The Evaluation of the IGF-1R as a Proposed Biomarker for DNA Damaging Cancer Therapies

by

Andrew Ross Gordon Worrall

St Edmund's Hall, Student Number 625893

A dissertation submitted to the University of Oxford for the degree of Master of Science By Research

Michaelmas 2013

The Evaluation of the IGF-1R as a Proposed Biomarker for DNA Damaging Cancer Therapies

Andrew Ross Gordon Worrall, St Edmunds Hall, Student Number 625893

Submitted for the degree of Master of Science By Research, Michaelmas 2013

Introduction

The IGF-1 receptor (IGF-1R) is overexpressed in many cancers, with roles in cell proliferation and survival. IGF-1R inhibition enhances radio- and chemo-sensitivity, potentially influencing DNA damage response, whilst *IGF1R* SNP rs4966013 has been identified as the SNP in the p53 stress response network most significantly associated with differences in chemosensitivity.

Aims:

1. Test whether IGF-1R protein expression correlates with *IGF-1R* mRNA, hence indirectly with SNP rs4966013 in high and low *IGF-1R* mRNA-expressing cell lines and the NCI60
2. Using cytotoxic drugs selected from sensitivity correlations with SNP rs4966013, assess:
    - whether cell lines expressing high IGF-1R exhibit greater chemo- and radio-resistance
    - the extent to which IGF-1R inhibition enhances chemo- and radiosensitivity, correlated with IGF-1R expression.

Methods

Protein expression was analysed using western blots. Sensitivity to irradiation, chemotherapy and IGF-1R inhibitors, and the effect of IGF-1R inhibition on radiosensitivity were assayed using cell viability assays. Published chemosensitivity and radiosensitivity data were compared with SNP genotype, *IGF1R* mRNA levels and published IGF-1R protein expression data.

Results

IGF-1R protein correlated with mRNA expression in the 8 cell line panel (Spearman's $r=-0.87$ $p=0.005$) and the wider NCI60 ($r=-0.71$ $p<0.0001$). Examination of IGF-1R protein and mRNA expression by SNP genotype suggested a dominant phenotype for the A allele.

Examination of public data demonstrated significant correlations between chemosensitivity and any measure of IGF-1R expression for 26 of 113 drugs. In cell viability assays, GI_{50}s for Paclitaxel and Topotecan were higher in cell lines with the GG genotype. However, in the 8 cell lines tested, viability assays showed no correlation between high IGF-1R and paclitaxel resistance, and a non-significant association with topotecan resistance.

Viability assays showed non-significantly increased radioresistance in cell lines with higher IGF-1R expression. Published NCI60 radiosensitivity data suggested no relationship with measures of IGF-1R expression.

Sigificant associations were identified between IGF-1R inhibitor sensitivity and pAKT but not measures of IGF-1R expression in cell viability assays. Public data showed cell lines of the GG genotype to be more sensitive to BMS754807 and possibly to OSI906 IGF-1R inhibitors.

Statement

I declare that, with the exception of the assistance acknowledged and sources quoted, all the work presented in the dissertation is my own work and has not been submitted in candidature for any other degree.

Andrew Ross Gordon Worrall

Word Count

Abstract	333	words
Text including tables and figures	19036	words
Text excluding tables and figures	14138	words

Acknowledgements

I have been lucky to have a great deal of help and support from many people, without whom I would not have been able to complete this project.

First and foremost, I would like to express my gratitude to Dr Valentine Macaulay, Head of the IGF Group of the Weatherall Institute of Molecular Medicine, and my principle supervisor. Val has been a constant and immensely patient source of exemplary help, explanation and scientific guidance throughout the project. Through her input into the project design and evolution, I have been able to investigate novel experimental methods for the laboratory and adapt the experimental design based upon their results. From initially teaching me the highest standards of experimental methods through to extensive advice and support with final write up, she has provided excellent supervision; many thanks.

Additionally, the supervision and access to the laboratory and data of Dr Gareth Bond, Ludwig Institute for Cancer Research, have been invaluable in the design and direction of the project. His personable approach to science has educated me in the benefits of collaboration within the research field.

From Dr Macaulay's laboratory, I would like to thank all the group members: Kunal, Tamara, Shan, Phil, Oliver and Aisha. I thank them for their frequent advice, help with troubleshooting, friendship and support through the year of study.

From Dr Bond's laboratory, I would like to thank and acknowledge Jorge, Elisabeth, Emmanouela, Anna, Juliet and Lukas, whose significant contributions in the supply of data and results were crucial for this project.

This project was funded by the generous donation of the Oxford Cancer Research Centre; for that I am very grateful.

Additionally, I would like to acknowledge the gift of K562 cells from Dr Catherine Porcher, Weatherall Institute of Molecular Medicine, and the gift of the IGF-1R inhibitor AZ12253801 to the laboratory from Elizabeth Anderson, Astra Zeneca, Alderley Park, UK.

Dedication

Thanks to my wife Caroline, whose constant love, support and immense patience has made this all possible. Thanks to my mum and my sister, Andrea, for their support and encouragement. To my daughter Tia, with love.

Declaration of author contributions

- All *IGF-1R* mRNA expression data was generated by RT-PCR by Jorge Zeron-Medina, and normalised to *GAPDH* mRNA expression (performed by Lukas Filip Grochola), with the normalisation being performed by Jorge Zeron-Medina, see 2.6 and 3.1. Whilst earlier analyses involving these data were performed by Jorge Zeron-Medina and Emmanouela Repapi, those presented within this document were performed by myself after exclusion of some of the cell lines previously included. The mRNA expression data described was used in analyses performed by myself and presented in figures 2D and E, 4, 5A,C and E, 12D, 13E, 14B, 15E, 16C, 17C, 19D, 20D, 22E and half of those described in Appendix V.
- SNP genotyping by Taqman assays were performed jointly by Jorge Zeron-Medina and Dr Elisabeth Bond (section 2.6). All SNP data used in this project was generated as such wherever it is reported, however analysis within the statistical comparisons reported here (with the exception of those mentioned in the introduction and those in Figure 11 C and D, which were performed by Emmanouela Repapi) were all performed by myself.
- Figure 1 Demonstrating the region in which SNP rs4966013 resides and similarity to FOX binding site is attributable to and reproduced by kind permission of Jorge Zeron-Medina. Section 1.5.
- Unpublished observations quoted from Dr Emmanouela Repapi for SNP contribution to chemoresistance are discussed in the sections 1.6 and 3.1; the contribution of these data to inspire an updated and extended analysis performed by myself is discussed in section 4.3.1. These data were used to select paclitaxel for further analysis by myself, see section 4.3.1, figure 11 (figure produced by myself according to the analysis performed by Emmanouela).
- All IGF-1R protein expression data generated by RPPA was downloaded from the NCI60 website http://dtp.nci.nih.gov/mtweb/targetinfo?moltid=MT18293&moltnbr=374556, as described in methods chapter 2.4.2, and is attributed to Park et al 2010, as referenced in the text; the uses of these data for analyses and comparisons with practical experiments performed by myself are discussed in section 3.3, 4.3.2, 4.4, 5.1.
- Radiosensitivity survival data: published post-irradiation survival data for the NCI60 cell line collection, generated using clonogenic assays, were obtained from Amundson et al 2008, methods chapter 2.4.3; I used these data to calculate SF_{50}s that are used in subsequent analysis, for example section 4.4.
- Chemotherapeutic GI_{50} data was downloaded from the NCI60 Human Tumor Cell Line Screen (http://dtp.nci.nih.gov/branches/btb/ivclsp.html) September 2012

release (methods: 2.4.1). The initial comparisons using this data (described in the introduction) and on which this project was based were performed by Emmanouela Repapi. All comparisons and analyses using this data and presented within the results were performed by myself.

- Where chemosensitivity data were not produced by myself with the resazurin assays I performed (chapters 4 & 5), they were otherwise obtained from the Genomics of Drug Sensitivity in Cancer (GDSC); data for sensitivity to IGF-1R inhibitors BMS754807 and OSI-906 were downloaded from http://www.cancerrxgene.org/translation/Drug, see chapter 2.5.1, with later analysis of these data performed by myself. Paclitaxel chemosensitivity data were additionally analysed by Dr Emmanouela Repapi (see comments re Figure 11, above).
- Gene mutation status, where not otherwise stated in the text, was downloaded from the Catalogue of Somatic Mutations in Cancer Project, part of the GDSC resource http://www.cancerrxgene.org/translation/Gene, section 2.5.2.

Table of Contents

Table of Contents vii
Table of Figures ix
Table of Tables xi
Abbreviations xii
1 Introduction 1
1.1 Cancer treatment 2
1.2 Mechanisms of resistance 5
1.3 Predicting response to chemotherapy and radiotherapy 8
1.4 Insulin-Like Growth Factor 1 Receptor 12
1.5 Project aims 16
2 Materials and Methods 17
2.1 Cell culture 18
2.1.1 General cell culture 18
2.1.2 Cell lines 19
2.1.3 Cell treatments 20
2.2 Protein analysis – western blotting 22
2.2.1 Collection and lysis of cells 22
2.2.2 Western blotting 22
2.3 Cell based assays 25
2.3.1 Clonogenic survival assays 25
2.3.2 Cell proliferation assays 25
2.4 NCI60 Developmental Therapeutic Program Human Tumor Cell Line Screen 27
2.4.1 Chemosensitivity data 27
2.4.2 IGF-1R Protein Expression Data 28
2.4.3 Radiosensitivity Data 28
2.5 Genomics of Drug Sensitivity In Cancer 29
2.5.1 Chemosensitivity data 29
2.5.1 Mutation Status of Cell Lines 29
2.6 SNP mRNA data source for NCI60 cell lines 30

2.7 Statistical Analysis 30
3 Examining the relationship between IGF-1R protein expression, *IGF-1R* mRNA expression and SNP rs4966013 32
3.1 Introduction 33
3.2 Examination of IGF-1R Protein Expression by Western Blot 33
3.3 Comparison of western blot derived protein expression data and IGF-1R mRNA with published IGF-1R protein expression data 33
3.4 Comparison of SNP rs4966013 genotype with IGF-1R protein and *IGF-1R* mRNA expression 38
3.5 Comparison of phosphorylated IGF-1R with total IGF-1R under steady state conditions and in relation to downstream signalling components 41
3.6 Summary and Discussion 49
4 Correlations between IGF-1R expression and chemo- and radio- resistance 51
4.1 Introduction 52
4.2 Assay Selection 52
4.3 Intrinsic Chemoresistance 56
4.3.1 Selection of Drugs 56
4.3.2 Paclitaxel and topotecan Sensitivity 61
4.5 Intrinsic Radioresistance 65
4.6 Summary 69
5 Testing associations between IGF-1R expression and the degree of radiosensitisation induced by IGF-1R inhibition 73
5.1 Introduction 74
5.2 Examining correlations between IGF-1R expression and sensitivity to IGF-1R inhibitors using publicly-available data. 75
5.3 Testing Intrinsic Sensitivity to IGF-1R inhibitors in 9 NCI60 cell lines 79
5.3.1 Inhibition of IGF-1R phosphorylation by AZ12253801 and BMS754807 80
5.3.2 AZ12253801 and BMS754807 sensitivity in cell viability assays 82
5.3.3 AZ12253801 sensitivity in colony assays 87
5.3.4 Correlations of IGF-1R inhibitor sensitivity 90
5.4 Effect of IGF-1R inhibition on radiosensitivity 92
5.4.1 Effect of AZ12253801 treatment on radiosensitivity 94
5.4.2 Effect of BMS754807 treatment on radiosensitivity 97

5.4.3 Summary and Discussion 100
References 107
Appendices 117
Appendix I: Cell Lines in the NCI60 tumour screen 118
Appendix II: Drugs examined 119
Appendix III: Boxplots - drug GI_{50} by SNP genotype 126
Alkylating agents 127
Antimitotic agents 133
Topoisomerase I inhibitors 136
Topoisomerase II inhibitors 139
RNA/ DNA antimetabolites 143
DNA antimetabolites 146
Appendix IV: Tables – drug GI_{50} by SNP genotype 150
Alkylating agents 151
Antimitotic agents 152
Topoisomerase I inhibitors 153
Topoisomerase II inhibitors 154
RNA/ DNA antimetabolites 155
DNA antimetabolites 156
Appendix V: Tables – correlations of drug GI_{50} with IGF-1R protein and mRNA 157
Alkylating agents 158
Antimitotic agents 159
Topoisomerase I inhibitors 160
Topoisomerase II inhibitors 161
RNA/ DNA antimetabolites 162
DNA antimetabolites 163

Table of Figures

Figure 1 The region of Intron 1 of the IGF-1R in which SNP rs4966013 resides. 15
Figure 2 IGF-1R protein expression in cell lines expressing high and low *IGF-1R* mRNA. 35
Figure 3 Comparison of IGF-1R protein expression assessed by western blot with publicly available data for the NCI60 cell line panel. 37
Figure 4 Comparison of IGF-1R protein and mRNA expression in NCI60 tumor cell lines. 37
Figure 5 Comparison of IGF-1R mRNA and protein expression with SNP rs4966013 genotype in cell lines from the NCI60. 40
Figure 6 Representative western blot for expression and phosphorylation of IGF-1R, AKT and ERK in 9 cell lines cultured under steady state conditions. 44
Figure 7 Comparison of phosphorylated IGF-1R with total IGF-1R in cell lines taken from the NCI60. 45
Figure 8 Comparison of pIGF-1R levels with pAKT and pERK levels in cell lines taken from the NCI60. 45
Figure 9 Growth pattern and morphology of cell lines under standard cell culture conditions. 53
Figure 10 Linearity of fluorescence versus cell number for the resazurin assay in 4 cell lines. 55
Figure 11 Comparison of Topotecan and Paclitaxel GI_{50}s between SNP rs4966013 genotypes in cell lines of the NCI60. 60
Figure 12 Examination of the relationship between intrinsic paclitaxel sensitivity and IGF-1R expression. 63
Figure 13 Examination of the relationship between intrinsic topotecan sensitivity and IGF-1R expression. 64
Figure 14 Comparison of Radiation SF_{50} with IGF-1R expression and SNP genotype within the NCI60. 66
Figure 15 Examination of the relationship between intrinsic radiosensitivity and IGF-1R expression. 68
Figure 16 Comparison of BMS754807 GI_{50} with IGF-1R SNP genotype, mRNA and protein expression. 76
Figure 17 Comparison of OSI-906 GI_{50} with IGF-1R SNP genotype, mRNA and protein expression. 78
Figure 18 Inhibition of IGF-1R phosphorylation by IGF-1R kinase inhibitors AZ12253801 and BMS 754801. 81
Figure 19 Examination of the relationship between intrinsic sensitivity to the IGF-1R inhibitor AZ12253801 and IGF-1R expression. 83
Figure 20 Examination of the relationship between intrinsic sensitivity to the IGF-1R inhibitor BMS754807 and IGF-1R expression. 84

Figure 21 Examination of the relationship between intrinsic sensitivity to IGF-1R inhibitors and phosphorylated ERK and AKT. 86
Figure 22 Examination of the relationship between intrinsic sensitivity to the IGF-1R inhibitor AZ12253801 and IGF-1R expression using clonogenic assays. 88
Figure 23 Correlation of sensitivity to IGF-1R inhibitors. 90
Figure 24 Examination of the effect of IGF-1R inhibition with AZ12253801 on radiosensitivity 95
Figure 25 Examination of the effect of IGF-1R inhibition with BMS754807 on radiosensitivity 98

Table of Tables

Table 1 Cell lines used in this project.....20
Table 2 Primary antibodies used in this project. 24
Table 3 Genetic mutations affecting major IGF-1R signalling pathways in the cell lines investigated.....48
Table 4 Summary of the Cytotoxic drugs examined per category within the Developmental Therapeutics Program (DTP) NCI60 Tumour Cell Line Sensitivity Screen. 57
Table 5 Drugs for which GI_{50} was significantly related to SNP rs4966013 genotype, *IGF-1R* mRNA and/or IGF-1R protein.....58
Table 6 GI_{50} values for Paclitaxel and Topotecan. 62
Table 7 Concentrations of the small molecule inhibitors AZ12253801, OSI-906 and BMS754807 required to cause half maximal inhibition of the IGF-1R and Insulin Receptor (IR). 79
Table 8 SNP genotype and Concentrations of AZ1225380 and BMS754807 required to inhibit growth of cell lines by 50%. 82
Table 9 SNP genotype and concentrations of AZ1225380 required to inhibit clonogenic survival (SF_{50}) and growth (GI_{50}) of cell lines by 50%.....89

Abbreviations

AH	anti-human
AM	anti-mouse
AP	apurinic/apyrimidinic
AR	anti-rabbit
ARF	alternate reading frame
ATM	ataxia telangiectasia mutated
ATP	adenosine triphosphate
ATR	ataxia telangiectasia and Rad3-related
Bak	Bcl-2 homologous antagonist/killer
Bax	Bcl-2-associated X protein
Bcl-X_L	B-cell lymphoma-extra large
BRCA1	breast cancer type 1 susceptibility protein
BRCA2	breast cancer type 2 susceptibility protein
BSA	bovine serum albumin
Chk	checkpoint kinase
CNS	central nervous system
CST	Cell Signalling Technologies
DMEM	Dulbecco's Modified Eagle's medium
DMSO	dimethyl sulfoxide
DNA	deoxyribonucleic acid
DNA-PKcs	DNA protein kinase catalytic subunit
DSB	double strand break
DTP	Developmental Therapeutics Program
EDTA	ethylenediaminetetraacetic acid

EGFR	epidermal growth factor receptor
ERCC1	excision repair cross-complementing rodent repair deficiency, group 1
ERK	extracellular-signal-regulated kinase
FCS	fetal calf serum
FEN1	flap structure-specific endonuclease 1
FLIP	FLICE-like inhibitory protein
GAPDH	glyceraldehyde 3-phophate dehydrogenase
GDSC	Genomics of Drug Sensitivity in Cancer
GI_{50}	concentration of drug to inhibit growth by 50%
H2AX	Histone H2A isoform X
Ham's F12	Hams F12 medium
HEPES	hydroxyethyl piperazineethanesulfonic acid
HER-2	human epidermal growth factor receptor 2
Het	heterozygous
Hom	homozygous
HRP	horseradish peroxidase
HRR	homologous recombination repair
IAP	inhibitor of apoptosis proteins
IC_{50}	half maximal inhibitory concentration
IGF-1R	insulin-like growth factor 1 receptor
IMDM	Iscove's modified Dulbecco's medium
IR	insulin receptor
IRS-1	insulin receptor substrate 1
MAPK	mitogen activated protein kinase
MDM2	murine double minute 2
MLH	mut L homolog

MM	monoclonal mouse
MR	monoclonal rabbit
Mre11	meiotic recombination 11
MRN	Mre11, Rad50, Nbs1
mRNA	messenger RNA
MSH	MutS protein homolog
n	number
NBS	Nijmegen breakage syndrome
NCI	National Cancer Institute
NFM	non-fat milk
NSC	National Service Center
O^6meG	O6-methylguanine
p53	protein 53
pAKT	phosphorylated AKT
PARP-1	poly(ADP-ribose) polymerase 1
PBS	phosphate buffered saline
PBST	PBS with 0.05% Tween 20
PCNA	proliferating cell nuclear antigen
pERK	phosphorylated ERK
PG	polyclonal goat
pIGFR-1R	phosphorylated IGF-1R
PMS2	post meiotic segregation increased 2
PR	polyclonal rabbit
PTEN	phosphatase and tensin homologue
RFC	replication factor C
RIPA	radio-immunoprecipitation assay

RNA	ribonucleic acid
RPA	replication protein A
RPMI	Roswell Park Memorial Institute medium
RPPA	reverse phase protein array
RT-PCR	real-time polymerase chain reaction
SDS	sodium dodecyl sulphate
SDS-PAGE	SDS polyacrylamide gel electrophoresis
SEM	standard error of mean
SF2	surviving fraction at 2Gy
SF_{50}	surviving fraction 50% cells
siRNA	small interfering RNA
SNP	single nucleotide polymorphism
SSB	single strand break
TBS	tris-buffered saline
TBST	TBS with 0.05% Tween 20
TFIIH	transcription factor II human
Tris	trisaminomethane
Trk	tropomyosin receptor kinase
XAB2	XPA-binding protein 2
XLF	XRCC4-like factor
XPF	xeroderma pigmentosum group F
XPG	xeroderma pigmentosum group G
XRCC	X-ray repair cross-complementing protein

1 Introduction

1.1 Cancer treatment

Cancer is a substantial health problem, with age standardised incidence rates of 431 and 375 per 100,000 population per year for men and women respectively during the period 2008-2010, and corresponding mortality rates of 204 and 148 per 100,000 population per year in the United Kingdom[1]. Whilst, for many of these cancers, early surgical intervention greatly reduces the risk of recurrence, for others, the likelihood of microscopic local infiltration or distant metastases requires radio- or chemotherapeutic management. Haematological malignancies are nearly always disseminated at presentation, thus systemic treatment is usually required.

Non-surgical treatments include radiotherapy, chemotherapy and targeted biological agents. This project focussed on cytotoxic drugs and irradiation. Radiotherapy exerts its effects via ionising damage to deoxyribonucleic acid (DNA) or proteins. Ionising radiation induces a wide spectrum of DNA lesions, including base modifications, crosslinks, single strand breaks (SSBs) and double strand breaks (DSBs)[2]. Whilst DSBs are the most cytotoxic lesion, SSBs may induce formation of DSBs either during their repair, or following replication block and fork collapse[2]. Following detection of DNA damage, activation of protein 53 (p53) may trigger cell cycle arrest, allowing repair of damage, senescence, or apoptosis via the intrinsic cell death pathway. However, the major mechanism of cell death following irradiation in solid tumours is mitotic catastrophe following impaired chromosome segregation[3]. Impaired enzymatic function due to oxidative protein damage, particularly that of DNA repair proteins, may exacerbate these effects and in some circumstances may be more critical than the degree of DNA damage itself[4].

The major categories of cytotoxic chemotherapeutic agent include alkylating agents, antimitotic agents, topoisomerase I and II inhibitors and ribonucleic acid (RNA) and DNA antimetabolites. Alkylating agents react with the cyclic nitrogen and extracyclic oxygen atoms within DNA bases, inducing formation of DNA adducts, abasic sites, and intra- and inter-strand crosslinks[5,6]. O^6-chloroethylguanine adducts, which may form G-C crosslinks with nearby cytosines, are removed by O^6-methylguanine (O^6meG) DNA methyltransferase. A number of the lesions formed may result in replication block, or failed repair and subsequent SSB, DSB and apoptosis. Platinum drugs such as Cisplatin also interact with cyclic nitrogen atoms within purine bases, but tend to produce intra- rather than inter- strand crosslinks, with futile cycles of mismatch repair contributing to DSB formation and apoptosis[7,8].

Antimitotic agents include tubulin binding agents and kinesin inhibitors. Microtubules are dynamic structures, growing and shortening as αβ heterodimers associate and dissociate. Interference with this inhibits the rapid assembly and disassembly needed for mitotic spindle assembly and the alignment and separation of chromosomes during mitosis[9]. Blocking mitotic spindle assembly and function results in G2/M cell cycle arrest and blocking of mitosis at the metaphase anaphase boundary, with subsequent mitotic catastrophe[10]. Agents such as the taxanes and epothilones bind and stabilise the βII subunit of polymerised tubulin, whereas the vinca alkaloids and halichondrins bind the β subunit at the microtubule ends, inhibiting assembly and, at higher doses, triggering depolymerisation, either of which result in mitotic block[11]. Kinesins are microtubule associated motor proteins which assemble and segregate

chromatids during mitosis[12], their inhibition prevents normal spindle assembly resulting in activation of the spindle checkpoint and mitotic catastrophe[13].

Topoisomerase I inhibitors include the camptothecin and camptothecin-like drugs such as irinotecan and topotecan. Topoisomerase I relaxes DNA supercoiling in advance of transcription and replication and also during DNA repair and chromatin remodelling[14]. It acts by binding DNA, inducing transient single strand DNA breaks, which allow rotation of the broken strand around the complementary strand to relax supercoiling, and completes its action by religating the broken strand[15]. The intermediate stage in which topoisomerase I is bound to the broken strand is termed the topoisomerase cleavage complex. Camptothecins intercalate between DNA and Topoisomerase I, stabilising the cleavage complex, preventing religation[16]. This lesion persists only as long as topotecan remains bound. However, when DNA replication complexes collide with the stabilised cleavage complex, DSB are created, triggering the DNA damage response and apoptosis[17]. Collision of transcription machinery with the topoisomerase cleavage complex may also induce transcription block and induction of the DNA damage response, though this requires higher concentrations for cytotoxicity[15].

Topoisomerase II inhibitors include anthracyclines, anthracenediones and epipodophyllotoxins. Topoisomerase II also relaxes DNA supercoiling, however, it binds to two DNA helices, induces a transient DSB in one helix, the G-segment, creating a gate, through which it guides the second captured helix before religating the double helix and dissociating[18,14]. Most topoisomerase II inhibitors in clinical use bind irreversibly to the intermediate topoisomerase II-DNA complex, preventing religation of the cleaved double helix[19]. Collision with replication and transcription machinery triggers the DNA damage

response, and attempted repair by nucleotide excision repair or by degradation of topoisomerase II and DSB repair by homologous recombination repair (HRR) or non-homologous end joining[20]. If repair is unsuccessful, then apoptosis may be triggered[20].

Antimetabolites include inhibitors of purine and pyrimidine synthesis and analogues inhibiting their utilisation. Folate antagonists chiefly inhibit dihydrofolate reductase, blocking thymidine and purine synthesis; this inhibits DNA and RNA synthesis, typically manifesting as stalled replications forks. Purine and pyrimidine analogues may inhibit DNA and/ or RNA synthesis by acting as competitive inhibitors of DNA or RNA polymerase, may act as false substrates which are then incorporated into DNA and RNA and then either have little effect on subsequent synthesis, or inhibit ongoing synthesis causing stalled replication forks and chain termination[21,22]. Thymidylate synthesis inhibition, by agents such as 5-fluorouracil, acts similarly to folate antagonists, depleting nucleotide supply and stalling replication forks. Some pyrimidine analogues also inhibit DNA methyltransferases, which may allow reactivation of tumour suppressor genes such as p53, leading to induction of apoptosis[23].

1.2 DNA Damage Repair

Cells employ three general mechanisms to repair the DNA damage induced by cytotoxic drugs and irradiation: direct reversal, for example of O^6meG adducts induced by dacarbazine and temozolomide[24], repair of single strand damage, via base excision repair, nucleotide excision repair or mismatch repair, and repair of DSBs, which are the most toxic lesions that arise from irradiation or chemotherapy. DSBs can be induced directly or indirectly from repair of other lesions, and are repaired by HRR or non-

homologous end joining (NHEJ)[25]. HRR allows for high fidelity repair of DSBs in S and G2 phases of the cell cycle, when sister chromatids are available[26]. The MRN complex (meiotic recombination 11 (Mre11), Rad50, Nbs1) recognises the damaged strand end and activates ataxia telangiectasia mutated (ATM), which in turn activates the histone H2A isoform (H2AX) anchoring the complex and preventing end dissociation[27]. MRN trims the 5' end to generate a 3' overhang, to which replication protein A (RPA) binds[28]. Breast cancer type 2 susceptibility protein (BRCA2) recruits Rad51, which mediates invasion of the homologous chromosome[28]; this is followed by DNA synthesis prior to the strands being released, and the nicks are sealed by DNA ligase. ATM also activates cell cycle damage checkpoints, G1/S via checkpoint kinase 1 (Chk1), Chk2 and p53, and the intra S phase and G2/M via multiple interactions[27].

NHEJ is an error-prone repair of DSBs that can be performed throughout the cell cycle. Ku70/80 heterodimers recognise, DNA protein kinase catalytic subunit (DNA-PKcs) bridges, and Artemis processes the damaged ends[29]. X-ray repair cross-complementing protein (XRCC) 4 acts as a scaffold for ligation by DNA ligase IV, and XRCC4-like factor (XLF)/cernunnos acts both to bridge the gap and stimulate DNA ligase IV activity[29]. DNA-PKcs cooperates with Ataxia telangiectasia and Rad3-related (ATR) and ATM to activate cell-cycle DNA damage checkpoints, allowing time for repair.

Single strand damage includes base damage, cross-links and SSBs. The latter are induced directly by numerous agents, or indirectly as a result of attempted damage repair. When recognised during replication, the MRN complex again provides recognition, whilst RPA serves as a scaffold and Rad52 aligns the sequences for annealing. Non-homologous ends are removed by Rad1 and 10, whilst DNA synthesis and ligation complete the process.

Crosslink repair involves a combination of nucleotide excision repair and DSB repair. Nucleotide excision repair is triggered by helix distorting DNA adducts and pyrimidine dimers[30]. Transcription factor II human (TFIIH) unwinds 20-30 nucleotides and allows xeroderma pigmentosum group G (XPG), RPA and xeroderma pigmentosum group F – excision repair cross-complementing rodent repair deficiency group 1 (XPF-ERCC1) to bind. XPF-ERCC1 and XPG cut and release the damaged DNA, followed by nucleotide replacement by the replication factor C (RFC)/ proliferating cell nuclear antigen (PCNA)/DNA polymerase δ complex prior to nick sealing by DNA ligase I[31]. Interstrand crosslinks prevent TFIIH from unwinding the DNA, in which case the lesion is excised by the concerted actions of XPG, XPF and ERCC1[30]. For intra-strand crosslinks this is followed by DNA synthesis and ligation, whilst for interstrand crosslinks, repair proceeds as for DSBs.

Base excision repair corrects small non-distorting lesions, and involves recognition of the lesion by Poly(ADP-ribose) polymerase 1 (PARP-1), which recruits ATM[32] and XRCC1[33]. XRCC1 coordinates removal of the damaged base by DNA glycosylase, whilst apurinic endonuclease and apurinic/apyrimidinic (AP) lyase remove the sugar residue[34]. Flap structure-specific endonuclease 1 (FEN1) trims the ends and DNA polymerase replaces bases before nick sealing by DNA ligase III and XRCC1[34]. Post replication mismatch repair involves protein recognition and excision of mismatched bases with complexes of mutS protein homolog (MSH) 2, 3 or 6 and mut L homolog (MLH) 1 or postmeiotic segregation increased 2 (PMS2), followed by base replacement as above.

1.3 Mechanisms of resistance

Mechanisms of resistance to radio- and chemotherapeutic agents may be intrinsic or extrinsic to tumour cells. Extrinsic factors include drug inactivation and tumour micro-environmental conditions, such as hypoxia and stromal cell interactions. Variations in extrinsic drug inactivation may be innate, such as single nucleotide polymorphisms (SNPs) affecting the promoter of gluconyltransferase, which inactivates the active form of irinotecan by glucoconjugation.[35] Alternatively, mechanisms of drug inactivation can be induced, such as upregulation of hepatic cytochrome P450 following exposure to corticosteroids, anticonvulsants or other xenobiotics[36]. Disordered tumour vascularity may reduce drug exposure and result in hypoxia. Hypoxia reduces sensitivity to indirectly ionising radiation, by reducing the formation of DNA damaging reactive oxygen species[37]. Furthermore, hypoxia upregulates expression of the transcriptional regulators hypoxia inducible factors, which may induce pro-survival metabolic changes, overexpression of multidrug resistance protein and inhibition of apoptosis and autophagy, increasing resistance to both chemo- and radiotherapy[38]. Paracrine signalling between tumour and stroma, and adhesion of tumour cells to stroma and extracellular matrix may also enhance chemo resistance[38].

Intrinsic mechanisms of resistance include reduced target exposure to the drug, reduced drug impact on the target, and alterations to DNA damage response, apoptosis and pro-survival signalling pathways. Reduced drug exposure may be achieved by increased cellular export via the multidrug resistance protein[39] or reduced import, such as follows inactivating mutations or epigenetic silencing of the folate transporter[40]. Alterations in intracellular activation and degradation, such as may occur with cytosine

arabinoside, may further reduce exposure[35]. Alternatively, mutations of the target may reduce sensitivity to the drug, for instance thymidylate synthetase and 5-fluorodeoxyuridine[41]. In contrast, overexpression of dihydrofolate reductase, for example, results in functional redundancy of the target and reduced drug impact[40].

The role of the DNA damage response in resistance to chemo- and radio-therapy is double-edged. There is a clear association of defects of the DNA damage sensory apparatus components ATM and Nijmegen breakage syndrome 1 (NBS-1) with both radiosensitivity and cancer formation as manifested in Ataxia-Telangiectasia and NBS[37]. Additionally, upregulation of proteins involved in homologous repair and recombination of DSBs, including RAD51 and RAD52, has been associated with earlier relapse following chemotherapy for melanoma[42], and overexpression of O^6meG DNA methyltransferase is associated with resistance to alkylating agents[43]. Increased expression of DNA damage repair proteins, such as ERCC1, which is involved in the nucleotide excision repair pathway, or breast cancer type 1 susceptibility protein (BRCA1), which is involved in repair of DSB via both HRR and nonhomologous end joining, are both associated with resistance and worse outcome in response to treatment of non-small cell lung cancer with platinum drugs[44].

In contrast, mutation or loss of the DNA damage signalling proteins, ATM, Mre11 and H2AX, have been associated in oral squamous cell carcinoma cell lines with resistance to cisplatin[45] and radiation[46]. Mutations in mismatch repair genes, such as *MLH1* and *MSH2*, confer resistance to cisplatin by avoiding futile repair cycles, which lead ultimately to apoptosis[43,38].

Resistance to cell death may be provided by activation of growth factor signalling pathways supplying a survival signal[47,48], or by alterations in the apoptosis pathway. The PI3K/AKT/mTOR pathway has prosurvival effects[49,50]. AKT phosphorylates and inactivates a number of proapoptotic targets including BAD, BAX, caspase 9 and the transcription factor FOXO3A[51,50]. Increased activity of this pathway is common in cancers and may arise from activity of overexpressed or mutated receptor tyrosine kinases such as insulin-like growth factor 1 receptor (IGF-1R), epidermal growth factor receptor (EGFR) or human epidermal growth factor receptor 2 (HER-2), from activating mutations of *PIK3CA* or *AKT,* or from inactivation of PTEN, which would otherwise inhibit PI3K[52]. Ras-Raf-MAPK signalling is another pathway commonly activated in tumours, and whilst primarily associated with proliferative effects, it may also provide prosurvival signals via crosstalk with the PI3K pathway[53].

Constitutive activation of the transcription factor NF-κB has been linked to apoptosis resistance[54] by promoting transcription of several antiapoptotic genes including inhibitor of apoptosis proteins (IAP) 1/2, B-cell lymphoma-extra large (Bcl-X_L) and FLICE-like inhibitory protein (FLIP)[55]. Alterations in the apoptotic pathway itself are also common, including both upregulation of anti-apoptotic proteins such as Bcl-2, FLIP, IAPs and downregulation or inactivation of proapoptotic proteins such as Bcl-2-associated X protein (Bax), Bcl-2 homologous antagonist/killer (Bak), Bim or the caspases.

1.4 Predicting response to chemotherapy and radiotherapy

Given the differences in intrinsic sensitivity of different tissues types to chemotherapy and radiotherapy, coupled with the genetic and epigenetic heterogeneity of cancer[56], it is inevitable that tumours will exhibit a range of sensitivity to these

treatment modalities. Even within tumours of apparently similar histopathology, treatment response varies. In order to avoid imposing adverse effects on those patients who will not benefit, it would be beneficial to identify biomarkers capable of differentiating between cancers that will and will not respond to therapy. The mechanisms of resistance described above, and the cellular pathways and regulatory networks linked to them seem likely candidates. Such biomarkers might include mutations or SNPs, epigenetic regulation by promoter methylation or micro RNA activity, measures of gene expression such as RNA or protein levels, or the metabolic products of protein activity.

The protein p53 lies at the hub of the DNA damage response, responding to DNA damage such as that caused by ionising radiation via the protein kinases ATM and Chk2[57]. In addition, p53 integrates signals from numerous additional cellular stresses, such as hypoxia via decreased expression of its inhibitor murine double minute 2 (MDM2)[58]; excessive growth signals, such as those due to overactivity of the oncogenes RAS and MYC, detected via $p14^{ARF}$ (alternate reading frame); and DNA damage due to ultraviolet irradiation or nucleotide depletion, or protein kinase inhibition, via the proteins ATR and Chk1[57,59,60]. Activation of p53 may then lead to cell cycle arrest at the G1/S or the G2/M checkpoint, senescence or apoptosis. Given the obvious importance of p53 and the genes it regulates in the response to genotoxic and other cellular stresses[61], the p53 stress response network is a logical area to investigate for potential biomarkers of chemotherapeutic response.

Such an approach has been taken using publicly available data for describing the growth inhibitory activity of a number of chemotherapeutic drugs examined in the

National Cancer Institute (NCI) tumor drug screen (http://dtp.nci.nih.gov/branches/btb/ivclsp.html). The NCI60 cell line panel consists of 59 tumour cell lines from nine different tissues types (blood, lung, colon, breast, central nervous system (CNS), skin, ovary, renal, and prostate). Cell lines with mutant p53 tended to exhibit less growth inhibition when exposed to antimetabolites, topoisomerase inhibitors and alkylating agents than cells with wild type p53. Antimitotic agents did not show such a correlation[62]. Dr Gareth Bond's group examined the effect of SNP309 in the promoter of the gene encoding MDM2, a negative regulator of p53, on chemosensitivity in tumour cell lines, using the same chemosensitivity information from the NCI60[61]. Dr Bond's group had previously found that the G allele of SNP309 was associated with increased *MDM2* messenger RNA (mRNA) and protein expression, and with accelerated tumour development[63]. More recently, they reported that the G allele of this SNP exhibited a similar pattern of correlation with response to cytotoxic drugs as that conferred by mutant p53[61].

1.5 Insulin-Like Growth Factor 1 Receptor

The Insulin like growth factor 1 receptor (IGF-1R) is overexpressed in several cancers including, renal[64], prostate[65], pharyngeal and breast cancer, in which it has been associated with reduced post-surgical survival[64], disease progression[66], metastasis[67] and resistance to endocrine[68] and radio- therapy[69] respectively. IGF-1R is a cell surface receptor tyrosine kinase, with each half receptor consisting of an extracellular ligand binding α subunit and a transmembrane/ intracellular β subunit with kinase activity responsible for intracellular signalling[70,71] It may form disulphide-bonded homodimers, or

heterodimers with the insulin receptor (IR)[71]. IGF-1 ligand binding triggers a conformational change, with activation of kinase activity and downstream signalling, primarily involving the PI3K/Akt/mTOR and Ras-Raf-MAPK pathways. IGF-1R signalling is involved in cell proliferation, protection from apoptosis[72,73], and motility and invasion through its interaction with integrins[74,75].

IGF-1R signalling has been shown to protect cancer cells from killing by cytotoxic drugs[76,77], and this has largely been attributed to the ability of IGFs to regulate cell survival by suppressing apoptosis[77-79]. Work from the Macaulay laboratory and others supports the involvement of the IGF-1R in the DNA damage response. Inhibition of IGF signalling using tyrosine kinase inhibitors, monoclonal antibodies and small interfering RNA (siRNA) knockdown has been shown to sensitise to DNA damaging therapies such as ionising radiation[80] and cytotoxic drugs including mitoxantrone, nitrogen mustard and etoposide[81-83]. Several studies have identified potential links between IGF-1R signalling and DNA damage repair. Inhibition or siRNA knockdown of IGF-1R has been reported to inhibit DSB repair by both HRR and non-homologous end joining[84,85]. Furthermore, these effects appear to occur at levels of IGF-1R inhibition lower than those required to influence cell cycle distribution and apoptosis induction[84]. In the HRR pathway, Rad51 appears to bind insulin receptor substrate 1 (IRS-1) within the perinuclear region and is released following phosphorylation of IRS-1 by IGF-1R, permitting RAD51 to localise to foci of DNA damage[83]. Monoclonal antibody mediated IGF-1R inhibition has also been shown to inhibit upregulation of ERCC1, XAB2, and RAD23A gene expression following cisplatin administration, suggesting an interaction between IGF-1R and the nucleotide excision repair pathway[86]. Finally, IGF-1R expression appears to be dependent on

expression of functional ATM[87], and mediated by the zinc finger transcription factors Sp1 and WT1[88]. Forced expression of IGF-1R in radiosensitive ATM mutant cells increases radioresistance[87].

1.6 Identification of an IGF-1R SNP associated with chemoresistance.

In an extension of their earlier work on functional SNPs that affect cancer phenotypes[63,61], the Bond group compared differences in sensitivity to 123 cytotoxic drugs with allelic differences in over 630 SNPs in the p53 response network using a custom made Illumina comparative genomic hybridisation platform. Within this analysis, IGF1R SNP rs4966013 (G/A) was identified as the highest ranking SNP, demonstrating significant allelic differences in growth inhibition for 56 of the 123 drugs (Dr Gareth Bond, unpublished data). These results were confirmed using Taqman SNP genotyping assays as described in section 2.6 later. When comparisons were made with drug concentrations required to achieve 50% growth inhibition (i.e. the GI_{50}), cell lines with the GG genotype were found to have higher GI_{50} values than cell lines with the AA genotype for 53 of the 56 drugs. In particular, 96% of these 53 drugs were DNA damaging, in comparison to 81% within the screen as a whole, whereas antimitotic agents were less common than in the screen as a whole (4% vs 18%, p=0.0096 Fishers Exact Test). Furthermore, the 7 relatively chemo- resistant cell lines with the GG genotype exhibited significantly higher *IGF-1R* mRNA levels (2.5 fold higher) than cells with the AA genotype (n=33, p=0.005) (Jorge Zeron Medina, Dr Emmanouela Repapi, unpublished data). SNP rs4996013 resides within a highly conserved region of the first intron of the IGF-1R (Figure 1) and in preliminary experiments has been identified by electromobility shift assay as a Forkhead C

transcription factor binding site with higher binding affinity for the G allele (Jorge Zeron-Medina unpublished data), consistent with the elevated *IGF-1R* mRNA expression in GG homozygotes.

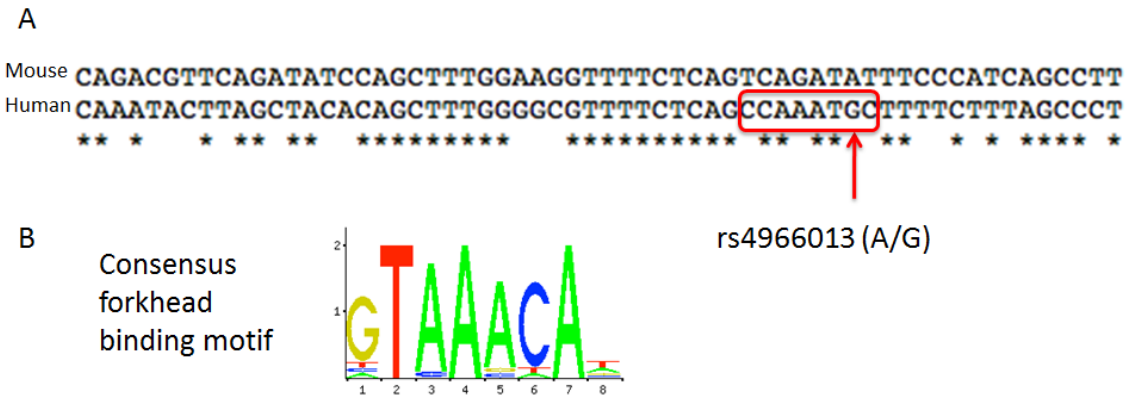


Figure 1 The region of Intron 1 of the IGF-1R in which SNP rs4966013 resides.
A. Conserved region of IGF-1R intron 1 with human and mouse sequences for comparison. Stars mark conserved base pairs. The predicted forkhead binding site is circled in red and the location of SNP rs4966013 marked with the red arrow. **B.** Consensus forkhead binding motif for comparison. Figure courtesy of Jorge Zeron-Medina.

The correlation of the GG genotype with both increased mRNA expression and chemoresistance suggests that the IGF-1R may contribute to chemoresistance, in particular to DNA damaging agents. Therefore, this finding is consistent with reports from our group and others of the association of the IGF-1R with chemo- and radio-resistance[83,89,85,86].

Given the associations of allelic differences of SNP rs4966013 with chemoresistance and the involvement of IGF-1R with DNA damage response and repair it seems possible that measures of IGF-1R expression may influence the degree of intrinsic chemo- and radio resistance. Furthermore, it is plausible that IGF-1R expression may also influence the extent to which IGF-1R inhibition may sensitise tumours to radiation or

chemotherapy. Finally, given that *IGF1R* mRNA has a complex 5' untranslated region and that its expression is subject to post-transcriptional regulation[90,91], it is important to assess whether IGF1R mRNA and protein expression correlate, and hence whether differences in *IGF1R* mRNA expression observed with SNP rs4966013 extend to protein expression.

1.7 Project aims

The aims of this project were therefore to

1 Test whether IGF-1R protein expression correlates with *IGF-1R* mRNA and hence indirectly with SNP rs4966013:

- In a panel of high and low IGF-1R mRNA expressing cell lines using western blot
- In the wider NCI60 using published protein array data

2 Test the following hypotheses using cytotoxic drugs selected based on sensitivity correlations with SNP rs4966013:

- Cell lines expressing high IGF-1R exhibit greater chemo- and radio- resistance
- The extent to which IGF-1R inhibition enhances chemo- and radiosensitivity correlates with IGF-1R expression

2 Materials and Methods

2.1 Cell culture

2.1.1 General cell culture

All cell lines were grown in sterile mycoplasma tested media (GIBCO / Invitrogen) in tissue culture grade flasks, dishes and plates (Corning). Culture media were supplemented with 100 units/ml Penicillin, 0.1mg/ml Streptomycin (GIBCO / Invitrogen) and 10% fetal calf serum (FCS, PAA Laboratories), except for the culture medium for Malme 3M, which was supplemented with 20% FCS. However, all cell lines were grown in medium supplemented with 10% FCS when grown for comparison of IGF-1R protein expression by western blot. Additionally, these cells were harvested in logarithmic growth phase and media were changed 2 hours prior to harvest. Cells were cultured in a humidified incubator at 37^{o}C, in either 5% CO_2 and 95% air, or 10% CO_2 and 90% air. Media and CO_2 requirements for specific cell lines are listed in table 1. Cell culture procedures were performed in a tissue culture hood and cell cultures were tested periodically to ensure absence of *Mycoplasma* spp.

Adherent cell lines were split for routine passage at approximately 80-90% confluence. Disaggregation of adherent cells for routine passage was performed by removing culture medium, washing cells in sterile phosphate buffered saline (PBS) then applying 1 x trypsin ethylenediaminetetraacetic acid (EDTA) (GIBCO/ Invitrogen; diluted from 10x stock using PBS) for 3-5 minutes at 37^{o}C. Cells were then resuspended in complete medium before reseeding at an appropriate dilution. Suspension cells were counted using a haemocytometer and split at a density of 2x10^{6}cells/ ml for CCRF-CEM or 1x10^{6}cells/ ml for K562 cells. After centrifugation at 1250g for 5 minutes, cells were resuspended in fresh media at a concentration of 3x10^{5} cells/ml for CCRF-CEM cells, and

$1x10^5$ cells/ml for K562 cells. Prior to experimental work, early passage cells were expanded for cryopreservation. Adherent cells were disaggregated as above, washed in complete medium and centrifuged at 1250g for 5 minutes then resuspended in a mixture of 10% dimethyl sulfoxide (DMSO), 50% FCS and 40% of their routine culture medium. Suspensions were frozen overnight at -80^oC in sterile Nunc cryovials prior to transfer to liquid nitrogen. Recovery of frozen cell suspensions involved rapid thawing, washing in complete growth medium, centrifugation and resuspension in complete growth medium for culture.

2.1.2 Cell lines

Cell lines used in this project are listed in Table 1. MCF-7, SK Mel 28 and SKUT-1 were obtained as low passage stocks from Cancer Research UK Cell Services, Clare Hall Laboratories, Hertfordshire, UK. CCRF-CEM, IGR-OV1, M14, MALME 3M and T47D were obtained via the laboratory of Dr Gareth Bond (Ludwig Institute for Cancer Research, Oxford, UK) from the NCI at Frederick in Maryland, USA. K562 and PC3 cells were obtained from the laboratories of Dr Catherine Porcher and Sir Walter Bodmer at the Weatherall Institute of Molecular Medicine, Oxford, UK. A375M were obtained from Prof Colin Goding, (Ludwig Institute for Cancer Research, Oxford, UK) and CHL-1 from the American Type Culture Collection.

Cell Line	Origin	Medium	CO_2 Concentration
A375M	Metastasis from human melanoma xenograft in mouse model	DMEM	10% CO_2
CCRF-CEM	Acute Lymphoblastic Leukaemia (T cell)	RPMI	5% CO_2
CHL-1	Melanoma	DMEM	10% CO_2
IGR-OV1	Ovarian Carcinoma	RPMI	5% CO_2
K562	Chronic Myelocytic Leukaemia	RPMI	5% CO_2
M14	Melanoma	RPMI	5% CO_2
Malme-3M	Melanoma	IMDM	5% CO_2
MCF-7	Breast carcinoma	IMDM	5% CO_2
PC3	Prostate Carcinoma	Ham's F12	5% CO_2
SK Mel 28	Melanoma	IMDM	5% CO_2
SKUT-1	Uterine Leiomyosarcoma	DMEM	10% CO_2
T47D	Breast carcinoma	IMDM	5% CO_2

Table 1 Cell lines used in this project.
The table details cell line, cancer type, base culture medium prior to additions, and CO_2 used in the incubators for their culture. DMEM = Dulbecco's Modified Eagle's Medium, RPMI = Roswell Park Memorial Institute Medium, Ham's F12 = Hams F12 medium and IMDM = Iscove's Modified Dulbecco's Medium.

2.1.3 Cell treatments

2.1.3.1 Ionising radiation

Cells growing in complete medium were irradiated or mock irradiated using doses of 0-10 Gy in an IBL 637 irradiator (CBS BIO International, France) containing four caesium 137 sources. Adherent and suspension cells were irradiated in 96 well plates; adherent cells were also irradiated in 10 cm dishes.

2.1.3.2 IGF-1R inhibition

AZ12253801 and BMS754807 are small molecule inhibitors of IGF-1R kinase activity that were obtained from Elizabeth Anderson, Astra Zeneca (Alderley Park, UK) and Chemietek (Indianapolis, US) respectively. Both were reconstituted to a stock concentration of 10mM in DMSO and stored in single use aliquots at -20^{o}C. Stock concentrations of inhibitor and control volumes of DMSO solution were further diluted in complete or serum free media as appropriate for individual experiments.

2.1.3.3 IGF-1R stimulation with IGF-1 ligand

Recombinant human IGF-1 (Sigma Aldrich, St. Louis, Mo, US) was used to activate the IGF-1R to test inhibition of the IGF-1R by AZ12253801 and BMS754807. Adherent cell lines were seeded in 6 well plates in complete media at sufficient density to achieve 70% confluence the next day, when media were removed and cells washed with PBS twice prior to incubation in serum free media for a further 24 hours. Suspension cells were washed twice in PBS following centrifugation and resuspended in serum free media for incubation for a further 24 hours as for adherent cells. K562 and CCRF-CEM cells were seeded at densities of $3x10^6$ and $10x10^6$ cells per well respectively. After 24 hours incubation, media were removed and 2.2ml serum free media containing IGF-1R inhibitors applied to each well for 1 hour before application of 1µl of 110uM IGF-1 ligand stock to each well to give a final concentration of 50nM IGF-1.

2.1.3.4 Chemotherapeutics

Paclitaxel and topotecan (Sigma Aldrich, Gillingham, UK) were reconstituted in DMSO to a stock concentration of 10mM and stored in single use aliquots at -20^{o}C. These were further diluted in complete media for individual experiments.

2.2 Protein analysis – western blotting

2.2.1 Collection and lysis of cells

Culture media were removed from dishes and adherent cells were washed twice with ice cold PBS, scraped into 1ml PBS and pelleted by centrifugation at 14000rpm for 2 minutes at 4^{o}C. Suspension cells were pelleted by centrifugation at 3000 rpm for 5 minutes at 4^{o}C then washed twice by resuspension in PBS and repeat centrifugation at 14000 rpm for 2 minutes at 4^{o}C. PBS was aspirated and cell pellets snap-frozen in dry ice and 100% ethanol for 1 minute. Cell pellets were either stored at -20^{o}C, or thawed and lysed on ice using either IGF-1R lysis buffer (50mM hydroxyethyl piperazine ethane sulfonic acid (HEPES) pH7.6, 100mM NaCl, 10mM EDTA, 1% Triton X-100, 4mM sodium pyrophosphate, 2mM sodium orthovanadate, 10mM NaF) or Radio-immunoprecipitation assay (RIPA) buffer (20mM trisaminomethane (Tris) pH 7.5, 1mM EDTA, 100mM NaCl, 1% Triton X-100, 0.5% sodium deoxycholate, 0.1% sodium dodecyl sulphate (SDS)). All lysis buffers were supplemented with EDTA free protease inhibitor cocktail (Roche, 1 tablet per 25-50ml buffer), 1.5mM Pefabloc SC Plus (Roche), Phosphatase inhibitor complex II (Sigma Aldrich, P5726) and complex III (Sigma Aldrich, P0044). Cell pellets were suspended in lysis buffer and lysed on ice for 30 minutes then centrifuged at 14000 rpm for 15 minutes to remove insoluble debris.

2.2.2 Western blotting

Soluble protein was quantified against bovine serum albumin (BSA) standards using the Pierce Bicinchoninic Acid assay (Thermo Fisher Scientific, UK) and analysed on a plate reader at 562nm (μQuant Universal Microplate Spectrophotometer, North Star Scientific, UK). Equal quantities of protein made up to the same volume of the appropriate lysis

buffer were denatured in 3X Laemmli Buffer (70mM Tris pH 6.8, 5% (v/v) β-mercaptoethanol, 40% (v/v) glycerol, 3% (w/v) SDS, 0.05% (w/v) Bromophenol Blue) at 95^{o}C for 5 min. Samples were separated by SDS polyacrylamide gel electrophoresis (SDS-PAGE) on 7.5 to 10% polyacrylamide gels. Proteins were transferred to nitrocellulose membrane (Hybond C Extra, Amersham Biosciences, UK) in a semi dry transfer buffer (48mM Tris, 39mM glycine, 20% methanol, 1.3mM SDS, final pH9.2) using a semi-dry transfer apparatus at a constant current of either 35mA per 10x8cm gel over 3 hours or 150mA per gel over 1 hour. Membranes were blocked for 1 hour at room temperature with 5% non-fat dairy milk or 5% BSA in TBST (Tris-buffered saline (TBS) with 0.05% Tween 20, Sigma) for one hour at room temperature on a rocker prior to overnight incubation at 4^{o}C on a rocker using primary antibodies as described in Table 2. Membranes were then washed 3 times for 5 minutes in PBS with 0.05% Tween 20 (PBST) before incubation in Horseradish peroxidase (HRP) conjugated anti-rabbit or anti-mouse secondary antibody (Dako, Ely UK) for 1 hour at room temperature. After three further 5 minute washes in PBST, antibodies were detected by enhanced chemiluminescence (ECL+, Amersham Biosciences, UK). Luminescence was detected using RX NIF Xray film (Fuji film) for varied exposure times aiming to minimise errors from signal saturation. Band intensity was quantified on scanned images using Image J. Measured protein levels were normalised to the loading control (Ku80 or β tubulin).

Primary Antibody Target	Manufacturer (Catalogue number)	Type (Clone if monoclonal)	Diluent	Dilution	Secondary antibody	Type	Dilution
IGF-1R	CST #3027	PR	5%BSA In TBST	1:1000	Dako P0448	PG AR	1:10000
pIGF-1R (Tyr1135/ 1136)	CST #3024	MR (IGH7)	5%BSA In TBST	1:250	Dako P0448	PG AR	1:1000
AKT	CST#9272	PR	5%BSA In TBST	1:1000	Dako P0448	PG AR	1:10000
pAKT (Ser473)	CST#4051	MM (587F11)	5%NFM in TBST	1:250	Dako P0447	PG AM	1:1000
ERK	CST #4695	MR (137F5)	5%BSA In TBST	1:1000	Dako P0448	PG AR	1:10000
pERK1/2 (Thr202/ Tyr202)	CST#4377	MR (197G2)	5%BSA In TBST	1:1000	Dako P0448	PG AR	1:10000
β-tubulin	Sigma T4026	MM (TUB 2.1)	5%BSA In TBST	1:10000	Dako P0447	PG AM	1:10000
Ku80	Neomarkers	MM (Ku-Ab-2(111))	5%BSA In TBST	1:500	Dako P0447	PG AM	1:10000

Table 2 Primary antibodies used in this project.
Secondary antibodies were all diluted in 5% non-fat milk (NFM) in TBST. Abbreviations: CST= Cell signalling Technologies. PR= polyclonal rabbit, MR= monoclonal rabbit, MM= monoclonal mouse, PG= polyclonal goat, AH= anti-human, AR= anti-rabbit, AM= anti-mouse immunoglobulin. BSA= bovine serum albumin. TBST= Tris buffered saline with 0.5% Tween. pIGF-1R= phosphorylated IGF-1R. pAKT= phosphorylated AKT. ERK= extracellular-signal-regulated kinase. pERK= phosphorylated ERK. Ser=Serine. Thr=Threonine. Tyr=Tyrosine.

2.3 Cell based assays

2.3.1 Clonogenic survival assays

Clonogenic assays were used to determine cell survival and ability to replicate following treatment. Cells were disaggregated from cultures at 60-80% confluence as described earlier and viable cells counted using a haemocytometer and trypan blue dye. To assess the possibility of testing the effect of treatments on anchorage independent cell survival, soft agar clonogenic assays were investigated. Cells were seeded at concentrations of 5000, 10000 and 20000 cells per well of a 6 well plate in complete medium plus 0.2% to 0.4% agar (Sigma A9414, melting temperature 65^{o}C, gelling temperature 30^{o}C) with a base layer of complete medium plus 1% agar. Plates were incubated for 8 to 14 days depending on cell line.

For adherent clonogenic assays, 1000 to 2000 cells depending on the cell line were seeded in triplicate 10cm dishes. MCF-7, IGR-OV1 and T47D were seeded at 2000 cells per dish, PC3 at 1200 cells per dish and Malme-3M at 1000 cells per dish. Cells were seeded 4-6 hours prior to treatment with irradiation or AZ12253801 as described earlier. Dishes were incubated for 8-10 days depending on cell line, in 5% CO_2 at 37^{o}C in a humidified incubator as per routine cell culture, and counted once colonies reached approximately 50 cells. Dishes were rinsed with PBS and fixed and stained for 30 minutes with 0.1% Coomassie, 7% acetic acid and 50% methanol at room temperature before rinsing with water, deionised water and air drying. Colonies were counted using an automated colony counter (Colcount, Oxford Optronix, UK). Results were expressed as a percentage of survival in solvent treated controls.

2.3.2 Cell proliferation assays

Resazurin (Sigma Aldrich R7107, Gillingham, UK) powder was reconstituted in RPMI medium to produce a 1mg/ml stock and stored at -20^{o}C. Cells were seeded into 3-8 replicate wells of 96 well plates at a density sufficient to achieve 90-95% confluence at 5 days for adherent cells, or for suspension cells, a similar coverage of settled cells on the plate base. For M14, MCF7, PC3 and SKMel 28 cells, this was 2000 cells per well; for IGR-OV1, T47D, K562 and CCRF-CEM cells, this was 2200, 2500, 3000 and 6000 cells per well respectively. Adherent cells were allowed to adhere for 4 hours before treatment, whilst suspension cells were treated upon completion of seeding. Cells were seeded in 200µl complete medium for assays involving treatment with irradiation alone, or in 100µl if also treating with IGF-1R inhibitors. IGF-1R inhibitors were administered 4 hours post cell seeding and 4 hours prior to irradiation. In order to minimise evaporation from the wells over the 5 day period of the assay, 150µl PBS was instilled into each of the spaces between wells, and the plates were placed in plastic containers with loosely fitting lids and water within the container.

Assays were incubated in 5% CO_2 at 37^{o}C in a humidified incubator as per routine cell culture and read at 5 days. For adherent cells, medium was removed and replaced with complete medium containing a 1:100 dilution of the 1mg/ml resazurin stock. For suspension cells, 20µl of medium was removed and replaced with a 1:10 dilution of resazurin. Cells were incubated for between 1 and 6 hours, dependent on cell line, before reading fluorescence at 585nm using an excitation wavelength of 555nm and a cut off of 570nm on a Spectra Max M2 microplate reader.

For investigation of the linearity of the relationship between cell number and fluorescence, defined numbers of cells were seeded per well in 100µl of complete medium in a 96 well plate. Then, 100µl of complete medium containing resazurin was added to give a final resazurin concentration of 1/100th of the stock concentration. For suspension cells, this addition was performed immediately after seeding, whilst it was performed after 4 hours for adherent cells. Cells were then incubated as above and the fluorescence at 585nm recorded at intervals.

2.4 NCI60 Developmental Therapeutic Program Human Tumor Cell Line Screen

2.4.1 Chemosensitivity data

The NCI60 Human Tumor Cell Line Screen (http://dtp.nci.nih.gov/branches/btb/ivclsp.html) uses a panel of tumour cell lines derived from leukaemias and breast, CNS, colon, lung, melanoma, ovarian, prostate and renal cancers (see Appendix I for list of cell lines included in the NCI60 screen) to identify compounds that selectively inhibit particular cell lines. Additionally, possible mechanisms of action may be ascribed to novel compounds by comparing their effect on cell lines to those of a library of compounds with defined mechanisms of action. The GI_{50} had been assessed using a Sulphorhodamine B assay as a measure of cell viability after 2 days culture with the investigational drug. Data for the GI_{50} concentrations for 163 drugs from the September 2012 release were downloaded from the NCI60 website http://dtp.nci.nih.gov /docs/dtp_search.html. Exclusion criteria for drug GI_{50} datasets were: data missing for more than 10% of cell lines; GI_{50} lying out of the concentration

range tested for more than 15% of cell lines; datasets with less than 2 replicates; a combination of these factors. The relationship of GI_{50} to SNP rs4966013 was examined using Jonckheere Terpstra and Mann-Whitney-U tests, and the relationship of GI_{50} to *IGF-1R* mRNA, and IGF-1R protein expression was examined using Spearman correlations.

2.4.2 IGF-1R Protein Expression Data

RNA and protein expression has been measured in the NCI 60 cell line panel for thousands of molecular targets and can be accessed at http://dtp.nci.nih.gov/mtargets/mt_index.html. Publicly available IGF-1R protein expression data generated by reverse phase protein array (RPPA)[92] were downloaded from http://dtp.nci.nih.gov/mtweb/targetinfo?moltid=MT18293&moltnbr=374556. These IGF-1R protein expression data were compared to protein expression data generated in this study by western blot, to *IGF-1R* mRNA expression and to chemotherapeutic GI_{50} using Spearman's correlation, and to SNP rs4966013 using Jonckheere Terpstra and Mann-Whitney-U tests.

2.4.3 Radiosensitivity Data

Published post-irradiation survival data for the NCI60 cell line collection, generated using clonogenic assays, were obtained from Amundson et al 2008[93]. These data were then used to calculate the dose of irradiation required to inhibit cell survival by 50% (SF_{50}). The relationship of SF_{50} to SNP rs4966013 was examined using Jonckheere Terpstra and Mann-Whitney-U tests, and the relationship of SF_{50} to *IGF-1R* mRNA and IGF-1R protein expression was examined using Spearman correlations.

2.5 Genomics of Drug Sensitivity In Cancer

2.5.1 Chemosensitivity data

The Genomics of Drug Sensitivity in Cancer (GDSC)[94] uses a panel of >1000 cell lines from diverse tumour types to screen for sensitivity to cytotoxic and targeted therapeutics and correlate them with genomic and expression data to identify features predictive of drug sensitivity. The GI_{50} is assessed after 3 days culture with the investigational drug. A Resazurin assay is used a measure of cell viability for suspension cells, whilst adherent cells were fixed in 4% formaldehyde prior to staining with the fluorescent nucleic acid stain Syto60 (Invitrogen) for one hour. Data for sensitivity to IGF-1R inhibitors BMS754807 and OSI-906 were downloaded from http://www.cancerrxgene.org/translation/Drug. Statistical comparisons were performed as for chemosensitivity data from the NCI60 described above.

2.5.2 Mutation Status of Cell Lines

The Catalogue of Somatic Mutations in Cancer Project, part of the GDSC resource has examined a panel of the genes most frequently mutated within cancer. Prior to Oct 24th 2013, this comprised a panel of 64 genes capillary sequenced across 800 cell lines and has since been upgraded to include 84 genes across 1015 cell lines, sequenced by whole exome sequencing. Unless otherwise stated within the text, the mutation status for genes described refers to the mutation status published in this resource http://www.cancerrxgene.org/translation/Gene [94].

2.6 SNP mRNA data source for NCI60 cell lines

SNP genotyping of cell lines in the NCI60 was performed by Jorge Zeron Medina and Dr Elizabeth Bond in the laboratory of Dr Gareth Bond using Taqman SNP genotyping assays on a 7500 real time polymerase chain reaction (RT-PCR) system (both Applied Biosystems). Briefly, genomic DNA was amplified using a SNP genotyping assay mix containing allele-specific probes consisting of either FAM or VIC dye attached to the 5' end, and a quencher attached to the 3' end. During the amplification process, bound probes were cleaved, releasing the dye from the quencher. Products were quantified using the 7500 RT-PCR system set to read emission maxima for probes labelled with the dye FAM (λ=518nm), VIC (λ=554nm), normalising the output to that of the passive reference dye, ROX (λ=610nm).

IGF-1R mRNA expression was assayed using real time quantitative polymerase chain reaction by Jorge Zeron Medina and normalised to expression of the housekeeping gene, glyceraldehyde 3-phosphate dehydrogenase (GAPDH) assayed in the same system by Dr Lukas Filip Grochola.

2.7 Statistical Analysis

Statistical analyses were performed in PRISM 6.0 (Graphpad Software Inc.) and SPSS 20 (IBM) to plot and analyse data. Kolgorov-Smirnov and Shapiro-Wilks tests were used to examine whether *IGF-1R* mRNA, IGF-1R protein and chemotherapeutic GI_{50} data were normally distributed. Spearman's coefficients and their significance were calculated

when examining correlations between scale datasets with non-parametric distributions. The Jonckheere Terpstra Test for ordered alternatives was used to examine associations between ordinal data and non-parametric scale data, whilst the Mann-Whitney U test was used to examine associations between dichotomous data and non-parametric scale data.

3 Examining the relationship between IGF-1R protein expression, *IGF-1R* mRNA expression and SNP rs4966013

3.1 Introduction

As described earlier, a SNP (rs4966013) located in the first intron of the *IGF-1R* was found by Dr Gareth Bond's group to show significant allelic differences in growth inhibition to 56 of 126 cytotoxic drugs examined in the NCI60 cell-line panel. Cell lines of the GG genotype were more chemo-resistant, requiring significantly higher concentrations of drug to inhibit growth than cells of either the AA or AG genotypes (Dr Emmanouela Repapi unpublished observations). Importantly, cell lines with the GG genotype also exhibited a 2.5 fold increase in *IGF-1R* mRNA transcript levels compared to those with the AA genotype (p=0.005 two sided Mann-Whitney-U Test; Jorge Zeron-Medina, unpublished data). This suggests that SNP rs4966013 may influence IGF-1R transcription. Since IGF-1R levels are regulated at the levels of translation[90] and protein degradation[95,96], it is important to examine whether *IGF-1R* mRNA expression correlates with protein expression.

3.2 Examination of IGF-1R Protein Expression by Western Blot

To test whether IGF-1R protein expression correlated with mRNA expression, protein expression was examined by western blot in a panel of cell lines selected from the NCI60 (Figure 2A). Cell lines were selected for high and low *IGF-1R* mRNA expression based on previous work examining *IGF-1R* mRNA expression in the NCI60 performed by Jorge Zeron-Medina. T47D, MCF7, Malme 3M, M14 and SK Mel28 were cell lines previously shown to exhibit the highest *IGF-1R* mRNA expression, whilst K562, CCRF-CEM, PC3 and IGR-OV1 exhibited the lowest *IGF-1R* mRNA expression. Quantification of protein levels observed in the western blot using Image J confirmed that those cell lines

demonstrating higher *IGF-1R* mRNA expression generally demonstrated higher IGF-1R protein expression (Figure 2B and C). Furthermore, *IGF-1R* mRNA and IGF-1R protein expressions were found to be significantly correlated (Spearman's correlation coefficient r=-0.77 (p=0.021); Figure 2D and E). One cell line, Malme-3M appeared to have lower protein expression than was predicted from its mRNA expression. This might represent impaired translation of protein, or increased degradation.

Figure 2 (overleaf) IGF-1R protein expression in cell lines expressing high and low *IGF-1R* mRNA. A. Independent replicates of western blots examining expression of IGF-1R protein in cell lines from the NCI60 tumour panel. The DNA repair protein Ku80 was used as a loading control. T47D, MCF7, MALME-3M, M14 and SKMel28 represent cell lines found to show the highest *IGF-1R* mRNA expression. K562, CCRF-CEM, PC3 and IGR-OV1 represent those with the lowest *IGF-1R* mRNA expression. **B**. The images in A were quantified using Image J, before normalising IGF-1R to the abundant DNA repair protein Ku80, which was used as a loading control. Bars represent mean and standard error of normalised IGF-1R protein expression. **C**. In order to examine the relative differences between cell lines and to minimise the effect of inter experiment variations in the band intensity detected by x-ray film, the IGF-1R/Ku80 ratios were then expressed as a percentage of the ratio observed in T47D. **D and E**. The normalised IGF-1R protein expression as presented in B and C was compared to *IGF-1R* mRNA expression (D and E respectively; real-time quantitative polymerase chain reaction (RT-PCR) data from Jorge Zeron-Medina). Points represent mean and standard error of IGF-1R protein expression normalised to Ku80. *IGF-1R* mRNA is represented as cycle threshold normalised to glyceraldehyde 3-phosphate dehydrogenase (*GAPDH*; expression data Dr Lucas Filip Grochola) , thus lower values equate to higher mRNA expression.

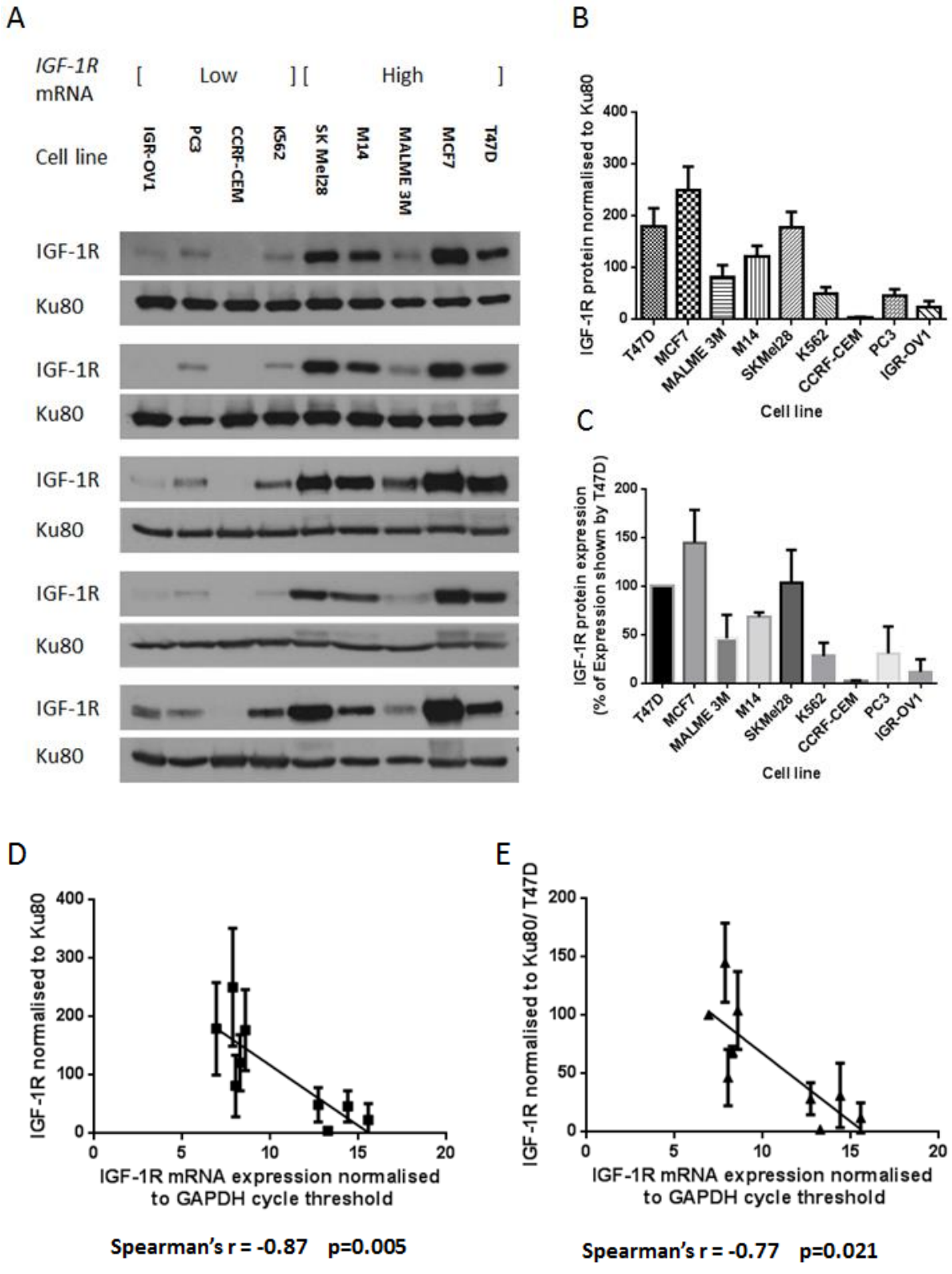


Figure 2 IGF-1R protein expression in cell lines expressing high and low *IGF-1R* mRNA.

3.3 Comparison of western blot derived protein expression data and *IGF-1R* mRNA with published IGF-1R protein expression data

In order to assess whether this correlation holds true for the wider NCI60, published IGF-1R protein expression data generated by RPPA[93] was downloaded from the NCI60 website (http://dtp.nci.nih.gov/mtweb/targetinfo?moltid=MT18293&moltnbr=374556 access date 01/03/2013). Within the cell lines examined here, protein expression data generated by quantification of western blot images showed a strong and highly significant correlation with published data generated by RPPA studies (Spearman's r=0.94, p=0.0004, Figure 3). Comparison of IGF-1R protein expression with the *IGF-1R* mRNA expression data (Jorge Zeron-Medina) across the entire NCI60 showed a strong and highly significant correlation of similar magnitude to that observed amongst the 9 cell-line subset examined by western blot (Spearman's r=-0.71, p<0.00001), further supporting the finding that IGF-1R protein expression followed *IGF-1R* mRNA expression.

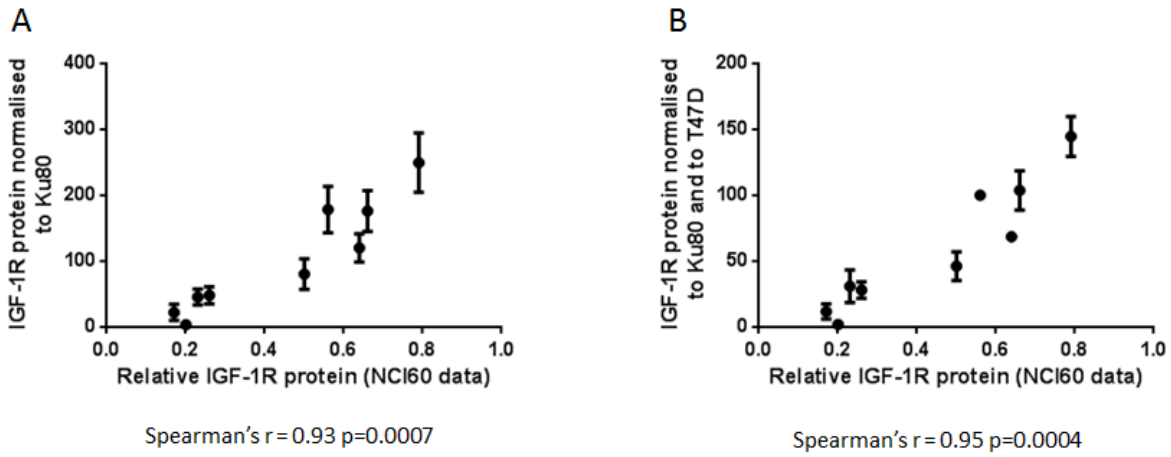


Figure 3 Comparison of IGF-1R protein expression assessed by western blot with publicly available data for the NCI60 cell line panel.
Points represent mean and standard error of IGF-1R protein expression normalised to Ku80 from 5 experiments, plotted against published protein expression data generated by reverse phase protein expression array (Park et al 2010[57], A). B differs from A in that having normalised the IGF-1R expression to that of Ku80 within cell lines, the normalised expression was then expressed as a percentage of that observed for T47D.

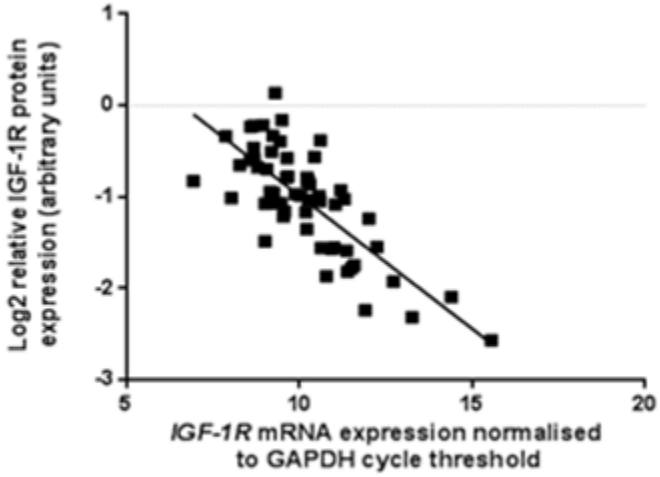


Figure 4 Comparison of IGF-1R protein and mRNA expression in NCI60 tumor cell lines.
Publicly available relative IGF-1R protein expression data generated by reverse phase protein expression array profiling (Park et al 2010[57]) was compared with *IGF-1R* mRNA expression data generated by RT-PCR (Jorge Zeron-Medina). *IGF-1R* mRNA expression data are expressed as cycle threshold normalised to *GAPDH*, hence lower values equate to higher mRNA expression. Whilst neither IGF-1R protein nor mRNA sample populations were found to differ significantly from normal using the Kolgorov-Smirnoff test, the distribution of mRNA expression data was found to differ significantly from normal using the Shapiro-Wilks test, so correlations were assessed using the non-parametric Spearman's correlation. IGF-1R protein and mRNA expression were found to correlate within the panel of NCI60 cell lines.

3.4 Comparison of SNP rs4966013 genotype with IGF-1R protein and *IGF-1R* mRNA expression

The original intent to ascertain whether *IGF-1R* mRNA expression correlated to IGF-1R protein aimed indirectly to address the question of whether the SNP rs4966013 genotype might be associated with IGF-1R protein expression, given that an association of SNP rs4966013 with *IGF-1R* mRNA expression had been demonstrated. Following identification of published IGF-1R protein expression data within the NCI60 cell line panel, this question was addressed directly.

Recent integrative genomic analyses and spectral karyotyping data have demonstrated the derivation of cell lines MDA-MB-N and MDA-MB-435 from M14, SNB 19 from U251 and NCI-ADR-RES from OVCAR-8[97]. Given this, the expression of *IGF-1R* mRNA with respect to SNP rs4966013 genotype was reanalysed in the same manner as originally performed by Dr Emmanouela Repapi, after excluding the derived cell lines MDA-MB-435, SNB-19 and NCI-ADR-RES in addition to the prior exclusion of MDA-MB-N.

Comparison of *IGF-1R* mRNA with the SNP rs4966013 demonstrated increased mRNA expression in the GG genotype compared to that of the AA or AG genotypes, with median cycle thresholds respectively of 10.23, 10.45 and 10.33 for AA, AG and combined AA+AG genotypes compared to 9.03 for the GG genotype (Figure 5). Comparison of the mRNA cycle thresholds for all three genotypes using the Jonckheere Terpstra test, when examining for an additive effect of SNP genotype, found no significant ordered differences between the three groups (Figure 5A). However, when expression of either the AA genotype (Figure 5C) or the combined AA and AG genotypes (when looking for a

dominant effect; Figure 5E) was compared to the GG genotype using the Mann-Whitney-U test, the differences were found to be significant.

Comparison of IGF-1R protein with SNP rs4966013 demonstrated increased protein expression in the GG genotype compared to that of the AA or AG genotypes, with median relative protein expressions of 0.48, 0.52 and 0.49 for AA, AG and combined AA+AG genotypes respectively, compared to 0.72 for the GG genotype (Figure 5). Comparison of the relative protein for all three genotypes using the Jonckheere Terpstra when examining for an additive effect of SNP genotype found no significant ordered differences between the three groups (Figure 5B). The differences were significant when comparing either the homozygotes (Figure 5D) or the combined AA and AG genotypes with the GG (Figure 5F), using the Mann-Whitney-U test.

The similarity of mRNA and protein expression for the AA and AG genotypes and significant difference of these from the GG genotype would be consistent with the A allele of SNP rs4966013 being dominant. However, this would need confirmation in a larger sample such as the Cancer Cell Line Encyclopaedia[98] or GDSC[94] cell line collections.

Figure 5 (Overleaf) Comparison of IGF-1R mRNA and protein expression with SNP rs4966013 genotype in cell lines from the NCI60. A and B. Comparison of *IGF-1R* mRNA and IGF-1R protein expression, respectively, between SNP rs4966013 genotypes AA, AG and GG representing a non-dominant model. **C and D.** Comparison of *IGF-1R* mRNA and IGF-1R protein expression respectively, between SNP rs4966013 homozygotes. **E and F.** Comparison of *IGF-1R* mRNA and IGF-1R protein expression respectively, between SNP rs4966013 genotypes AA and AG combined, and the GG genotype. SNP genotyping data generated by Taqman assays (Jorge Zeron-Medina and Dr Elisabeth Bond). *IGF-1R* mRNA expression data generated by RT-PCR (Jorge Zeron-Medina)*, IGF-1R* levels are expressed as cycle thresholds normalised to GAPDH, lower values equate to higher mRNA expression. Publicly available relative IGF-1R protein expression data generated by reverse phase protein expression array profiling (Park et al 2010[57]). Boxplots: Horizontal bars represent the median, boxes the interquartile range and whiskers the range. Circles and asterisks represent statistical outliers.

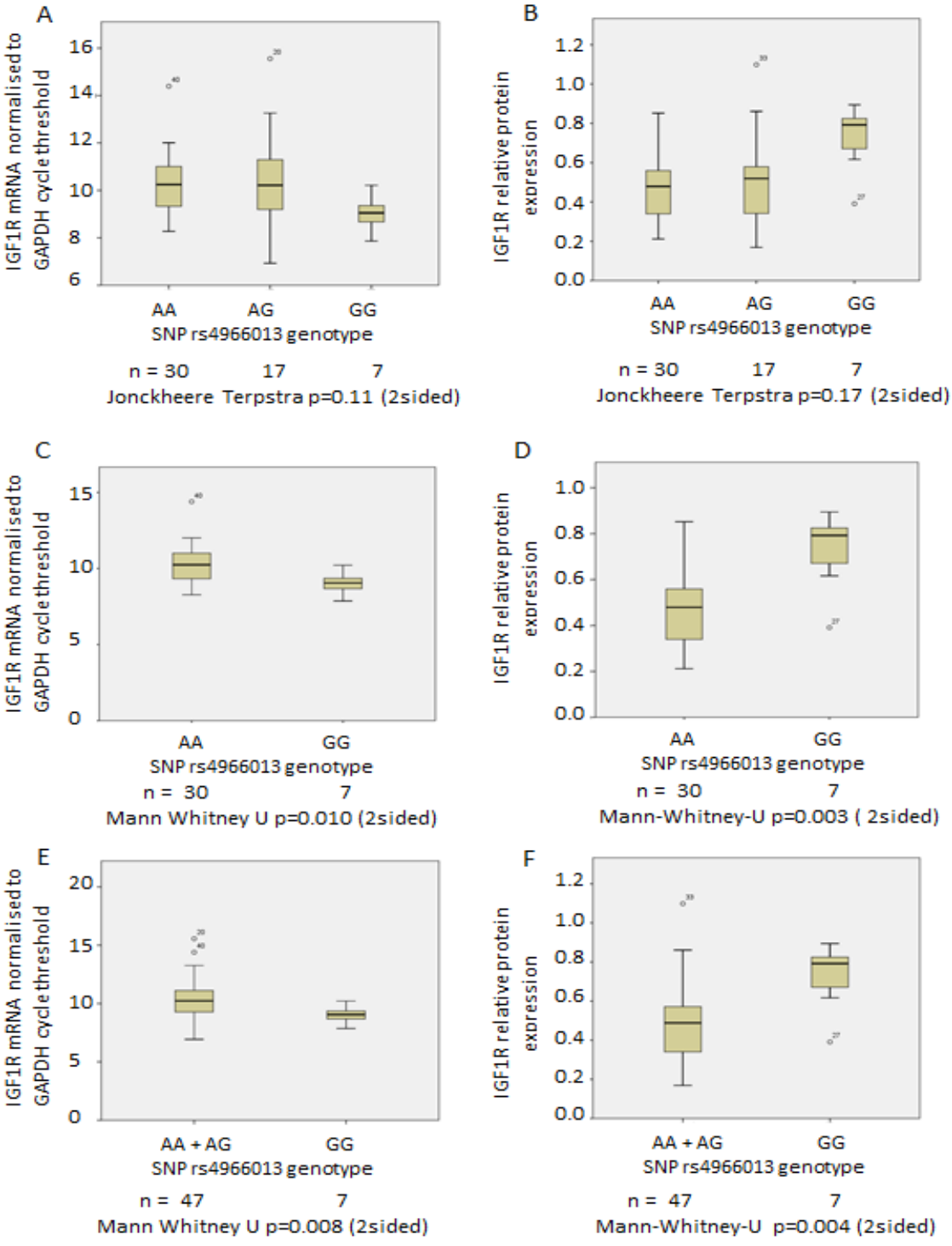


Figure 5 Comparison of IGF-1R mRNA and protein expression with SNP rs4966013 genotype in cell lines from the NCI60.

3.5 Comparison of phosphorylated IGF-1R with total IGF-1R under steady state conditions and in relation to downstream signalling components

IGF-1R expression does not necessarily have implications for the activity of the IGF signalling axis. In order to examine the relation of total IGF-1R protein to phosphorylated IGF-1R (pIGF-1R) and potential implications for downstream signalling pathways, western blots were used to examine the expression and phosphorylation of IGF-1R, AKT and ERK under steady state conditions (cells grown in complete medium including 10% FCS). Relatively high levels of pIGF-1R were observed in SkMel28 and to a lesser extent MCF7, with intermediate levels in M14, K562 and PC3 and very little in T47D, Malme-3M, CCRF-CEM and IGR-OV1 (Figure 6, and Figure 7A, 1 and 2 pages overleaf respectively). Comparatively high levels of pAKT were observed in T47D, SKMel28, CCRF-CEM, PC3 and

IGROV1 and pERK in the melanoma cell lines MALME-3M, M14 and SKMel28 (

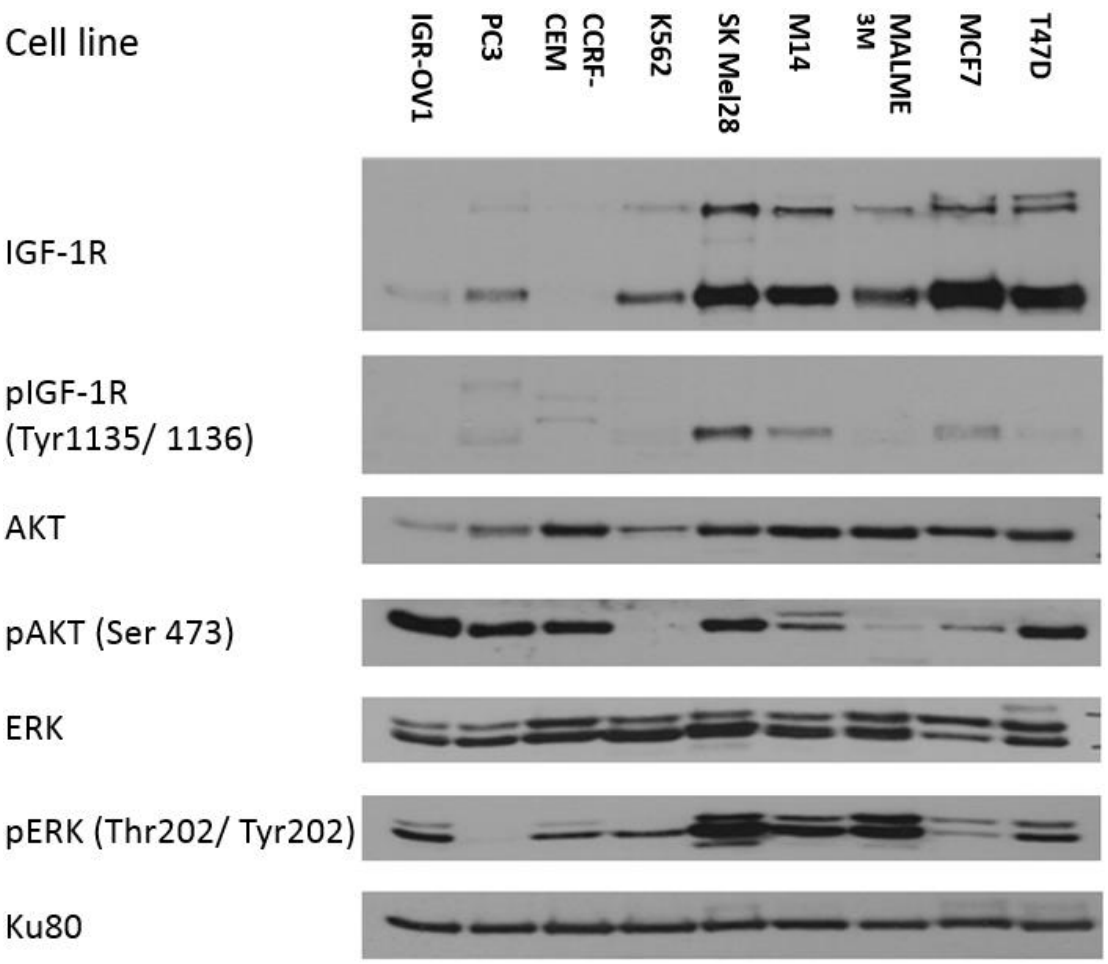


Figure 6 and Figure 7A). Comparison of pIGF-1R and total IGF-1R quantified by Image J demonstrated pIGF-1R to be significantly correlated with total IGF-1R (Spearman correlation

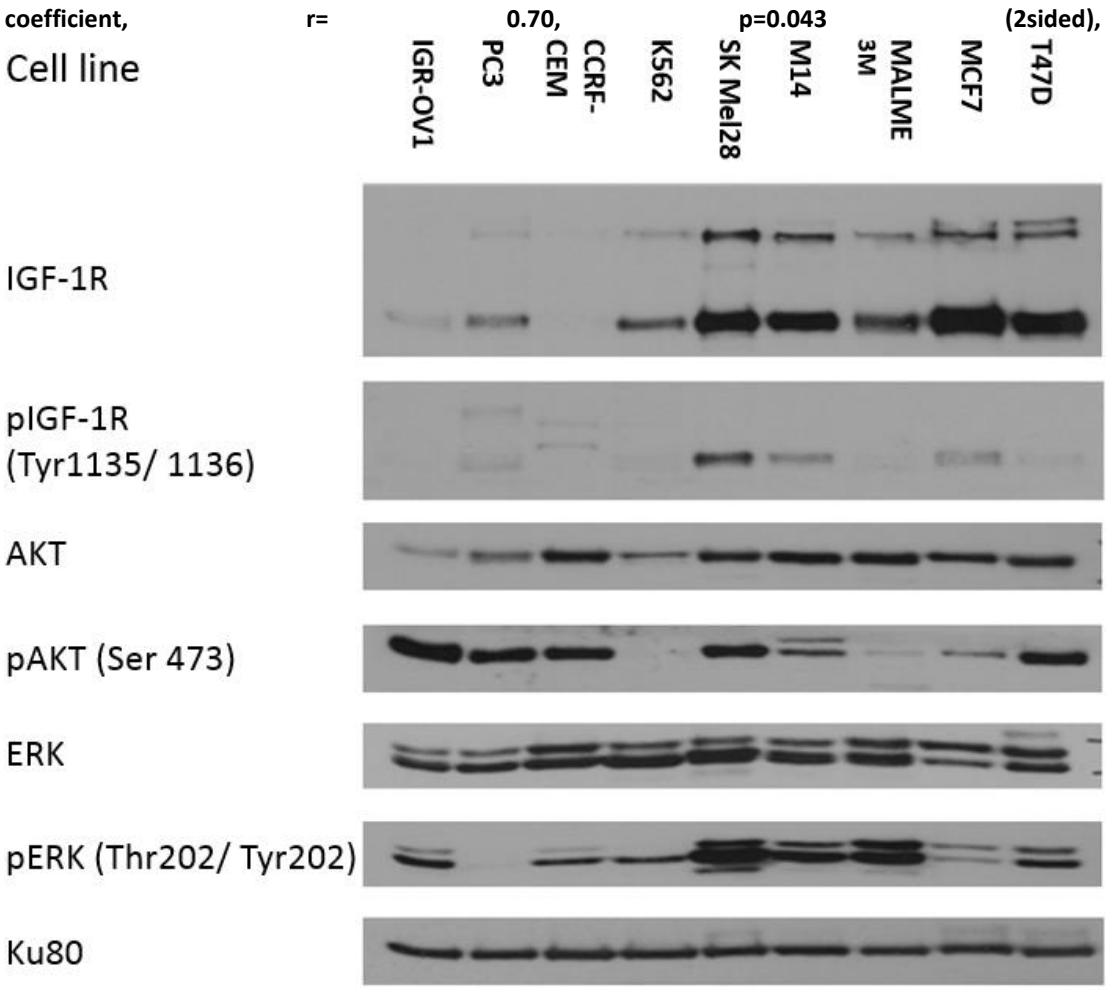


Figure 6B). No significant correlation was seen between levels of pIGF-1R and those of pAKT or pERK (Figure 7B).

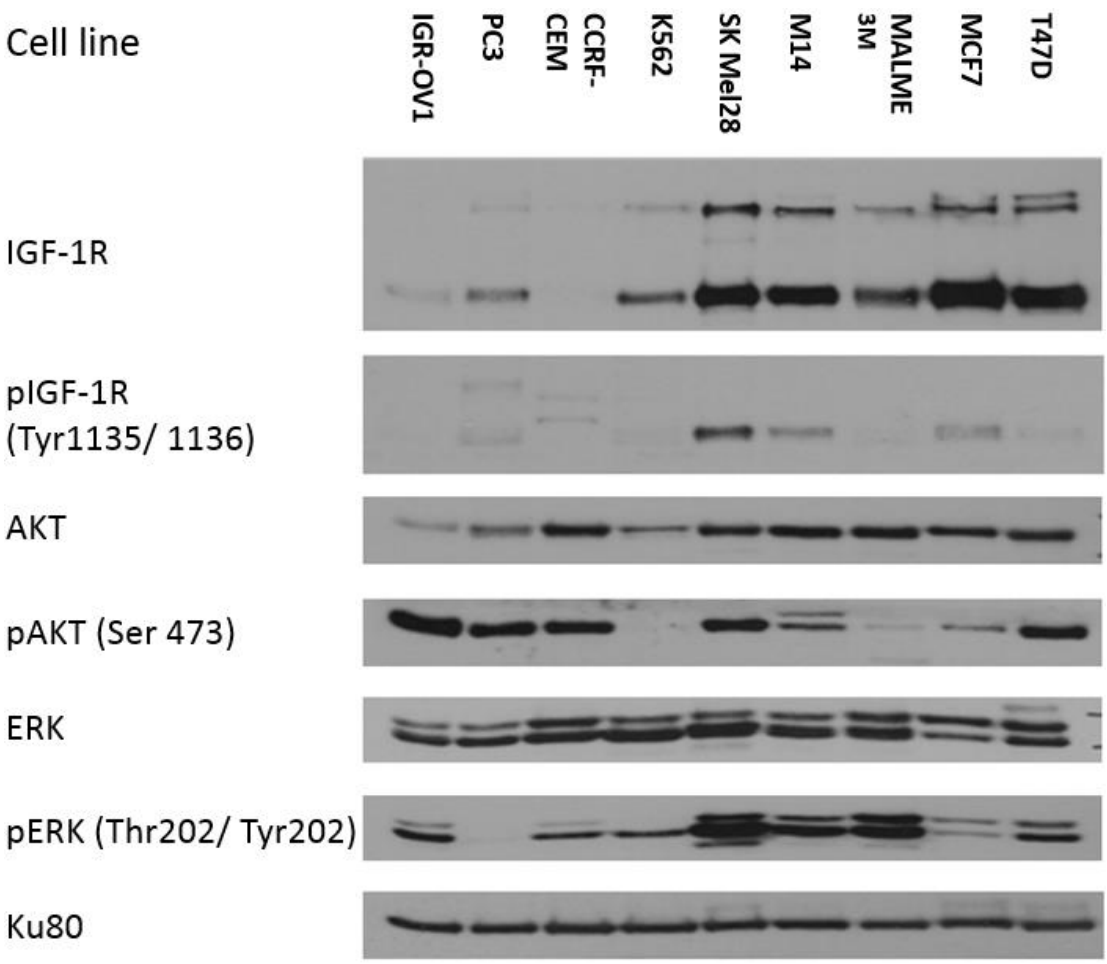


Figure 6 Representative western blot for expression and phosphorylation of IGF-1R, AKT and ERK in 9 cell lines cultured under steady state conditions.

Cells were cultured in media containing 10% FCS. Cells were harvested 2 days after seeding whilst in logarithmic growth phase. Media were changed 2 hours prior to harvesting. Upper band in IGF-1R blot represents the 210kDa proreceptor. Both bands observed on the pIGF-1R blot for the CCRF-CEM cell line (95kDa and 120kDa), and the upper band for the PC3 cell line (130kDa) do not correspond to the expected 80kDa molecular weight of the IGF-1R and may represent non-specific bands. Double band observed for ERK represents ERK 1 and 2. The double band observed in on the blot for pAKT in the M14 cell line may be non-specific, or may represent differing states of phosphorylation as has been observed by Kim et al.

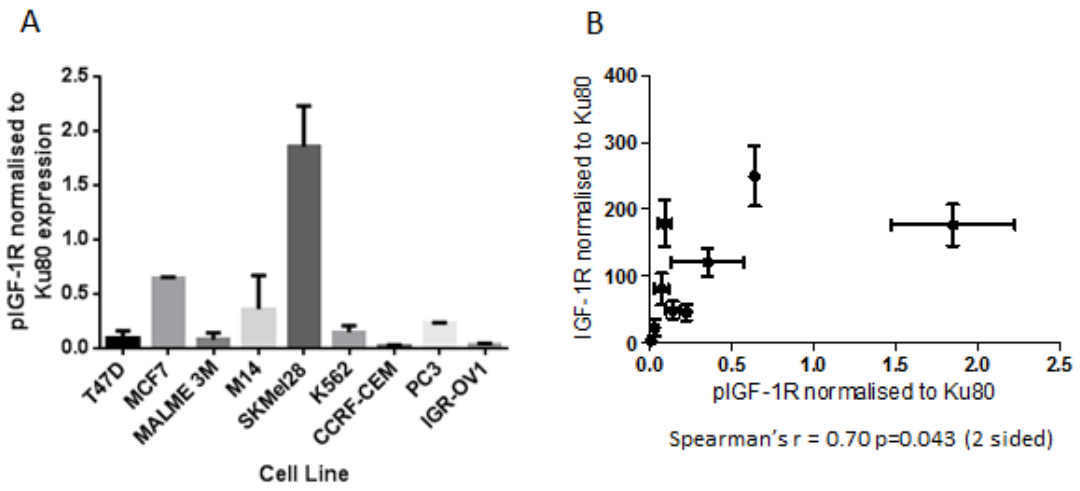


Figure 7 Comparison of phosphorylated IGF-1R with total IGF-1R in cell lines taken from the NCI60. **A.** pIGF-1R protein levels. T47D, MCF7, MALME-3M, M14 and SKMel28 represent cell lines found to show the highest *IGF-1R* mRNA expression. K562, CCRF-CEM, PC3 and IGR-OV1 represent those with the lowest *IGF-1R* mRNA expression. **B.** Total IGF-1R (IGF-1R) compared to pIGF-1R. **Both**: Protein expression examined by western blot and assessed using Image J before normalising the expression to that of the loading control, Ku80. Bars represent mean and standard error of pIGF-1R protein normalised to Ku80 from 2 experiments, expressed in arbitrary units.

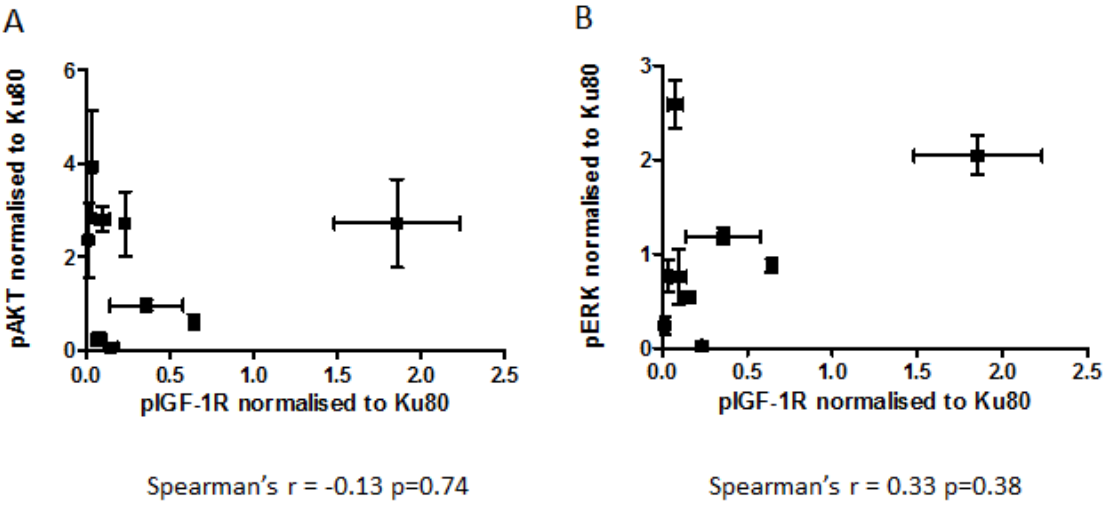


Figure 8 Comparison of pIGF-1R levels with pAKT and pERK levels in cell lines taken from the NCI60. **A.** pAKT compared to pIGF-1R. **B.** pERK compared to pIGF-1R. **Both**: Protein expression examined by western blot and assessed using Image J before normalising the expression to that of the loading control, Ku80. Bars represent mean and standard error of phosphorylated protein normalised to Ku80 from 2 experiments, expressed in arbitrary units.

The relatively high levels of pAKT observed here would be consistent with the loss of functional phosphatase and tensin homologue (PTEN) found in CCRF-CEM, PC3 and IGR-OV1, and the activating kinase domain mutation in PIK3CA in T47D (Table 3, overleaf). However, elevated pAKT in SKMel 28 has been observed inconsistently in cells cultured in serum-containing media, with some authors reporting pronounced pAKT, becoming more pronounced in the absence of serum[99]. However, others report no elevations in AKT phosphorylation in this cell line, and comment that wild type PTEN function appears to be retained[100,101]. Here, the relatively high pIGF-1R may contribute to the pAKT elevation, although why this should differ from other the other experimental settings is unclear.

The low pAKT seen in MCF-7 is consistent with the observations of Vasudevan and colleagues[102], who observed that cell lines such as MCF7 that harbour helical domain mutations of PIK3CA often have much lower pAKT than those harbouring either kinase domain mutations or inactivating PTEN mutations[102]. The elevations in pERK observed in the melanoma cell lines MALME-3M, M14 and SKMel28 are consistent with their harbouring the V600E activating BRAF mutation (http://cancer.sanger.ac.uk/cosmic).

It must be noted that the assessment of phosphorylation of IGF-1R, AKT and ERK in western blots does not assess the functional activity the IGF-1R kinase directly. Other methods such as peptide substrate reporters of kinase activity in whole cell lysates[103] may detect kinase activity specifically, although whether they can be said to reflect kinase activity in the native setting is a different matter. Equally

they may detect kinase activity present in cell fractions that would not normally be activated by ligand.

Cell Line	Tissue	SNP rs4966013 genotype	Mutated Gene(s)	Coding sequence alteration	Amino Acid change	Reported functional effect	Expected effect: pAKT +pERK	Observed here	Ref.
T47D	Breast	AG	PIK3CA	Het 3140A>G	H1047R	activating	↑ pAKT	↑ pAKT	104,102
MCF7	Breast	GG	PIK3CA	Het 1633G>A	E545K	activating	↑pAKT*	no pAKT ↑	102
Malme-3M	Melanoma	unknown	BRAF	Het 1799T>A	V600E	activating	↑ pERK	↑ pERK	101
M14	Melanoma	AA	BRAF	Het 1799T>A	V600E	activating	↑ pERK	↑ pERK	
SKMel28	Melanoma	AG	BRAF	Hom 1799T>A	V600E	activating	↑ pERK	↑ pERK	101
			PTEN	499A>G	T167A	unclear	none/** ↑ pAKT	↑ pAKT	101,100, 99
K562	Leukaemia	unknown	None relevant					no ↑ pERK or pAKT	
CCRF-CEM	Leukaemia	AG	PTEN	Hom c.1_471 del 471	No protein	inactivating	↑ pAKT	↑ pAKT	105,106
PC3	Prostate	AA	PTEN	Hom c.165-1026 del 862	No protein	inactivating	↑ pAKT	↑ pAKT	106
IGR-OV1	Ovarian	AA	PTEN	Het c.955_958delACTT	T319fsX1	inactivating	↑ pAKT	↑ pAKT	106,107

Table 3 Genetic mutations affecting major IGF-1R signalling pathways in the cell lines investigated.
Based on information contained in the Catalogue of Somatic Mutations in Cancer (Access date 20th August 2013) with other sources as referenced. *The PIK3CA mutation in MCF-7 affects the helical domain and has been observed to produce little pAKT in comparison to the mutations in the kinase domain such as T47D[102]. **Elevated pAKT has been observed inconsistently in SKMel28 when cultured in serum containing medium. Some authors report pronounced pAKT, becoming more pronounced in the absence of serum, whilst others report no elevations in AKT phosphorylation, particularly in relation to PTEN function[101,100,99]. Het = heterozygous. Hom = homozygous.

3.6 Summary and Discussion

IGF-1R mRNA expression shows a significant correlation with IGF-1R protein expression within the subset of cell lines examined by western blot, and a highly significant correlation when examined within the wider NCI60 panel using published data generated elsewhere by RPPA[92]. IGF-1R protein expression examined by western blot exhibits a strong and highly significant correlation with published data generated by RPPA suggesting that findings relating to protein expression here are likely to be more widely applicable.

RPPA involves the production of dot-blot arrays of tens to hundreds of serial protein lysate dilutions per slide to allow simultaneous quantification of individual proteins from multiple samples using immunochemical detection[108]. The colorimetric or fluorescent signal intensities of serial lysate dilution dots are used to calculate a "dose-response" curve and a single protein expression value for each sample. Proteins are not separated by molecular weight; hence it is not possible to ascertain the molecular size or specificity of the detected signal. Thus the specificity of all antibodies used for this process must first be validated using conventional western blotting techniques. Therefore, with appropriate antibody selection, results should be comparable to data generated by western blotting.

SNP rs4966013 did not show a significant association with either *IGF-1R* mRNA or protein expression when examining an additive model of expression using the Jonckheere Terpstra test. However, a significant association of the GG genotype with increased mRNA and protein expression was seen using the Mann-Whitney-U test to examine a model with the A allele dominant. It is unclear as to how the A allele of SNP

rs4966013 might exert a dominant negative effect on IGF-1R mRNA and protein expression by its reduced affinity for FOXC2 binding. Levels of pIGF-1R correlated significantly with total IGF-1R, but not with pAKT or pERK.

In summary, a correlation was identified between SNP rs4966013, *IGF-1R* mRNA and IGF-1R protein, providing a basis for future testing in larger cell line panels and in tumour tissue.

4 Correlations between IGF-1R expression and chemo- and radio- resistance

4.1 Introduction

The finding that underpinned this project was the identification of an association between allelic differences in SNP rs4966013 in the first intron of the *IGF-1R* gene, both with *IGF-1R* mRNA expression and resistance to numerous chemotherapeutic drugs using the NCI60 tumour screen (Dr Emmanouela Repapi, unpublished data). This finding was in accord with reports from the Macaulay laboratory indicating that IGF-1R depletion or inhibition enhances chemo- and radio- sensitivity, at least in part via effects on the DNA damage response[81,85,84].

To test the hypothesis that IGF-1R expression correlated with chemo- and/ or radio-resistance, chemotherapeutic and radiation dose responses were examined in cell lines exhibiting high and low *IGF-1R* mRNA expression levels.

4.2 Assay Selection

These assays included A375M, CHL-1, SKUT-1 and the 9 cell lines from the NCI60 that had been used previously, including four of the five cell lines expressing the highest *IGF-1R* mRNA, and the four lowest. Under standard culture conditions these cell lines showed a range of different growth characteristics (Figure 9). Given the importance of the IGF-1R for anchorage independent cell survival[109], initial soft agar colony assays were assessed to determine suitability for growth of both suspension and adherent cell lines.

Using the standard assay protocol, epithelial cell lines PC3 and MCF7 formed colonies in 0.2% agar when overlaid on medium with 1% agar. None of the other cell lines formed consistent countable colonies under these conditions; melanoma cell lines A375M and CHL-1 migrated through the top layer of agar and grew at the interface with the lower 1% agar. This prompted assessment of a range of assay conditions. Melanoma cells

grew in colonies at higher concentrations (0.35 and 0.4%) of the top layer of agar, but PC3 and MCF7 did not. At 0.25 and 0.3% agar, colony formation by PC3 and MCF7 was inconsistent.

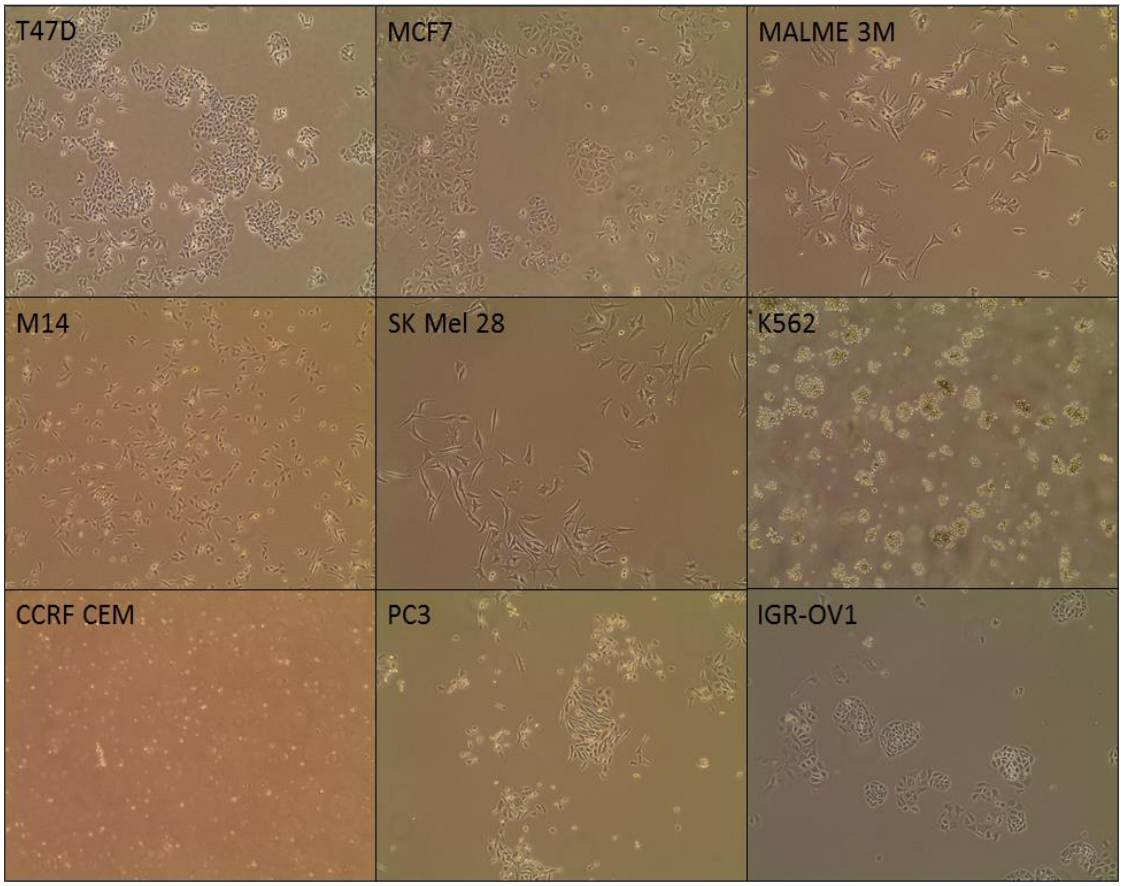


Figure 9 Growth pattern and morphology of cell lines under standard cell culture conditions.
Within the adherent cell lines, the epithelial cell lines T47D, MCF7, IGR-OV1 and to a lesser extent PC3 exhibited more clustered growth patterns, whilst the melanoma cell lines (MALME 3M, M14 and SK Mel28) tended to grow in a more diffuse pattern. Of the suspension cell lines, K562 tended to grow in dense clumps, while CCRF-CEM grew in single cells or small clusters. Magnification 100x.

Monolayer colony assays proved unsuitable for some of the melanoma cell lines given the tendency of these cells to grow and spread in loose aggregates rather than discrete colonies (see Figure 9 for cell line morphology). Ultimately, it did not prove possible to find a clonogenic assay format that was compatible with the growth patterns of all 9 cell lines, and so an alternative assay was sought. Malme-3M exhibited very slow growth, with 4-8 cell clusters being observed after 30 days culture in a clonogenic assay. Additionally, doubling times of approximately 7 days were observed in routine culture, in contrast to the reported doubling time of approximately 2 days reported in the NCI60 tumor screen. Consequently, this cell line was excluded from subsequent assays.

The resazurin assay, a cell viability assay, was investigated as a means to compare all cell lines under investigation. This assay is based on the principle that cytosolic, mitochondrial and microsomal enzymes, including oxidoreductases, dehydrogenases and cytochromes in viable, metabolically active cells reduce the non-fluorescent resazurin to the fluorescent resorufin[110]. Furthermore, it is reported that the rate of resazurin reduction is both proportional to the number of viable cells and is very sensitive, detecting as few as 40 cells[111]. Later reports suggested that this assay gives results comparable to clonogenic assays for assessment of radiosensitivity[112,113].

Initial tests demonstrated the linearity of the relationship between cell number and fluorescence at 585nm. The relationship was broadly linear when plates were read from 1 to 6 hours after addition of resazurin, until the fluorescence exceeded approximately 20 000 units (see Figure 10 for examination of linearity in 4 cell lines). Whether the loss of linearity beyond this point related to exhaustion of the resazurin within the test media, to the limits of the fluorescence reader, or to further reduction of resorufin to the colourless

and non-fluorescent hydroresorufin as observed by O'Brien and colleagues[111] was not tested.

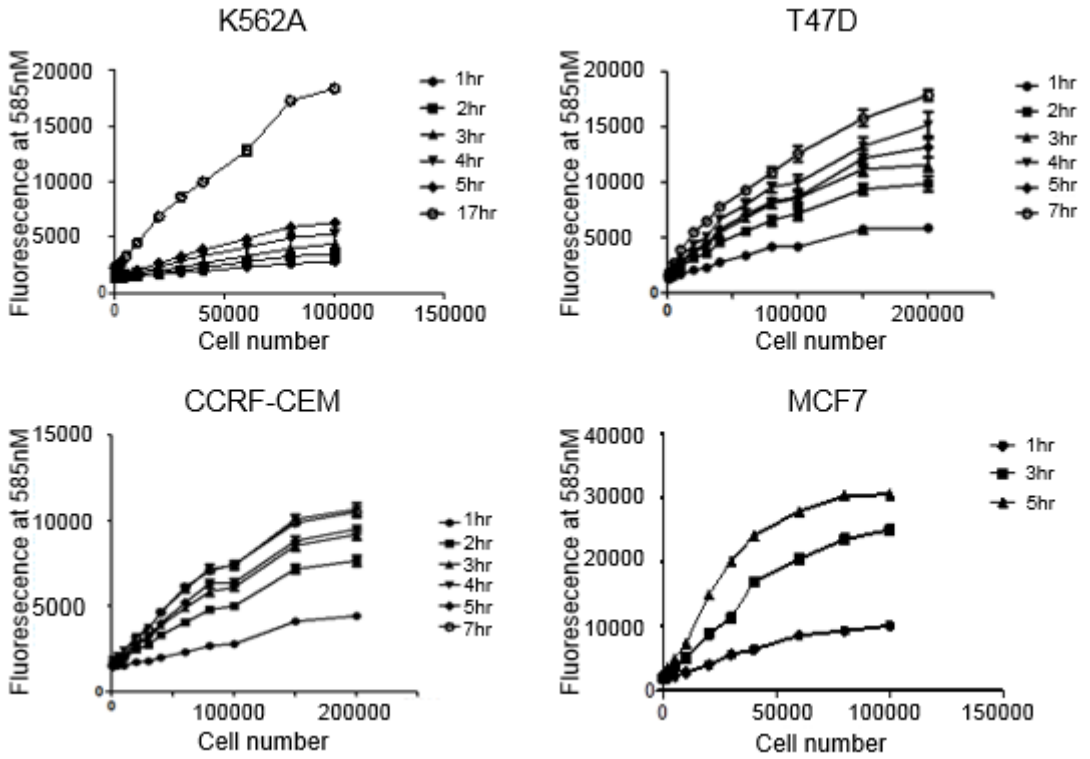


Figure 10 Linearity of fluorescence versus cell number for the resazurin assay in 4 cell lines.
Graphs show the fluorescence at 585nm following incubation of defined numbers of cells with Resazurin for variable time periods. Defined numbers of cells were seeded in 96 well plates. Resazurin was added to suspension cells (K562 and CCRF-CEM) immediately post seeding and to adherent cells (T47D and MCF-7) 4 hours post seeding prior to incubation at 37°C and reading fluorescence at 585nm at intervals. Points represent mean and standard error of a minimum of two independent experiments, each with 8 replicates per data point.

4.3 Intrinsic Chemoresistance

4.3.1 Selection of Drugs

Using information from the NCI60 Human Tumor Cell Line Screen (http://dtp.nci.nih.gov/branches/btb/ivclsp.html), Dr Emmanouela Repapi examined the association between allelic differences in SNP rs4966013 genotype and GI_{50} for a number of chemotherapeutic drugs, finding 56 of 113 to differ significantly between the combined AA + AG group and the GG group. These data were explored to identify drugs with larger differences in median GI_{50} between SNP groups that might be used to test the hypothesis that cell lines expressing high IGF-1R exhibited greater chemoresistance.

Following Dr Repapi's analysis, this examination was expanded in an attempt to identify a wider selection of drugs from the different drug groups and to include more chemotherapeutics in clinical or trial use, using the most recent (September 2012 NCI60) data release. Furthermore, the initial examination was repeated in the light of the recent findings that 4 of the 60 cell lines were in fact derived from 3 of the others (see comment in 3.3). GI_{50} datasets for 50 chemotherapeutic drugs were excluded from statistical analysis where: i) more than 15% of the GI_{50}s were recorded as being above or below the concentration range tested; ii) chemosensitivity data were not recorded for more than 10% of the cell lines; iii) fewer than 2 replicates were present; iv) If a combination of the above factors were present (summarised in Table 4 and detailed in Appendix II). Using the 113 remaining datasets, drug GI_{50}s were compared to SNP genotype, IGF-1R protein expression and *IGF-1R* mRNA expression (see Table 5 for summary of drugs with significant associations, and Appendices III, IV and V for a complete list). Non-parametric tests were used to examine these interactions as Kologorov-Smirnov and Shapiro-Wilks

tests demonstrated that a large proportion of the GI_{50} datasets were not normally distributed (data not shown).

Drug Class	Total no. of drugs considered	Exclusions				Final no. of drugs analysed
		>15% GI_{50}s outside of concentration tested	Data missing for > 10% cell lines	<2 replicates	Combination	
Alkylating agents	41	4	2	0	1	34
Antimitotic agents	23	7	1	0	2	13
Topoisomerase I inhibitors	34	4	2	0	13	15
Topoisomerase II inhibitors	20	0	0	0	0	20
RNA/DNA antimetabolites	24	0	0	0	11	12
DNA antimetabolites	21	0	0	0	2	19
Total	163	15	5	0	29	113

Table 4 Summary of the Cytotoxic drugs examined per category within the Developmental Therapeutics Program (DTP) NCI60 Tumour Cell Line Sensitivity Screen.
All datasets without 2 replicates also fulfilled one of the other exclusion criteria, so no datasets were excluded for this reason alone.

Drug Group (total number of drugs examined)	Drugs with significant association with IGF-1R SNP genotype or correlation with IGF-1R expression at the 0.05 level	IGF-1R related with significant association / correlation				
		SNP AA vs AG vs AA	SNP AA vs GG	SNP AA +AG vs GG	Protein	mRNA
Alkylating agents (33)	Uramustine		●			
	Clomesone		●	●		
	Cyclodisone		●	●		
	Carmustine				●	●
	Lomustine				●	●
	Semustine			●	●	●
	PCNU					●
	Mitozolomide					●
	Carboplatin			●		
	Cisplatin			●		
Antimitotic Agents (13)	Thiocolchicine			●		●
	Maytansin			●		
	Dolastatin 15				●	●
Topoisomerase I inhibitors (15)	Camptothecin Sodium salt			●		
	MLS000766263		●	●		
	Camptothecin dimethyl glycinate			●		
	Camptothecin diethylglycinate			●		
	Camptothecin ethylglycinate		●			
	Topotecan			●		
Topoisomerase II inhibitors (20)	Cyanomorpholinodoxorubicin	●	●	●		
	Pyrazoloacridine					●
RNA/DNA anti-metabolites (12)	Dichloroallyl lawsone					●
	Brequinar					●
	Methotrexate			●		
	Trimetrexate					●
	Piritrexim		●	●		
DNA anti-metabolites (20)						
Total 113	26	1	7	15	4	11

Table 5 Drugs for which GI_{50} was significantly related to SNP rs4966013 genotype, *IGF-1R* mRNA and/or IGF-1R protein.

The interaction of the SNP genotype with drug GI_{50}s was examined in 3 ways. Using the Jonckheere Terpstra test, which assumed a non-dominant / additive model for the effect, a significant association of SNP genotype with GI_{50} was found only for Cyanomorpholinodoxorubicin, a Topoisomerase II inhibitor. When examining a dominant model using the Mann-Whitney-U test and comparing AA+AG to GG, significant interactions of drug GI_{50} with genotype were identified for 15 drugs involving all drug groups except DNA antimetabolites (Table 5). When comparing differences between the homozygotes alone, significant associations between GI_{50} and SNP genotype were found for 7 drugs. Spearman's correlations were performed to examine the significance of any associations between drug GI_{50} and IGF-1R expression at the protein and mRNA levels. Significant associations were found for 4 and 11 drugs respectively, particularly amongst the nitrosourea group of alkylating agents (Table 5). However, the effects No significant associations between protein or mRNA expression and drug GI_{50} were found in groups other than the alkylating and antimitotic agents. Additionally, DNA antimetabolites showed no significant associations with IGF-1R SNP, mRNA or protein expression. The demonstration of significant associations between IGF-1R SNP, mRNA or protein expression scattered across multiple classes may reflect the level of significance chosen and the lack of use of a Bonferroni correction. However, given the clusters of associations involving the camptothecins and the nitrosorueas, it seems possible that for these two drug groups, the observed associations may represent real rather than chance effects.

There was approximately a 20 fold difference in median GI_{50} for topotecan between the combined AA and AG genotypes and the GG genotype for SNP rs4996013 (Figure 11 A and B). Comparison of these groups using the Mann-Whitney-U test suggested that their GI_{50}s were significantly different ($p=0.046$). In addition, paclitaxel was selected to examine

based on unpublished data from the Bond group demonstrating significantly greater resistance to paclitaxel in cell lines of the GG genotype compared to the combined AA and AG genotypes (p=0.035, Mann-Whitney-U) using data obtained from the GDSC (Dr Emmanouela Repapi, Figure 11 C and D). These drugs were chosen to test the hypothesis that cells expressing high IGF-1R exhibit greater chemoresistance; and to test whether IGF-1R expression correlates with the extent to which IGF-1R inhibition enhances chemosensitivity. A large proportion of drugs exhibited chemosensitivity differences between the SNPrs4966013 genotypes consistent (see Figure 11 and Appendix III) with a dominant effect of the A allele, similar to the pattern observed with IGF-1R protein and mRNA expression.

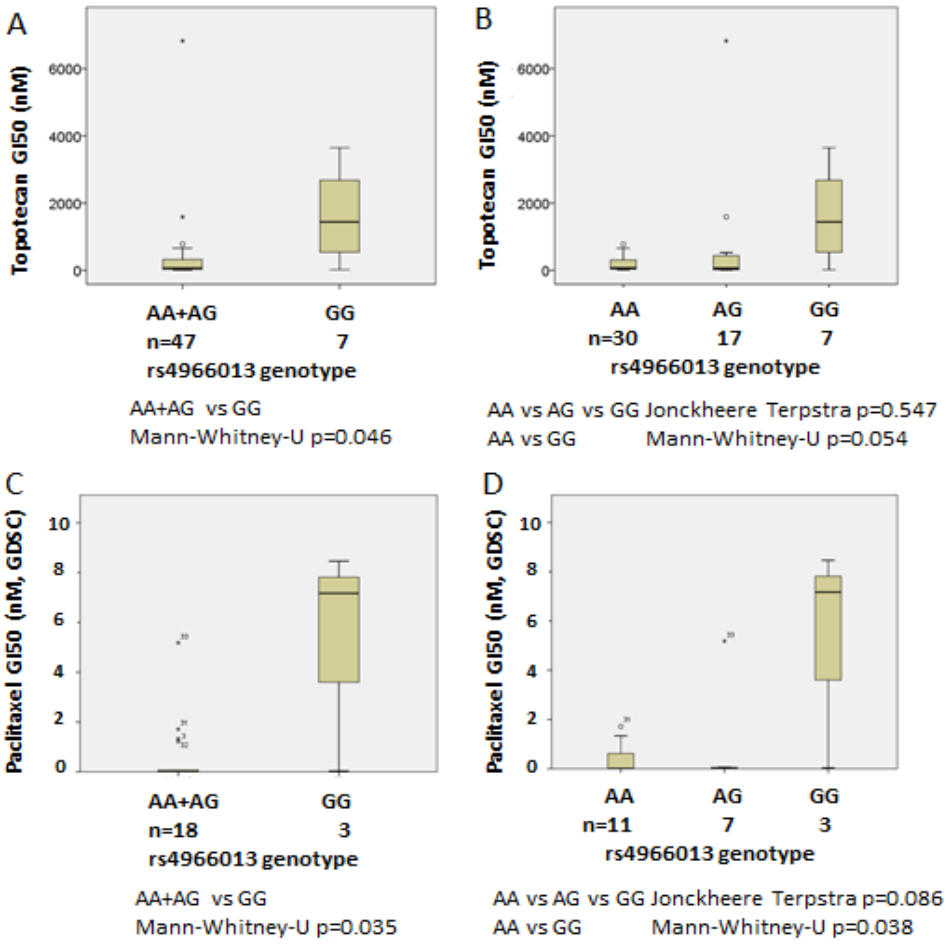


Figure 11 Comparison of Topotecan and Paclitaxel GI_{50}s between SNP rs4966013 genotypes in cell lines of the NCI60.

A and B. Comparison of topotecan GI_{50} using data from the NCI60 screen. **C and D.** Comparison of paclitaxel GI_{50} using data from the Genomics of Drug Sensitivity in Cancer. **A and C.** Combined AA and AG genotype compared with GG genotype. **B and D.** Comparison of individual genotypes demonstrating similar GI_{50}s for AA and AG groups. Boxplots: Horizontal bars represent the median, boxes the interquartile range and whiskers the range. Circles and asterisks represent statistical outliers. SNP genotyping as described earlier (Dr Jorge Zeron-Medina and Elisabeth Bond) Comparisons C and D performed by Dr Emmanouela Repapi.

4.3.2 Paclitaxel and topotecan sensitivity

Paclitaxel stabilises polymerised tubulin, inhibiting microtubule disassembly and blocking cells in mitosis, with prolonged arrest triggering apoptosis. Topotecan stabilises topoisomerase I cleavage complexes inducing the formation of DNA DSBs when the replication machinery collides with the stabilised cleavage complex, triggering the DNA damage response, cell cycle arrest and apoptosis. Resazurin assays were performed to examine the dose response to these cytotoxic drugs.

Cells were seeded in 96 well plates, allowed 4 hours to adhere if required and exposed to a range of paclitaxel or topotecan concentrations or solvent for 5 days prior to measuring cell viability using the resazurin assay. The paclitaxel GI_{50} values for all cell lines excluding PC3 lay between 0.1 and 0.8nM, whilst that for PC3 was 35nM (see Figure 12 A for dose response curves, Table 6 for GI_{50} values). No correlations were observed between paclitaxel GI_{50} and *IGF-1R* mRNA, total IGF-1R protein measured using publically available data (generated by RPPA), or total and phospho- IGF-1R levels measured in this study (Figure 2)), whether the outlier PC3 was included (Figure 12 B to E) or excluded in the analysis (data not shown). As the panel of cell lines examined was both small and incompletely genotyped (see Table 3, Ch3), no attempt was made to assess correlations of chemo/radio resistance with SNP genotype.

It was noted that the paclitaxel GI_{50} concentrations measured here were 10 to 100 fold lower than those reported in the NCI60 tumor drug screen, likely reflecting the 5 day chemotherapeutic exposure in this assay compared to the 2 day exposure in the NCI60 screen. More importantly, the GI_{50} concentrations observed here were much lower than

the 100-8000nM range reported to be attainable in clinical use[114]. Therefore, the effects of IGF-1R inhibition on response to paclitaxel sensitivity were not investigated.

Assays using topotecan revealed GI_{50} values ranging from 1 to 49nM, with all bar SKMel28 (49nM) being between 1 and 8nM (see Figure 13 A for dose response curves, Table 6 for GI_{50} values). Whilst there were trends towards higher topotecan GI_{50} values amongst cell lines expressing higher IGF-1R mRNA, protein and pIGF-1R, these were not significant (see Figure 13 B to F). As with paclitaxel, the GI_{50} concentrations for topotecan were below those observed in the NCI60 screen (Table 6). However, the difference was not as marked for topotecan, and most GI_{50}s lay within or near the 4-15nM range of reported peak plasma concentrations achieved clinically[115-117].

Cell Line	SNP rs4966013 Genotype	Paclitaxel GI_{50} (nM)		Topotecan GI_{50} (nM)	
		This study	NCI60	This study	NCI60
T47D	AG	0.4	40.7	7.9	21.4
MCF7	GG	0.4	2.8	4.1	16.8
M14	AA	0.6	3.5	8	31.9
SKMel28	AG	0.1	65.2	49.2	1588
K562	Unknown	0.2	4.3	1.1	181
CCRF-CEM	AG	0.8	3	1.1	11.4
PC3	AA	35	4	4.6	278
IGR-OV1	AA	0.5	7.1	4.6	438

Table 6 GI_{50} values for Paclitaxel and Topotecan.
Those measured in this study are compared listed along with those reported by the NCI60. SNP rs4966013 genotype (Jorge Zeron-Medina and Elisabeth Bond) is included for comparison

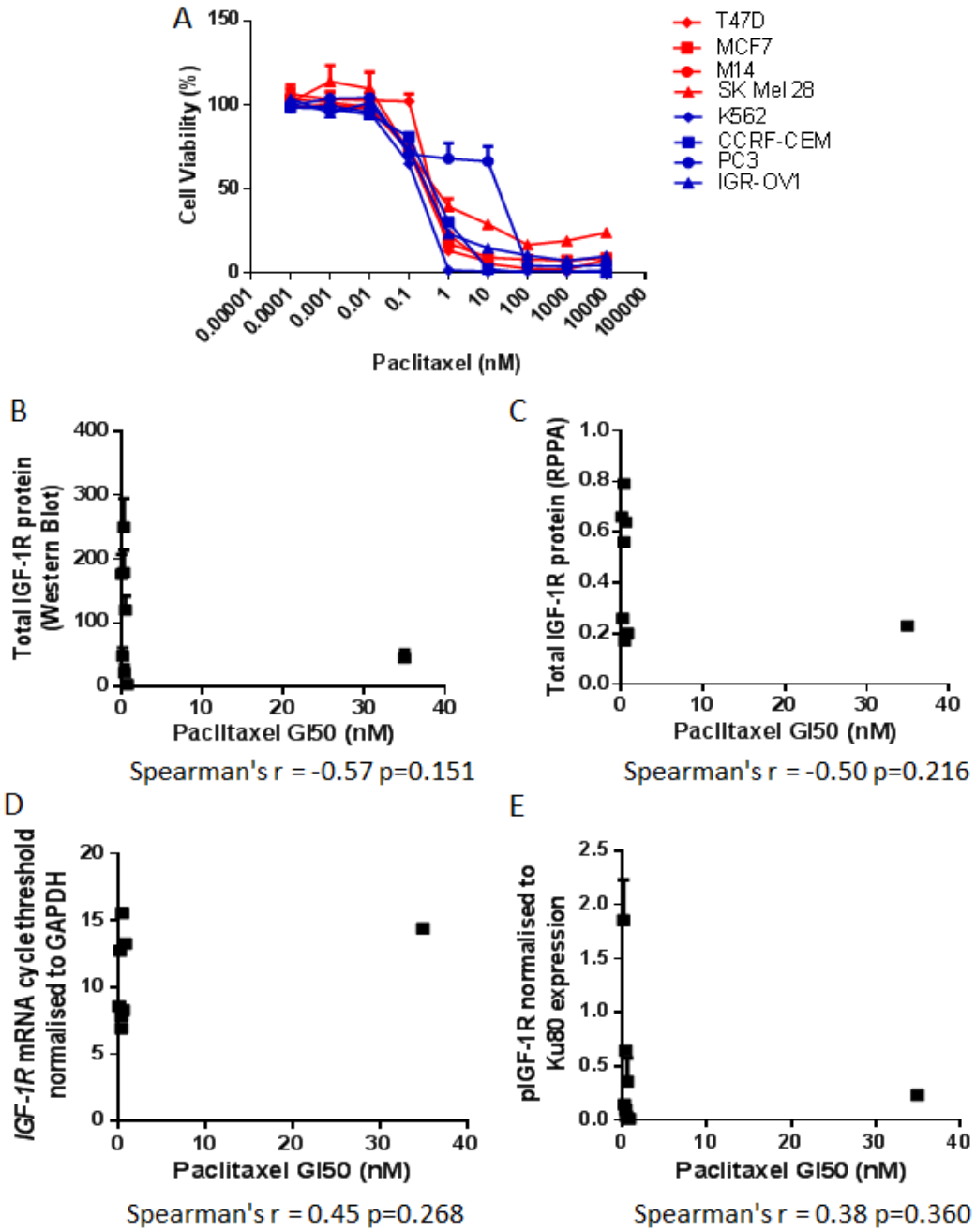


Figure 12 Examination of the relationship between intrinsic paclitaxel sensitivity and IGF-1R expression. **A.** Cell viability following paclitaxel treatment. Viability is represented as a percentage of untreated controls. Cells were seeded, allowed to adhere if appropriate, and then treated with solvent or paclitaxel. 5 days later, cell viability was measured by fluorescence using the resazaurin assay. Results represent mean ± SEM for three independent experiments. Cell line plots: Red plots = high and blue = low *IGF-1R* mRNA expression. **B.** Paclitaxel GI_{50} (nM) values from A compared to total IGF-1R protein expression as measured by western blot. IGF-1R protein expression was quantified using Image J and normalised according to expression of the loading control, Ku80. Results represent mean ± SEM for a minimum of two independent experiments. **C.** Paclitaxel GI_{50} from A compared to published total IGF-1R protein expression as measured by reverse phase protein array (RPPA). **D.** Paclitaxel GI_{50} (nM) from A is compared to *IGF-1R* mRNA expression expressed as cycle threshold normalised to *GAPDH (*Jorge Zeron-Medina). **E.** Paclitaxel GI_{50} (nM) from A is compared to levels of phosphorylated IGF-1R (pIGF-1R) as measured by western blot under steady state conditions (See Ch. 3.5). Quantification and normalisation are as for B. Results represent mean ± standard error of mean (SEM) for a minimum of two independent experiments.

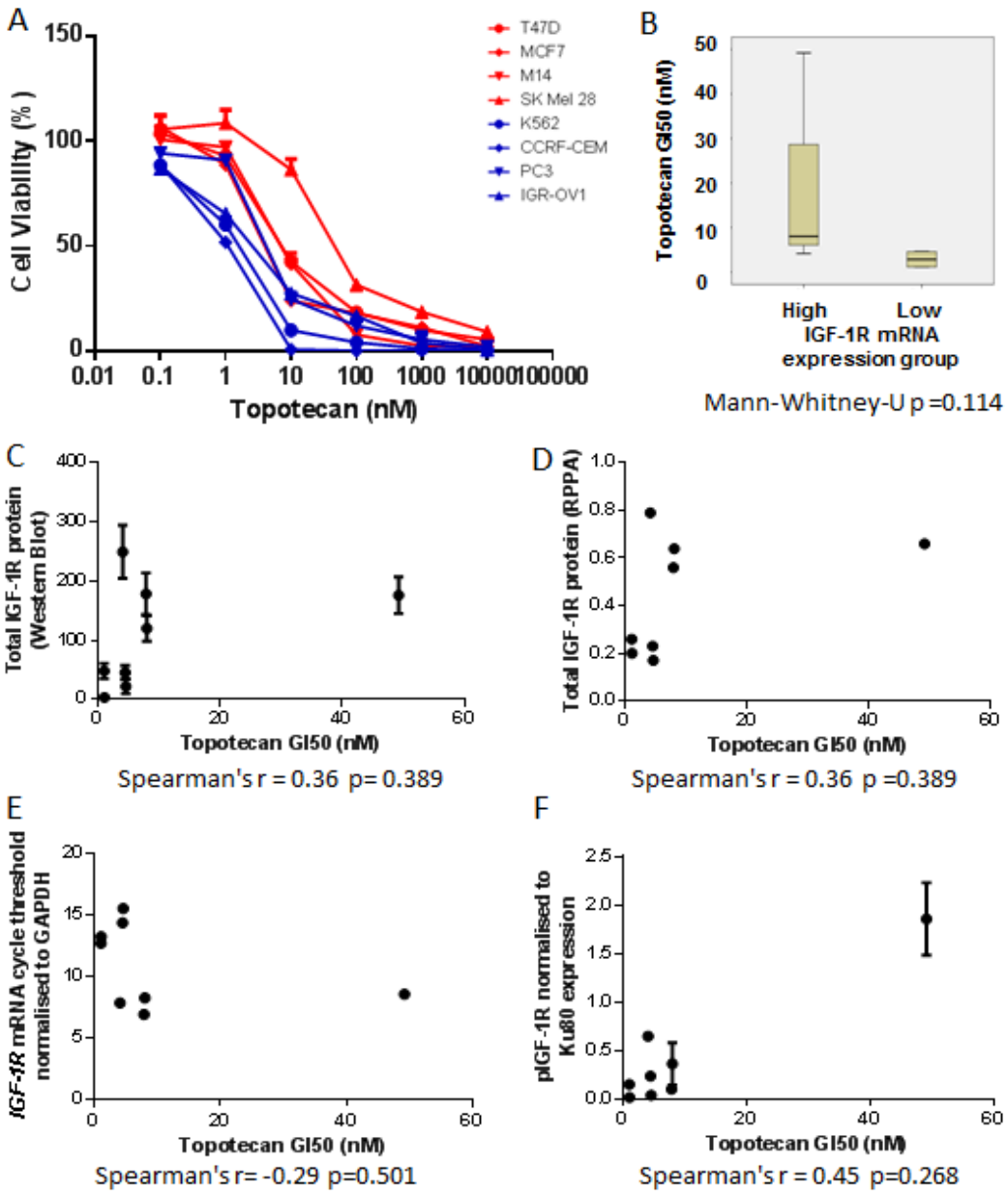


Figure 13 Examination of the relationship between intrinsic topotecan sensitivity and IGF-1R expression. **A.** Cell viability following topotecan treatment. Viability is represented as a percentage of untreated controls. Cells were seeded, allowed to adhere if appropriate, then treated with solvent or topotecan. Five days later, cell viability was measured by resazaurin assay. Results represent mean ± SEM for three independent experiments. Cell line plots: Red plots = high and blue = low *IGF-1R* mRNA expression. **B.** Comparison of topotecan GI_{50} between high and low *IGF-1R* mRNA expressing groups. Boxplots show median, range and interquartile range. Exact 2 sided significance reported. **C.** Topotecan GI_{50} (nM) from A compared to total IGF-1R protein expression measured by western blot. IGF-1R protein expression was quantified using Image J and normalised according to expression of the loading control, Ku80. Results represent mean ± SEM for a minimum of two independent experiments. **D.** Topotecan GI_{50} (nM) from A compared to published total IGF-1R protein expression as measured by reverse phase protein array (RPPA). **E.** Topotecan GI_{50} (nM) from A compared to *IGF-1R* mRNA expression expressed as cycle threshold normalised to *GAPDH* (Jorge Zeron-Medina). **F.** Topotecan GI_{50} (nM) from A compared to levels of phosphorylated IGF-1R (pIGF-1R) as measured by western blot under steady state conditions (See Ch. 3.5). Quantification and normalisation are as for B. Results represent mean ± SEM for a minimum of two independent experiments.

4.4 Intrinsic Radioresistance

SNP rs4966013 was identified by Dr Gareth Bond's laboratory on the basis of its association with differences in chemoresistance (Dr Emmanouela Repapi and Jorge Zeron-Medina, unpublished data). Given the interest of the host laboratory in the effects of IGF-1R inhibition on radiosensitivity and the DNA damage response[80,81,85,84], experiments were also performed to investigate correlations between IGF-1R SNP rs4966013, mRNA and protein expression and intrinsic radioresistance.

Initial assessments compared radiation SF_{50}s derived from published radiosensitivity data for the NCI60[93], generated using clonogenic assays, to SNP genotype, IGF-1R mRNA or protein. No associations or correlations were found between SNP genotype, IGF-1R mRNA or protein and radioresistance (see Figure 14). However given previous demonstrations of radiosensitisation following IGF-1R inhibition or siRNA knockdown of IGF-1R within this laboratory and others[89,84,80,81,85], this was investigated further.

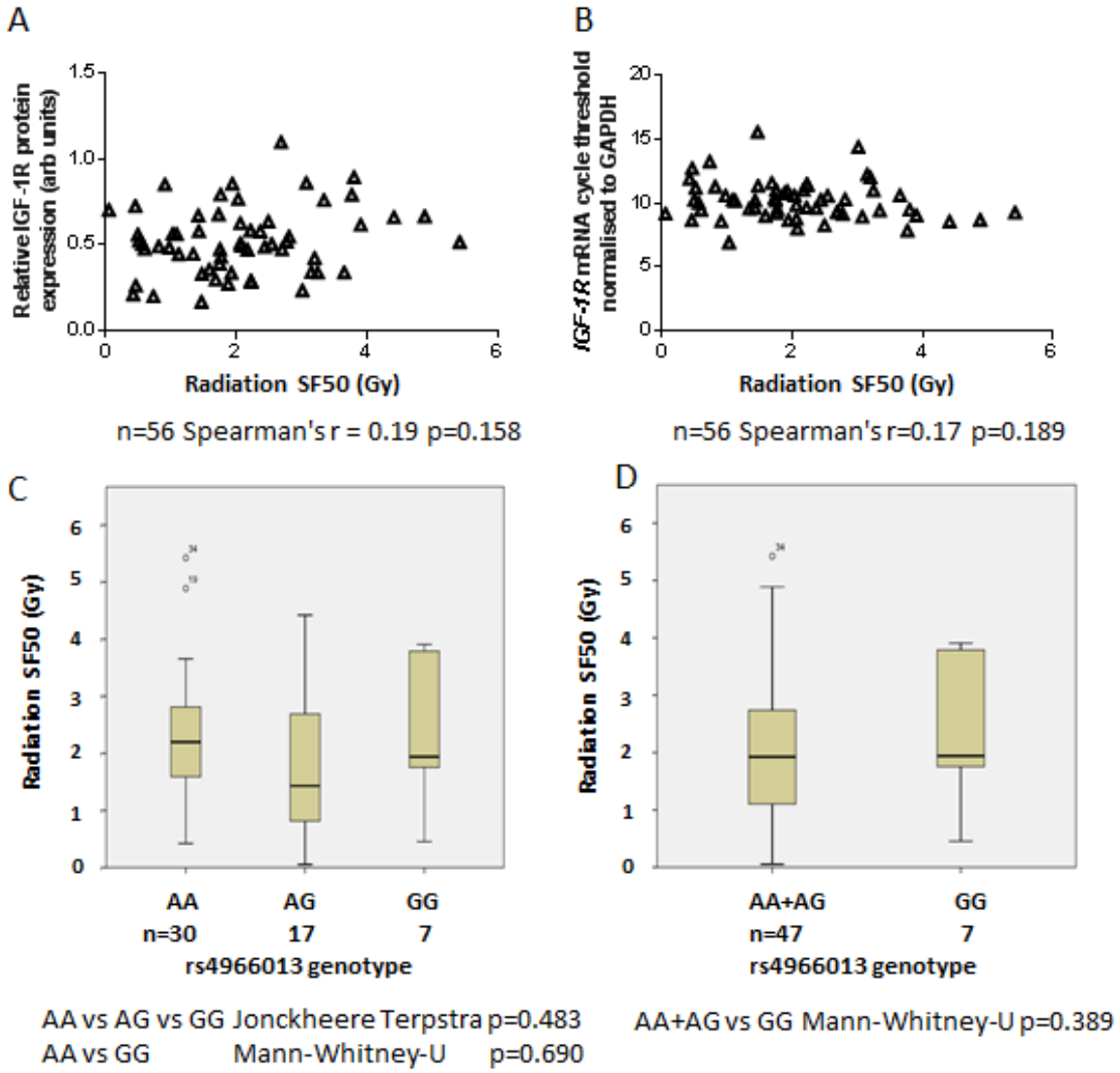


Figure 14 Comparison of Radiation SF_{50} with IGF-1R expression and SNP genotype within the NCI60.
Irradiation SF_{50}s were calculated from dose response curves plotted using published clonogenic assay data for surviving fraction (SF) at 2, 5 and 8 Gy in cell lines of the NCI60 (Amundson et al 2008[93]). **A.** Comparison of relative IGF-1R protein expression (**A**) and mRNA expression (**B**) with radiation SF_{50}. **C and D**. Boxplots showing distribution of radiation SF_{50} between SNP genotypes. **C.** AA vs AG vs GG **D.** Combined AA+AG vs GG. Boxplots: Horizontal bars represent the median, boxes the interquartile range and whiskers the range. Circles and asterisks represent statistical outliers. Publicly available relative IGF-1R protein expression data generated by reverse phase protein expression array profiling (Park et al 2010[92]), http://dtp.nci.nih.gov/mtweb/targetinfo?moltid=MT18293&moltnbr=374556). *IGF-1R* mRNA expression data generated using RT-PCR by Jorge Zeron-Medina, levels are expressed as cycle thresholds normalised to GAPDH, lower values equate to higher mRNA expression. SNP genotyping data generated by comparative genomic hybridisation and confirmed by Taqman Assay (Jorge Zeron-Medina and Dr Elisabeth Bond).

.

To investigate correlations of intrinsic radioresistance with IGF-1R expression, cell viability assays were performed. Cells were seeded in 96 well plates, allowed 4 hours to adhere if required and exposed to 0, 2, 5 or 8 Gy of radiation then cultured for 5 days prior to measuring cell viability using the resazurin assay. Whilst it is conventional to examine radiation sensitivity using clonogenic assays, resazurin assays were used here also because of the reasons outlined earlier. To maintain consistency with previous assays, results were compared using SF_{50}s rather than surviving fraction at 2, 5 or 8 Gy. The GI_{50} for irradiation ranged from 1.3 Gy for CCRF-CEM to 9.8 Gy for SKMel28 (see Figure 15 A, for radiation dose response curves in all cell lines). There was a non-significant trend towards relative radioresistance in cell lines with higher IGF-1R mRNA, protein, pIGF-1R and pERK, but not pAKT (Figure 15 B to H).

Figure 15 (overleaf) Examination of the relationship between intrinsic radiosensitivity and IGF-1R expression. A. Cell viability following irradiation. Viability is represented as a percentage of unirradiated controls. Cells were seeded, allowed to adhere if appropriate, irradiated, and 5 days later, cell viability was measured by fluorescence using the resazurin assay. Results represent mean ± SEM for a minimum of two independent experiments. Cell line plots: Red plots = high, and blue = low *IGF-1R* mRNA expression. **B.** Comparison of radiation GI_{50} derived from A between high and low *IGF-1R* mRNA expressing groups. Boxplots show median, range and interquartile range. Exact 2 sided significance reported **C.** Irradiation GI_{50} values from A compared to total IGF-1R protein expression as measured by western blot. IGF-1R protein expression was quantified using Image J and normalised according to expression of the loading control, Ku80. Results represent mean ± SEM for a minimum of two independent experiments. **D.** Irradiation GI_{50} from A compared to published total IGF-1R protein expression as measured by reverse phase protein array (RPPA). **E.** Irradiation GI_{50} from A compared to *IGF-1R* mRNA expression expressed as cycle threshold normalised to *GAPDH* (Jorge Zeron-Medina). **F, G and H.** Irradiation GI_{50} from A compared to levels of phosphorylated IGF-1R (pIGF-1R), AKT (pAKT) and ERK (pERK) respectively as measured by western blot under steady state conditions (See Ch. 3.5). Quantification and normalisation for F, G and H are as for C. Results represent mean ± SEM for a minimum of two independent experiments.

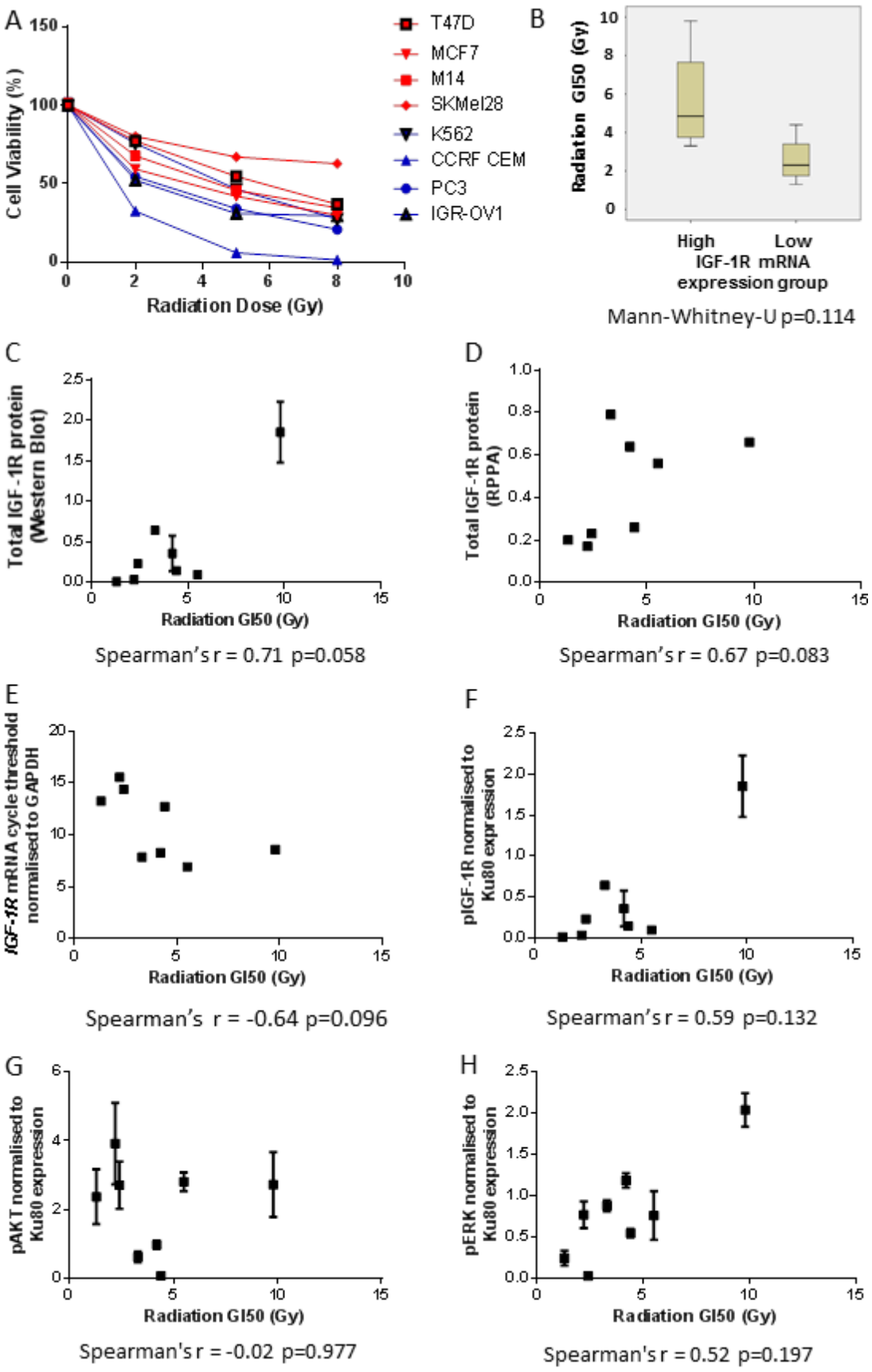


Figure 15 Examination of the relationship between intrinsic radiosensitivity and IGF-1R expression.

The differences between the trends observed here and those seen from examination of the published radiosensitivity data may relate to the effects of different sample sizes, differences in gene/protein importance for survival in clonogenic assays (used for the data generated by Amundson and colleagues[93]) or to changes in the relative positions of cell GI_{50}s due to the use of time as a defined endpoint for the 96 well plate assay as opposed to a defined number of doublings required to reach a colony size of 50 cells as per Amundson and colleagues. In order to make a more comparable assay, it might be more appropriate to seed a uniform number of cells (approximately $1/50^{th}$ of the desired final confluence) across all cell lines and end the assay after a defined number of doubling times.

4.5 Summary

Initial data from Dr Bond's group suggested a correlation between the GG genotype of IGF-1R SNP rs4966013 and resistance to 53 of the 123 cytotoxic drugs examined, particularly those known to damage DNA. Further analysis of 113 cytotoxic drugs, within this study indicated a correlation between IGF-1R SNP and/or IGF-1R expression in 26 drugs of which 17 showed significant associations with SNP rs4966013 genotype, 4 with IGF-1R protein expression and 11 with *IGF-1R* mRNA expression. Significant correlations with SNP genotype were found across all drug groups except DNA antimetabolites, particularly amongst topoisomerase I inhibitors and alkylating agents. Interestingly, whilst significant associations were found between IGF-1R protein and/or mRNA expression and drug resistance for a number of alkylating agents, particularly nitrosoureas, none were found for topoisomerase I inhibitors, indeed none approached significance (see Appendix V). Whether this difference reflects chance, or is repeatable in a wider panel of cell lines remains to be seen. If so, then it may reflect activities of the SNP rs4966013 other than

the enhancement of transcription. Ideally these examinations would be pursued in larger panels of cell lines, preferably of a single type. Given the importance of p53 in the response to cellular stress and genotoxic damage, it would be useful to reanalyse the data by p53 mutation status. Similar analyses may be performed by pathway activation status. For example cell lines with or without mutations activating the PI3K/AKT/MTOR pathway such as PTEN deletions or PIK3CA could be examined as separate groups, or those with RAS/RAF/MAPK pathway activation.

The correlation of *IGF-1R* mRNA with resistance to mitozolomide (Spearman's r =-0.341 p=0.010, as mentioned in Table 5 and detailed in Appendix V) correlates with data from the host lab indicating that IGF-1R inhibitors AZ12253801 and OSI-906 sensitize melanoma cells to the mitozolomide derivative temozolomide (Ramcharan et al submitted). To examine SNP rs4966013 genotype and immunohistochemical expression of IGF-1R in tissue from patients with metastatic melanoma treated with dacarbazine, attempts were made to optimise IGF-1R immunohistochemical staining and SNP genotyping.

Qiagen kit and the Levi methods[118] of DNA extraction from formalin fixed paraffinised tissue were compared and the Qiagen kit found to produce smaller quantities of higher quality DNA, which produced more consistent results when genotyping using Taqman assays. Attempts were also made to optimise immunohistochemistry staining techniques using a polyclonal rabbit antibody that had been proven to provide reliable immunohistochemical staining in previous studies (Cell Signalling Technology catalogue number 3027)[64,66]. However, the batch used failed to exhibit appropriate staining in controls prepared from formalin-fixed tissues and cell pellets of known IGF-1R expression.

On-going work in the host lab has been able to achieve staining of control cell pellets and tissues using a newly-available IGF-1R monoclonal antibody. If time had permitted, this method would have been applied to the melanomas of Oxford patients treated with dacarbazine.

Whilst not significantly different in this small, heterogeneous cell line panel, topotecan GI_{50} values were generally higher in high *IGF-1R* mRNA expressing cell lines than in low *IGF-1R* mRNA expressing cell lines. These are worth investigating further in larger cell line panels and potentially in tumour samples if confirmed. Other studies demonstrating sensitization of cell lines to topotecan and the related irinotecan following inhibition of IGF-1R provide further evidence linking the IGF-1R to topotecan resistance[119,76]. Future experiments could test whether significant differences in topotecan sensitivity were observed between high and low IGF-1R expressing cell lines of tumour types where topoisomerase I inhibitors are used, such as ovarian[120] and small cell lung cancer[121,122], where topotecan is used or trialed, and colorectal cancer, where irinotecan is used[123].

No correlations or trends were observed between paclitaxel GI_{50} and total IGF-1R protein, *IGF-1R* mRNA or pIGF-1R levels. Whilst this did not support the observations from the GDSC data, it was consistent with the lack of relation between IGF-1R SNP genotype, mRNA and protein expression and paclitaxel GI_{50} within the larger NCI60 dataset. Observations with respect to sensitisation of cell lines to paclitaxel treatment by IGF-1R inhibition or silencing have been similarly variable[124,82,81,125,126]. Whilst several mechanisms of taxane resistance have been identified, such as aberrant signal transduction pathways, increased expression of βIII tubulin or p-glycoprotein, these have

not proven to be convincing biomarkers by which the paclitaxel data from the NCI60 might be stratified for reanalysis[127,128,10]. However, given the demonstration of IGF-1R dependent induction of AKT phosphorylation by paclitaxel in ovarian carcinoma cell lines[125] it may be worth exploring the interactions of IGF-1R expression and paclitaxel sensitivity in a panel of cell lines that lack PTEN deletions, activating PIK3CA mutations and do not demonstrate elevated pAKT under serum starved conditions.

Similarly the relative radioresistance in high *IGF-1R* mRNA expressing cell lines, whilst not significantly different from that of the low expressors, seems worth further investigation. This seems particularly so, given the association of IGF-1R expression with poor outcome or lack of response in a number of radiotherapy or radio-chemotherapy trials involving breast cancer, cervical cancer, and oral squamous cell carcinomas[69,129,130]. Further support is provided by the sensitization to radiation observed in a number of cell lines[81,84,89]. Indeed, forced expression of IGF-1R in cells with mutant ATM, which naturally have low IGF-1R levels, increases radioresistance[87].

5 Testing associations between IGF-1R expression and the degree of radiosensitisation induced by IGF-1R inhibition

5.1 Introduction

IGF-1R inhibition has been shown to enhance tumour cell radiosensitivity *in vitro*[80,86,84] and in vivo[80,86]. If IGF-1R is not only a marker of, but a contributor to, chemo- and radio- resistance, it was hypothesised that cells in which high IGF-1R expression is a major driver of resistance might be more effectively chemo- or radio- sensitized by IGF-1R inhibition, compared with low IGF-1R cell lines.

Initially, publicly-available data from the GDSC were used to assess correlations between IGF-1R inhibitor sensitivity and IGF-1R expression. Then, the ability of two IGF-1R inhibitors, AZ12253801 and BMS754807, to inhibit IGF-1R phosphorylation, downstream phosphorylation of AKT and ERK, and cell growth in viability assays was examined. Finally, the same inhibitors were used in cell viability assays to assess the effects on intrinsic radiosensitivity of IGF-1R inhibition in cell lines expressing high vs low *IGF-1R* mRNA.

5.2 Examining correlations between IGF-1R expression and sensitivity to IGF-1R inhibitors using publicly-available data.

In order to examine correlations between sensitivity to IGF-1R inhibition and IGF-1R expression within the NCI60, publicly available GI_{50} data for BMS754807 and OSI-906 were downloaded from the GDSC website (http://www.cancerrxgene.org/translation/Drug access date 24/02/2013) and compared to the IGF-1R rs4966013 SNP genotype, *IGF-1R* mRNA and IGF-1R protein expression data described earlier (Figure 16 and **Figure 17**).

Comparison of BMS754807 GI_{50} with the SNP rs4966013 revealed the median BMS754807 GI_{50} for the GG genotype to be lower than that of the AA or AG genotypes, with median GI_{50}s respectively of 3.0, 2.8 and 2.8μM for AA, AG and combined AA+AG genotypes compared to 1.4μM for the GG genotype (Figure 16 A and B). Comparison of BMS754807 GI_{50}s for all three genotypes using the Jonckheere Terpstra test, when examining for an additive effect of SNP genotype, found the differences between the three groups to be significant (p=0.011, Figure 16 A). However, comparisons of either the homozygotes (p=0.071, Figure 16 A), or, when assuming dominance of the A allele, the combined AA and AG genotypes with the GG genotype (p=0.080, Figure 16 B) using the Mann-Whitney-U test did not show significant differences. No correlations were found between *IGF-1R* mRNA expression or relative IGF-1R protein expression and BMS754807 GI_{50} (Figure 16 C and D).

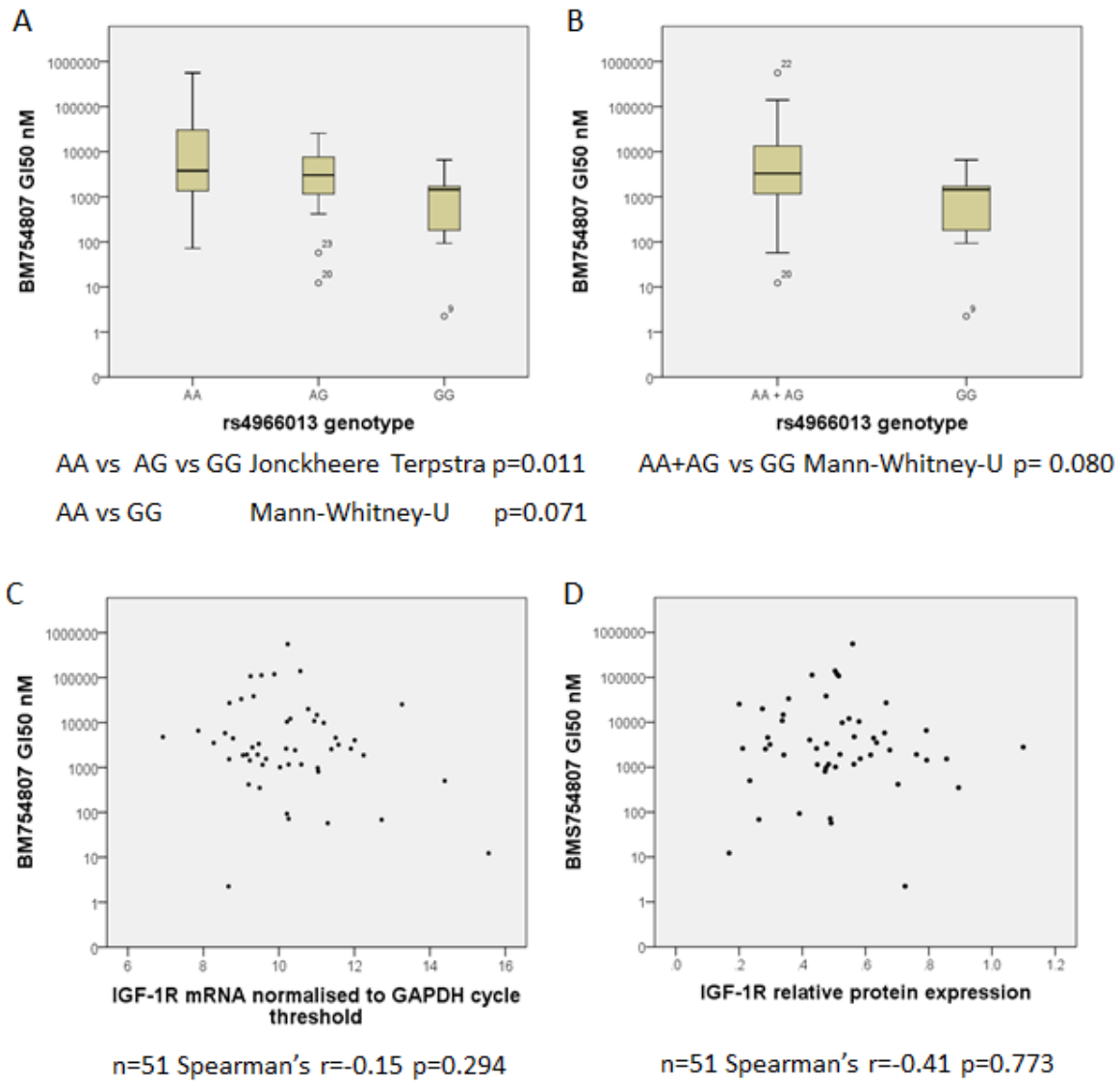


Figure 16 Comparison of BMS754807 GI_{50} with IGF-1R SNP genotype, mRNA and protein expression.
A. and B. Comparison of BMS754807 GI_{50} with SNP rs4966013 genotype. **A**. Additive/ non-dominant model. **B.** Model with A allele dominant. **Boxplots for A and B:** Horizontal bars represent the median, boxes the interquartile range and whiskers the range. Circles and asterisks represent statistical outliers. **C**. Comparison of BMS754807 GI_{50} with *IGF-1R* mRNA expression. **D.** Comparison of BMS754807 GI_{50} with IGF-1R protein expression. Data for BMS754807 GI_{50} were downloaded from the Genomics of Drug Sensitivity in Cancer website (http://www.cancerrxgene.org/translation/Drug access date 24/02/2013), generated in a 3 day, resazurin based cell viability assay. SNP genotyping data generated by comparative genomic hybridisation and confirmed by Taqman Assay (Jorge Zeron-Medina and Dr Elisabeth Bond). *IGF-1R* mRNA expression data generated using RT-PCR by Dr Gareth Bond's laboratory, levels are expressed as cycle thresholds normalised to GAPDH, lower values equate to higher mRNA expression. Publicly available relative IGF-1R protein expression data generated by reverse phase protein expression array profiling (Park et al 2010[92], http://dtp.nci.nih.gov/mtweb/targetinfo?moltid=MT18293&moltnbr=374556).

Comparison of OSI-906 GI_{50} with the SNP rs4966013 revealed the median OSI-906 GI_{50} for the GG genotype to be lower than that of the AA or AG genotypes, with median GI_{50}s respectively of 37.7, 72.5 and 40.9μM for AA, AG and combined AA+AG genotypes compared to 7.5μM for the GG genotype (Figure 17). Comparison of OSI-906 GI_{50}s for all three genotypes using the Jonckheere Terpstra test, when examining for an additive effect of SNP genotype, found no significant ordered differences (p=0.734, Figure 17 A). Nor did these differences reach significance when comparing OSI-906 GI_{50}s between either the homozygotes (p=0.178, Figure 17 A) or, when looking for a dominant effect of the A allele, between the combined AA and AG, and the GG genotypes (p=0.102; Figure 17 B) using the Mann-Whitney-U test. No correlations were found between *IGF-1R* mRNA expression or relative IGF-1R protein expression and OSI-906 GI_{50} (Figure 17 C and D).

In summary, neither *IGF-1R* mRNA nor IGF-1R protein expression correlated with sensitivity to either IGF-1R inhibitor. The differences in sensitivity noted between the SNP genotypes, although not significant, may be worth examining in a larger dataset. The lack of correlation of IGF-1R protein expression with sensitivity to IGF-1R inhibition contrasts with some cell line studies in a variety of tumour types including breast, colon and non-small cell lung carcinoma, rhabdomyosarcoma, Ewing's sarcoma and neuroblastoma[131-134]. It is not clear whether this difference might relate to differing mechanisms of action or off target effects of the agents used to inhibit IGF-1R or to the use of more homogenous cell line panels. However, the lack of correlation is consistent with some preclinical studies and clinical trial results, although the clinical studies have largely involved monoclonal antibodies targeting the IGF-1R only, rather than dual targeting of the IR, as for OSI-906 and BMS754807[135,136,84,137].

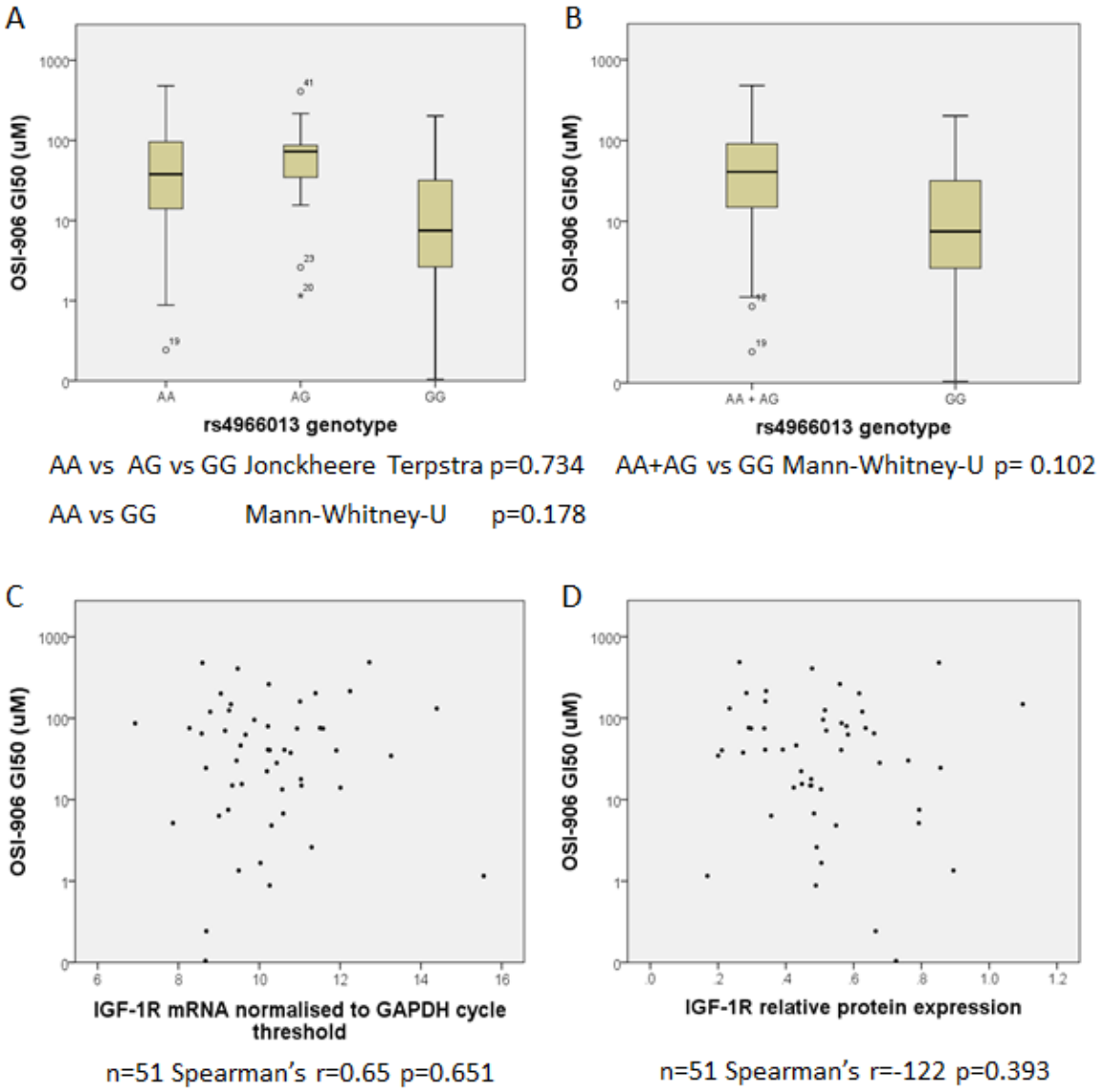


Figure 17 Comparison of OSI-906 GI_{50} with IGF-1R SNP genotype, mRNA and protein expression.
A. and B. Comparison of OSI-906 GI_{50} with SNP rs4966013 genotype. **A**. Additive/ non-dominant model. **B.** Model with A allele dominant. **Boxplots for A and B:** Horizontal bars represent the median, boxes the interquartile range and whiskers the range. Circles and asterisks represent statistical outliers. **C**. Comparison of OSI-906 GI_{50} with *IGF-1R* mRNA expression. **D.** Comparison of OSI-906 GI_{50} with IGF-1R protein expression. Data for OSI-906 GI_{50} was downloaded from the Genomics of Drug Sensitivity in Cancer website (http://www.cancerrxgene.org/translation/Drug access date 24/02/2013), it was generated in a 3 day, resazurin based cell viability assay. SNP genotyping data generated by comparative genomic hybridisation and confirmed by Taqman Assay (Jorge Zeron-Medina and Dr Elisabeth Bond). *IGF-1R* mRNA expression data generated by RT-PCR (Jorge Zeron-Medina) and, levels are expressed as cycle thresholds normalised to *GAPDH* (Dr Lucas Filip Grochola), lower values equate to higher mRNA expression. Publicly available relative IGF-1R protein expression data generated by reverse phase protein expression array profiling (Park et al 2010[92], http://dtp.nci.nih.gov/mtweb/targetinfo?moltid=MT18293&moltnbr=374556).

5.3 Testing Intrinsic Sensitivity to IGF-1R inhibitors in 9 NCI60 cell lines

The IGF-1R inhibitors, AZ12253801, OSI-906 and BMS754807, are small molecule adenosine triphosphate (ATP) competitive IGF-1R kinase inhibitors with varying specificities for kinase inhibition. AZ12253801 is more specific, with an IC_{50} (half maximal inhibitory concentration) for IGF-1R approximately 10 fold lower than for the IR, whilst for OSI-906 it is 2 fold, and BMS-754807 is equipotent for IGF-1R and IR inhibition[64,78,138] (Table 7). For AZ12253801 and OSI-906, all other kinases tested demonstrated IC_{50}s greater than 1µM and 10µM respectively. BMS754807 is much less specific, with the most potent off target activities reported being against Met, RON, tropomyosin receptor kinase (Trk) A and B, Aurora A and Aurora B with IC_{50}s of 6, 44, 7, 4, 9 and 25nM respectively[78].

	AZ12252801[64]	OSI-906[137]	BMS754807[78]
IGF-1R IC_{50} (nM)	2.1	35	1.8
IR IC_{50} (nM)	19	75	1.7

Table 7 Concentrations of the small molecule inhibitors AZ12253801, OSI-906 and BMS754807 required to cause half maximal inhibition of the IGF-1R and Insulin Receptor (IR).

5.3.1 Inhibition of IGF-1R phosphorylation by AZ12253801 and BMS754807

Initially, the ability of AZ12253801 and BMS754807 to inhibit IGF-1R activation was examined. Serum starved cells were incubated with AZ12253801, BMS754807 or solvent prior to stimulation with 50nM IGF-1. MCF-7 cells demonstrated inhibition of phosphorylation of IGF-1R, and the downstream signalling components, AKT and ERK in response to AZ12253801 administration (Figure 18A). In T47D cells there was evidence of inhibition of IGF-1R phosphorylation, with dose dependent inhibition of AKT and ERK, following treatment with BMS 754807 or AZ12253801 (Figure 18B). A second set of experiments was performed in MCF-7 cells using BMS754807, and in IGR-OV1 cells with both inhibitors (Figure 18C and D). There was no detectable IGF-1 induced IGF-1R activation, later found to be due to a problem with the bioactivity of that batch of ligand. However, these experiments did demonstrate the ability of these inhibitors to block basal IGF-1R activation. These findings were consistent with the observations of others demonstrating inhibition of IGF-1R and downstream phosphorylation by AZ12253801 and BMS754807[64,139,140,84].

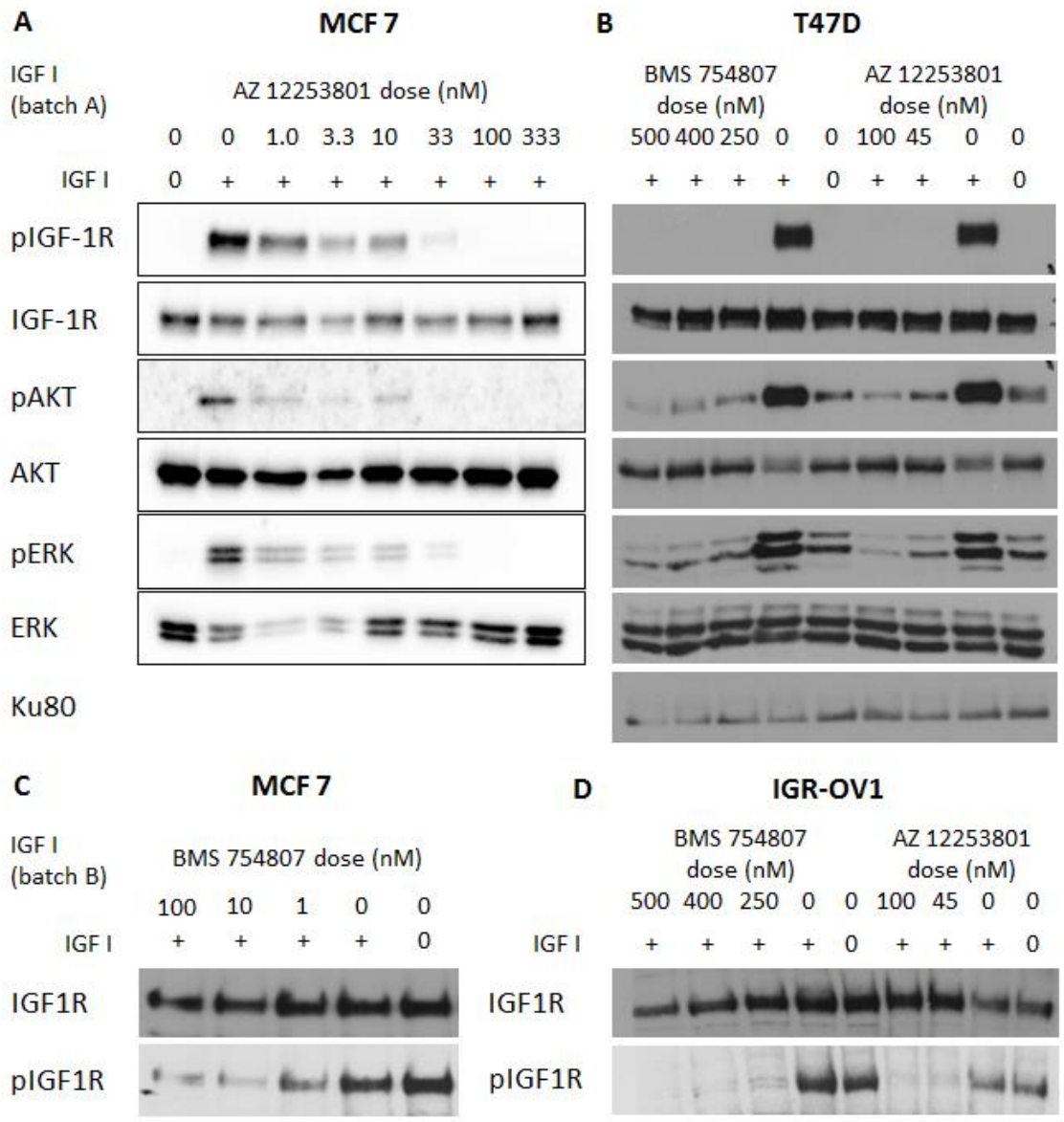


Figure 18 Inhibition of IGF-1R phosphorylation by IGF-1R kinase inhibitors AZ12253801 and BMS 754801.

For all experiments, cells were serum starved for 24 hours, treated with AZ12253801, BMS7548076 or solvent for one hour then stimulated by 50nM IGF-1 for 15 minutes. Antibodies used recognise proteins phosphorylated proteins at the following sites Tyr1135/1136 (pIGF-1R), Ser 473(pAKT) and Thr202/Tyr202 (pERK1/2).**A and B.** Inhibition of IGF-1R and downstream AKT and ERK phosphorylation. **A.** MCF7 cells treated with AZ12253801. **B.** T47D cells treated with AZ12253801 or BMS754807 to assess inhibition of IGF-1R and downstream signalling at concentrations of IGF-1R inhibitors approximating to the GI_{50}s of cell lines used in the panel. **C and D.** Repetition of the same experiment as in **B,** in MCF7 and IGR-OV1 cell lines using a 2nd batch of IGF-1 (subsequently found to be inactive), demonstrating no IGF-induced IGF-1R activation, but confirming ability of inhibitors to block basal IGF-1R phosphorylation.

5.3.2 AZ12253801 and BMS754807 sensitivity in cell viability assays

Having confirmed the ability of AZ12253801 and BMS754807 to inhibit IGF-1R phosphorylation and activation, their ability to inhibit cell growth was examined. Cells were seeded in 96 well plates, allowed 4 hours to adhere if required and exposed to a range of AZ12253801 and BMS754807 concentrations or solvent for 5 days prior to measuring cell viability using the resazurin assay. Both IGF-1R inhibitors inhibited the growth of all cell lines examined. The AZ12253801 GI_{50} values ranged from 39nM for K562 to 196nM for T47D (see Figure 19 A for dose response curves, Table 8 for GI_{50} values). Most of the GI_{50} values for BMS754807 were between 217nM for CCRF-CEM and 545nM for SKMel28, with MCF7 exhibiting a substantially lower GI_{50} at 1nM (see Figure 20A for dose response curves, Table 8 for GI_{50} values). No correlations were observed between either AZ12253801 or BMS754807 GI_{50} and total IGF-1R protein, *IGF-1R* mRNA or pIGF-1R levels (Figure 19 and 19, B to E). As for paclitaxel and topotecan, the GI_{50} values for BMS754807 were substantially lower than those reported in the GDSC data, again likely a reflection of assay duration.

Cell Line	SNP rs4966013 genotype	AZ12253801 GI_{50} (nM)	BMS754807 GI_{50} (nM)	
		This study	This study	GDSC*
T47D	AG	196	538	4766
MCF7	GG	42	1	93
M14	AA	92	369	6588
SKMel28	AG	110	545	139742
K562	unknown	39	260	558078
CCRF-CEM	AG	48	217	25452
PC3	AA	130	436	1926
IGR-OV1	AA	100	460	69

Table 8 SNP genotype and Concentrations of AZ1225380 and BMS754807 required to inhibit growth of cell lines by 50%.
AZ12253801 and BMS754807 GI_{50} interpolated from resazurin assay data using Graphpad PRISM.*BMS754807 GI_{50} reported on the GDSC website is detailed for comparison. SNP genotyping data generated by comparative genomic hybridisation and confirmed by Taqman Assay (Jorge Zeron-Medina and Dr Elisabeth Bond).

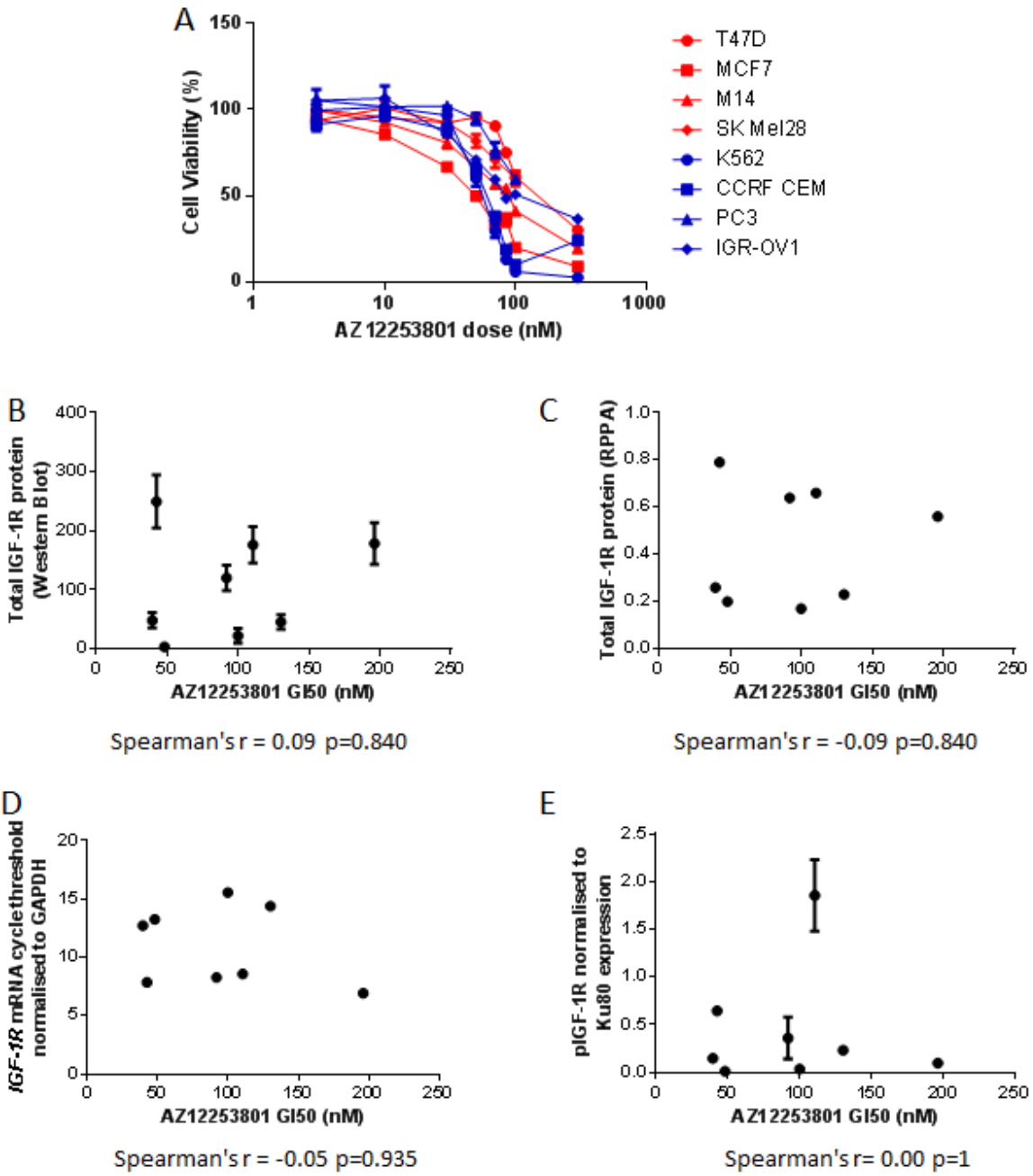


Figure 19 Examination of the relationship between intrinsic sensitivity to the IGF-1R inhibitor AZ12253801 and IGF-1R expression.

A. Cell viability following AZ12253801 treatment. Viability is represented as a percentage of untreated controls. Cells were seeded, allowed to adhere if appropriate, and then treated with solvent or AZ12253801. Five days later, cell viability was measured by fluorescence using the resazurin assay. Results represent mean ± SEM for a minimum of three independent experiments. Cell line plots: Red plots = high and blue = low *IGF-1R* mRNA expression. **B.** AZ12253801 GI_{50} from A compared to total IGF-1R protein expression as measured by western blot, and quantified as described previously. Results represent mean ± SEM for a minimum of two independent experiments. **C.** AZ12253801 GI_{50} from A compared to published total IGF-1R protein expression as measured by reverse phase protein array (RPPA). **D.** AZ12253801 GI_{50} from A compared to *IGF-1R* mRNA expression, expressed as cycle threshold normalised to GAPDH *IGF-1R* mRNA expression data generated by RT-PCR (Jorge Zeron-Medina). **E.** AZ12253801 GI_{50} from A compared to levels of phosphorylated IGF-1R (pIGF-1R) as measured by western blot under steady state conditions (See Ch. 3.5). Quantification and normalisation are as for B. Results represent mean ± SEM for a minimum of two independent experiments.

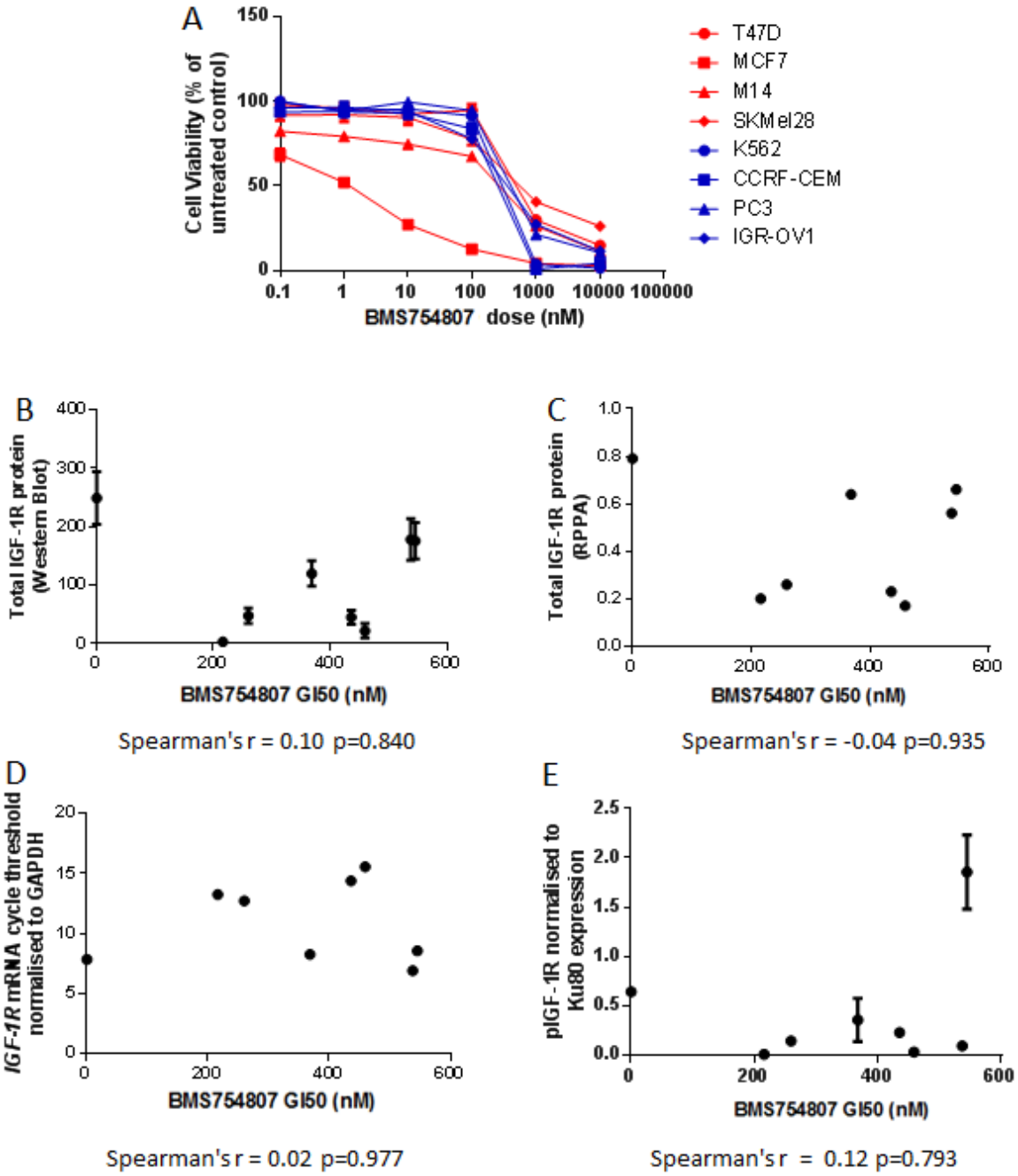


Figure 20 Examination of the relationship between intrinsic sensitivity to the IGF-1R inhibitor BMS754807 and IGF-1R expression.

Cell viability following BMS754807 treatment. Viability was assessed as described in legend to Figure 19 5 days after treatment with BMS754807, and represented as a percentage of untreated controls. Results represent mean ± SEM for a minimum of three independent experiments. Cell line plots: Red plots = high and blue = low *IGF-1R* mRNA expression. **B.** BMS754807 GI_{50} from A compared to total IGF-1R protein expression corrected for the loading control, Ku80. Results represent mean ± SEM for a minimum of two independent experiments. **C.** BMS754807 GI_{50} from A compared to published total IGF-1R protein expression as measured by reverse phase protein array (RPPA). **D.** BMS754807 GI_{50} from A compared to *IGF-1R* mRNA expression expressed as cycle threshold normalised to *GAPDH IGF-1R* mRNA expression data generated by RT-PCR (Jorge Zeron-Medina). **E.** BMS754807 GI_{50} from A compared to levels of phosphorylated IGF-1R (pIGF-1R) as measured by western blot under steady state conditions (See Ch. 3.5). Quantification and normalisation are as for B. Results represent mean ± SEM for a minimum of two independent experiments.

The lack of correlation between measures of IGF-1R expression and inhibition by either AZ12253801 or BMS754807 is consistent both with clinical trials[137] and other *in vitro* studies[141,135,136]. Indeed the clinical picture is not dissimilar to the lack of correlation of immunohistochemical EGFR expression with sensitivity to the anti EGFR monoclonal antibody, cetuximab[142].

The GI_{50} values for both inhibitors were found to correlate with pAKT, with higher GI_{50} values in cells expressing high levels of pAKT (Figure 21A and B). This feature is consistent with previous reports that IGF-1R inhibition fails to inhibit AKT phosphorylation in resistant cell lines[143], expression of constitutively active AKT reduces sensitivity to IGF-1R inhibition in rhabdomyosarcoma cells[131], and pAKT increases post treatment in sarcomas resistant to IGF-1R monoclonal antibody therapy[144]. Furthermore, *PTEN* deletions and activating *PIK3CA* mutations are associated with resistance to IGF-1R inhibitors reported in the GDSC database[145,94]. All these observations highlight the importance of the PI3K-AKT pathway in IGF-1R signalling.

Elevated levels of pERK under steady state or basal conditions might also be expected to associate with relative resistance to IGF-1R inhibitors, however, no such correlation was found here. This would be consistent with observations that cell lines harbouring activating mutations of *KRAS* and *BRAF* retain their sensitivity to IGF-1R inhibition[146,147]. Indeed, somewhat counterintuitively, cell lines harbouring activating *KRAS* mutations demonstrated increased sensitivity to IGF-1R inhibitors, including OSI-906 and BMS754807, in the GDSC panel and some studies[76,148] but not that of Zinn and colleagues[149]. However, it must be noted that the correlation of elevated ERK phosphorylation with resistance to IGF-1R in small cell lung carcinoma cell lines observed

by Zinn and colleagues appears to be just that, as mitogen activated protein kinase (MAPK) inhibition did not restore sensitivity[149].

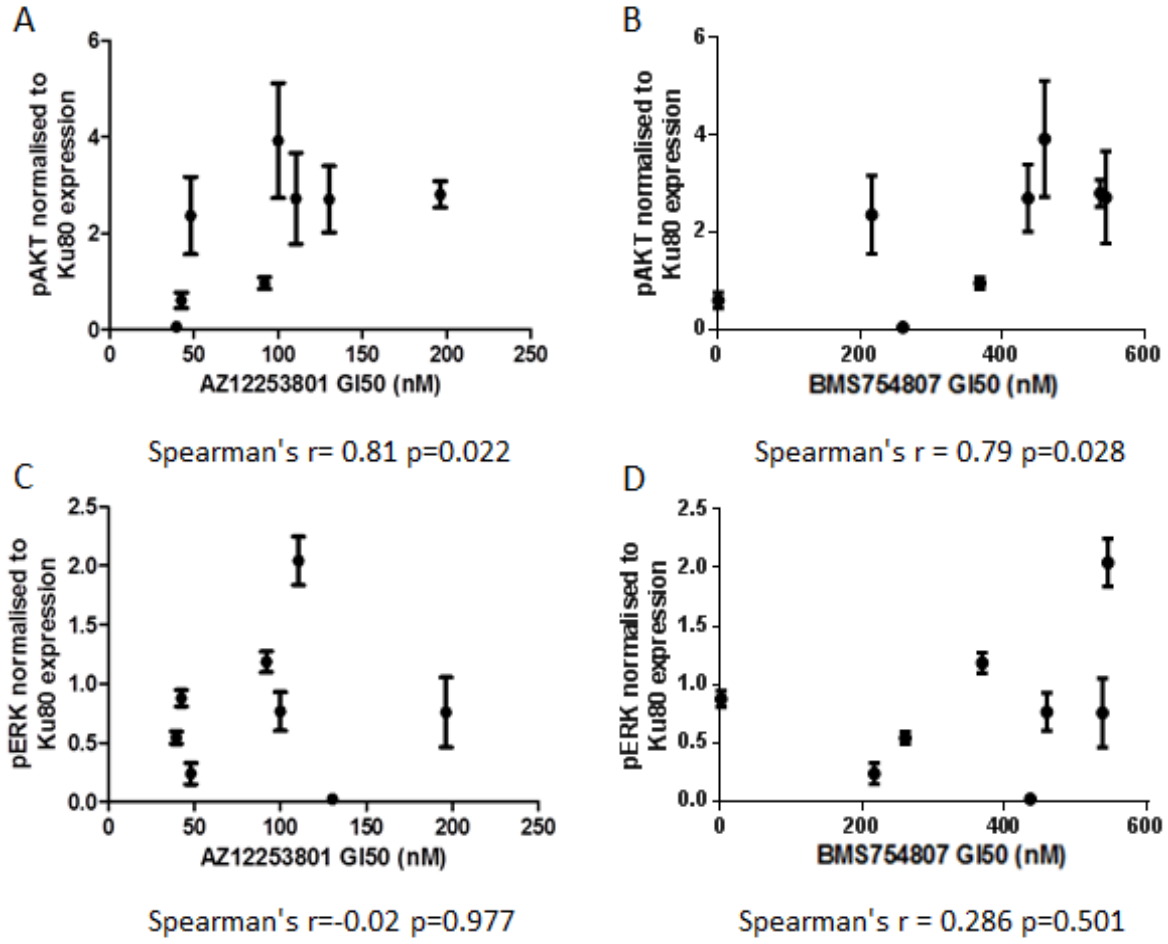


Figure 21 Examination of the relationship between intrinsic sensitivity to IGF-1R inhibitors and phosphorylated ERK and AKT.

A and C. AZ12253801 GI_{50} from experiment depicted in Figure 19A compared with phosphorylated AKT (**A**) and ERK (**C**) proteins as measured by western blot under steady state conditions (See Ch. 3.5) and corrected for the loading control, Ku80. **B** and **D**. As for A and C, but using BMS754807 GI_{50} derived from experimental data in Figure 20A. Results represent mean ± SEM for a minimum of two independent experiments.

5.3.3 AZ12253801 sensitivity in colony assays

Monolayer colony assays were used to assess the ability of IGF-1R inhibition by AZ12253801 to inhibit clonogenic survival in a subset of cell lines that grow as adherent monolayers and are amenable to this assay format. As described previously (section 4.2), initial experiments had attempted to determine conditions for clonogenic assays in all 9 cell lines under anchorage-independent conditions in soft agar, but this proved not to be technically feasible, and so monolayer survival assays were used instead. Cells were seeded sparsely in 10cm dishes, allowed to adhere for 4 hours before exposing to AZ12253801 or solvent control and incubating for 1-2 weeks. Colonies were counted when untreated control colonies reached 50 cells.

AZ12253801 inhibited the survival of all cell lines examined, with SF_{50} values ranging from 15nM for IGR-OV1 to 63nM for PC3 (see Figure 22A, overleaf for dose response curves; Table 9, 2 pages overleaf for SF_{50} values). No correlations were observed between AZ12253801 SF_{50} and AZ12253801 GI_{50}, total IGF-1R protein, *IGF-1R* mRNA, pIGF-1R, pERK or pAKT levels (Figure 22B to E). Whilst not reaching significance in this small selection of cell lines, visual inspection suggested a trend to correlation between AZ12253801 SF_{50} and AZ12253801 GI_{50} measured in resazurin assay (Figure 22B), and also between increasing AZ12253801 SF_{50} and decreasing pERK (Figure 22H), which might be worth investigating in a larger sample size. The latter observation would be consistent with the aforementioned association of activating *KRAS* mutations with sensitivity to IGF-1R inhibitors in the GDSC data.

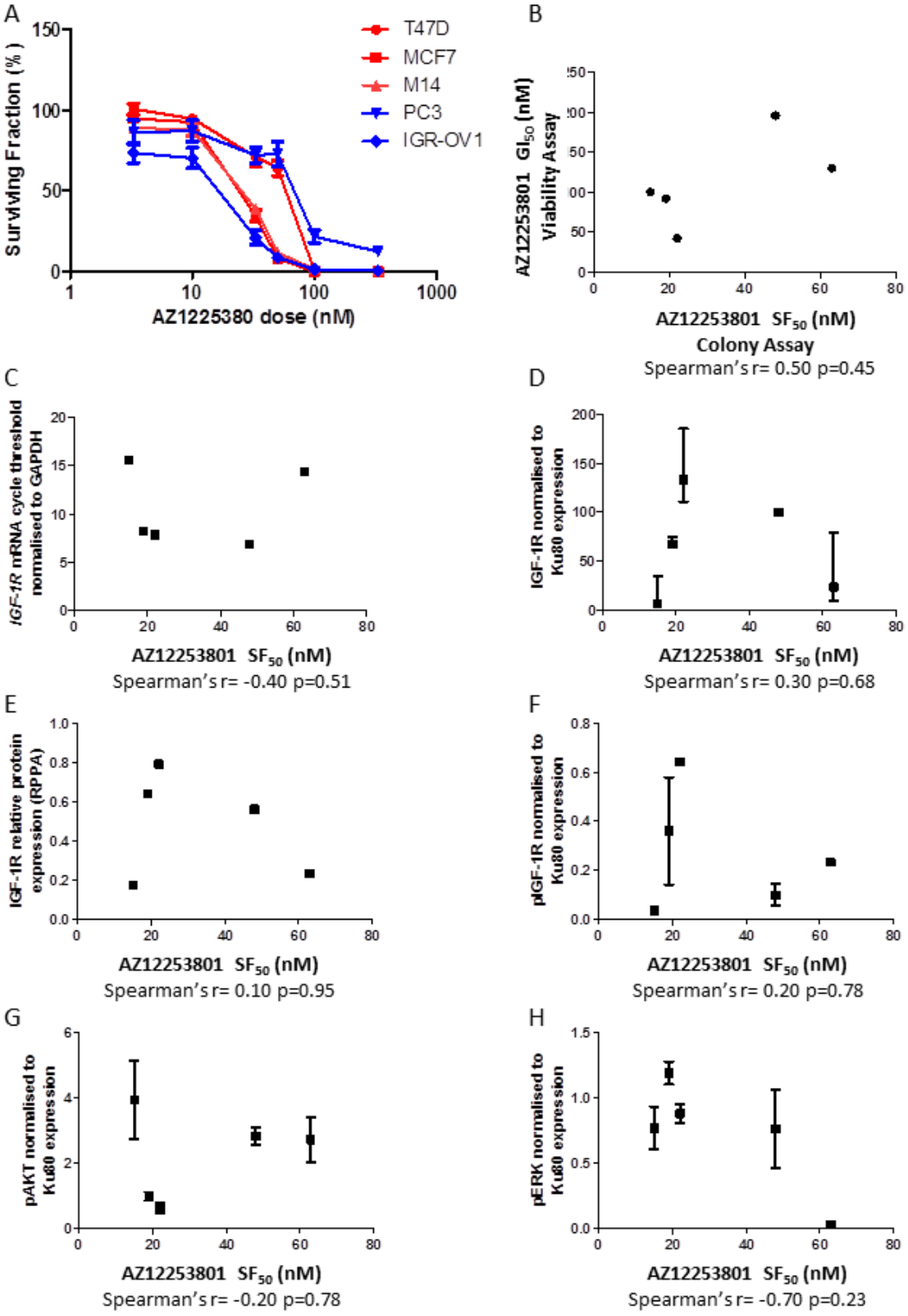


Figure 22 Examination of the relationship between intrinsic sensitivity to the IGF-1R inhibitor AZ12253801 and IGF-1R expression using clonogenic assays.
Legend overleaf.

Figure 22 Examination of the relationship between intrinsic sensitivity to the IGF-1R inhibitor AZ12253801 and IGF-1R expression using clonogenic assays. A. Cell survival following AZ12253801 treatment. Cell survival is represented as a percentage of untreated controls. Cells were seeded into 10cm dishes, allowed to adhere, and then treated with solvent or AZ12253801. Colonies were counted 7-14 days later, when the untreated controls had formed 50 cell colonies. Results represent mean ± SEM for four independent experiments. Cell line plots: red plots = high and blue = low *IGF-1R* mRNA expression. **B.** AZ12253801 SF_{50} from A compared to AZ12253801 GI_{50} derived from experiment Figure 19A. **C.** AZ12253801 SF_{50} from A compared to with *IGF-1R* mRNA expression data generated by RT-PCR and expressed as cycle threshold normalised to *GAPDH* (Jorge Zeron-Medina, Dr Lucas Filip Grochola). **D.** AZ12253801 SF_{50} from A compared to total IGF-1R protein expression as measured by western blot, and quantified as described previously. Results represent mean ± SEM for a minimum of two independent experiments. **E.** AZ12253801 SF_{50} from A compared to published total IGF-1R protein expression as measured by reverse phase protein array (RPPA) by Park and colleagues[92]. **F.** AZ12253801 SF_{50} from A compared to levels of phosphorylated IGF-1R (pIGF-1R) as measured by western blot, and quantified as described previously. Results represent mean ± SEM for a minimum of two independent experiments. **G.** AZ12253801 SF_{50} from A compared to pAKT protein as measured by western blot, and quantified as described previously. **H.** AZ12253801 SF_{50} from A compared to pERK protein as measured by western blot, and quantified as described previously. Results represent mean ± SEM for a minimum of two independent experiments. Spearman's correlations performed using Graphpad PRISM.

Cell Line	SNP rs4966013 genotype	AZ12253801 SF_{50} (nM) Colony Assay	AZ12253801 GI_{50} (nM) Viability assay
T47D	AG	48	196
MCF7	GG	22	42
M14	AA	19	92
PC3	AA	63	130
IGR-OV1	AA	15	100

Table 9 SNP genotype and concentrations of AZ1225380 required to inhibit clonogenic survival (SF_{50}) and growth (GI_{50}) of cell lines by 50%.
AZ12253801 SF_{50} values were derived from curve fitting and interpolation of clonogenic survival data using Graphpad PRISM. Survival data represents 4 independent experiments, each with 3 replicates. AZ12253801 GI_{50} values were derived from resazurin assay data as described in Table 8 above). SNP genotyping data generated by comparative genomic hybridisation and confirmed by Taqman Assay (Jorge Zeron-Medina and Dr Elisabeth Bond).

5.3.4 Correlations of IGF-1R inhibitor sensitivity

In order to examine whether cell lines exhibited similar sensitivity to different IGF-1R inhibitors, GI_{50} values for IGF-1R inhibitors were compared using both public data from the GDSC and data generated within this project. Within the cell line sample examined here, sensitivity to AZ12253801 and BMS754807 were significantly correlated (Spearman's r=0.81, p=0.022; Figure 23A). Although non-significant, a similar trend was observed when comparing sensitivity to OSI-906 and BMS754807 within the GDSC data (Spearman's r=0.26, p=0.068; Figure 23B). This supports the concept that, at concentrations around the $GI_{50,}$ and, despite its lower selectivity, the predominant mechanism of action responsible for the observed effects of BMS754807 is IGF-1R kinase inhibition.

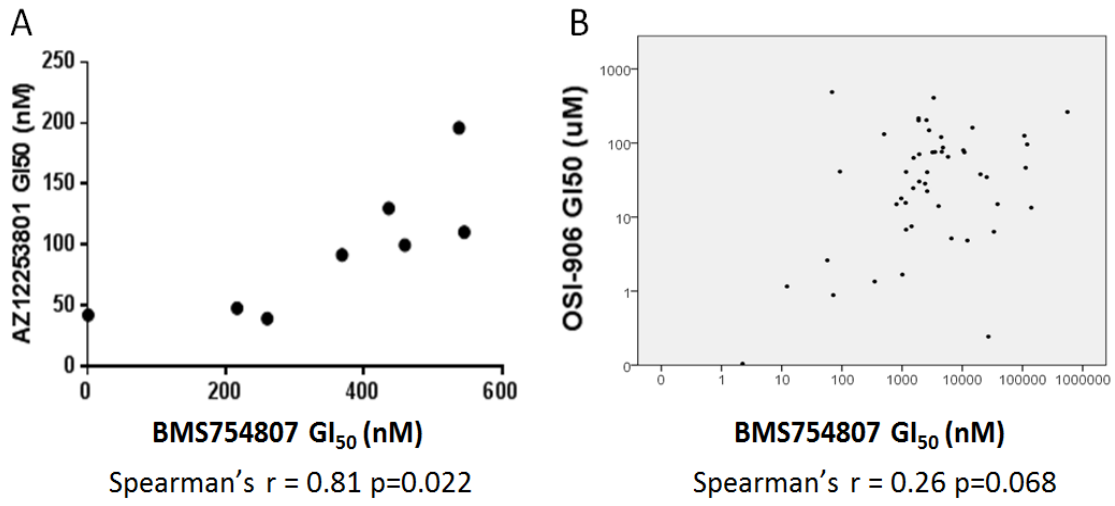


Figure 23 Correlation of sensitivity to IGF-1R inhibitors.
A. Comparison of GI_{50} values for AZ12253801 and BMS754807 GI_{50}. Graphpad PRISM was used to generate GI_{50} values by interpolation of data generated using the resazurin assay as above. **B.** Comparison of GI_{50} values for OSI906 and BMS754807, data for both inhibitors was sourced from the GDSC as described earlier.

It would be interesting to see if this correlation extends to allosteric IGF-1R inhibitors, such as picropodophyllin, monoclonal antibodies directed against the IGF-1R, or siRNA knockdown. If it did, then it might be reasonable to expect that mechanisms of resistance and thus clinical biomarkers predicting resistance would be similar. However, this seems unlikely to be the case given the lessons from EGFR, where point mutations in the ATP binding pocket confer sensitivity to the small molecule tyrosine kinase inhibitors erlotinib and gefitinib[150-152], whilst mutations in downstream signalling components *KRAS* and more recently *BRAF*, *NRAS*, *PTEN* and *PIK3CA* have been shown to confer resistance to monoclonal antibody therapy[153].

5.4 Effect of IGF-1R inhibition on radiosensitivity

The ability of IGF-1R inhibition to influence radiosensitivity in cells expressing high vs low *IGF-1R* mRNA was tested, given the interest of the host laboratory in investigating the effects of IGF-1R as a mediator of radioresistance. If time had permitted these investigations would have been extended to examine the effects of IGF-1R inhibition on chemoresistance, focussing initially on topotecan given the trend to association between intrinsic topotecan resistance and IGF-1R expression (Chapter 4 Figure 13). This might be further extended to include alkylating agents, particularly the nitrosoureas, given the associations between various measures of IGF-1R expression and GI_{50} value observed for a number of compounds in this group.

Cells were seeded in 96 well plates, allowed 4 hours to adhere if required, and exposed to a range of AZ12253801 and BMS754807 concentrations or solvent for a further 4 hours. They were then exposed to 0, 2, 5 or 8 Gy of radiation and incubated for 5 days prior to measuring cell viability using the resazurin assay. Curve fitting would ideally have been used to take all data into account when comparing cell viability curves. However, the radiation response curves for a number of inhibitor concentrations did not converge enough to allow comparison of GI_{50} values and identification of GI_{25} using curve fitting was visibly inaccurate for a number of cell lines. Hence, comparisons were made using the viable or surviving fraction at 2Gy (SF2). Examination of the sample distributions using Shapiro-Wilks test confirmed the visual impression that many did not conform to a normal distribution, and further inspection with Bartlett's test demonstrated that the variances were unequal (data not shown). Whilst the Kruskal Wallis test assumes equal variances, it is more robust to assumptions of this violation than the parametric one way ANOVA[154], and was therefore used to compare the distribution of SF2 between different

AZ12253801 treatment groups. The Jonckheere-Terpstra test might have been preferable to the Kruskal-Wallis test given its ability to detect ordered trends in difference rather than the existence of simple differences, regardless of the direction of difference, however, it was not supported by the software used in this analysis.

The SF_{50} data for most of the cell lines were derived from 2 independent experimental repeats. Due to time constraints, data for IGR-OV1 and T47D are from single experiments only, as is data for CCRF-CEM following exposure to BMS754807.

5.4.1 Effect of AZ12253801 treatment on radiosensitivity

The dose response curves for irradiation and the SF2 values after exposure to different concentrations of AZ12253801 are presented in Figure 24, the first 4 graphs showing responses in the high IGF-1R cell lines, and the second set of 4 graphs in the low IGF-1R cell lines. AZ12253801 caused only minor changes in radiosensitivity of T47D cells (Figure 24A), and the observed differences in SF2 were not significant ($p=0.194$), however, they suggested a trend towards decreasing SF2 with increasing AZ12253801 dose, which if repeatable might suggest that AZ12253801 modestly radiosensitises this cell line. In cell lines SKMel28, K562 and CCRF-CEM there were no consistent concentration-dependent changes in radiosensitivity, and changes in SF_{50} values were not significant ($p=0.937$, $p=0.245$ and $p=0.085$ respectively). Changes in SF_{50} values observed for IGR-OV1 and M14 were significant ($p<0.001$ for both), but again did not appear to follow a discernible pattern.

In contrast, AZ12253801 appeared to induce concentration-dependent increases in relative cell viabilities in MCF7 and PC3 cells, and the observed differences between SF2 for different concentrations of AZ12253801 were significant, with most of the significance appearing to derive from an apparent increase in surviving fraction observed at 70 and 100nM AZ12253801. This was an unexpected finding and contrasts with other data, including a recent report from our group, that IGF-1R inhibition induces radiosensitivity[85,84,86].

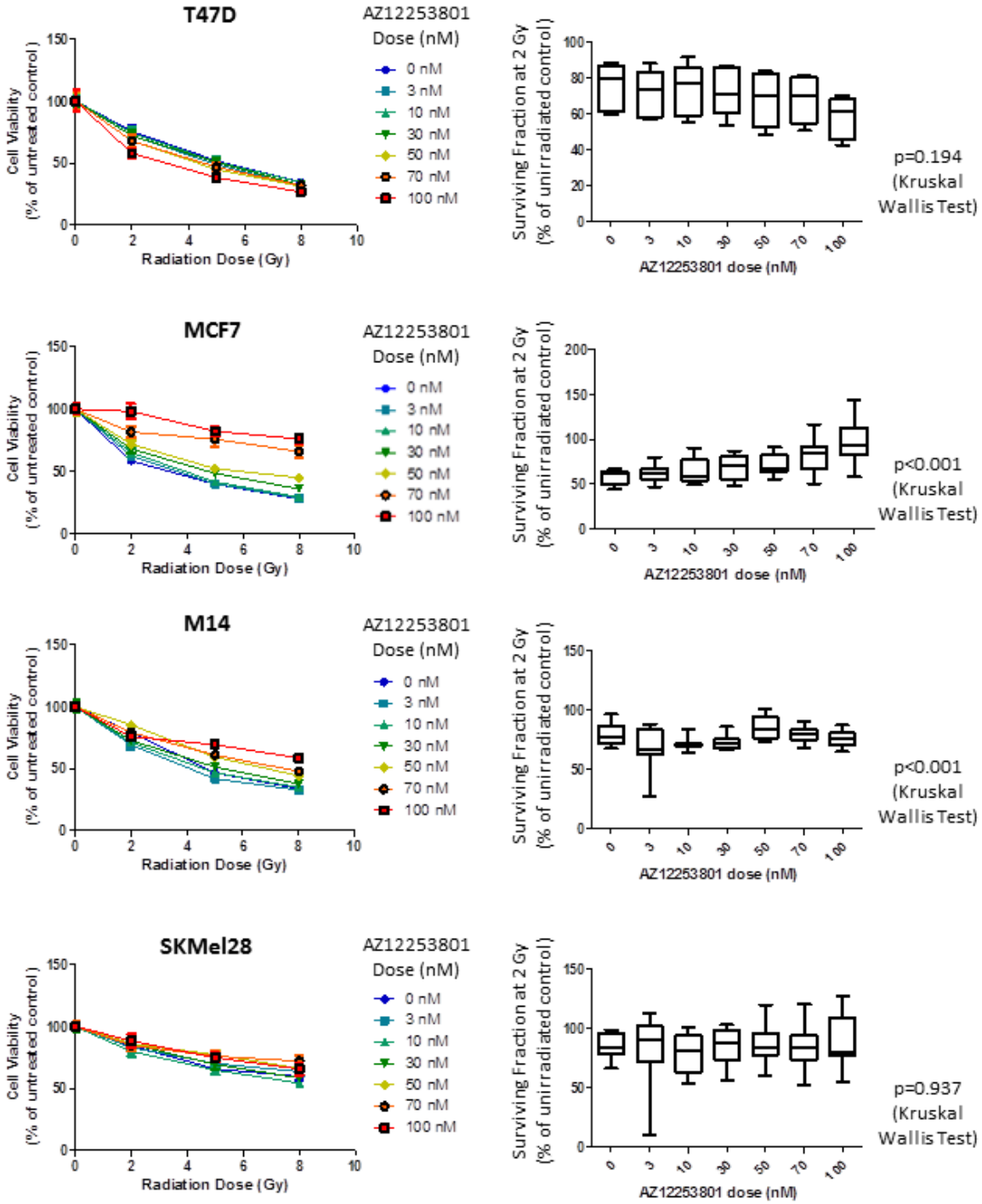


Figure 24 Examination of the effect of IGF-1R inhibition with AZ12253801 on radiosensitivity (continued overleaf). Cell viability following AZ12253801 and subsequent irradiation presented by cell line. **Left column.** Viability is represented as a percentage of unirradiated controls. Cells were seeded, allowed to adhere if appropriate, treated with solvent or AZ12253801 then irradiated 4 hours later. Five days later, cell viability was measured by fluorescence using the resazurin assay. Results represent mean ± SEM for 2 independent experiments of 8 replicates each, except data for IGR-OV1 and T47D, which represent one experiment with 8 replicates only. Cell line plots are coloured from blue through to red in order of increasing AZ12253801 concentration. **Right column.** The percentage cell viability at a radiation dose of 2Gy relative to unirradiated controls is compared between cells exposed to differing concentrations of AZ12253801 pre-treatment. Boxplots show median, range and interquartile range of viability relative to the mean of unirradiated controls. Differences between dose groups were compared using the Kruskal Wallis test.

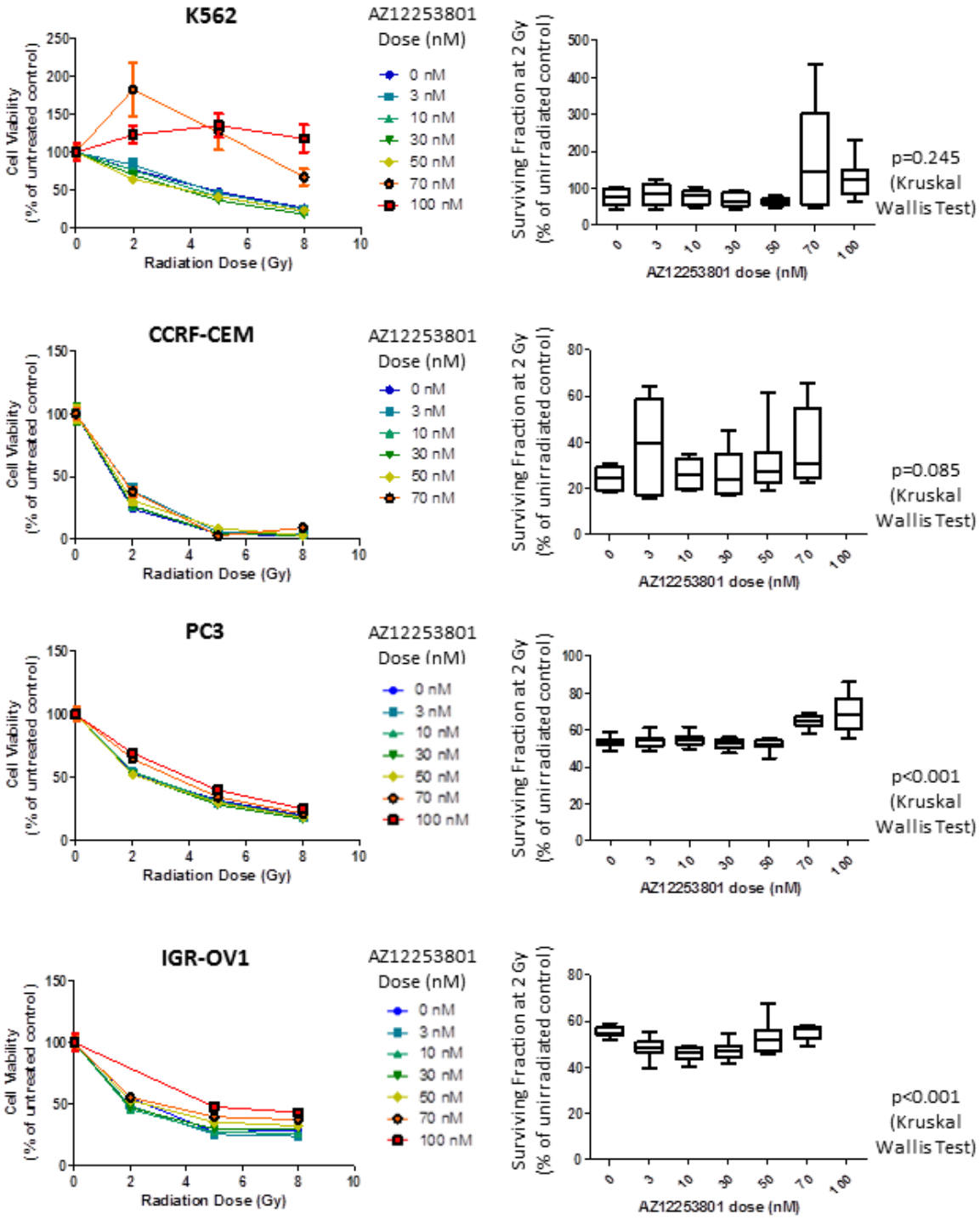


Figure 24 continued. Examination of the effect of IGF-1R inhibition with AZ12253801 on radiosensitivity

5.4.2 Effect of BMS754807 treatment on radiosensitivity

The next experiments tested effects of BMS754807 on response to irradiation, and as above the dose-response curves were used to derive SF2 values upon exposure to different concentrations of BMS754807 (Figure 25). With the exception of IGR-OV1, all cell lines appeared to show an increase in relative viability post-irradiation following exposure to increasing concentrations of BMS754807. These observed differences between SF2 for different doses of BMS754807 were significant for all cell lines bar T47D. These data suggest that BMS754807 enhances radioresistance in these cell lines, as was found for experiments using AZ12253801 in MCF7 and PC3 cells (Figure 25). In contrast, IGR-OV1 cells showed a significant reduction in SF2 values with increasing BMS754807 concentrations; suggesting modest radiosensitisation by BMS754807. The significance of this may be due to the differences between the highest 3 concentrations and further replicates of this experiment are needed before this result can be interpreted with confidence.

Figure 25 Examination of the effect of IGF-1R inhibition with BMS754807 on radiosensitivity (next 2 pages) Cell viability following BMS754807 treatment and subsequent irradiation, presented by cell line. Left column. Viability is represented as a percentage of unirradiated controls. Cells were seeded, allowed to adhere if appropriate, treated with solvent or BMS754807, then irradiated 4 hours later. Five days later, cell viability was measured by fluorescence using the resazurin assay. Results represent mean ± SEM for 2 independent experiments of 8 replicates each, except data for IGR-OV1 and T47D, which represent one experiment with 8 replicates only. Cell line plots are coloured from blue through to red in order of increasing BMS754807 concentration. Right column. The percentage cell viability at a radiation dose of 2Gy relative to unirradiated controls is compared between cells exposed to differing concentrations of BMS754807 pre-treatment. Boxplots show median, range and interquartile range of viability relative to the mean of unirradiated controls. Differences between dose groups were compared using the Kruskal Wallis test.

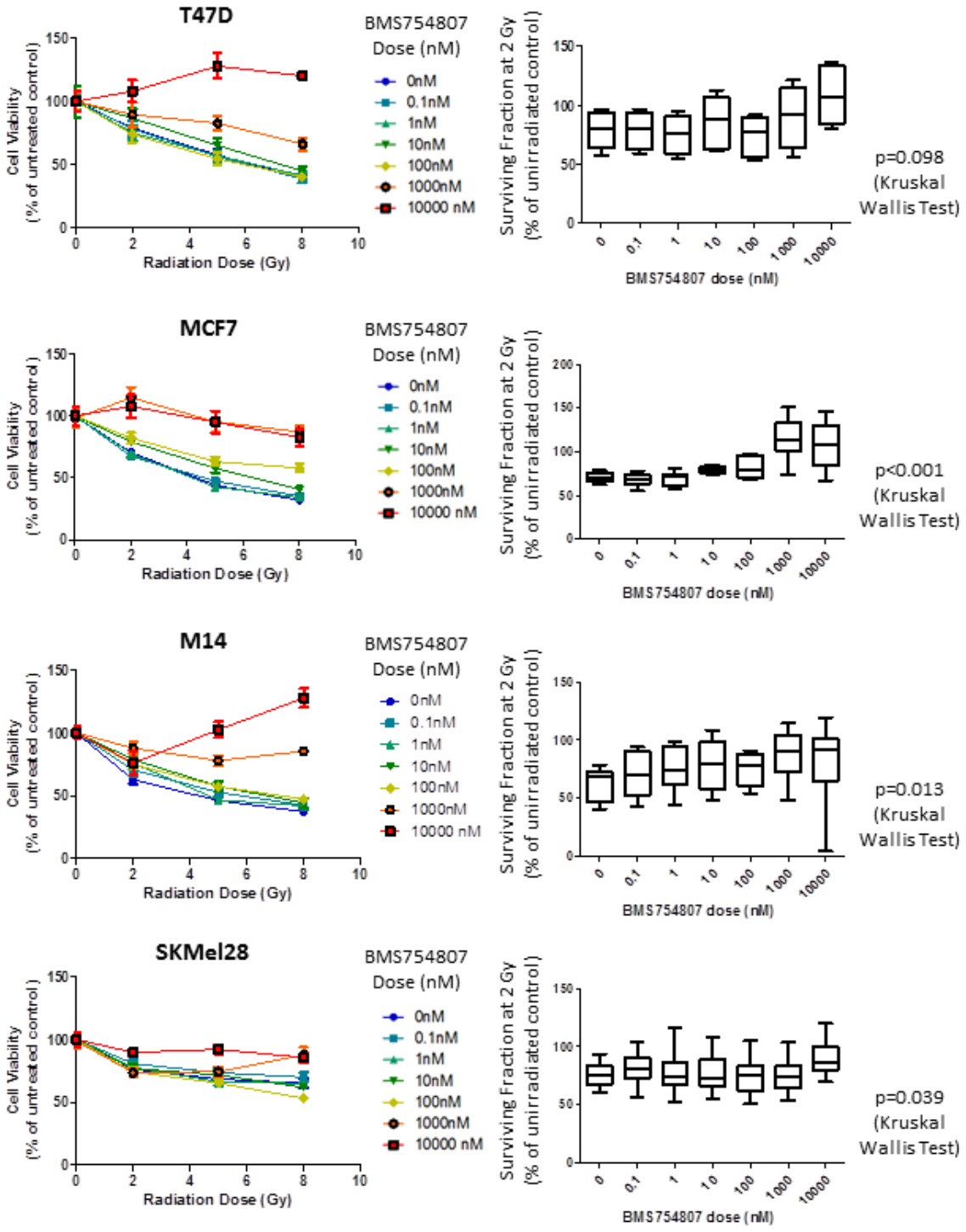


Figure 25 Examination of the effect of IGF-1R inhibition with BMS754807 on radiosensitivity

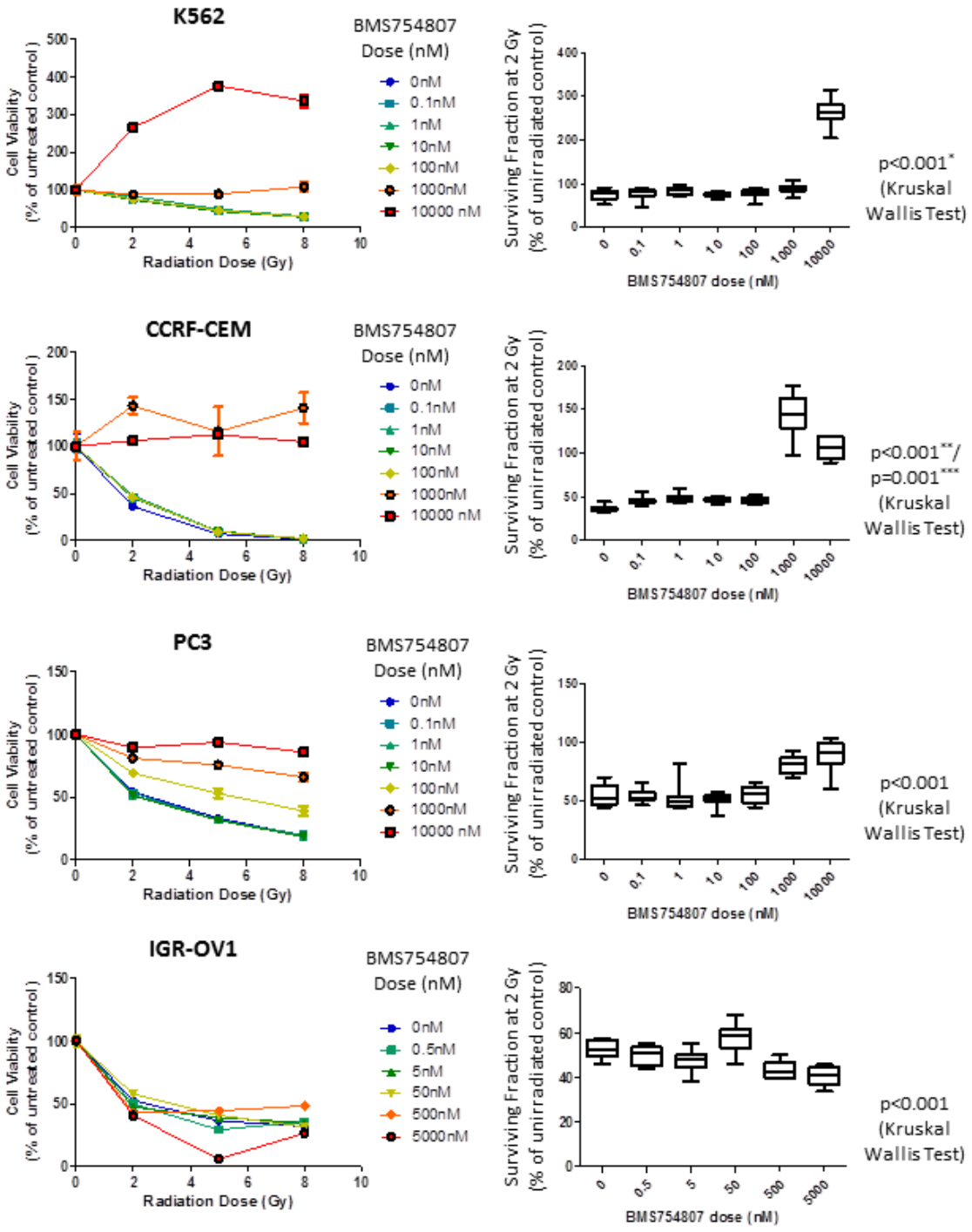


Figure 25 continued. Examination of the effect of IGF-1R inhibition with BMS754807 on radiosensitivity

5.4.3 Summary and Discussion

Examination of the raw data indicated that post-irradiation cell viability was clearly lower following pre-treatment with either AZ12253801 or BMS754807. There was evidence of a trend to radiosensitisation in T47D cells following treatment with AZ12253801 (although this represented only one experiment, which should be repeated), and significant though relatively minor radiosensitisation in IGR-OV1 cells following treatment with BMS754807. However, for most cell lines, as the concentration of BMS754807 increased, the proportion of viable cells relative to unirradiated control cells also increased. This suggested that, for most cell lines in this assay format, irradiation and BMS754807 pre-treatment were antagonistic, with BMS754807 pre-treatment inducing relative radioresistance. A similar pattern was observed following treatment of MCF7 and PC3 cells with AZ12253801: relative cell viability post-irradiation was increased by AZ12253801; again suggesting AZ12253801 pre-treatment was antagonistic to irradiation in these cell lines. For MCF7 this appeared to be a steady trend to increasing relative viability with increasing dose, whereas for PC3 no obvious difference was apparent until the concentration of AZ1225380 reached 70nM.

These results, particularly those obtained using BMS754807, seem at odds with other studies demonstrating radiosensitisation by IGF-1R inhibition[84-86,81,89,80], in particular, at the AZ12253801 concentrations found by Chitnis et al to induce a 3.8 fold sensitisation of PC3 cells, increased radioresistance was noted (Figure 24). Given the results of Chitnis and colleagues[84], the difference between these assays and those of others in the field cannot be explained away by invoking non-kinase dependent activities of the IG1-R that would be abolished by its knockdown using siRNA or antisense oligonucleotides. If the relative radioresistance observed following BMS754807 or

AZ12253801 treatment was due to IGF-1R inhibition specifically, it might be explained by delayed cell cycle progression allowing more time for DNA damage repair before cells enter mitosis, the point in the cell cycle at which cells are most radiosensitive[155]. This in turn might reduce the number of cells entering mitosis with incompletely repaired DNA and undergoing delayed nuclear fragmentation, for which our group found evidence in IGF-1R inhibited irradiated DU145 prostate cancer cells[84].

Whilst the resazurin assay has been reported to give results comparable to clonogenic assays for measuring radiation survival[112,113] it is possible that the differences observed here may reflect either the shorter duration of the resazurin assay and the fact that the assay measures cell viability rather than cell survival. The higher seeding densities in these assays may result in higher concentrations of secreted growth factors, potentially providing some degree of radioprotection. This effect could be examined by repeating these experiments in a clonogenic assay setting using media preconditioned by cells grown at a higher density.

Indeed these effects are likely not limited to increased density of tumour cells, as both cellular and matrix components of the microenvironment may modulate radiosensitivity[156-160] and chemosensitivity[161,162]. It seems likely therefore, that the inclusion of micro-environmental components in a co-culture system would help to more reliably predict the *in vivo* effect of interference in growth factor signalling on chemosensitivity and radiosensitivity. For example, the lower growth rate of prostatic carcinoma cells in the presence of osteoblasts or osteoblast conditioned media inhibited response to chemotherapy[162] and may similarly affect the ability of targeted signalling inhibition to modulate chemo- and radio-sensitivity. At their simplest, such experiments

may involve growth in medium preconditioned by stromal cells or co culture with fibroblasts, and may extend to 3D co-culture in collagen gels.

There are no reports of radiosensitisation using BMS754807, so it is difficult to ascertain from comparison with other similar studies whether the differences might relate to differences in assay format, scheduling effects or to off-target effects on the kinases such aurora kinases or Trk A and B. The correlation observed between the GI_{50} values for BMS754807 and the more specific AZ12253801 suggests that at levels around the GI_{50}, the major mechanism by which BMS754807 inhibits cell viability is IGF-1R kinase inhibition. Whilst inhibition of the IGF-1R kinase has been shown to impair the DNA damage response and sensitise to radiation [84], this does not imply that all effects of BMS754807 with regards response to radiation are IGF-1R related, nor does it mean that the effects on IGF-1R are the predominant effect.

Indeed, given the apparent difference in effect between these two inhibitors, with BMS754807 inducing radioresistance to a greater degree than observed with AZ12253801, these effects may not be IGF-1R related. The IC_{50} values of BMS754807 for Trk A and Trk B are 7 and 4nM respectively[78], well within the ranges examined in the current study. Inhibition of these receptor tyrosine kinases has been shown to be radioprotective in human umbilical vein endothelial cells[163]. This could be tested by re-examining the effect of BMS754807 on radiosensitivity in TrkA/B null cells or in the radio-protected cell lines following siRNA knockdown of Trk A and B. Further support could be garnered by comparing expression and activation of Trk A and B in the cell lines examined, if IGR-OV1 were to have low or non-functional TrkA and TrkB, that might suggest that the sensitisation observed on exposure to BMS754807 reflected the effects

of IGF-1R kinase inhibition unmasked by lack of Trk A or B. It would also be interesting to see whether OSI-906, a more specific IGF-1R inhibitor than BMS754807 produced similar results.

6 Conclusion

In conclusion, SNP rs4966013 significantly correlated with both IGF-1R protein and mRNA expression when assuming a dominant model, whilst *IGF-1R* mRNA expression significantly correlates with IGF-1R protein expression. Given the higher topotecan GI_{50}s in high IGF-1R expressing cell lines, it seems worth examining this further in a larger more homogenous panel of cell lines of tumour types in which topotecan and other topoisomerase I inhibitors are used clinically. Furthermore, both SNP rs4966013 genotype and immunohistochemical IGF-1R expression could be examined in patient tissues. Given the correlation of resistance to mitozolomide with *IGF-1R* mRNA, and that tumour tissues from melanoma patients treated with a closely related drug, dacarbazine, are available, SNP genotype and immunohistochemical investigations could be performed in future.

Whilst data regarding BMS754807 in particular suggested that IGF-1R inhibition was antagonistic to the effects of radiation, these may well relate to off target effects including inhibition of TrkA and TrkB as described above. Other studies performed in this laboratory and elsewhere support a role for IGF-1R in radioresistance[84,81,85,80,89] and would be consistent with the increased radiation GI_{50} amongst high *IGF-1R* mRNA expressing cell lines in this small panel. If time had permitted, the role of IGF-1R would have been explored further in prostate biopsy tissues from patients with localised cancer treated with radiotherapy.

Ideally, the link between SNP rs4966013 and chemo-radiosensitivity would be tested in material from patients treated with IGF-1R inhibitors or antagonistic antibodies in clinical trials. The magnitude of sensitisation observed in patients with either a GG genotype or high IGF-1R expression could be examined to test the hypothesis that high IGF-1R or SNP genotype would predict the benefit obtained from IGF-1R inhibitory drugs. However, due to trial consents, access to this material is currently not possible despite

the willingness of pharmaceutical companies to participate. This in turn could be addressed by widening trial consents to allow post hoc analysis of newly identified or candidate biomarkers.

References

1. Office of National Statistics. Cancer Incidence and Mortality in the United Kingdom, 2008-10 http://www.ons.gov.uk/ons/rel/cancer-unit/cancer-incidence-and-mortality/2008-2010/stb-cancer-incidence-and-mortality-in-the-united-kindom--2008-2010.html: UK Statistics Authority; 2012 [updated 06 December 2012 cited 2013 22/11/2013].
2. Roos WP, Kaina B. DNA damage-induced cell death: from specific DNA lesions to the DNA damage response and apoptosis. Cancer Lett. 2013 May 28;332(2):237-48.
3. Eriksson D, Stigbrand T. Radiation-induced cell death mechanisms. Tumour Biol. 2010 Aug;31(4):363-72.
4. Daly MJ. Death by protein damage in irradiated cells. DNA Repair (Amst). 2012 Jan 2;11(1):12-21.
5. Middleton MR, Margison GP. Improvement of chemotherapy efficacy by inactivation of a DNA-repair pathway. Lancet Oncol. 2003 Jan;4(1):37-44.
6. Fu D, Calvo JA, Samson LD. Balancing repair and tolerance of DNA damage caused by alkylating agents. Nat Rev Cancer. 2012 Feb;12(2):104-20.
7. Siddik ZH. Cisplatin: mode of cytotoxic action and molecular basis of resistance. Oncogene. 2003 Oct 20;22(47):7265-79.
8. Faivre S, Chan D, Salinas R, Woynarowska B, Woynarowski JM. DNA strand breaks and apoptosis induced by oxaliplatin in cancer cells. Biochem Pharmacol. 2003 Jul 15;66(2):225-37.
9. Perez EA. Microtubule inhibitors: Differentiating tubulin-inhibiting agents based on mechanisms of action, clinical activity, and resistance. Mol Cancer Ther. 2009 Aug;8(8):2086-95.
10. Murray S, Briasoulis E, Linardou H, Bafaloukos D, Papadimitriou C. Taxane resistance in breast cancer: mechanisms, predictive biomarkers and circumvention strategies. Cancer Treat Rev. 2012 Nov;38(7):890-903.
11. Jordan MA, Wilson L. Microtubules as a target for anticancer drugs. Nat Rev Cancer. 2004 Apr;4(4):253-65.
12. Sharp DJ, Rogers GC, Scholey JM. Microtubule motors in mitosis. Nature. 2000 Sep 7;407(6800):41-7.
13. Cox CD, Breslin MJ, Mariano BJ, Coleman PJ, Buser CA, Walsh ES, et al. Kinesin spindle protein (KSP) inhibitors. Part 1: The discovery of 3,5-diaryl-4,5-dihydropyrazoles as potent and selective inhibitors of the mitotic kinesin KSP. Bioorg Med Chem Lett. 2005 Apr 15;15(8):2041-5.
14. Chen SH, Chan NL, Hsieh TS. New mechanistic and functional insights into DNA topoisomerases. Annu Rev Biochem. 2013;82:139-70.
15. Tomicic MT, Kaina B. Topoisomerase degradation, DSB repair, p53 and IAPs in cancer cell resistance to camptothecin-like topoisomerase I inhibitors. Biochim Biophys Acta. 2013 Jan;1835(1):11-27.
16. Pommier Y. DNA topoisomerase I inhibitors: chemistry, biology, and interfacial inhibition. Chem Rev. 2009 Jul;109(7):2894-902.
17. Pommier Y, Redon C, Rao VA, Seiler JA, Sordet O, Takemura H, et al. Repair of and checkpoint response to topoisomerase I-mediated DNA damage. Mutat Res. 2003 Nov 27;532(1-2):173-203.
18. Martinez-Garcia B, Fernandez X, Diaz-Ingelmo O, Rodriguez-Campos A, Manichanh C, Roca J. Topoisomerase II minimizes DNA entanglements by proofreading DNA topology after DNA strand passage. Nucleic Acids Res. 2013 Oct 31.

19. Pommier Y, Leo E, Zhang H, Marchand C. DNA topoisomerases and their poisoning by anticancer and antibacterial drugs. Chem Biol. 2010 May 28;17(5):421-33.
20. Nitiss JL. Targeting DNA topoisomerase II in cancer chemotherapy. Nat Rev Cancer. 2009 May;9(5):338-50.
21. Parker WB. Enzymology of purine and pyrimidine antimetabolites used in the treatment of cancer. Chem Rev. 2009 Jul;109(7):2880-93.
22. Sampath D, Rao VA, Plunkett W. Mechanisms of apoptosis induction by nucleoside analogs. Oncogene. 2003 Dec 8;22(56):9063-74.
23. Gowher H, Jeltsch A. Mechanism of inhibition of DNA methyltransferases by cytidine analogs in cancer therapy. Cancer Biol Ther. 2004 Nov;3(11):1062-8.
24. Verbeek B, Southgate TD, Gilham DE, Margison GP. O6-Methylguanine-DNA methyltransferase inactivation and chemotherapy. Br Med Bull. 2008;85:17-33. Epub 2008/02/05.
25. Mladenov E, Iliakis G. Induction and repair of DNA double strand breaks: the increasing spectrum of non-homologous end joining pathways. Mutat Res. 2011 Jun 3;711(1-2):61-72.
26. Thompson LH. Recognition, signaling, and repair of DNA double-strand breaks produced by ionizing radiation in mammalian cells: the molecular choreography. Mutat Res. 2012 Oct-Dec;751(2):158-246.
27. Lamarche BJ, Orazio NI, Weitzman MD. The MRN complex in double-strand break repair and telomere maintenance. FEBS Lett. 2010 Sep 10;584(17):3682-95.
28. Jackson SP. Sensing and repairing DNA double-strand breaks. Carcinogenesis. 2002 May;23(5):687-96.
29. Mahaney BL, Meek K, Lees-Miller SP. Repair of ionizing radiation-induced DNA double-strand breaks by non-homologous end-joining. Biochem J. 2009 Feb 1;417(3):639-50.
30. McHugh PJ, Spanswick VJ, Hartley JA. Repair of DNA interstrand crosslinks: molecular mechanisms and clinical relevance. Lancet Oncol. 2001 Aug;2(8):483-90.
31. Tapias A, Auriol J, Forget D, Enzlin JH, Scharer OD, Coin F, et al. Ordered conformational changes in damaged DNA induced by nucleotide excision repair factors. J Biol Chem. 2004 Apr 30;279(18):19074-83.
32. Sousa FG, Matuo R, Soares DG, Escargueil AE, Henriques JA, Larsen AK, et al. PARPs and the DNA damage response. Carcinogenesis. 2012 Aug;33(8):1433-40.
33. Dantzer F, Ame JC, Schreiber V, Nakamura J, Menissier-de Murcia J, de Murcia G. Poly(ADP-ribose) polymerase-1 activation during DNA damage and repair. Methods Enzymol. 2006;409:493-510.
34. Krokan HE, Bjoras M. Base excision repair. Cold Spring Harb Perspect Biol. 2013 Apr;5(4):a012583.
35. Tobias J, Hochhauser D. Systemic Treatment for Cancer. Cancer and its Management: Wiley-Blackwell; 2009. p. 77-106.
36. Ennulat D, Walker D, Clemo F, Magid-Slav M, Ledieu D, Graham M, et al. Effects of Hepatic Drug-metabolizing Enzyme Induction on Clinical Pathology Parameters in Animals and Man. Toxicologic Pathology. 2010;38(5):810-28.
37. Hall E JGA, J. Radiobiology for the Radiologist. 7th ed: Lippincott, Williams and Williams; 2011.
38. Rebucci M, Michiels C. Molecular aspects of cancer cell resistance to chemotherapy. Biochem Pharmacol. 2013 May 1;85(9):1219-26.
39. Cui Y, Konig J, Buchholz JK, Spring H, Leier I, Keppler D. Drug resistance and ATP-dependent conjugate transport mediated by the apical multidrug resistance protein, MRP2, permanently expressed in human and canine cells. Mol Pharmacol. 1999 May;55(5):929-37.
40. Gonen N, Assaraf YG. Antifolates in cancer therapy: structure, activity and mechanisms of drug resistance. Drug Resist Updat. 2012 Aug;15(4):183-210.

41. Kawate H, Landis DM, Loeb LA. Distribution of mutations in human thymidylate synthase yielding resistance to 5-fluorodeoxyuridine. J Biol Chem. 2002 Sep 27;277(39):36304-11.
42. Jewell R, Conway C, Mitra A, Randerson-Moor J, Lobo S, Nsengimana J, et al. Patterns of expression of DNA repair genes and relapse from melanoma. Clin Cancer Res. 2010 Nov 1;16(21):5211-21.
43. Curtin NJ. DNA repair dysregulation from cancer driver to therapeutic target. Nat Rev Cancer. 2012 Dec;12(12):801-17.
44. Felip E, Martinez P. Can sensitivity to cytotoxic chemotherapy be predicted by biomarkers? Ann Oncol. 2012 Sep;23 Suppl 10:x189-92.
45. Wang L, Mosel AJ, Oakley GG, Peng A. Deficient DNA damage signaling leads to chemoresistance to cisplatin in oral cancer. Mol Cancer Ther. 2012 Nov;11(11):2401-9.
46. Parikh RA, White JS, Huang X, Schoppy DW, Baysal BE, Baskaran R, et al. Loss of distal 11q is associated with DNA repair deficiency and reduced sensitivity to ionizing radiation in head and neck squamous cell carcinoma. Genes, Chromosomes and Cancer. 2007;46(8):761-75.
47. Geier A, Beery R, Haimsohn M, Karasik A. Insulin-like growth factor-1 inhibits cell death induced by anticancer drugs in the MCF-7 cells: involvement of growth factors in drug resistance. Cancer Invest. 1995;13(5):480-6.
48. Duxbury MS, Ito H, Zinner MJ, Ashley SW, Whang EE. Inhibition of SRC tyrosine kinase impairs inherent and acquired gemcitabine resistance in human pancreatic adenocarcinoma cells. Clin Cancer Res. 2004 Apr 1;10(7):2307-18.
49. Chen J. Roles of the PI3K/Akt pathway in Epstein-Barr virus-induced cancers and therapeutic implications. World J Virol. 2012 Dec 12;1(6):154-61.
50. Matheny RW, Jr., Adamo ML. Current perspectives on Akt Akt-ivation and Akt-ions. Exp Biol Med (Maywood). 2009 Nov;234(11):1264-70.
51. Whang YE, Yuan XJ, Liu Y, Majumder S, Lewis TD. Regulation of sensitivity to TRAIL by the PTEN tumor suppressor. Vitam Horm. 2004;67:409-26. Epub 2004/04/28.
52. Burris HA, 3rd. Overcoming acquired resistance to anticancer therapy: focus on the PI3K/AKT/mTOR pathway. Cancer Chemother Pharmacol. 2013 Apr;71(4):829-42.
53. De Luca A, Maiello MR, D'Alessio A, Pergameno M, Normanno N. The RAS/RAF/MEK/ERK and the PI3K/AKT signalling pathways: role in cancer pathogenesis and implications for therapeutic approaches. Expert Opin Ther Targets. 2012 Apr;16 Suppl 2:S17-27.
54. Staudt LM. Oncogenic activation of NF-kappaB. Cold Spring Harb Perspect Biol. 2010 Jun;2(6):a000109.
55. Glasgow JN, Qiu J, Rassin D, Grafe M, Wood T, Perez-Pol JR. Transcriptional regulation of the BCL-X gene by NF-kappaB is an element of hypoxic responses in the rat brain. Neurochem Res. 2001 Jun;26(6):647-59.
56. Burrell RA, McGranahan N, Bartek J, Swanton C. The causes and consequences of genetic heterogeneity in cancer evolution. Nature. 2013 Sep 19;501(7467):338-45.
57. Vogelstein B, Lane D, Levine AJ. Surfing the p53 network. Nature. 2000 Nov 16;408(6810):307-10.
58. Appella E, Anderson CW. Post-translational modifications and activation of p53 by genotoxic stresses. Eur J Biochem. 2001 May;268(10):2764-72.
59. Agarwal ML, Agarwal A, Taylor WR, Chernova O, Sharma Y, Stark GR. A p53-dependent S-phase checkpoint helps to protect cells from DNA damage in response to starvation for pyrimidine nucleotides. Proc Natl Acad Sci U S A. 1998 Dec 8;95(25):14775-80.
60. Hastak K, Paul RK, Agarwal MK, Thakur VS, Amin AR, Agrawal S, et al. DNA synthesis from unbalanced nucleotide pools causes limited DNA damage that triggers ATR-CHK1-dependent p53 activation. Proc Natl Acad Sci U S A. 2008 Apr 29;105(17):6314-9.

61. Vazquez A, Bond EE, Levine AJ, Bond GL. The genetics of the p53 pathway, apoptosis and cancer therapy. Nat Rev Drug Discov. 2008;7(12):979-87.
62. O'Connor PM, Jackman J, Bae I, Myers TG, Fan S, Mutoh M, et al. Characterization of the p53 tumor suppressor pathway in cell lines of the National Cancer Institute anticancer drug screen and correlations with the growth-inhibitory potency of 123 anticancer agents. Cancer Res. 1997 Oct 1;57(19):4285-300.
63. Bond GL, Hu W, Bond EE, Robins H, Lutzker SG, Arva NC, et al. A single nucleotide polymorphism in the MDM2 promoter attenuates the p53 tumor suppressor pathway and accelerates tumor formation in humans. Cell. 2004 Nov 24;119(5):591-602.
64. Aleksic T, Chitnis MM, Perestenko OV, Gao S, Thomas PH, Turner GD, et al. Type 1 insulin-like growth factor receptor translocates to the nucleus of human tumor cells. Cancer Res. 2010 Aug 15;70(16):6412-9.
65. Hellawell GO, Turner GD, Davies DR, Poulsom R, Brewster SF, Macaulay VM. Expression of the type 1 insulin-like growth factor receptor is up-regulated in primary prostate cancer and commonly persists in metastatic disease. Cancer Res. 2002 May 15;62(10):2942-50.
66. Turney BW, Turner GD, Brewster SF, Macaulay VM. Serial analysis of resected prostate cancer suggests up-regulation of type 1 IGF receptor with disease progression. BJU Int. 2011 May;107(9):1488-99.
67. Liu J, Pan S, Zhou Y, Yu Z, Liu L. [Expression and significance of IGF-IR and PKC in laryngeal squamous cell carcinoma]. Lin Chung Er Bi Yan Hou Tou Jing Wai Ke Za Zhi. 2010 Feb;24(4):152-5.
68. Bhargava R, Beriwal S, McManus K, Dabbs DJ. Insulin-like growth factor receptor-1 (IGF-1R) expression in normal breast, proliferative breast lesions, and breast carcinoma. Appl Immunohistochem Mol Morphol. 2011 May;19(3):218-25.
69. Turner BC, Haffty BG, Narayanan L, Yuan J, Havre PA, Gumbs AA, et al. Insulin-like growth factor-I receptor overexpression mediates cellular radioresistance and local breast cancer recurrence after lumpectomy and radiation. Cancer Res. 1997 Aug 1;57(15):3079-83.
70. Adams TE, Epa VC, Garrett TP, Ward CW. Structure and function of the type 1 insulin-like growth factor receptor. Cell Mol Life Sci. 2000 Jul;57(7):1050-93.
71. Pandini G, Frasca F, Mineo R, Sciacca L, Vigneri R, Belfiore A. Insulin/insulin-like growth factor I hybrid receptors have different biological characteristics depending on the insulin receptor isoform involved. J Biol Chem. 2002 Oct 18;277(42):39684-95.
72. Baserga R. The IGF-I receptor in cancer research. Exp Cell Res. 1999 Nov 25;253(1):1-6.
73. Sell C, Baserga R, Rubin R. Insulin-like growth factor I (IGF-I) and the IGF-I receptor prevent etoposide-induced apoptosis. Cancer Res. 1995 Jan 15;55(2):303-6.
74. Jackson JG, Zhang X, Yoneda T, Yee D. Regulation of breast cancer cell motility by insulin receptor substrate-2 (IRS-2) in metastatic variants of human breast cancer cell lines. Oncogene. 2001 Nov 1;20(50):7318-25.
75. Maile LA, Imai Y, Clarke JB, Clemmons DR. Insulin-like growth factor I increases alpha Vbeta 3 affinity by increasing the amount of integrin-associated protein that is associated with non-raft domains of the cellular membrane. J Biol Chem. 2002 Jan 18;277(3):1800-5.
76. Flanigan SA, Pitts TM, Eckhardt SG, Tentler JJ, Tan AC, Thorburn A, et al. The Insulin-like Growth Factor I Receptor/Insulin Receptor Tyrosine Kinase Inhibitor PQIP Exhibits Enhanced Antitumor Effects in Combination with Chemotherapy Against Colorectal Cancer Models. Clinical Cancer Research. 2010 November 15, 2010;16(22):5436-46.
77. Dunn SE, Hardman RA, Kari FW, Barrett JC. Insulin-like growth factor 1 (IGF-1) alters drug sensitivity of HBL100 human breast cancer cells by inhibition of apoptosis induced by diverse anticancer drugs. Cancer Res. 1997 Jul 1;57(13):2687-93.
78. Carboni JM, Wittman M, Yang Z, Lee F, Greer A, Hurlburt W, et al. BMS-754807, a small molecule inhibitor of insulin-like growth factor-1R/IR. Mol Cancer Ther. 2009 Dec;8(12):3341-9.

79. Kai K, D'Costa S, Sills RC, Kim Y. Inhibition of the insulin-like growth factor 1 receptor pathway enhances the antitumor effect of cisplatin in human malignant mesothelioma cell lines. Cancer Lett. 2009 Jun 8;278(1):49-55.
80. Macaulay VM, Salisbury AJ, Bohula EA, Playford MP, Smorodinsky NI, Shiloh Y. Downregulation of the type 1 insulin-like growth factor receptor in mouse melanoma cells is associated with enhanced radiosensitivity and impaired activation of Atm kinase. Oncogene. 2001 Jul 5;20(30):4029-40.
81. Rochester MA, Riedemann J, Hellawell GO, Brewster SF, Macaulay VM. Silencing of the IGF1R gene enhances sensitivity to DNA-damaging agents in both PTEN wild-type and mutant human prostate cancer. Cancer Gene Ther. 2005 Jan;12(1):90-100.
82. Hellawell GO, Ferguson DJ, Brewster SF, Macaulay VM. Chemosensitization of human prostate cancer using antisense agents targeting the type 1 insulin-like growth factor receptor. BJU Int. 2003 Feb;91(3):271-7.
83. Trojanek J, Ho T, Del Valle L, Nowicki M, Wang JY, Lassak A, et al. Role of the insulin-like growth factor I/insulin receptor substrate 1 axis in Rad51 trafficking and DNA repair by homologous recombination. Mol Cell Biol. 2003 Nov;23(21):7510-24.
84. Chitnis MM, Lodhia KA, Aleksic T, Gao S, Protheroe AS, Macaulay VM. IGF-1R inhibition enhances radiosensitivity and delays double-strand break repair by both non-homologous end-joining and homologous recombination. Oncogene. 2013 Nov 4.
85. Turney BW, Kerr M, Chitnis MM, Lodhia K, Wang Y, Riedemann J, et al. Depletion of the type 1 IGF receptor delays repair of radiation-induced DNA double strand breaks. Radiother Oncol. 2012 Jun;103(3):402-9.
86. Ferte C, Loriot Y, Clemenson C, Commo F, Gombos A, Bibault JE, et al. IGF-1R targeting increases the antitumor effects of DNA-damaging agents in SCLC model: an opportunity to increase the efficacy of standard therapy. Mol Cancer Ther. 2013 Jul;12(7):1213-22.
87. Peretz S, Jensen R, Baserga R, Glazer PM. ATM-dependent expression of the insulin-like growth factor-I receptor in a pathway regulating radiation response. Proc Natl Acad Sci U S A. 2001 Feb 13;98(4):1676-81.
88. Shahrabani-Gargir L, Pandita TK, Werner H. Ataxia-telangiectasia mutated gene controls insulin-like growth factor I receptor gene expression in a deoxyribonucleic acid damage response pathway via mechanisms involving zinc-finger transcription factors Sp1 and WT1. Endocrinology. 2004 Dec;145(12):5679-87.
89. Riesterer O, Yang Q, Raju U, Torres M, Molkentine D, Patel N, et al. Combination of anti-IGF-1R antibody A12 and ionizing radiation in upper respiratory tract cancers. Int J Radiat Oncol Biol Phys. 2011 Mar 15;79(4):1179-87.
90. Blume SW, Jackson NL, Frost AR, Grizzle WE, Shcherbakov OD, Choi H, et al. Northwestern profiling of potential translation-regulatory proteins in human breast epithelial cells and malignant breast tissues: evidence for pathological activation of the IGF1R IRES. Exp Mol Pathol. 2010 Jun;88(3):341-52.
91. Meng Z, Snyder RC, Shrestha K, Miller DM, Emanuel PD, Blume SW. Evidence for differential ribonucleoprotein complex assembly in vitro on the 5'-untranslated region of the human IGF-IR transcript. Mol Cell Endocrinol. 2003 Feb 28;200(1-2):127-40.
92. Park ES, Rabinovsky R, Carey M, Hennessy BT, Agarwal R, Liu W, et al. Integrative analysis of proteomic signatures, mutations, and drug responsiveness in the NCI 60 cancer cell line set. Mol Cancer Ther. 2010 Feb;9(2):257-67.
93. Amundson SA, Do KT, Vinikoor LC, Lee RA, Koch-Paiz CA, Ahn J, et al. Integrating global gene expression and radiation survival parameters across the 60 cell lines of the National Cancer Institute Anticancer Drug Screen. Cancer Res. 2008 Jan 15;68(2):415-24.
94. Yang W, Soares J, Greninger P, Edelman EJ, Lightfoot H, Forbes S, et al. Genomics of Drug Sensitivity in Cancer (GDSC): a resource for therapeutic biomarker discovery in cancer cells. Nucleic Acids Res. 2013 Jan;41(Database issue):D955-61.

95. Girnita L, Shenoy SK, Sehat B, Vasilcanu R, Girnita A, Lefkowitz RJ, et al. {beta}-Arrestin is crucial for ubiquitination and down-regulation of the insulin-like growth factor-1 receptor by acting as adaptor for the MDM2 E3 ligase. J Biol Chem. 2005 Jul 1;280(26):24412-9.
96. Vecchione A, Marchese A, Henry P, Rotin D, Morrione A. The Grb10/Nedd4 complex regulates ligand-induced ubiquitination and stability of the insulin-like growth factor I receptor. Mol Cell Biol. 2003 May;23(9):3363-72.
97. Garraway LA, Widlund HR, Rubin MA, Getz G, Berger AJ, Ramaswamy S, et al. Integrative genomic analyses identify MITF as a lineage survival oncogene amplified in malignant melanoma. Nature. 2005 Jul 7;436(7047):117-22.
98. Barretina J, Caponigro G, Stransky N, Venkatesan K, Margolin AA, Kim S, et al. The Cancer Cell Line Encyclopedia enables predictive modelling of anticancer drug sensitivity. Nature. 2012 Mar 29;483(7391):603-7.
99. Gomez-Gutierrez JG, Souza V, Hao HY, Montes de Oca-Luna R, Dong YB, Zhou HS, et al. Adenovirus-mediated gene transfer of FKHRL1 triple mutant efficiently induces apoptosis in melanoma cells. Cancer Biol Ther. 2006 Jul;5(7):875-83.
100. Packer L, Pavey S, Parker A, Stark M, Johansson P, Clarke B, et al. Osteopontin is a downstream effector of the PI3-kinase pathway in melanomas that is inversely correlated with functional PTEN. Carcinogenesis. 2006 Sep;27(9):1778-86.
101. Tsao H, Goel V, Wu H, Yang G, Haluska FG. Genetic interaction between NRAS and BRAF mutations and PTEN/MMAC1 inactivation in melanoma. J Invest Dermatol. 2004 Feb;122(2):337-41.
102. Vasudevan KM, Barbie DA, Davies MA, Rabinovsky R, McNear CJ, Kim JJ, et al. AKT-independent signaling downstream of oncogenic PIK3CA mutations in human cancer. Cancer Cell. 2009 Jul 7;16(1):21-32.
103. Wu D, Sylvester JE, Parker LL, Zhou G, Kron SJ. Peptide reporters of kinase activity in whole cell lysates. Biopolymers. 2010;94(4):475-86. Epub 2010/07/02.
104. Kataoka Y, Mukohara T, Shimada H, Saijo N, Hirai M, Minami H. Association between gain-of-function mutations in PIK3CA and resistance to HER2-targeted agents in HER2-amplified breast cancer cell lines. Ann Oncol. 2010 Feb;21(2):255-62.
105. Hales EC, Orr SM, Larson Gedman A, Taub JW, Matherly LH. Notch1 receptor regulates AKT protein activation loop (Thr308) dephosphorylation through modulation of the PP2A phosphatase in phosphatase and tensin homolog (PTEN)-null T-cell acute lymphoblastic leukemia cells. J Biol Chem. 2013 Aug 2;288(31):22836-48.
106. Ikediobi ON, Davies H, Bignell G, Edkins S, Stevens C, O'Meara S, et al. Mutation analysis of 24 known cancer genes in the NCI-60 cell line set. Mol Cancer Ther. 2006 Nov;5(11):2606-12.
107. Domcke S, Sinha R, Levine DA, Sander C, Schultz N. Evaluating cell lines as tumour models by comparison of genomic profiles. Nat Commun. 2013;4:2126.
108. Spurrier B, Ramalingam S, Nishizuka S. Reverse-phase protein lysate microarrays for cell signaling analysis. Nat Protoc. 2008;3(11):1796-808.
109. Prager D, Li HL, Asa S, Melmed S. Dominant negative inhibition of tumorigenesis in vivo by human insulin-like growth factor I receptor mutant. Proc Natl Acad Sci U S A. 1994 Mar 15;91(6):2181-5.
110. Gonzalez RJ, Tarloff JB. Evaluation of hepatic subcellular fractions for Alamar blue and MTT reductase activity. Toxicol In Vitro. 2001 Jun;15(3):257-9.
111. O'Brien J, Wilson I, Orton T, Pognan F. Investigation of the Alamar Blue (resazurin) fluorescent dye for the assessment of mammalian cell cytotoxicity. Eur J Biochem. 2000 Sep;267(17):5421-6.
112. Anoopkumar-Dukie S, Carey JB, Conere T, O'Sullivan E, van Pelt FN, Allshire A. Resazurin assay of radiation response in cultured cells. Br J Radiol. 2005 Oct;78(934):945-7.

113. Buch K, Peters T, Nawroth T, Sanger M, Schmidberger H, Langguth P. Determination of cell survival after irradiation via clonogenic assay versus multiple MTT Assay--a comparative study. Radiat Oncol. 2012;7:1.
114. Huizing MT, Vermorken JB, Rosing H, Huinink WWtB, Mandjes I, Pinedo HM, et al. Pharmacokinetics of paclitaxel and three major metabolites in patients with advanced breast carcinoma refractory to anthracycline therapy treated with a 3-hour paclitaxel infusion: A European Cancer Centre (ECC) trial. Annals of Oncology. 1995 September 1, 1995;6(7):699-704.
115. Schellens JHGC, J.;Beijnen, J. H. ; Rosing, H.; de Boer-Dennert, M.; McDonald, M.; Davies, B.; Verweij, J. . Bioavailability and pharmacokinetics of oral topotecan: a new topoisomerase I inhibitor. Br J Cancer. 1996 1996 May;73(10):1268–71.
116. de Jonge MJ, Loos WJ, Gelderblom H, Planting AS, van der Burg ME, Sparreboom A, et al. Phase I pharmacologic study of oral topotecan and intravenous cisplatin: sequence-dependent hematologic side effects. J Clin Oncol. 2000 May;18(10):2104-15.
117. Kruijtzer CMF, Beijnen JH, Rosing H, ten Bokkel Huinink WW, Schot M, Jewell RC, et al. Increased Oral Bioavailability of Topotecan in Combination With the Breast Cancer Resistance Protein and P-Glycoprotein Inhibitor GF120918. Journal of Clinical Oncology. 2002 July 1, 2002;20(13):2943-50.
118. Campos PF, Gilbert TM. DNA extraction from formalin-fixed material. Methods Mol Biol. 2012;840:81-5.
119. Bielen A, Box G, Perryman L, Bjerke L, Popov S, Jamin Y, et al. Dependence of Wilms tumor cells on signaling through insulin-like growth factor 1 in an orthotopic xenograft model targetable by specific receptor inhibition. Proc Natl Acad Sci U S A. 2012 May 15;109(20):E1267-76.
120. Stein SM, Tiersten A, Hochster HS, Blank SV, Pothuri B, Curtin J, et al. A phase 2 study of oxaliplatin combined with continuous infusion topotecan for patients with previously treated ovarian cancer. Int J Gynecol Cancer. 2013 Nov;23(9):1577-82. Epub 2013/11/01.
121. Owonikoko TK, Aisner J, Wang XV, Dahlberg SE, Rubin EH, Ramalingam SS, et al. E5501: phase II study of topotecan sequenced with etoposide/cisplatin, and irinotecan/cisplatin sequenced with etoposide for extensive-stage small-cell lung cancer. Cancer Chemother Pharmacol. 2013 Nov 28.
122. Rossi A, Martelli O, Di Maio M. Treatment of patients with small-cell lung cancer: from meta-analyses to clinical practice. Cancer Treat Rev. 2013 Aug;39(5):498-506.
123. Spindler KG, Appelt AL, Pallisgaard N, Andersen RF, Jakobsen A. KRAS-mutated plasma DNA as predictor of outcome from irinotecan monotherapy in metastatic colorectal cancer. Br J Cancer. 2013 Nov 21.
124. Dunn SE, Ehrlich M, Sharp NJ, Reiss K, Solomon G, Hawkins R, et al. A dominant negative mutant of the insulin-like growth factor-I receptor inhibits the adhesion, invasion, and metastasis of breast cancer. Cancer Res. 1998 Aug 1;58(15):3353-61.
125. Huang GS, Brouwer-Visser J, Ramirez MJ, Kim CH, Hebert TM, Lin J, et al. Insulin-like growth factor 2 expression modulates Taxol resistance and is a candidate biomarker for reduced disease-free survival in ovarian cancer. Clin Cancer Res. 2010 Jun 1;16(11):2999-3010.
126. Mukohara T, Shimada H, Ogasawara N, Wanikawa R, Shimomura M, Nakatsura T, et al. Sensitivity of breast cancer cell lines to the novel insulin-like growth factor-1 receptor (IGF-1R) inhibitor NVP-AEW541 is dependent on the level of IRS-1 expression. Cancer Letters. 2009 9/8/;282(1):14-24.
127. Orr GA, Verdier-Pinard P, McDaid H, Horwitz SB. Mechanisms of Taxol resistance related to microtubules. Oncogene. 2003 Oct 20;22(47):7280-95.
128. Kavallaris M. Microtubules and resistance to tubulin-binding agents. Nat Rev Cancer. 2010 Mar;10(3):194-204.
129. Moreno-Acosta P, Gamboa O, Sanchez de Gomez M, Cendales R, Diaz GD, Romero A, et al. IGF1R gene expression as a predictive marker of response to ionizing radiation for

patients with locally advanced HPV16-positive cervical cancer. Anticancer Res. 2012 Oct;32(10):4319-25.
130. Lara PC, Bordon E, Rey A, Moreno M, Lloret M, Henriquez-Hernandez LA. IGF-1R expression predicts clinical outcome in patients with locally advanced oral squamous cell carcinoma. Oral Oncol. 2011 Jul;47(7):615-9.
131. Cao L, Yu Y, Darko I, Currier D, Mayeenuddin LH, Wan X, et al. Addiction to elevated insulin-like growth factor I receptor and initial modulation of the AKT pathway define the responsiveness of rhabdomyosarcoma to the targeting antibody. Cancer Res. 2008 Oct 1;68(19):8039-48.
132. Gong Y, Yao E, Shen R, Goel A, Arcila M, Teruya-Feldstein J, et al. High expression levels of total IGF-1R and sensitivity of NSCLC cells in vitro to an anti-IGF-1R antibody (R1507). PLoS One. 2009;4(10):e7273.
133. Huang F, Greer A, Hurlburt W, Han X, Hafezi R, Wittenberg GM, et al. The mechanisms of differential sensitivity to an insulin-like growth factor-1 receptor inhibitor (BMS-536924) and rationale for combining with EGFR/HER2 inhibitors. Cancer Res. 2009 Jan 1;69(1):161-70.
134. Zha J, O'Brien C, Savage H, Huw LY, Zhong F, Berry L, et al. Molecular predictors of response to a humanized anti-insulin-like growth factor-I receptor monoclonal antibody in breast and colorectal cancer. Mol Cancer Ther. 2009 Aug;8(8):2110-21.
135. Browne BC, Eustace AJ, Kennedy S, O'Brien NA, Pedersen K, McDermott MS, et al. Evaluation of IGF1R and phosphorylated IGF1R as targets in HER2-positive breast cancer cell lines and tumours. Breast Cancer Res Treat. 2012 Dec;136(3):717-27.
136. Wynes M, W; Ekman, S; Asuncion, B,R; Dziadziuszko, R; S. Glisson,B,S; Wistuba, I,I; Hirsch F,R. Insulin-like growth factor 1 (IGF-1R) protein expression (PE) and gene copy number (GCN) for discrimination of response and outcome to figitumumab in NSCLC. J Clin Oncol 2012;30(suppl; abstr 7597):abstr.
137. Schwartz GK, Tap WD, Qin LX, Livingston MB, Undevia SD, Chmielowski B, et al. Cixutumumab and temsirolimus for patients with bone and soft-tissue sarcoma: a multicentre, open-label, phase 2 trial. Lancet Oncol. 2013 Apr;14(4):371-82.
138. Mulvihill MJ, Cooke A, Rosenfeld-Franklin M, Buck E, Foreman K, Landfair D, et al. Discovery of OSI-906: a selective and orally efficacious dual inhibitor of the IGF-1 receptor and insulin receptor. Future Med Chem. 2009 Sep;1(6):1153-71.
139. Awasthi N, Zhang C, Ruan W, Schwarz MA, Schwarz RE. BMS-754807, a small-molecule inhibitor of insulin-like growth factor-1 receptor/insulin receptor, enhances gemcitabine response in pancreatic cancer. Mol Cancer Ther. 2012 Dec;11(12):2644-53.
140. Dayyani F, Parikh NU, Varkaris AS, Song JH, Moorthy S, Chatterji T, et al. Combined Inhibition of IGF-1R/IR and Src family kinases enhances antitumor effects in prostate cancer by decreasing activated survival pathways. PLoS One. 2012;7(12):e51189.
141. Luk F, Yu Y, Walsh WR, Yang JL. IGF1R-targeted therapy and its enhancement of doxorubicin chemosensitivity in human osteosarcoma cell lines. Cancer Invest. 2011 Oct;29(8):521-32.
142. Chung KY, Shia J, Kemeny NE, Shah M, Schwartz GK, Tse A, et al. Cetuximab shows activity in colorectal cancer patients with tumors that do not express the epidermal growth factor receptor by immunohistochemistry. J Clin Oncol. 2005 Mar 20;23(9):1803-10.
143. Yeh J, Litz J, Hauck P, Ludwig DL, Krystal GW. Selective inhibition of SCLC growth by the A12 anti-IGF-1R monoclonal antibody correlates with inhibition of Akt. Lung Cancer. 2008 May;60(2):166-74.
144. Subbiah V, Naing A, Brown RE, Chen H, Doyle L, LoRusso P, et al. Targeted morphoproteomic profiling of Ewing's sarcoma treated with insulin-like growth factor 1 receptor (IGF1R) inhibitors: response/resistance signatures. PLoS One. 2011;6(4):e18424.
145. Genomics of Drug Sensitivity in Cancer http://www.cancerrxgene.org/translation/Drug [cited 2013 16/09/2013].

146. Yeh AH, Bohula EA, Macaulay VM. Human melanoma cells expressing V600E B-RAF are susceptible to IGF1R targeting by small interfering RNAs. Oncogene. 2006 Oct 26;25(50):6574-81.
147. Klinakis A, Szabolcs M, Chen G, Xuan S, Hibshoosh H, Efstratiadis A. Igf1r as a therapeutic target in a mouse model of basal-like breast cancer. Proc Natl Acad Sci U S A. 2009 Feb 17;106(7):2359-64.
148. Molina-Arcas M, Hancock DC, Sheridan C, Kumar MS, Downward J. Coordinate direct input of both KRAS and IGF1 receptor to activation of PI3 kinase in KRAS-mutant lung cancer. Cancer Discov. 2013 May;3(5):548-63.
149. Zinn RL, Gardner EE, Marchionni L, Murphy SC, Dobromilskaya I, Hann CL, et al. ERK phosphorylation is predictive of resistance to IGF-1R inhibition in small cell lung cancer. Mol Cancer Ther. 2013 Jun;12(6):1131-9.
150. Lynch TJ, Bell DW, Sordella R, Gurubhagavatula S, Okimoto RA, Brannigan BW, et al. Activating mutations in the epidermal growth factor receptor underlying responsiveness of non-small-cell lung cancer to gefitinib. N Engl J Med. 2004 May 20;350(21):2129-39.
151. Paez JG, Janne PA, Lee JC, Tracy S, Greulich H, Gabriel S, et al. EGFR mutations in lung cancer: correlation with clinical response to gefitinib therapy. Science. 2004 Jun 4;304(5676):1497-500.
152. Pao W, Miller V, Zakowski M, Doherty J, Politi K, Sarkaria I, et al. EGF receptor gene mutations are common in lung cancers from "never smokers" and are associated with sensitivity of tumors to gefitinib and erlotinib. Proc Natl Acad Sci U S A. 2004 Sep 7;101(36):13306-11.
153. De Roock W, Claes B, Bernasconi D, De Schutter J, Biesmans B, Fountzilas G, et al. Effects of KRAS, BRAF, NRAS, and PIK3CA mutations on the efficacy of cetuximab plus chemotherapy in chemotherapy-refractory metastatic colorectal cancer: a retrospective consortium analysis. Lancet Oncol. 2010 Aug;11(8):753-62.
154. Khan ARG, D. Robustness to Non-Normality of Common Tests for the Many-Sample Location Problem. Journal of Applied Mathematics & Decision Sciences. 2003 December 2003(4).
155. Biade S, Stobbe CC, Chapman JD. The intrinsic radiosensitivity of some human tumor cells throughout their cell cycles. Radiat Res. 1997 Apr;147(4):416-21.
156. Koto M, Cho H, Riesterer O, Giri U, Story MD, Ha CS, et al. Human lymphoma cells develop resistance to radiation in the presence of astrocytes in vitro. Anticancer Res. 2011 Jan;31(1):33-8.
157. Bochet L, Meulle A, Imbert S, Salles B, Valet P, Muller C. Cancer-associated adipocytes promotes breast tumor radioresistance. Biochem Biophys Res Commun. 2011 Jul 22;411(1):102-6.
158. Rossi L, Boccardo F, Corvo R. Endothelial cells increase the radiosensitivity of oropharyngeal squamous carcinoma cells in collagen gel. Oral Oncol. 2004 Feb;40(2):214-22.
159. Rossi L, Reverberi D, Podesta G, Lastraioli S, Corvo R. Co-culture with human fibroblasts increases the radiosensitivity of MCF-7 mammary carcinoma cells in collagen gels. Int J Cancer. 2000 Mar 1;85(5):667-73.
160. Gery B, Coppey J, Little JB. Modulation of clonogenicity, growth, and radiosensitivity of three human epidermoid tumor cell lines by a fibroblastic environment. Int J Radiat Oncol Biol Phys. 1996 Mar 15;34(5):1061-71.
161. Kucerova L, Skolekova S, Matuskova M, Bohac M, Kozovska Z. Altered features and increased chemosensitivity of human breast cancer cells mediated by adipose tissue-derived mesenchymal stromal cells. BMC Cancer. 2013 Nov 9;13(1):535.
162. Pinski J, Parikh A, Bova GS, Isaacs JT. Therapeutic implications of enhanced G(0)/G(1) checkpoint control induced by coculture of prostate cancer cells with osteoblasts. Cancer Res. 2001 Sep 1;61(17):6372-6.

163. Jarboe JS, Jaboin JJ, Anderson JC, Nowsheen S, Stanley JA, Naji F, et al. Kinomic profiling approach identifies Trk as a novel radiation modulator. Radiother Oncol. 2012 Jun;103(3):380-7.

Appendices

Appendix I: Cell Lines in the NCI60 tumour screen

Cell Line	Tumour Type	Cell Line	Tumour Type
IGROV1	Ovarian	LOX IMVI	Melanoma
NCI/ADR-RES	Ovarian	M14	Melanoma
OVCAR-3	Ovarian	MALME-3M	Melanoma
OVCAR-4	Ovarian	MDA-MB-435	Melanoma
OVCAR-5	Ovarian	SK-MEL-2	Melanoma
OVCAR-8	Ovarian	SK-MEL-28	Melanoma
SK-OV-3	Ovarian	SK-MEL-5	Melanoma
DU-145	Prostate	UACC-257	Melanoma
PC-3	Prostate	UACC-62	Melanoma
BT-549	Breast	SF-268	Central Nervous System
HS 578T	Breast	SF-295	Central Nervous System
MCF7	Breast	SF-539	Central Nervous System
MDA-MB-231/ATCC	Breast	SNB-19	Central Nervous System
T-47D	Breast	SNB-75	Central Nervous System
A549/ATCC	Non-Small Cell Lung	U251	Central Nervous System
EKVX	Non-Small Cell Lung	786-0	Renal
HOP-62	Non-Small Cell Lung	A498	Renal
HOP-92	Non-Small Cell Lung	ACHN	Renal
NCI-H226	Non-Small Cell Lung	CAKI-1	Renal
NCI-H23	Non-Small Cell Lung	RXF-393	Renal
NCI-H322M	Non-Small Cell Lung	SN12C	Renal
NCI-H460	Non-Small Cell Lung	TK-10	Renal
NCI-H522	Non-Small Cell Lung	U0-31	Renal
COLO 205	Colon	CCRF-CEM	Leukaemia
HCC-2998	Colon	HL-60(TB)	Leukaemia
HCT-116	Colon	K-562	Leukaemia
HCT-15	Colon	MOLT-4	Leukaemia
HT29	Colon	RPMI-8226	Leukaemia
KM12	Colon	SR	Leukaemia
SW-620	Colon		

Appendix II: Drugs examined

The following pages show chemotherapeutic drugs for which sensitivity data in the form of GI_{50} concentrations was downloaded from the NCI60 website: http://dtp.nci.nih.gov/docs/dtp_search.html. The data examined relate to the September 2012 release. Drugs are grouped by mechanism of action as described on the NCI60 website (and see Introduction section 1). The National Service Center (NSC) number is the identification number for drugs submitted to the NCI for screening and may be used to search for chemosensitivity data from the above website. Also noted is the number of cell lines within the 56 of the NCI60 examined in this study for which data was either missing, or where the GI_{50} was recorded as being outside of the concentration range tested. Cell lines were excluded from further analysis if any of the following criteria applied: i) more than 15% of the GI_{50}s were recorded simply as being above or below the concentration range tested ii) chemosensitivity data was not recorded for more than 10% of the cell lines iii) less than 2 replicates were present iv) if a combination of the above factors were present.

Alkylating agents

Mechanism of action Drug Group	Drug name	NSC Identification number	Number of cell lines for which:		Number of replicates	Analysed further (yes/no)
			Data is absent	GI_{50} is outside of the concentration range tested		
Alkylating agents:						
Nitrogen Mustards	Asaley	167780	0	0	11	Yes
	Chlorambucil	3088	0	0	63	Yes
	Cyclophosphamide	26271	0	43	40	No
	Fluorodopan	73754	1	0	7	Yes
	Ifosfamide	109724	0	6	39	Yes
	Mechlorethamine (mustine)	762	1	0	39	Yes
	Melphalan	8806	1	0	40	Yes
	Uramustine (uracil nitrogen mustard)	34462	1	0	41	Yes
Aziridines and epoxides	Diaziquone (AZQ)	182986	7	0	39	No
	Mitomycin C	26980	0	0	67	Yes
	Actinomycin D	3053	0	0	22	Yes
	Porfiromycin	56410	1	0	5	Yes
	Thiotepa	6396	0	0	71	Yes
	Triethylenemelamine	9706	0	0	67	Yes
	Hexamethylmelamine	13875	0	40	40	No
	Dianhydrogalacticol	132313	1	0	6	Yes
	Teroxirone	296934	1	0	5	Yes
Alkyl sulfonates	Busulfan	750	1	0	38	Yes
	Clomosone	338947	1	0	5	Yes
	Cyclodisone	348948	0	0	5	Yes
	Hepsulfam	329680	1	0	11	Yes
	Hycanthone	142982	14	0	4	No
	Yoshi 684	102627	1	0	8	Yes
Nitrosoureas	Chlorotozocin (DCNU)	178248	0	0	8	Yes
	Carmustine (BCNU)	409962	0	0	65	Yes
	Lomustine (CCNU)	79037	1	0	40	Yes
	PCNU	95466	1	0	8	Yes
	Semustine (methylCCNU)	95441	1	0	7	Yes
	Spiromustine	172112	12	7	10	No
Tetrazines	Procarbazine	77213	0	42	37	No
	Dacarbazine	45388	1	5	42	Yes
	Mitozolomide	353451	0	0	5	Yes
	Temozolomide	362856	0	51	2	No
Piperazines	Piperazine	34007	0	1	5	Yes
	Piperazinedione	135758	1	5	7	Yes
	Pipobroman	25154	1	0	40	Yes
Platinum agents	Carboxypthaloplatinum	271674	0	0	7	Yes
	Carboplatin (CBDCA)	241240	0	0	44	Yes
	Cisplatin	119875	0	0	62	Yes
	Iproplatin (CHIP)	256927	1	0	11	Yes
	Tetraplatin (Ormaplatin)	363812	0	0	3	Yes

Antimitotic agents

Mechanism of action Drug Group	Drug name	NSC Identification number	Number of cell lines for which:		Number of replicates	Analysed further (yes/no)
			Data is absent	GI_{50} is outside of the concentration range tested		
Antimitotic agents:						
Tubulin Modulators:						
Microtubule stabilising						
Taxanes	Paclitaxel (taxol)	125973	0	0	24	Yes
	Taxol derivative	608832	0	43	5	No
	Docetaxel	628503	2	4	2	Yes
	Carbazitaxel (XRP-6258)	761432	0	46	2	No
Epothilones	Epothilone A	684362	0	55	2	No
	Epothilone B (Patupilone, EPO906)	684363	0	56	2	No
	Epothilone B analogue (Ibaxepilone)	747973	2	4	2	Yes
	Epothilone D (KOS-862)	703147	0	56	1	No
Microtubule destabilising						
Vinca Alkaloids	Vinblastine sulphate	49842	0	0	59	Yes
	Vincristine sulphate	67574	0	28	42	No
Halichondrin B	Halichondrin B	609395	9	0	4	No
	Halichondrin B analogue (Erubilin mesylate, E7389)	707389	0	1	3	Yes
Dolastatins	Dolastatin 10	376128	1	2	5	Yes
	Dolastatin 15	617668	0	4	6	Yes
	Auristatin PE	654663	2	1	2	Yes
Colchicine	Colchicine	757	2	7	3	No
	Allocolchicine	406042	0	46	4	No
	Colchicine derivative	33410	0	4	4	Yes
	Thiocolchicine	361792	0	6	4	Yes
Maytansine	Maytansine	153858	0	4	12	Yes
Rhizoxin	Rhizoxin	332598	3	16	6	No
Kinesin inhibitors:						
	Trityl cysteine	83265	1	0	8	Yes
	Monastrol	716782	0	3	4	Yes

Topoisomerase I inhibitors

Mechanism of action Drug Group	Drug name	NSC Identification number	Number of cell lines for which:		Number of replicates	Analysed further (yes/no)
			Data is absent	GI_{50} is outside of the concentration range tested		
Topoisomerase I Inhibitors:						
Camptothecins	Camptothecin	94600	6	4	6	No
	Camptothecin, Na salt	100880	0	0	2	Yes
	9-aminocamptothecin	603071	0	17	6	No
	Camptothecin acetate	95382	9	2	3	No
	10-hydroxycamptothecin	107124	12	1	5	No
	14-Cl-20(S)-camptothecin hydrate	643833	0	0	3	Yes
	MLS002701638	629971	3	12	4	No
	AC1L6X8Y	295500	8	1	2	No
	7-ethyl-10-OH camptothecin, SN-38 (irinotecan active metabolite)	249910	2	23	4	No
	MLS00766263	606985	0	0	2	Yes
	Camptothecin,20-O-(4-(2-hydroxyethyl)-1-piperazino) OAC	374028	0	0	3	Yes
	9-methoxy-camptothecin	176323	1	19	3	No
	1H-pyranol[3',7] indolizino [1,2-b]quinolone-3,14 (4H, 12H) –dione,4-ethyl-4hydroxy-11-methoxy-camptothecin	295501	8	19	2	No
	11-formyl-20(RS)-camptothecin	606172	0	0	3	Yes
	Hydroxymethyl-20(RS)-camptothecin	606173	7	0	2	No
	Camptothecin phosphate	610458	11	0	1	No
	Camptothecin-20-O-(N,N-dimethyl) glycinate HCl	618939	1	0	2	Yes
	Camptothecin lysinate hydrochloride	610457	0	15	3	No
	Camptothecin glutamate hydrochloride	610459	0	5	3	Yes
	Camptothecin butylglycinate ester hydrochloride	606499	6	2	2	No
	Camptothecin, N-diethyl glycinate	610456	0	4	3	Yes
	Camptothecin hemisuccinate sodium salt	364830	9	9	1	No
	Camptothecin ethylglycinate ester hydrochloride	606497	0	0	3	Yes
	Irinotecan	616348	0	0	8	Yes
	Silatecan	708298	0	31	2	No
	Topotecan	609699	0	1	7	Yes
Indeno-isoquinolines	2,3-dimethoxy-6-methyl-5H-(1,3)dioxolo(4',5':5,6)indeno(1,2-c)isoquinoline-5,12(6H)dione	314622	0	4	5	Yes
	MJ-III-65	706744	0	12	2	No
	Indotecan	724998	0	2	2	Yes
	Indimitecan HCl	725776	1	20	2	No
	NSC 726972	726972	1	13	2	No
	Bisindenoisoquinolone	727357	3	12	2	No
Indolocarbazoles	Staurosporine	618487	0	0	3	Yes
Anthracyclines	Morpholinodoxorubicin	354646	0	0	5	Yes

Topoisomerase II inhibitors

Mechanism of action Drug Group	Drug name	NSC Identification number	Number of cell lines for which:		Number of replicates	Analysed further (yes/no)
			Data is absent	GI_{50} is outside of the concentration range tested		
Topoisomerase II inhibitors:						
Anthracyclines	Aclarubicin	208734	2	0	5	Yes
	Cyanomorpholinodoxorubicin	357704	0	0	8	Yes
	Daunorubicin	82151	0	0	24	Yes
	Deoxydoxorubicin (escorubicin)	267469	1	0	10	Yes
	Doxorubicin	123127	0	0	1722	Yes
	Epirubicin	256942	3	2	3	Yes
	Idarubicin	256439	2	0	3	Yes
	Menogaril	269148	1	1	12	Yes
	NN-Dibenzylaunorubicin	268242	1	0	5	Yes
	Zorubicin (rubidazone)	164011	2	0	11	Yes
Anthracenediones	Mitoxantrone	301739	1	0	9	Yes
	Piroxantrone (oxantrozole)	349174	2	0	11	Yes
	Teloxantrone (anthrapyrazole derivative)	355644	0	0	7	Yes
Benzoquinolene-diones	Amonafide	308847	1	0	11	Yes
Anthracenes	Bisantrene	337766	5	0	6	Yes
Pyrazoles	Pyrazoloacridine	366140	0	0	5	Yes
Miscellaneous	Amsacrine.mAMSA	249992	0	0	65	Yes
	Merbarone	336628	2	0	10	Yes
Epipodophyllotoxins	Etopiside (VP-16)	141540	1	0	33	Yes
	Topotecan	609699	0	1	7	Yes

RNA/ DNA antimetabolites

Mechanism of action Drug Group	Drug name	NSC Identification number	Number of cell lines for which:		Number of replicates	Analysed further (yes/no)
			Data is absent	GI_{50} is outside of the concentration range tested		
RNA/DNA Antimetabolites:						
Purine antimetabolites	L-alanosine (SDX-102)	153353	2	0	11	Yes
Pyrimidine antimetabolites	5-fluorouracil	19893	0	0	1487	Yes
	Ftorafur (pro-drug, tegafur)	148958	1	10	7	No
	Pyrazofurin	143095	0	0	9	Yes
	5-azacytidine	102816	1	0	7	Yes
	5,6-dihydro-5-azacytidine	264880	2	0	11	Yes
	Acivicin	163501	3	0	11	Yes
	Dichloroallyl lawsone	126771	0	0	3	Yes
	Brequinar	368390	3	0	7	Yes
	L-aspartic acid, N-(phosphonoacetyl)-, tetrasodium salt (PALA)	224131	1	2	10	Yes
Folate antagonists Dihydrofolate reductase inhibitors Classical antifolates	Methotrexate	740	0	0	65	Yes
	Methotrexate derivative	174121	1	16	2	No
	Raltitrexed	639186	7	27	1	No
	Pralatrexate	754230	2	45	2	No
	Edatrexate	626715	13	17	1	No
	L-aspartic acid, N-(2-chloro-5-(((2,4-diamino-5-methyl-6-quinazolinyl)methyl)amino) benzoyl)	132483	9	7	2	No
	L-aspartic acid, N-(4-(((2,4-diamino-5-ethyl-6-quinazolinyl)methyl)amino) benzoyl)	184692	11	7	2	No
	Aspartic acid, 4-diamino-6-pteridinyl)methyl]amino]benzoyl]-monohydrate,L-	134033	15	3	2	No
	N(sup).alpha.-(4-amino-4-deoxypteroyl)-N(sup).delta.-hemiphthaloyl-L-ornithine	623017	14	31	2	No
Nonpolyglutamable classical antifolates	Talotrexin (PT-523)	633713	0	10	2	No
	Triazinate	139105	1	11	6	No
Nonclassical antifolates	Trimetrexate (TMQ)	352122	0	0	11	Yes
	Piritrexim (PTX)	351521	1	5	2	Yes
Multitargeted antifolates	Pemetrexed (LY231514)	698037	1	40	2	No

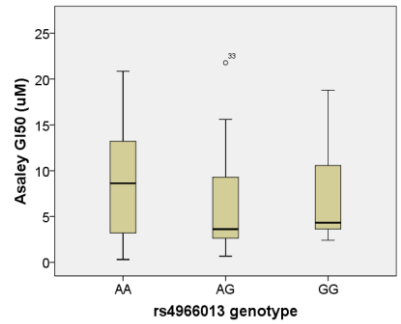
DNA antimetabolites

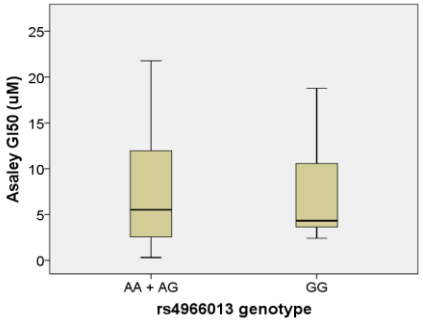
Mechanism of action Drug Group	Drug name	NSC Identification number	Number of cell lines for which:		Number of replicates	Analysed further (yes/no)
			Data is absent	GI_{50} is outside of the concentration range tested		
DNA Antimetabolites:						
Purine antimetabolites						
	Floxuridine (2'-deoxy-5-fluorouridine)	27640	0	0	59	Yes
	Fludarabine (2-fluoroadenosine arabinoside)	312887	2	0	12	Yes
	Nelarabine (O^6-methylarabinofuranosyl guanine)	686673	2	35	1	No
	Clofarabine (2'fluoro-2'-deoxyarabinofuranosyl-2-chloroadenine)	606869	0	4	3	Yes
	Cladribine (2-chloro-2'-deoxyadenosine)	105014	0	5	6	Yes
	Alpha-TGDR thiodeoxyguanidine	71851	1	0	7	Yes
	Guanazole	1895	1	7	1	Yes
	6 Mercaptopurine (thiopurine)	755	0	0	66	Yes
	6 Thioguanine	752	0	0	68	Yes
	Inosine glycoaldehyde	118994	1	0	6	Yes
Pyrimidine antimetabolites						
	Cytarabine (cytosine arabinoside, ara-C)	63878	0	0	62	Yes
	Decitabine (5-aza-2'deoxycytidine)	127716	1	0	8	Yes
	Gemcitabine (2,2-difluoro-2'-deoxycytidine)	613327	0	7	7	Yes
	Pentostatin (2'-deoxycoformycin)	218321	1	12	39	No
	Ancitabine (cyclocytidine)	145668	1	7	7	Yes
Other						
	Macbecin II	330500	2	0	3	Yes
	Aphidicolin	303812	0	0	7	Yes
	3HP	95678	2	0	5	Yes
	5HP	107392	0	0	7	Yes
	Pyrazoloimidazole	51143	1	3	8	Yes
	Hydroxyurea	32065	1	0	39	Yes

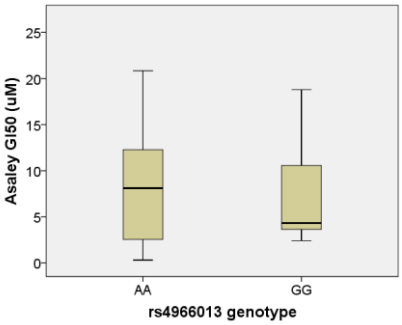
Appendix III: Boxplots - drug GI_{50} by SNP genotype

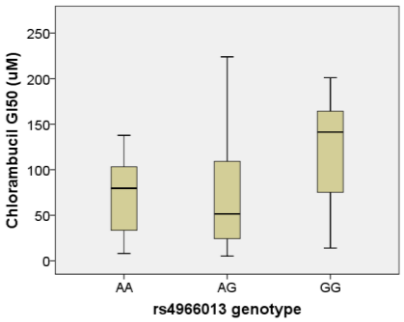
The following pages show boxplots comparing SNP rs4966013 genotype with GI_{50} concentration for drugs analysed. Boxplots are arranged by drug mechanism of action. Horizontal bars represent the median, boxes the interquartile range and whiskers the range. Circles and asterisks represent statistical outliers. Left hand column compares AA, AG and GG genotypes, middle column compares the combined AA and AG genotypes with the GG genotype and the right column compares the homozygotes only. Plots across the row examine the same drug. The same arrangement applies to the subsequent pages.

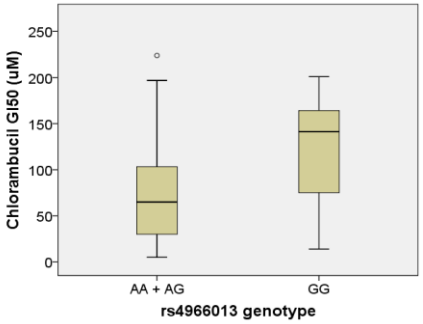
Alkylating agents

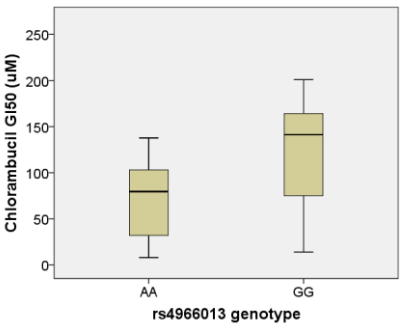


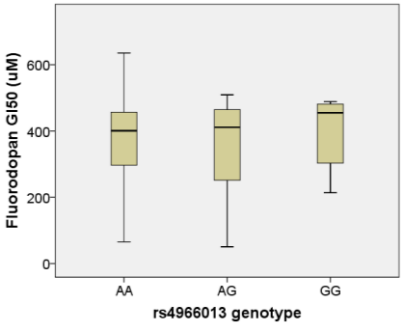


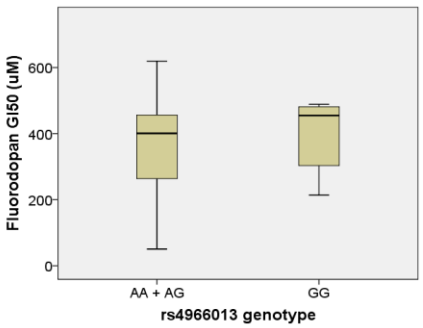


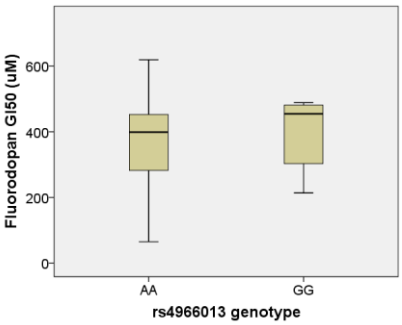


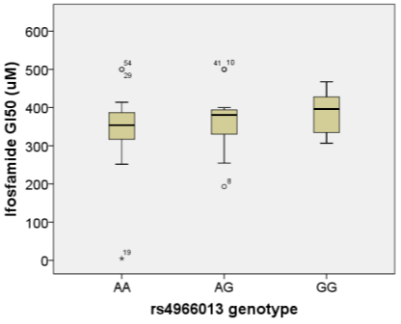


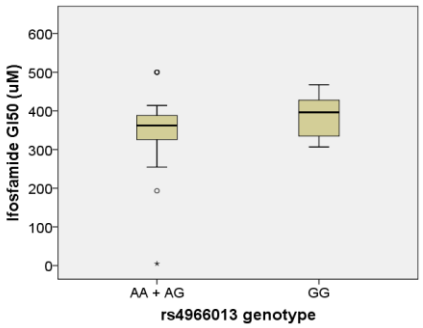


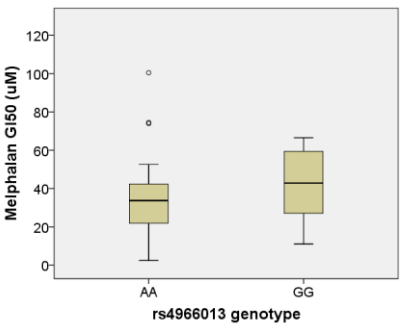


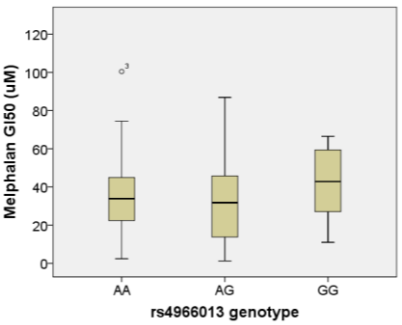


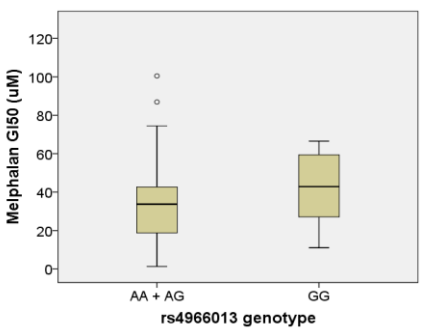


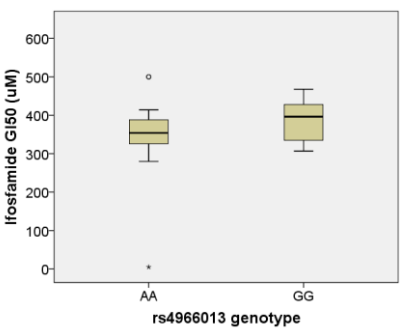


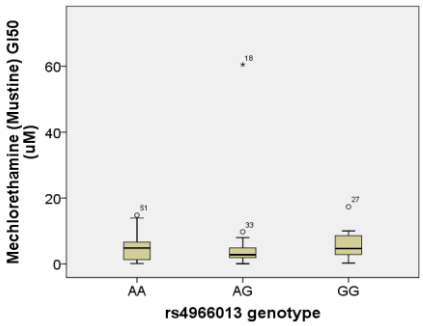


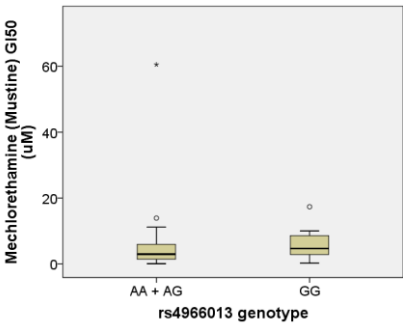


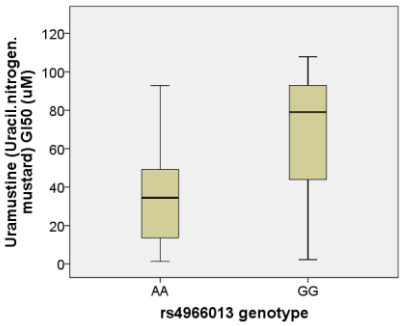


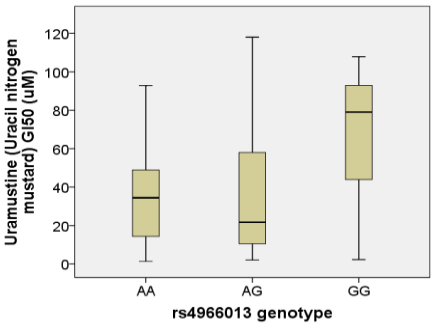


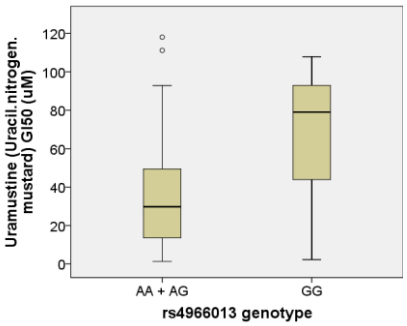


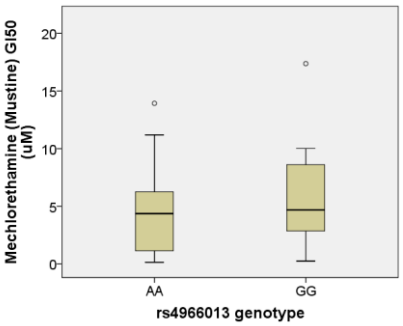

Mechlorethamine (Mustine) GI50 (uM)
AA
AG
GG
rs4966013 genotype

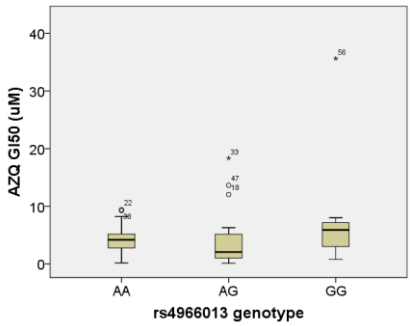

Mechlorethamine (Mustine) GI50 (uM)
AA + AG
GG
rs4966013 genotype

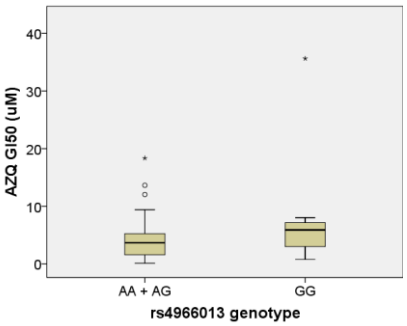

Uramustine (Uracil.nitrogen. mustard) GI50 (uM)
AA
GG
rs4966013 genotype

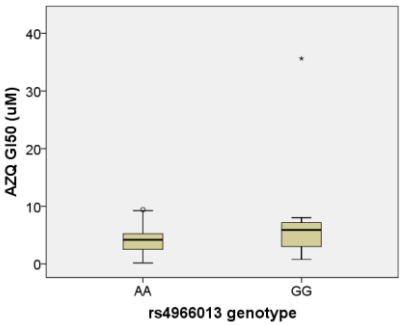

Uramustine (Uracil nitrogen mustard) GI50 (uM)
AA
AG
GG
rs4966013 genotype

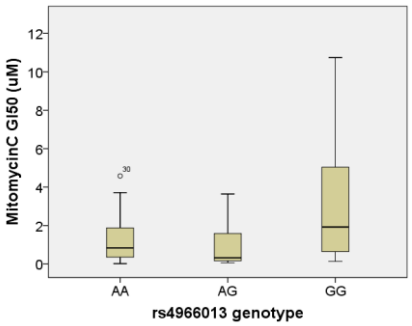

Uramustine (Uracil.nitrogen. mustard) GI50 (uM)
AA + AG
GG
rs4966013 genotype

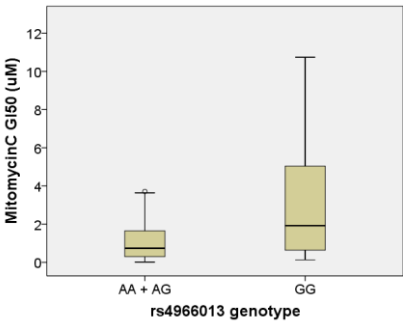

Mechlorethamine (Mustine) GI50 (uM)
AA
GG
rs4966013 genotype

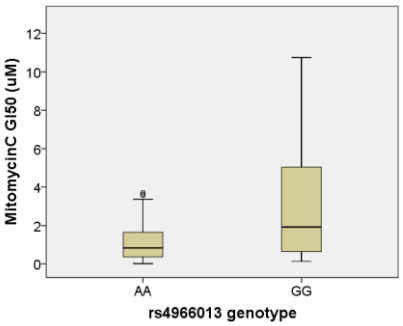

AZQ GI50 (uM)
AA
AG
GG
rs4966013 genotype

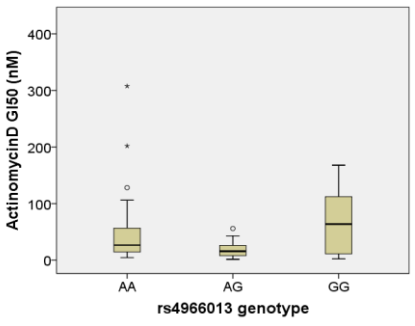

AZQ GI50 (uM)
AA + AG
GG
rs4966013 genotype

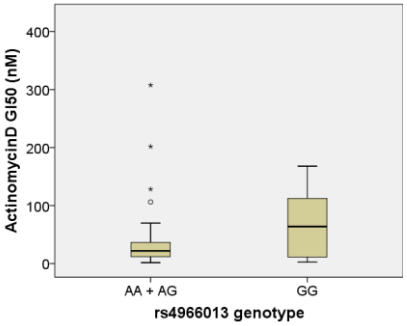

AZQ GI50 (uM)
AA
GG
rs4966013 genotype

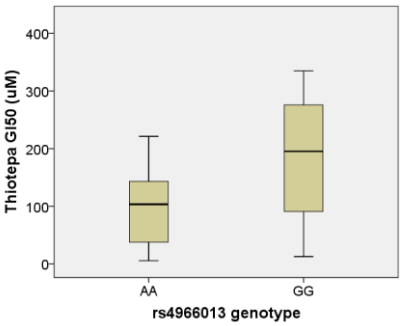

MitomycinC GI50 (uM)
AA
AG
GG
rs4966013 genotype

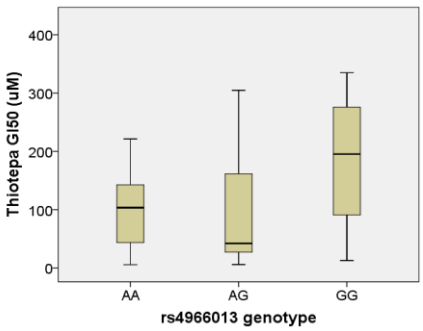

MitomycinC GI50 (uM)
AA + AG
GG
rs4966013 genotype

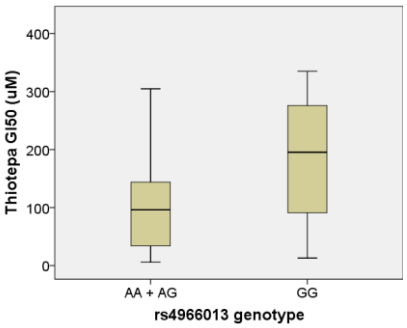

MitomycinC GI50 (uM)
AA
GG
rs4966013 genotype

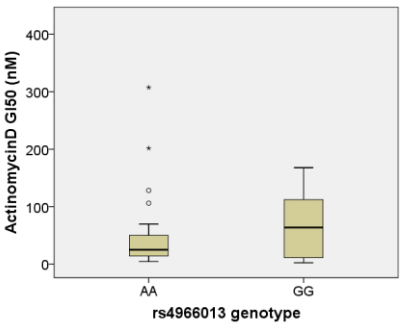

ActinomycinD GI50 (nM)
AA
AG
GG
rs4966013 genotype

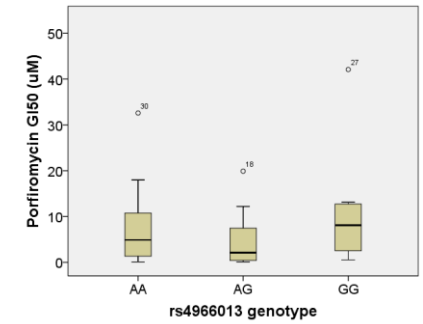

ActinomycinD GI50 (nM)
AA + AG
GG
rs4966013 genotype

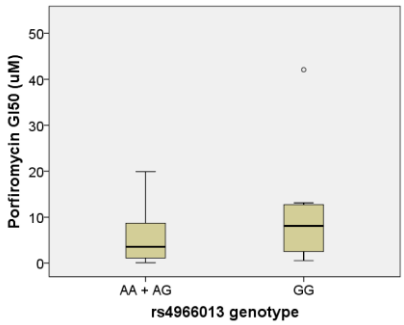

Thiotepa GI50 (uM)
AA
GG
rs4966013 genotype

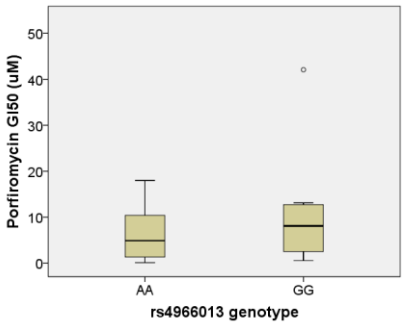

Thiotepa GI50 (uM)
AA
AG
GG
rs4966013 genotype

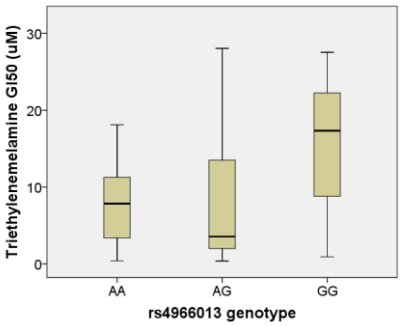

Thiotepa GI50 (uM)
AA + AG
GG
rs4966013 genotype

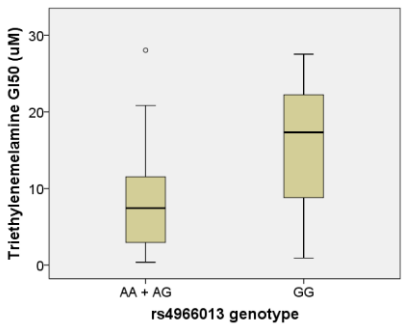

ActinomycinD GI50 (nM)
AA
GG
rs4966013 genotype

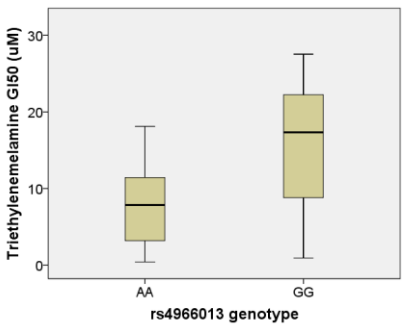

Porfiromycin GI50 (uM)
50
40
30
20
10
0
30
18
27
AA
AG
GG
rs4966013 genotype

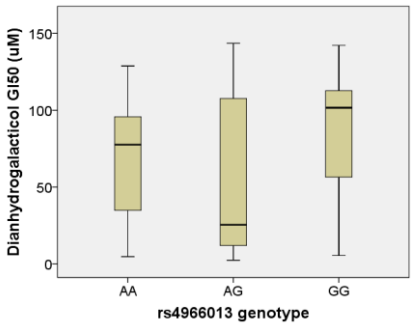

Porfiromycin GI50 (uM)
50
40
30
20
10
0
AA + AG
GG
rs4966013 genotype

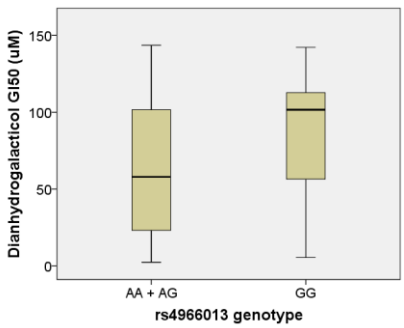

Porfiromycin GI50 (uM)
50
40
30
20
10
0
AA
GG
rs4966013 genotype

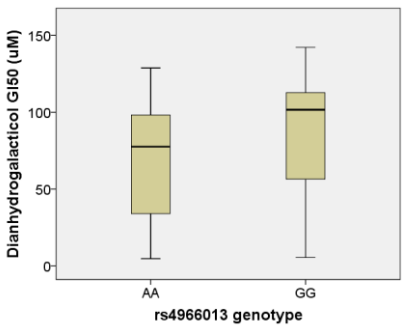

Triethylenemelamine GI50 (uM)
30
20
10
0
AA
AG
GG
rs4966013 genotype

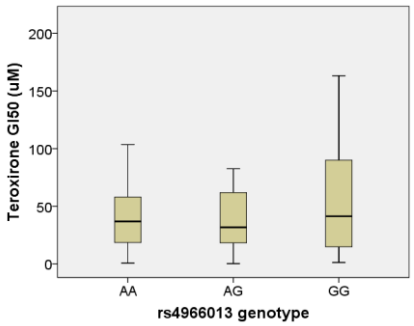

Triethylenemelamine GI50 (uM)
30
20
10
0
AA + AG
GG
rs4966013 genotype

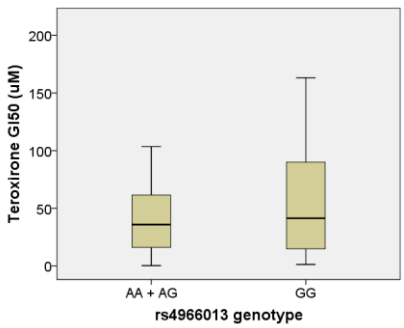

Triethylenemelamine GI50 (uM)
30
20
10
0
AA
GG
rs4966013 genotype

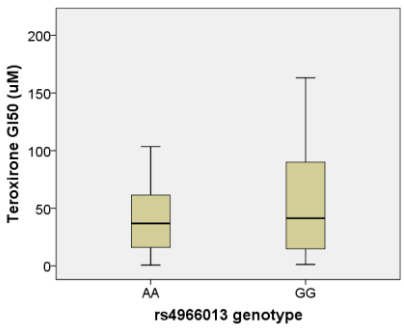

Dianhydrogalacticol GI50 (uM)
150
100
50
0
AA
AG
GG
rs4966013 genotype

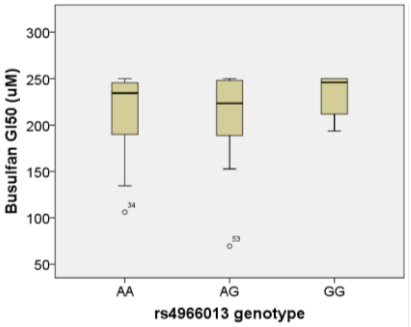

Dianhydrogalacticol GI50 (uM)
150
100
50
0
AA + AG
GG
rs4966013 genotype

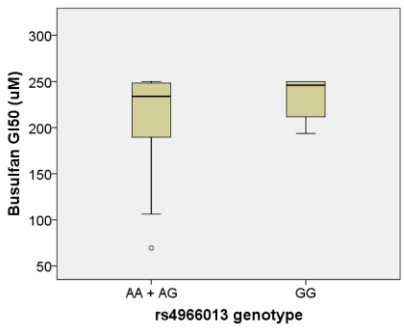

Dianhydrogalacticol GI50 (uM)
150
100
50
0
AA
GG
rs4966013 genotype

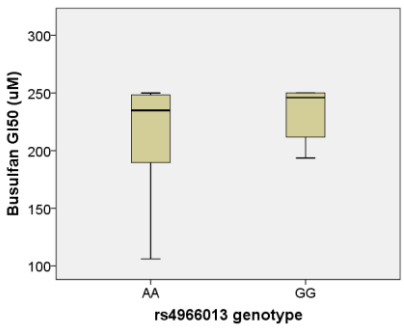

Teroxirone GI50 (uM)
200
150
100
50
0
AA
AG
GG
rs4966013 genotype

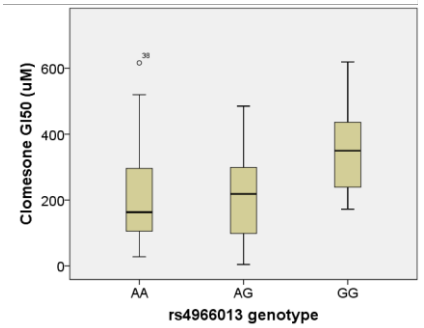

Teroxirone GI50 (uM)
200
150
100
50
0
AA + AG
GG
rs4966013 genotype

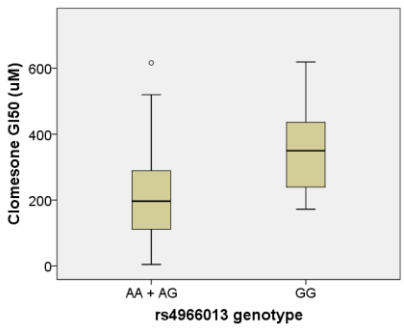

Teroxirone GI50 (uM)
200
150
100
50
0
AA
GG
rs4966013 genotype

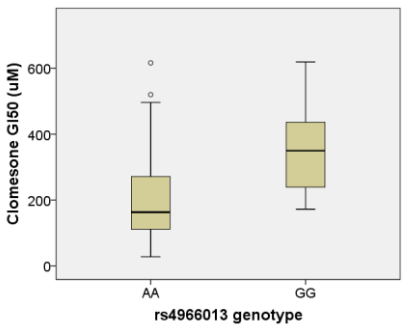

Busulfan GI50 (uM)
300
250
200
150
100
50
34
53
AA
AG
GG
rs4966013 genotype

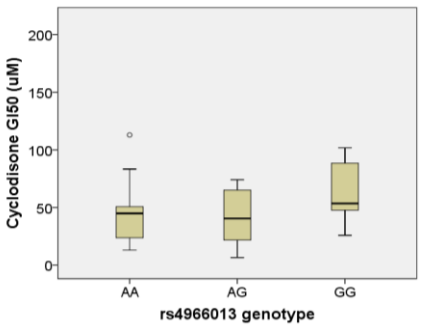

Busulfan GI50 (uM)
300
250
200
150
100
50
AA + AG
GG
rs4966013 genotype

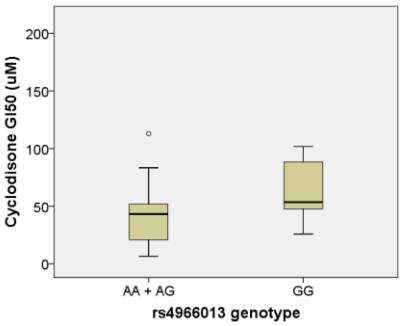

Busulfan GI50 (uM)
300
250
200
150
100
AA
GG
rs4966013 genotype

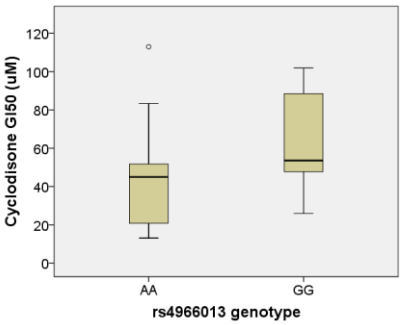

Clomesone GI50 (uM)
600
400
200
0
38
AA
AG
GG
rs4966013 genotype

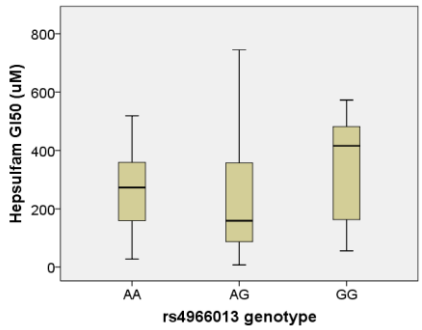

Clomesone GI50 (uM)
600
400
200
0
AA + AG
GG
rs4966013 genotype

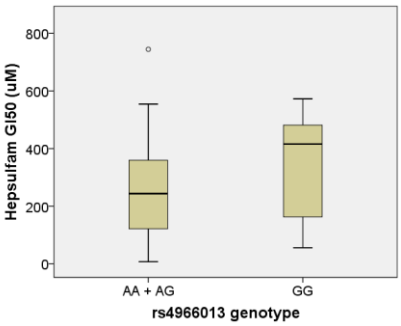

Clomesone GI50 (uM)
600
400
200
0
AA
GG
rs4966013 genotype

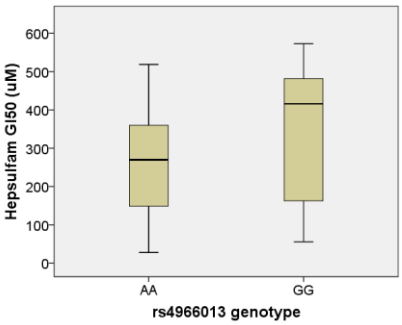

Cyclodisone GI50 (uM)
200
150
100
50
0
AA
AG
GG
rs4966013 genotype

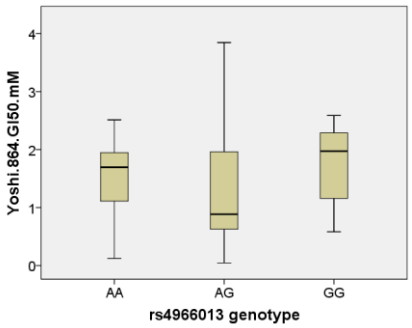

Cyclodisone GI50 (uM)
200
150
100
50
0
AA + AG
GG
rs4966013 genotype

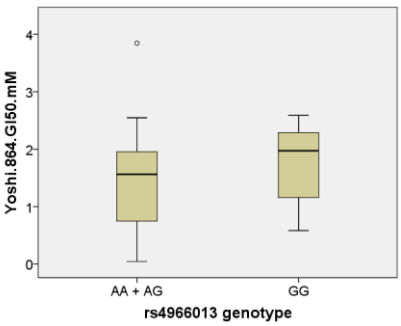

Cyclodisone GI50 (uM)
120
100
80
60
40
20
0
AA
GG
rs4966013 genotype

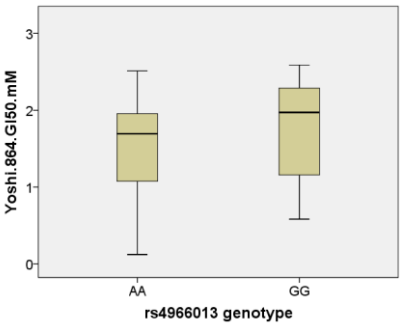

Hepsulfam GI50 (uM)
800
600
400
200
0
AA
AG
GG
rs4966013 genotype

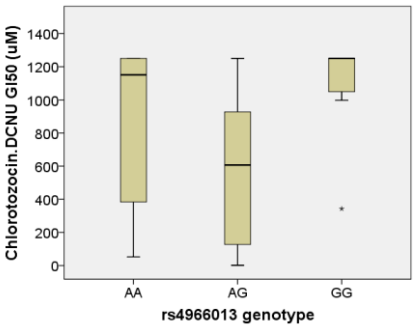

Hepsulfam GI50 (uM)
800
600
400
200
0
AA + AG
GG
rs4966013 genotype

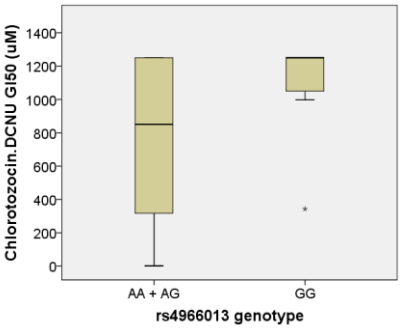

Hepsulfam GI50 (uM)
600
500
400
300
200
100
0
AA
GG
rs4966013 genotype

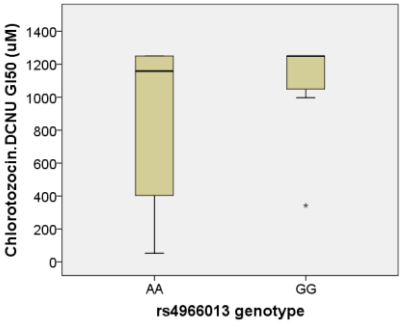

Yoshi.864.GI50.mM
4
3
2
1
0
AA
AG
GG
rs4966013 genotype

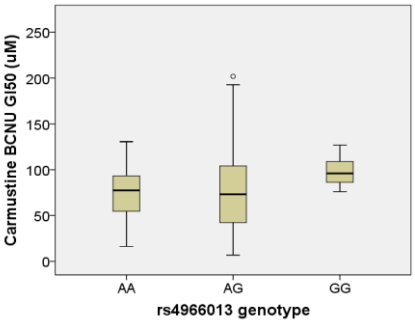

Yoshi.864.GI50.mM
4
3
2
1
0
AA + AG
GG
rs4966013 genotype

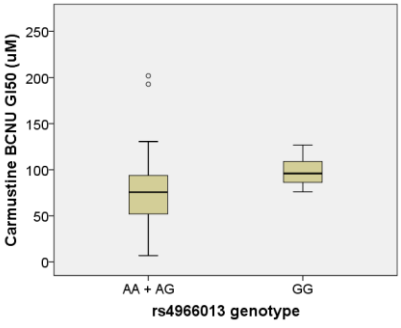

Yoshi.864.GI50.mM
3
2
1
0
AA
GG
rs4966013 genotype

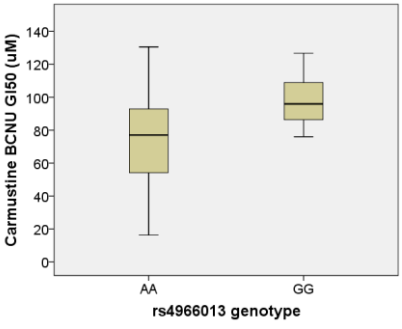

Chlorotozocin.DCNU GI50 (uM)
1400
1200
1000
800
600
400
200
0
AA
AG
GG
rs4966013 genotype

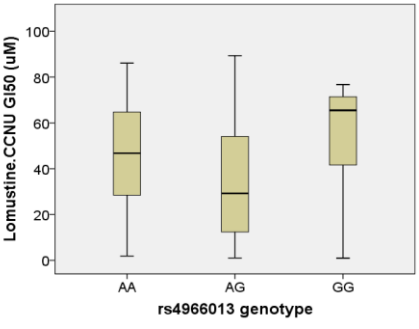

Chlorotozocin.DCNU GI50 (uM)
1400
1200
1000
800
600
400
200
0
AA + AG
GG
rs4966013 genotype

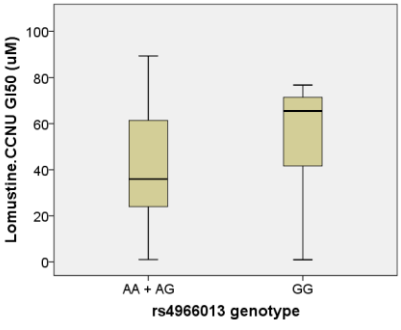

Chlorotozocin.DCNU GI50 (uM)
1400
1200
1000
800
600
400
200
0
AA
GG
rs4966013 genotype

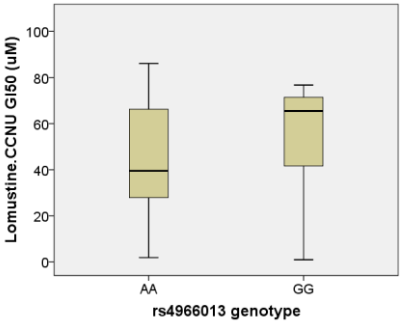

Carmustine BCNU GI50 (uM)
250
200
150
100
50
0
AA
AG
GG
rs4966013 genotype

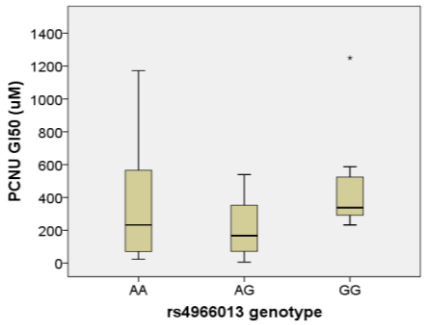

Carmustine BCNU GI50 (uM)
250
200
150
100
50
0
AA + AG
GG
rs4966013 genotype

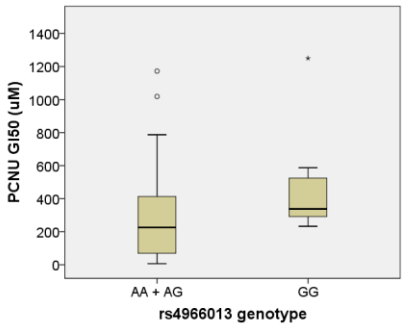

Carmustine BCNU GI50 (uM)
140
120
100
80
60
40
20
0
AA
GG
rs4966013 genotype

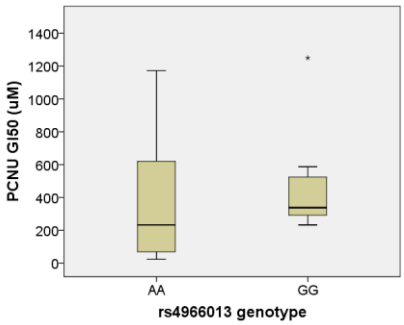

Lomustine.CCNU GI50 (uM)
100
80
60
40
20
0
AA
AG
GG
rs4966013 genotype

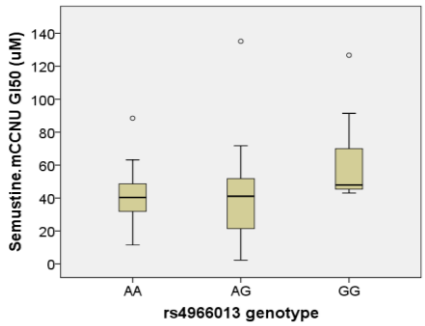

Lomustine.CCNU GI50 (uM)
100
80
60
40
20
0
AA + AG
GG
rs4966013 genotype

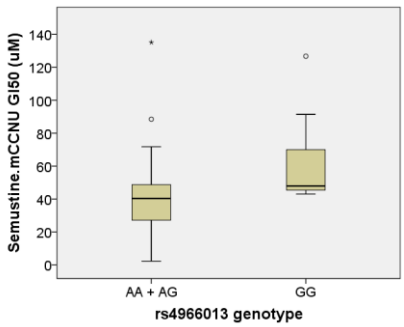

Lomustine.CCNU GI50 (uM)
100
80
60
40
20
0
AA
GG
rs4966013 genotype

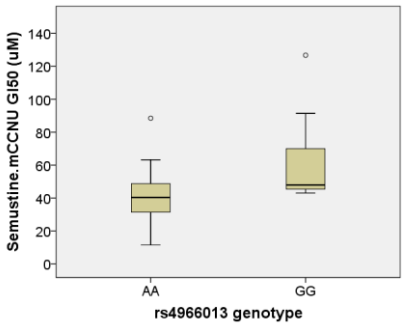

PCNU GI50 (uM)
1400
1200
1000
800
600
400
200
0
AA
AG
GG
rs4966013 genotype

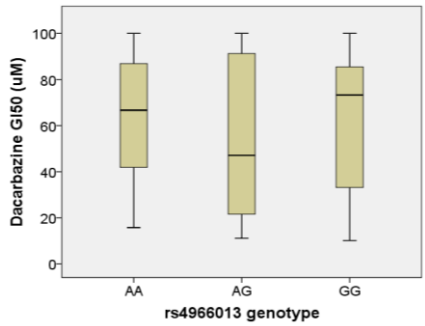

PCNU GI50 (uM)
1400
1200
1000
800
600
400
200
0
AA + AG
GG
rs4966013 genotype

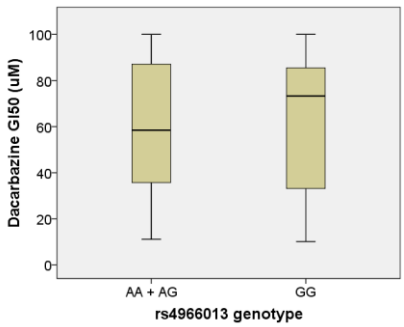

PCNU GI50 (uM)
1400
1200
1000
800
600
400
200
0
AA
GG
rs4966013 genotype

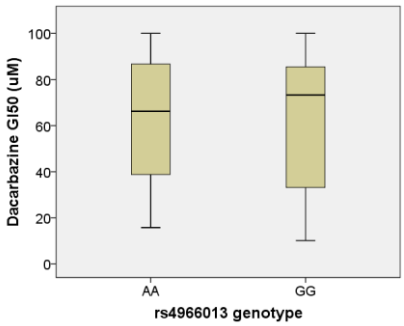

Semustine.mCCNU GI50 (uM)
140
120
100
80
60
40
20
0
AA
AG
GG
rs4966013 genotype

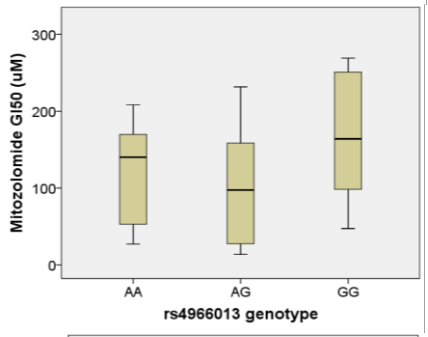

Semustine.mCCNU GI50 (uM)
140
120
100
80
60
40
20
0
AA + AG
GG
rs4966013 genotype

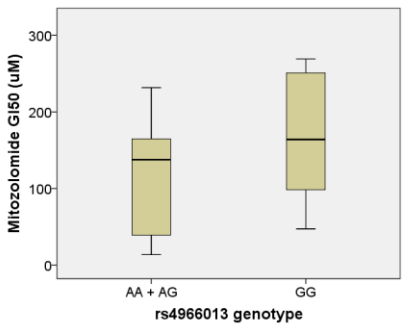

Semustine.mCCNU GI50 (uM)
140
120
100
80
60
40
20
0
AA
GG
rs4966013 genotype

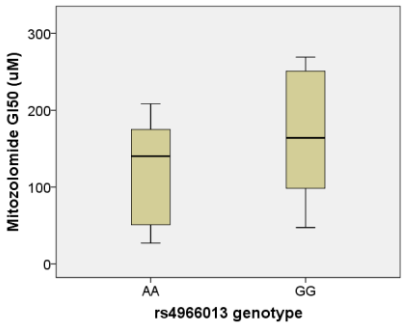

Dacarbazine GI50 (uM)
100
80
60
40
20
0
AA
AG
GG
rs4966013 genotype

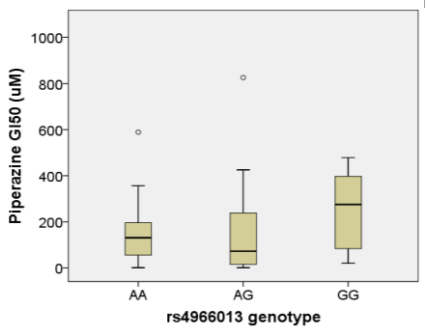

Dacarbazine GI50 (uM)
100
80
60
40
20
0
AA + AG
GG
rs4966013 genotype

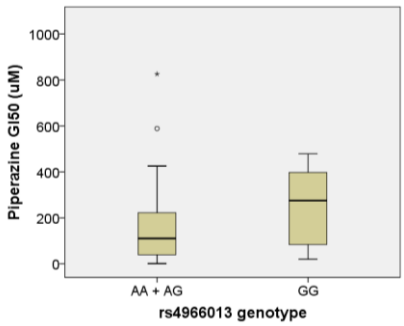

Dacarbazine GI50 (uM)
100
80
60
40
20
0
AA
GG
rs4966013 genotype

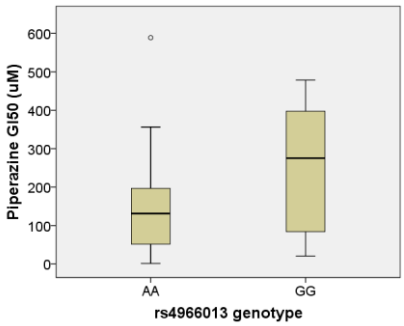

Mitozolomide GI50 (uM)
300
200
100
0
AA
AG
GG
rs4966013 genotype

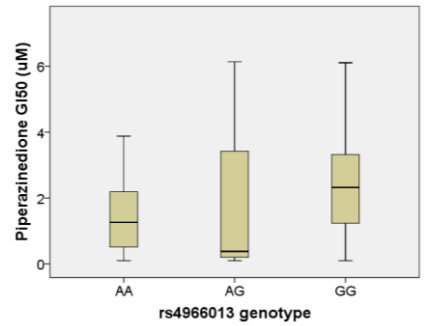

Mitozolomide GI50 (uM)
300
200
100
0
AA + AG
GG
rs4966013 genotype

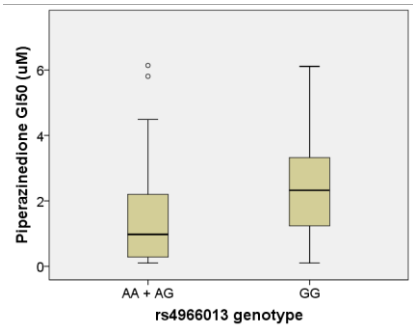

Mitozolomide GI50 (uM)
300
200
100
0
AA
GG
rs4966013 genotype

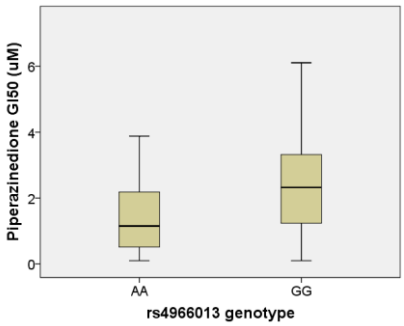

Piperazine GI50 (uM)
1000
800
600
400
200
0
AA
AG
GG
rs4966013 genotype

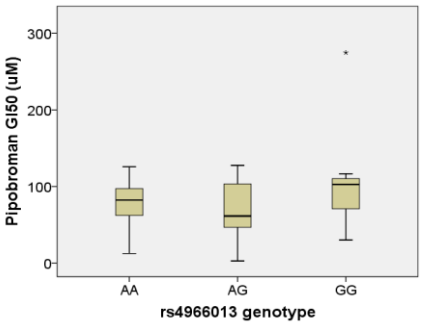

Piperazine GI50 (uM)
1000
800
600
400
200
0
AA + AG
GG
rs4966013 genotype

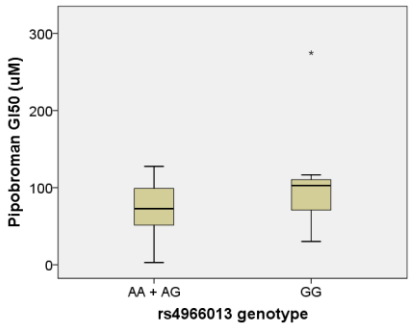

Piperazine GI50 (uM)
600
500
400
300
200
100
0
AA
GG
rs4966013 genotype

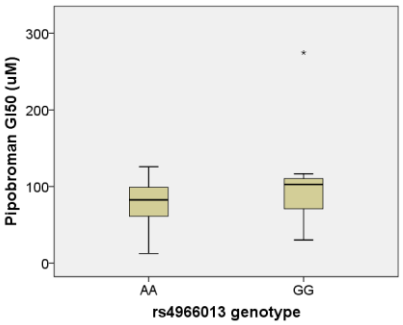

Piperazinedione GI50 (uM)
6
4
2
0
AA
AG
GG
rs4966013 genotype

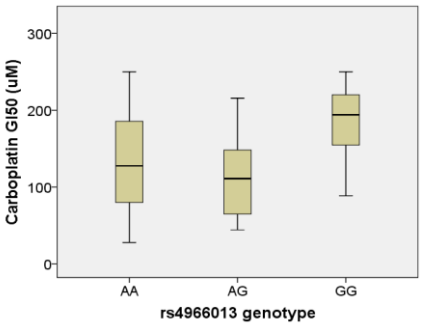

Piperazinedione GI50 (uM)
6
4
2
0
AA + AG
GG
rs4966013 genotype

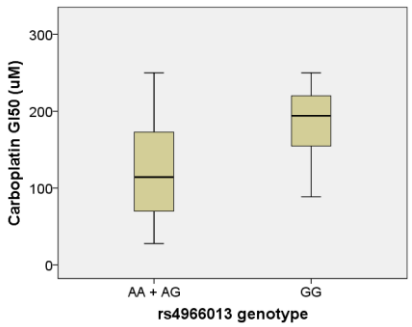

Piperazinedione GI50 (uM)
6
4
2
0
AA
GG
rs4966013 genotype

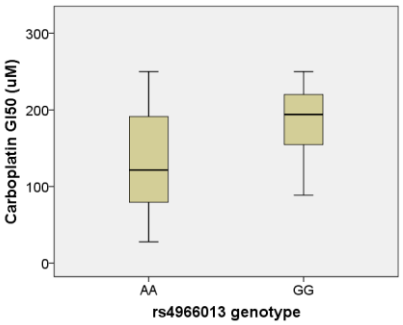

Pipobroman GI50 (uM)
300
200
100
0
AA
AG
GG
rs4966013 genotype

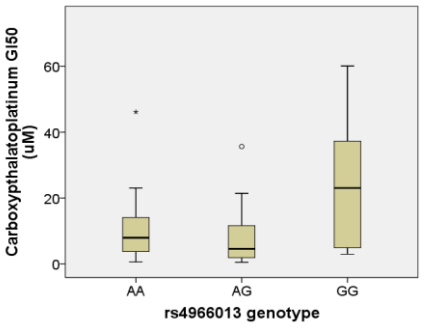

Pipobroman GI50 (uM)
300
200
100
0
AA + AG
GG
rs4966013 genotype

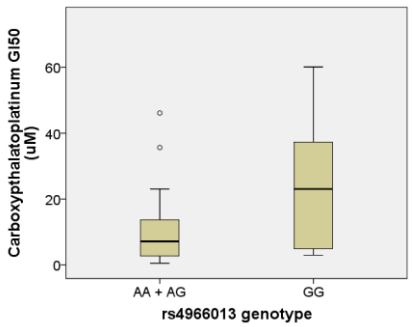

Pipobroman GI50 (uM)
300
200
100
0
AA
GG
rs4966013 genotype

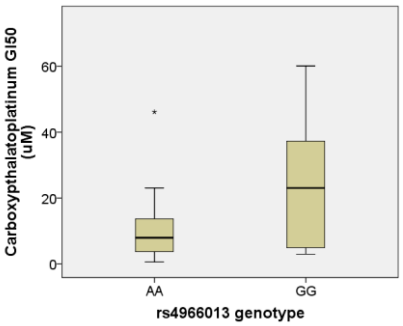

Carboplatin GI50 (uM)
300
200
100
0
AA
AG
GG
rs4966013 genotype

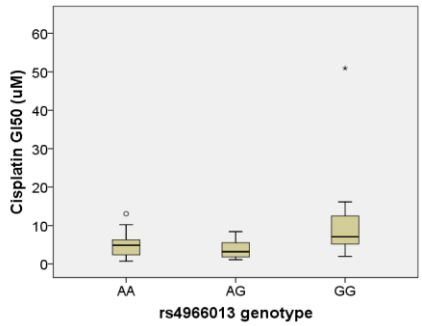

Carboplatin GI50 (uM)
300
200
100
0
AA + AG
GG
rs4966013 genotype

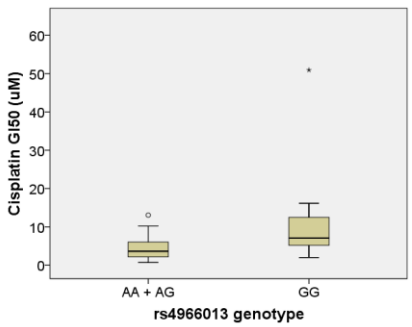

Carboplatin GI50 (uM)
300
200
100
0
AA
GG
rs4966013 genotype

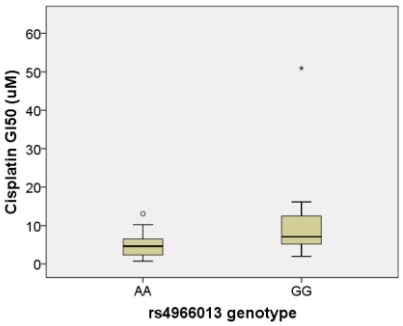

Carboxypthalatoplatinum GI50 (uM)
60
40
20
0
AA
AG
GG
rs4966013 genotype

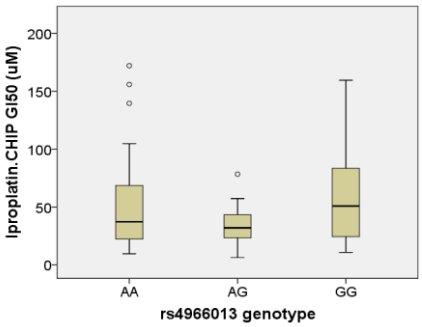

Carboxypthalatoplatinum GI50 (uM)
60
40
20
0
AA + AG
GG
rs4966013 genotype

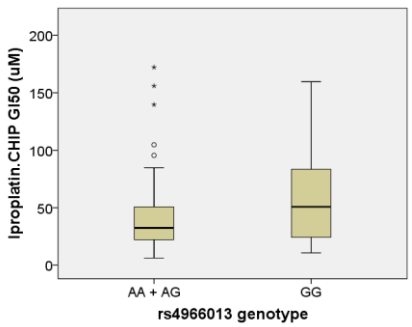

Carboxypthalatoplatinum GI50 (uM)
60
40
20
0
AA
GG
rs4966013 genotype

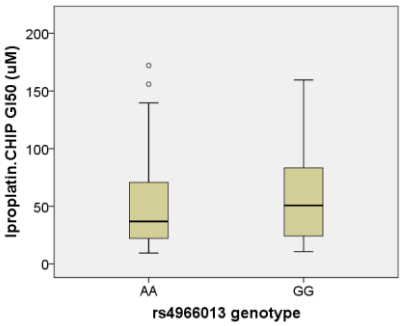

Cisplatin GI50 (uM)
60
50
40
30
20
10
0
AA
AG
GG
rs4966013 genotype

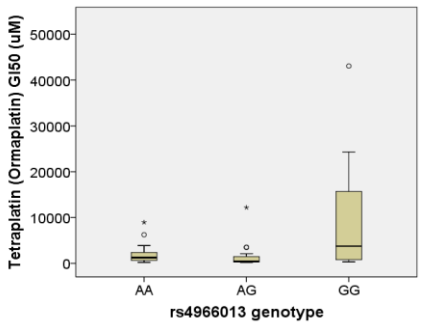

Cisplatin GI50 (uM)
60
50
40
30
20
10
0
AA + AG
GG
rs4966013 genotype

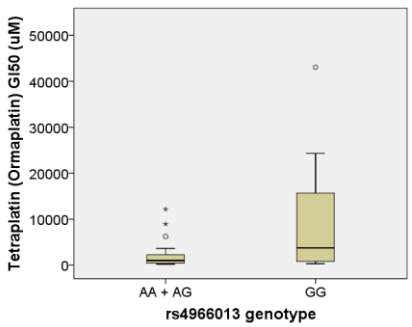

Cisplatin GI50 (uM)
60
50
40
30
20
10
0
AA
GG
rs4966013 genotype

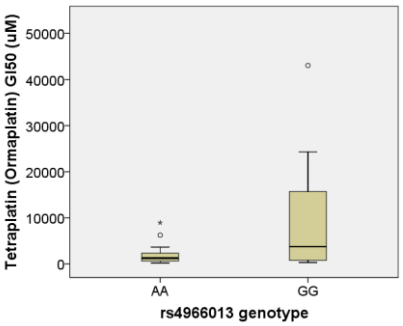

Iproplatin.CHIP GI50 (uM)
200
150
100
50
0
AA
AG
GG
rs4966013 genotype


Iproplatin.CHIP GI50 (uM)
200
150
100
50
0
AA + AG
GG
rs4966013 genotype

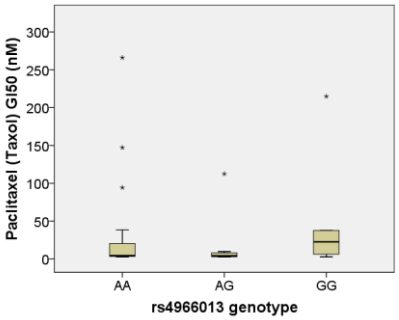

Iproplatin.CHIP GI50 (uM)
200
150
100
50
0
AA
GG
rs4966013 genotype

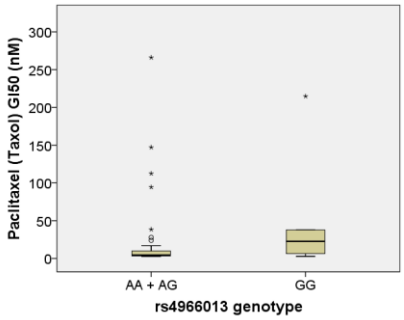

Tetraplatin (Ormaplatin) GI50 (uM)
50000
40000
30000
20000
10000
0
AA
AG
GG
rs4966013 genotype

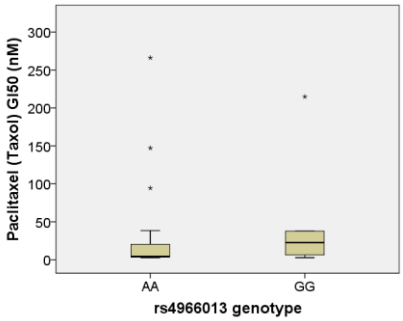

Tetraplatin (Ormaplatin) GI50 (uM)
50000
40000
30000
20000
10000
0
AA + AG
GG
rs4966013 genotype

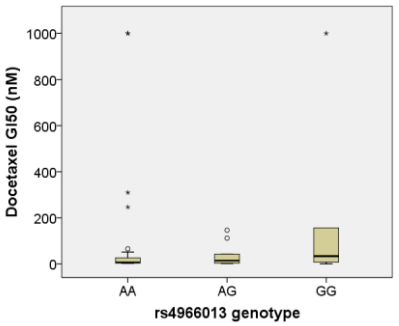

Tetraplatin (Ormaplatin) GI50 (uM)
50000
40000
30000
20000
10000
0
AA
GG
rs4966013 genotype

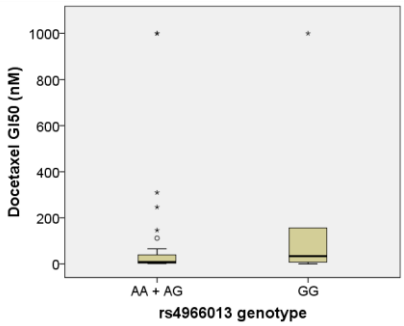
Antimitotic agents

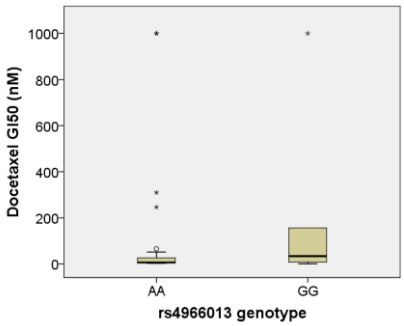


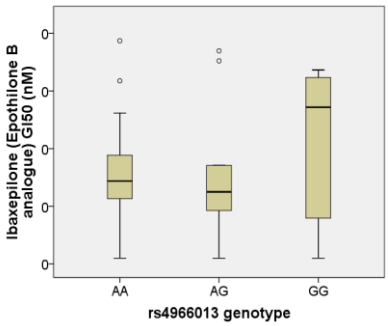


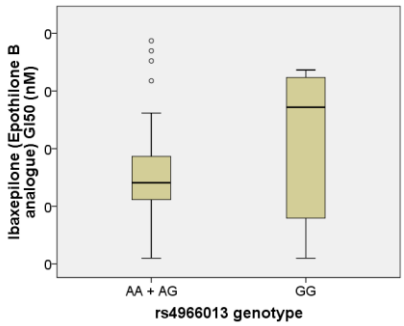


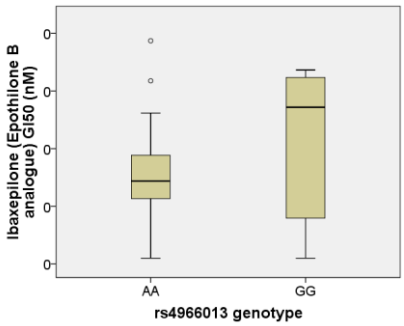


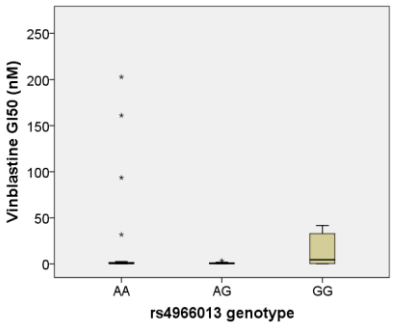


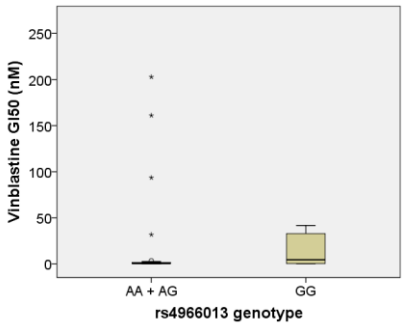


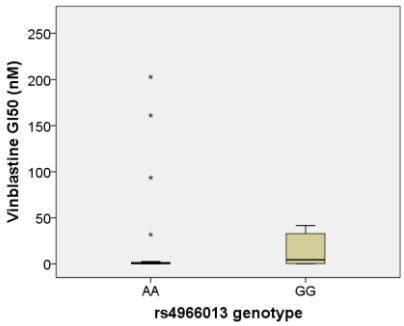


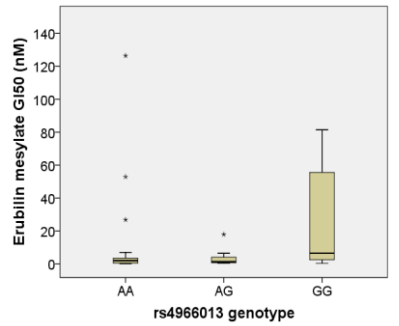


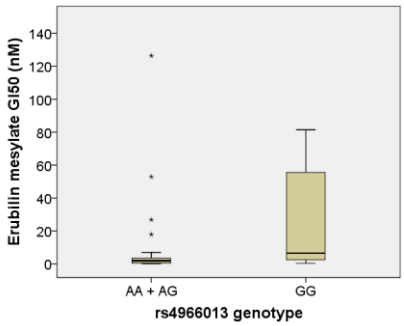


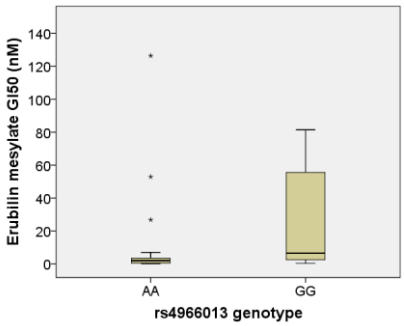


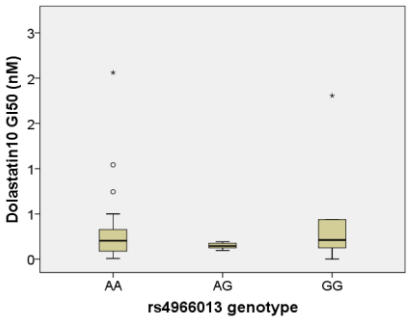


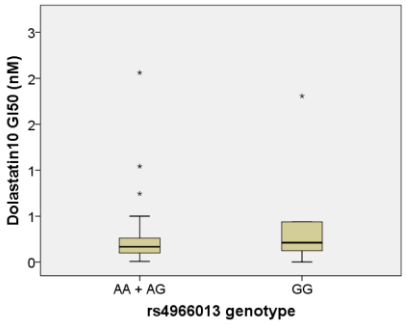


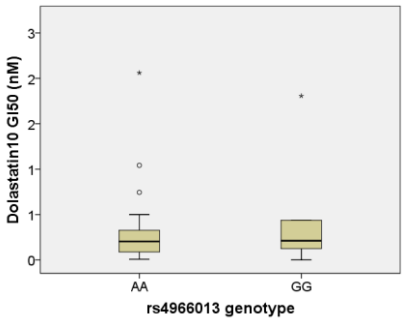


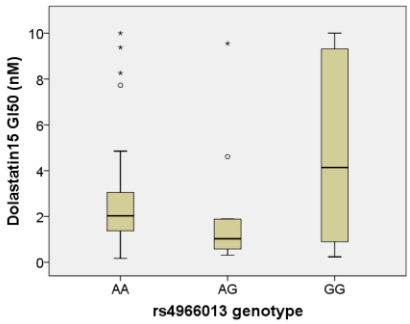


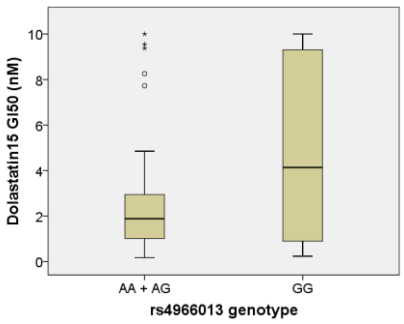


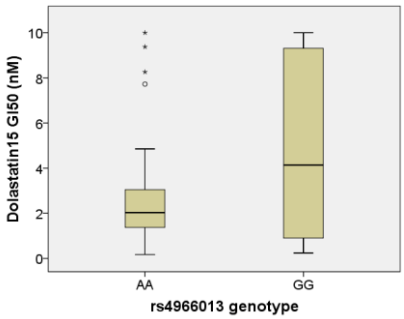

Dolastatin10 GI50 (nM)
AA
AG
GG
rs4966013 genotype

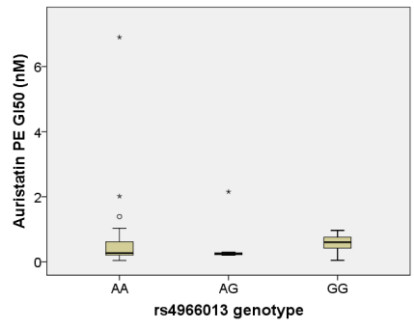

Dolastatin10 GI50 (nM)
AA + AG
GG
rs4966013 genotype

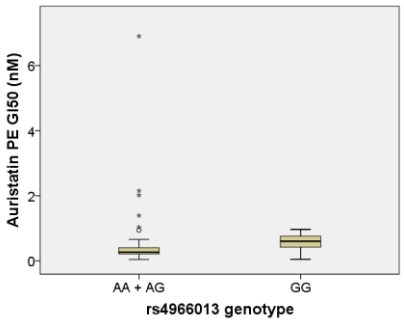

Dolastatin10 GI50 (nM)
AA
GG
rs4966013 genotype

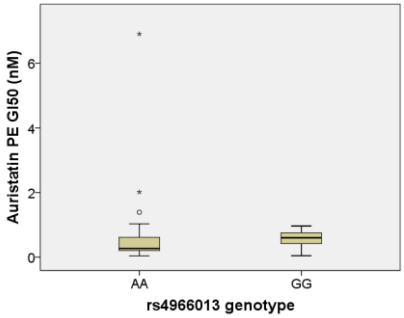

Dolastatin15 GI50 (nM)
AA
AG
GG
rs4966013 genotype

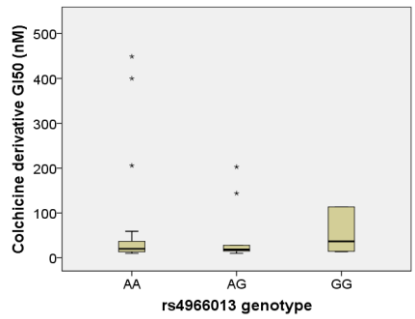

Dolastatin15 GI50 (nM)
AA + AG
GG
rs4966013 genotype

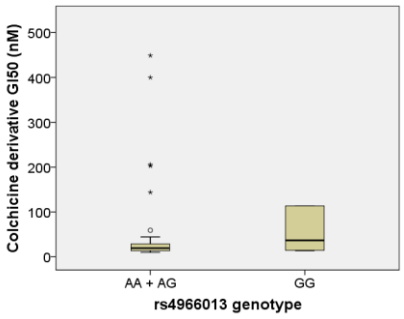

Dolastatin15 GI50 (nM)
AA
GG
rs4966013 genotype

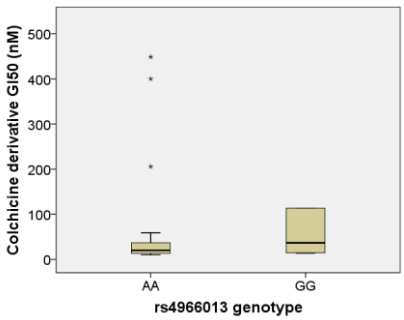

Auristatin PE GI50 (nM)
AA
AG
GG
rs4966013 genotype

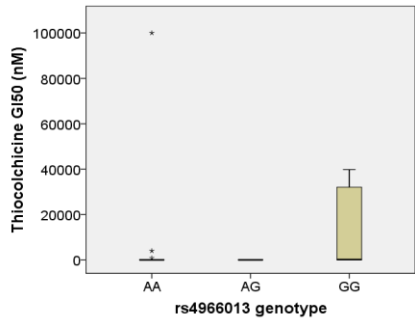

Auristatin PE GI50 (nM)
AA + AG
GG
rs4966013 genotype

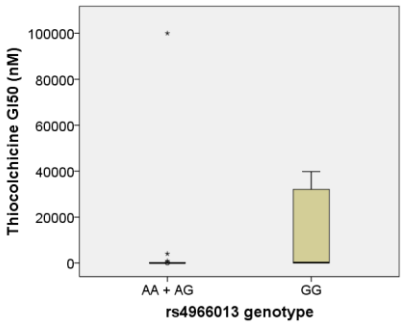

Auristatin PE GI50 (nM)
AA
GG
rs4966013 genotype

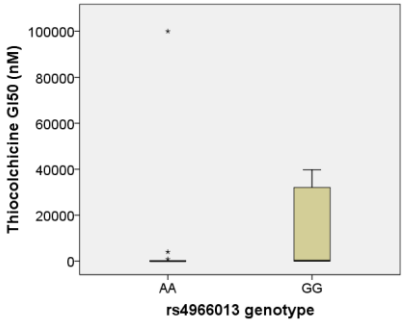

Colchicine derivative GI50 (nM)
AA
AG
GG
rs4966013 genotype

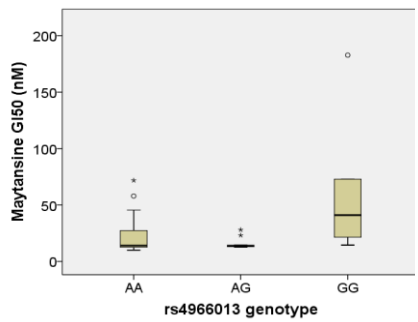

Colchicine derivative GI50 (nM)
AA + AG
GG
rs4966013 genotype

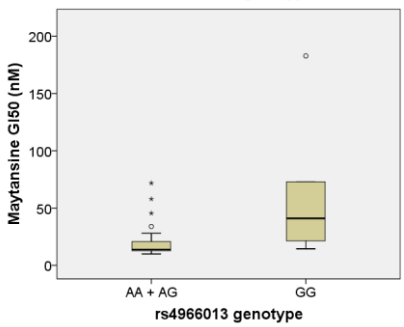

Colchicine derivative GI50 (nM)
AA
GG
rs4966013 genotype

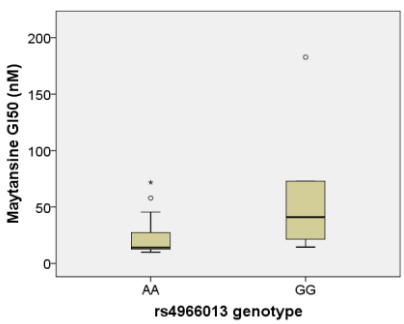

Thiocolchicine GI50 (nM)
AA
AG
GG
rs4966013 genotype

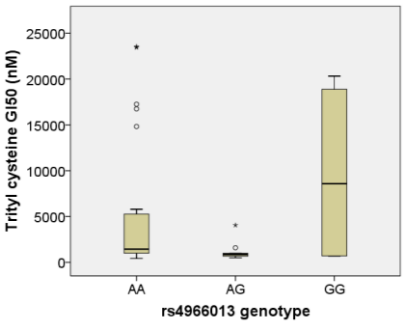

Thiocolchicine GI50 (nM)
AA + AG
GG
rs4966013 genotype

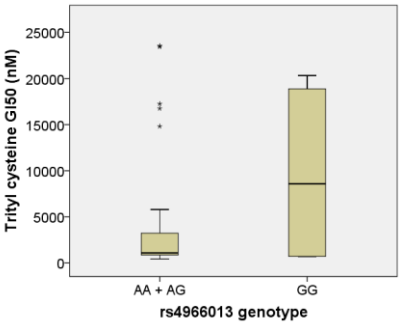

Thiocolchicine GI50 (nM)
AA
GG
rs4966013 genotype

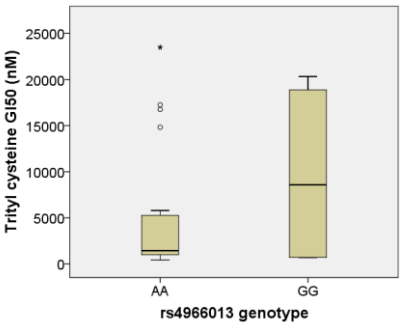

Maytansine GI50 (nM)
AA
AG
GG
rs4966013 genotype

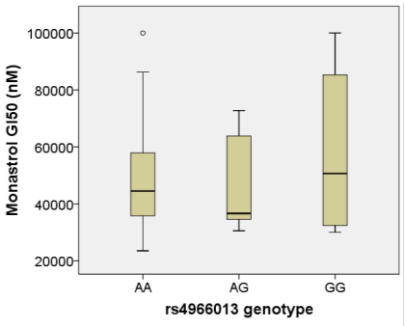

Maytansine GI50 (nM)
AA + AG
GG
rs4966013 genotype

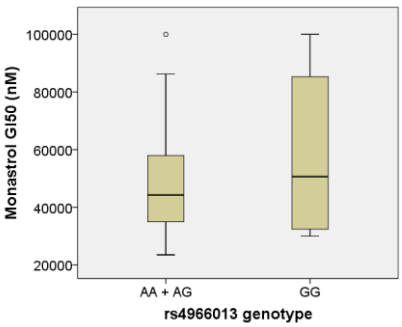

Maytansine GI50 (nM)
AA
GG
rs4966013 genotype

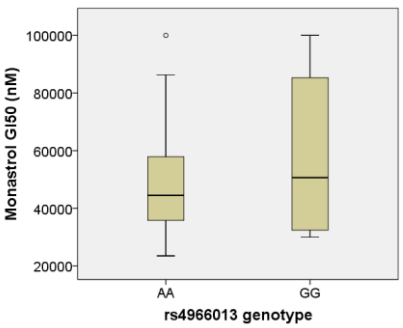

Trityl cysteine GI50 (nM)
25000
20000
15000
10000
5000
0
AA
AG
GG
rs4966013 genotype


Trityl cysteine GI50 (nM)
25000
20000
15000
10000
5000
0
AA + AG
GG
rs4966013 genotype

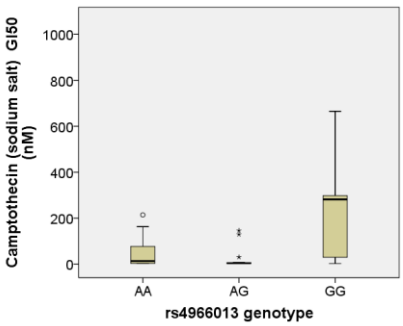

Trityl cysteine GI50 (nM)
25000
20000
15000
10000
5000
0
AA
GG
rs4966013 genotype

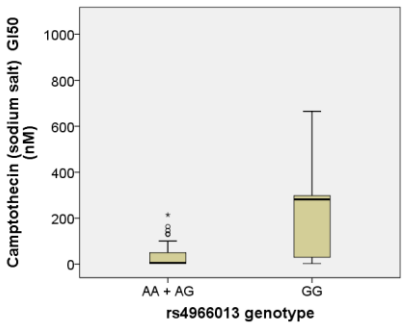

Monastrol GI50 (nM)
100000
80000
60000
40000
20000
AA
AG
GG
rs4966013 genotype

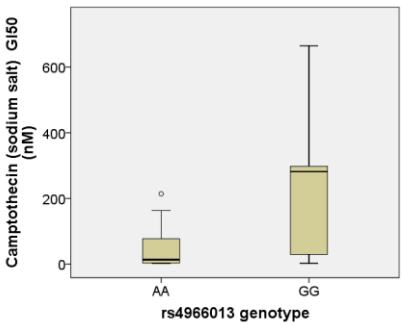

Monastrol GI50 (nM)
100000
80000
60000
40000
20000
AA + AG
GG
rs4966013 genotype

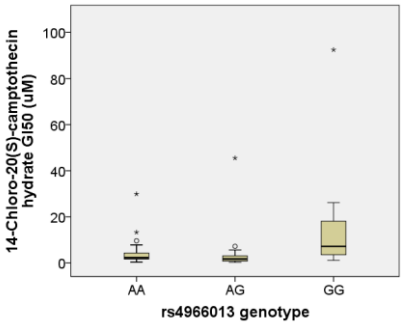

Monastrol GI50 (nM)
100000
80000
60000
40000
20000
AA
GG
rs4966013 genotype

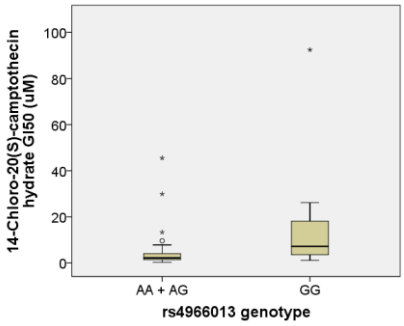
Topoisomerase I inhibitors

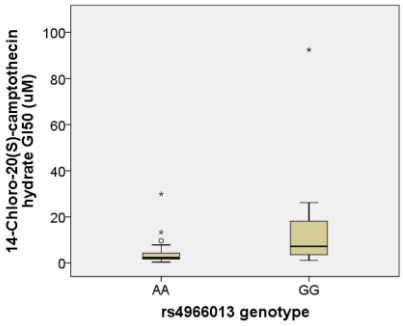


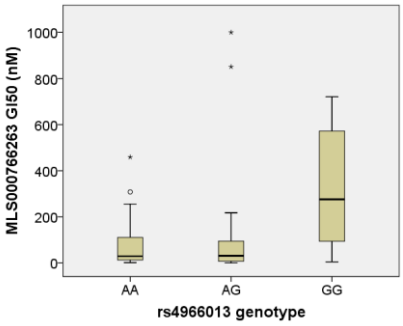


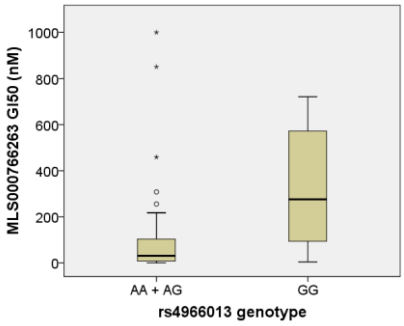


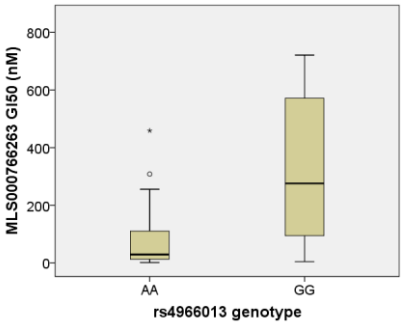


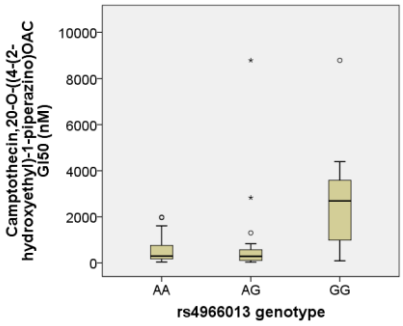


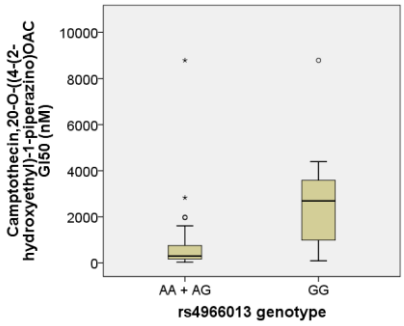


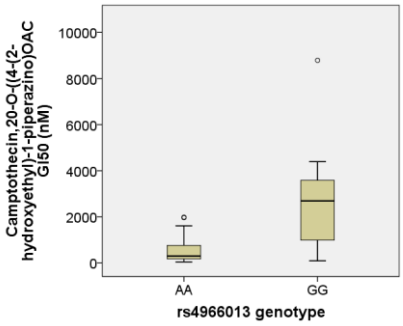


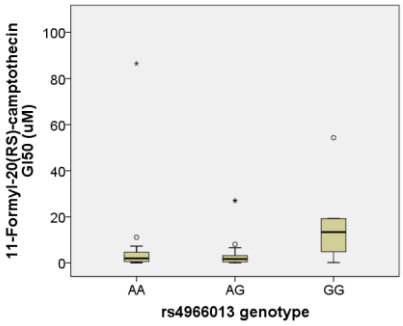


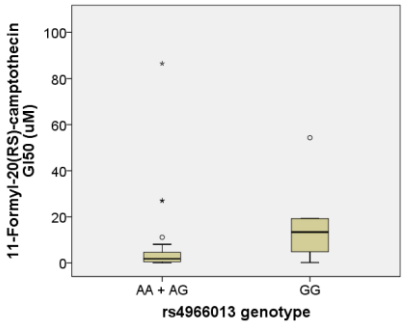


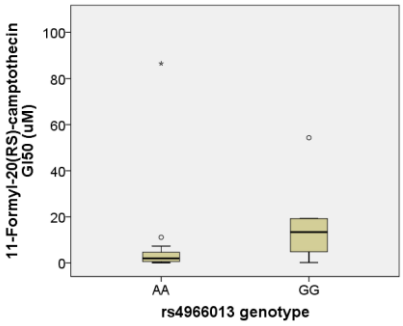


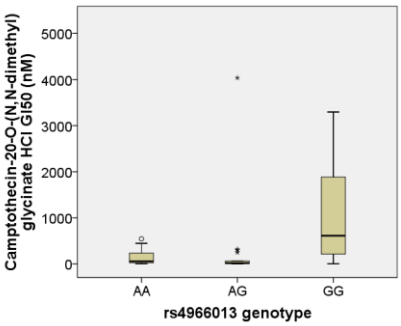


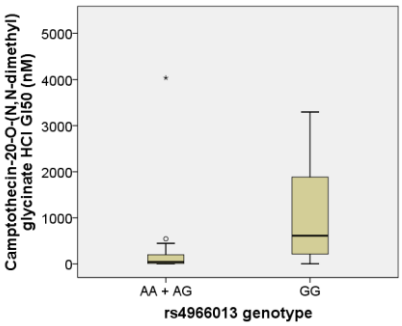


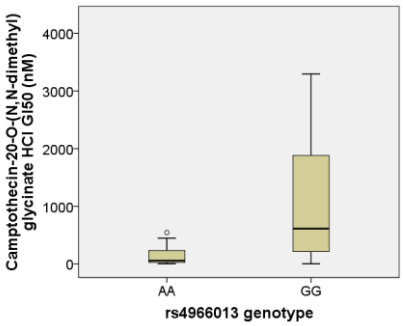


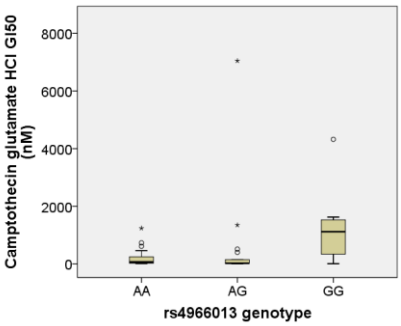


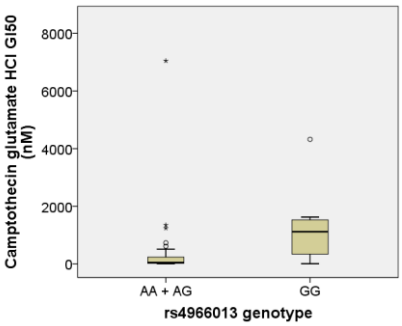


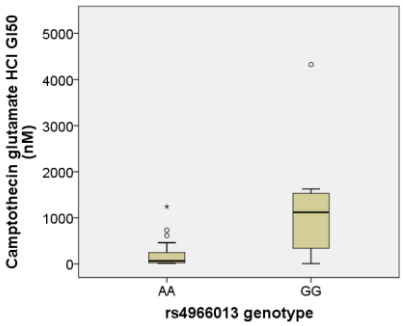

Camptothecin-20-O-(N,N-dimethyl) glycinate HCl GI50 (nM)
5000
4000
3000
2000
1000
0
AA
AG
GG
rs4966013 genotype

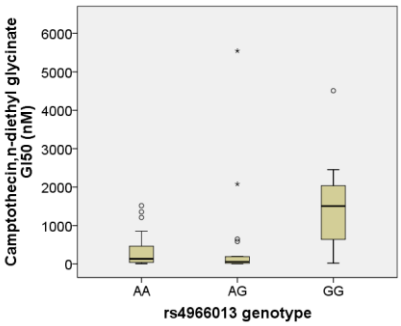

Camptothecin-20-O-(N,N-dimethyl) glycinate HCl GI50 (nM)
5000
4000
3000
2000
1000
0
AA + AG
GG
rs4966013 genotype

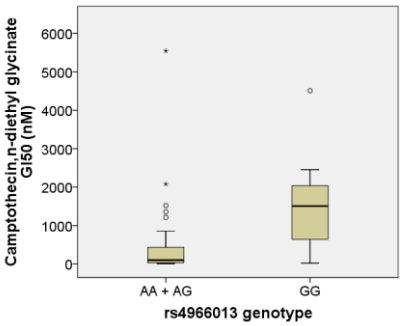

Camptothecin-20-O-(N,N-dimethyl) glycinate HCl GI50 (nM)
4000
3000
2000
1000
0
AA
GG
rs4966013 genotype

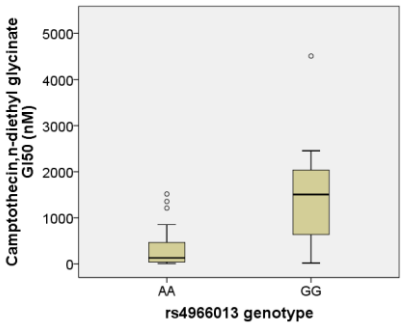

Camptothecin glutamate HCl GI50 (nM)
8000
6000
4000
2000
0
AA
AG
GG
rs4966013 genotype

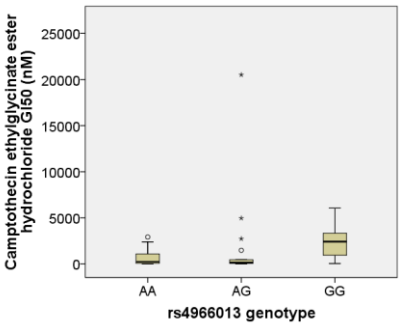

Camptothecin glutamate HCl GI50 (nM)
8000
6000
4000
2000
0
AA + AG
GG
rs4966013 genotype

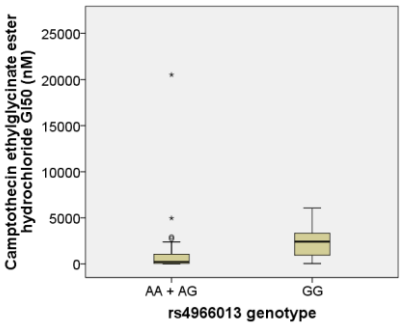

Camptothecin glutamate HCl GI50 (nM)
5000
4000
3000
2000
1000
0
AA
GG
rs4966013 genotype

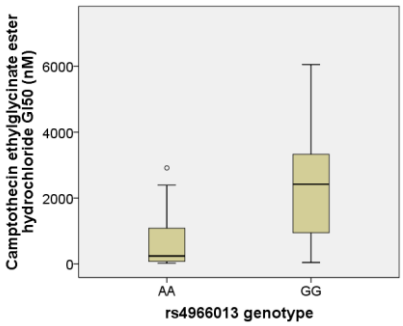

Camptothecin,n-diethyl glycinate GI50 (nM)
6000
5000
4000
3000
2000
1000
0
AA
AG
GG
rs4966013 genotype

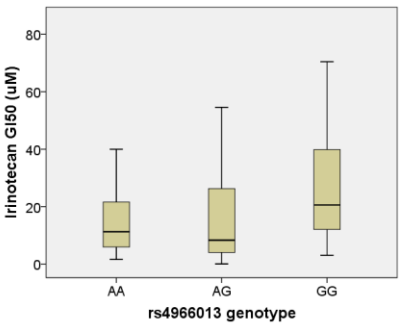

Camptothecin,n-diethyl glycinate GI50 (nM)
6000
5000
4000
3000
2000
1000
0
AA + AG
GG
rs4966013 genotype

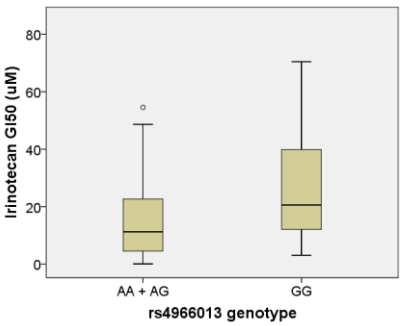

Camptothecin,n-diethyl glycinate GI50 (nM)
5000
4000
3000
2000
1000
0
AA
GG
rs4966013 genotype

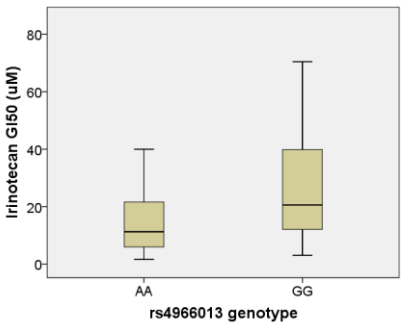

Camptothecin ethylglycinate ester hydrochloride GI50 (nM)
25000
20000
15000
10000
5000
0
AA
AG
GG
rs4966013 genotype

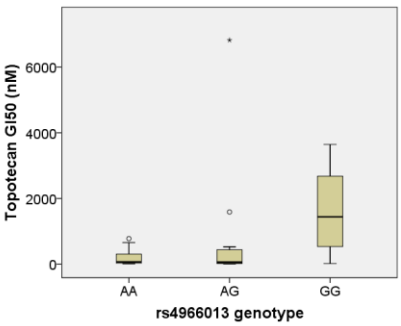

Camptothecin ethylglycinate ester hydrochloride GI50 (nM)
25000
20000
15000
10000
5000
0
AA + AG
GG
rs4966013 genotype

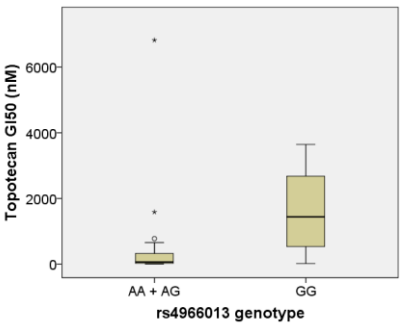

Camptothecin ethylglycinate ester hydrochloride GI50 (nM)
6000
4000
2000
0
AA
GG
rs4966013 genotype

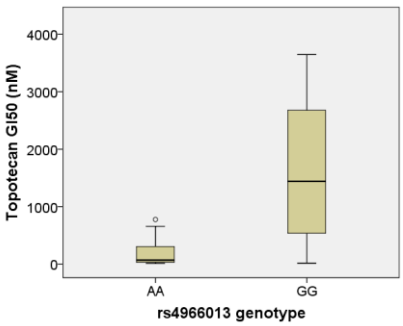

Irinotecan GI50 (uM)
80
60
40
20
0
AA
AG
GG
rs4966013 genotype

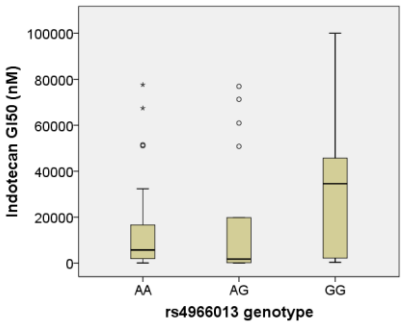

Irinotecan GI50 (uM)
80
60
40
20
0
AA + AG
GG
rs4966013 genotype

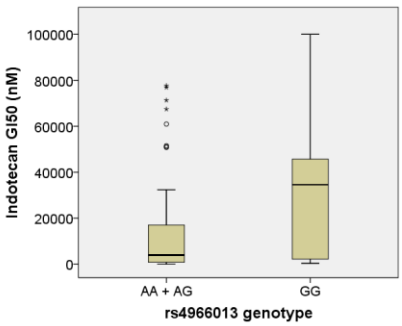

Irinotecan GI50 (uM)
80
60
40
20
0
AA
GG
rs4966013 genotype

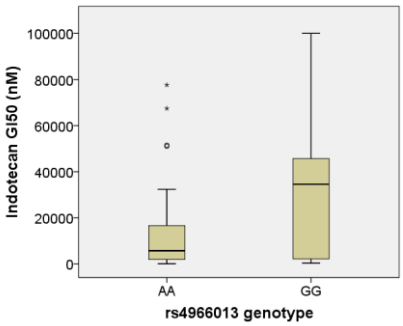

Topotecan GI50 (nM)
6000
4000
2000
0
AA
AG
GG
rs4966013 genotype

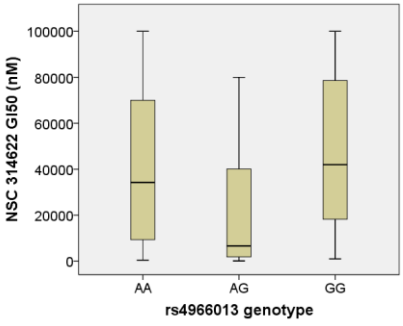

Topotecan GI50 (nM)
6000
4000
2000
0
AA + AG
GG
rs4966013 genotype

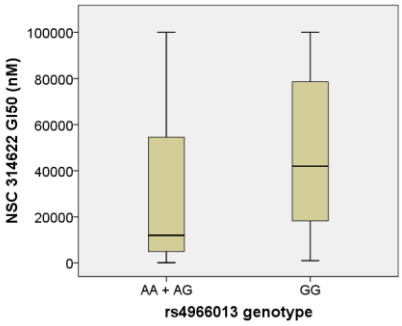

Topotecan GI50 (nM)
4000
3000
2000
1000
0
AA
GG
rs4966013 genotype

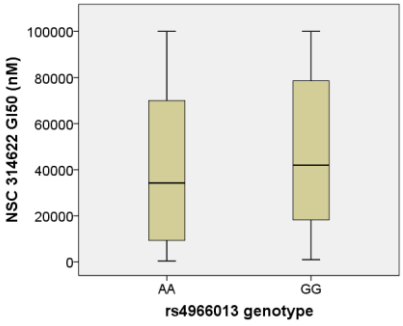

Indotecan GI50 (nM)
100000
80000
60000
40000
20000
0
AA
AG
GG
rs4966013 genotype

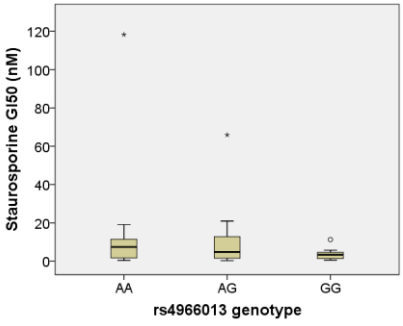

Indotecan GI50 (nM)
100000
80000
60000
40000
20000
0
AA + AG
GG
rs4966013 genotype

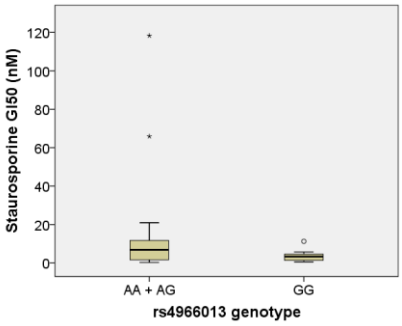

Indotecan GI50 (nM)
100000
80000
60000
40000
20000
0
AA
GG
rs4966013 genotype

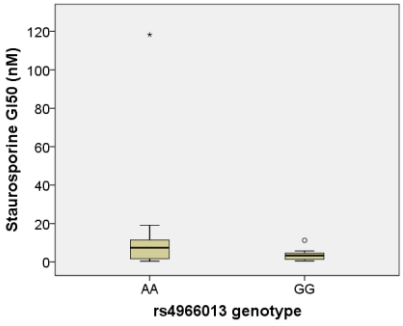

NSC 314622 GI50 (nM)
100000
80000
60000
40000
20000
0
AA
AG
GG
rs4966013 genotype

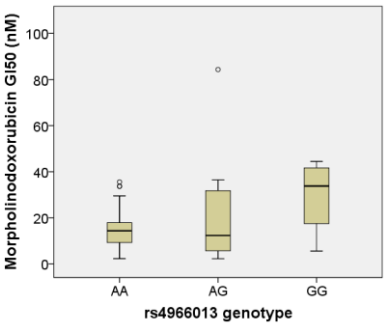

NSC 314622 GI50 (nM)
100000
80000
60000
40000
20000
0
AA + AG
GG
rs4966013 genotype

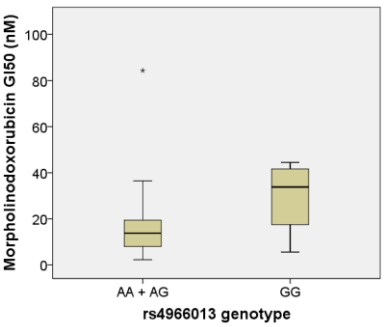

NSC 314622 GI50 (nM)
100000
80000
60000
40000
20000
0
AA
GG
rs4966013 genotype

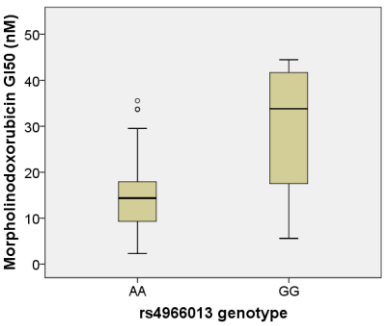

Staurosporine GI50 (nM)
120
100
80
60
40
20
0
AA
AG
GG
rs4966013 genotype


Staurosporine GI50 (nM)
120
100
80
60
40
20
0
AA + AG
GG
rs4966013 genotype

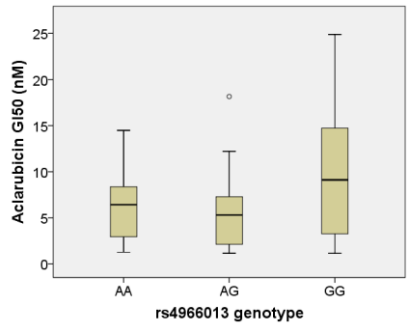

Staurosporine GI50 (nM)
120
100
80
60
40
20
0
AA
GG
rs4966013 genotype

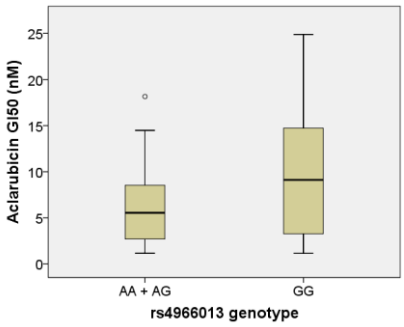

Morpholinodoxorubicin GI50 (nM)
100
80
60
40
20
0
AA
AG
GG
rs4966013 genotype

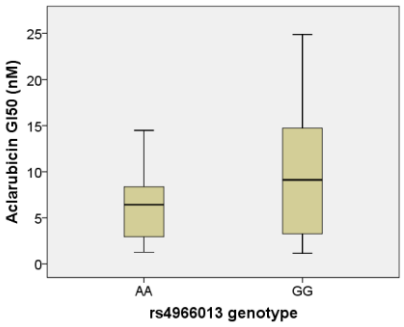

Morpholinodoxorubicin GI50 (nM)
100
80
60
40
20
0
AA + AG
GG
rs4966013 genotype

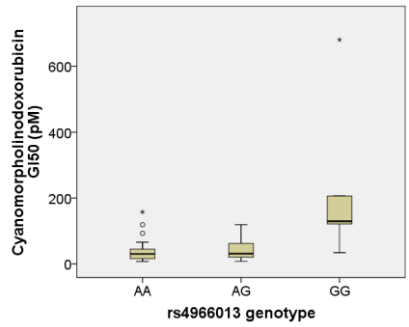

Morpholinodoxorubicin GI50 (nM)
50
40
30
20
10
0
AA
GG
rs4966013 genotype

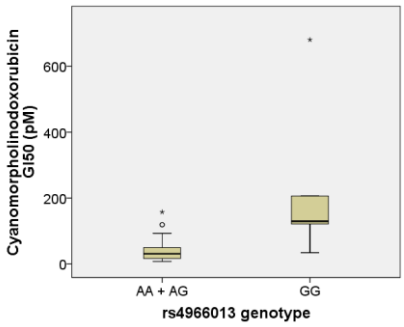
Topoisomerase II inhibitors

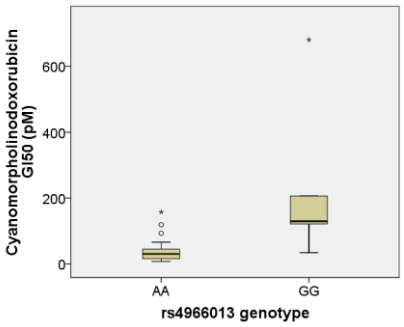


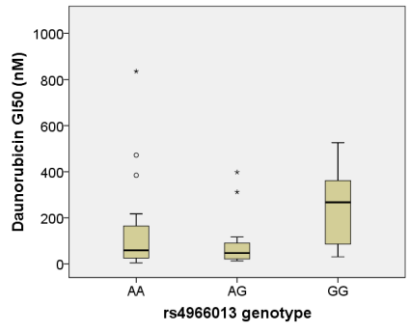


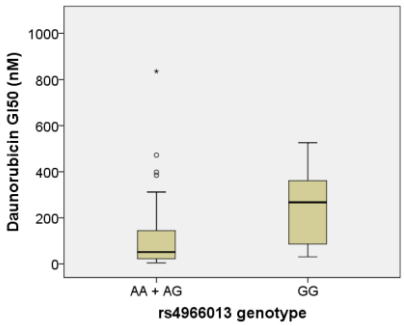


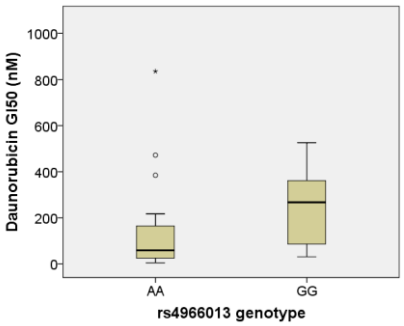


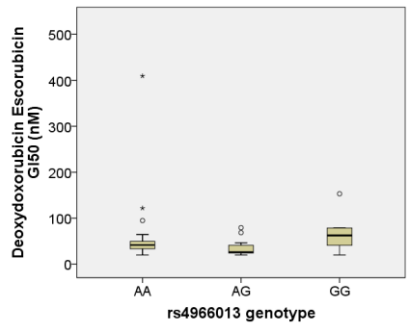


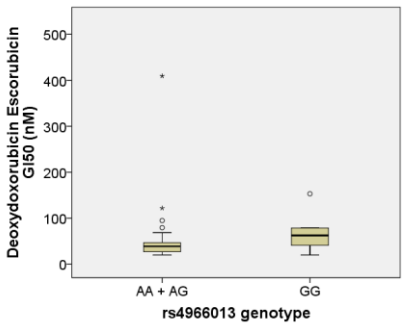


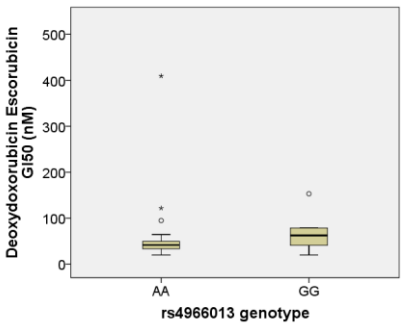


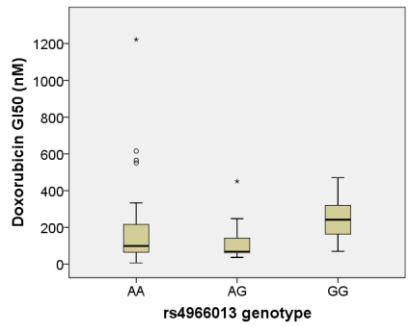


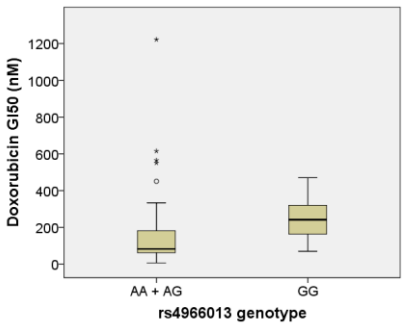


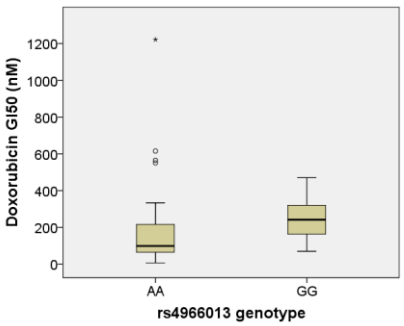


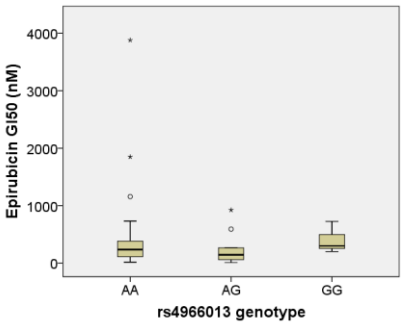


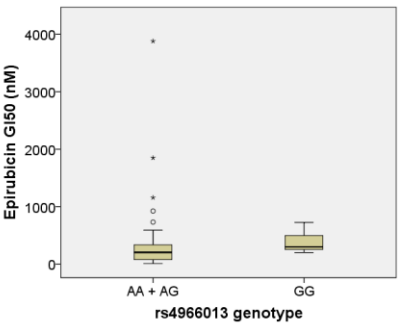


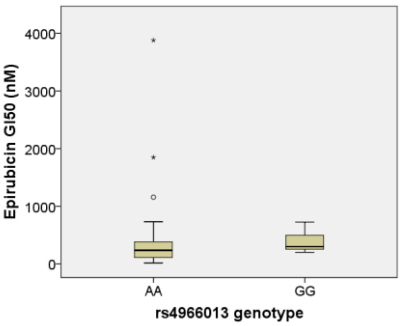


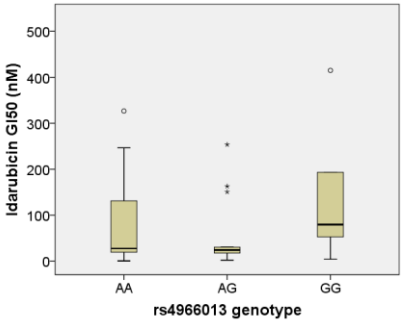


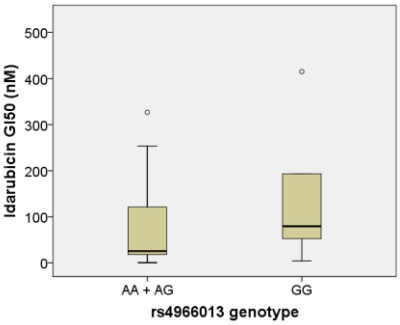


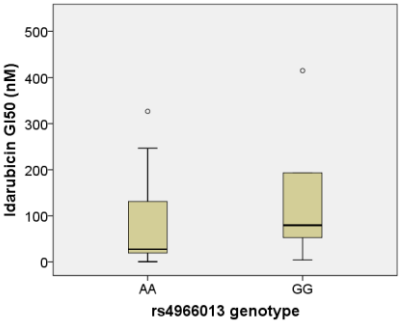

Epirubicin GI50 (nM)
4000
3000
2000
1000
0
AA
AG
GG
rs4966013 genotype

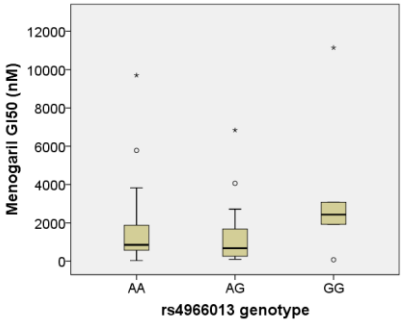

Epirubicin GI50 (nM)
4000
3000
2000
1000
0
AA + AG
GG
rs4966013 genotype

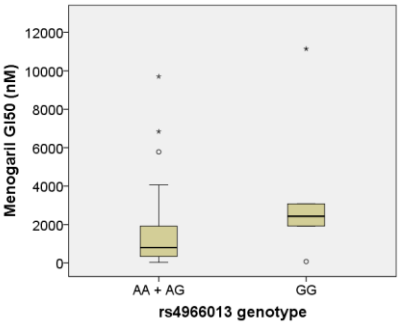

Epirubicin GI50 (nM)
4000
3000
2000
1000
0
AA
GG
rs4966013 genotype

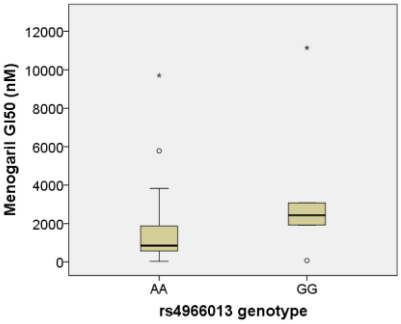

Idarubicin GI50 (nM)
500
400
300
200
100
0
AA
AG
GG
rs4966013 genotype

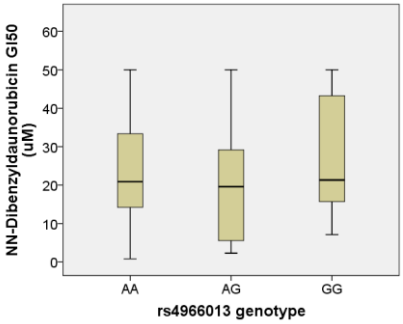

Idarubicin GI50 (nM)
500
400
300
200
100
0
AA + AG
GG
rs4966013 genotype

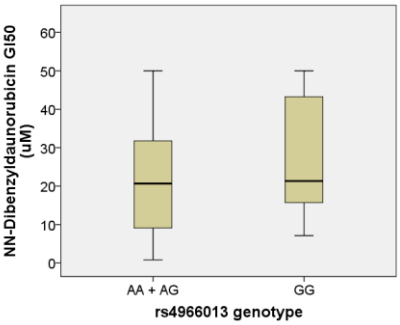

Idarubicin GI50 (nM)
500
400
300
200
100
0
AA
GG
rs4966013 genotype

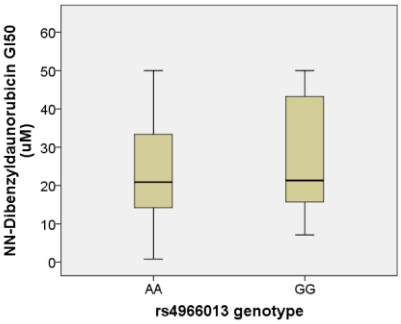

Menogaril GI50 (nM)
12000
10000
8000
6000
4000
2000
0
AA
AG
GG
rs4966013 genotype

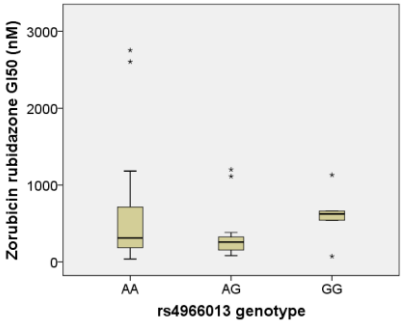

Menogaril GI50 (nM)
12000
10000
8000
6000
4000
2000
0
AA + AG
GG
rs4966013 genotype

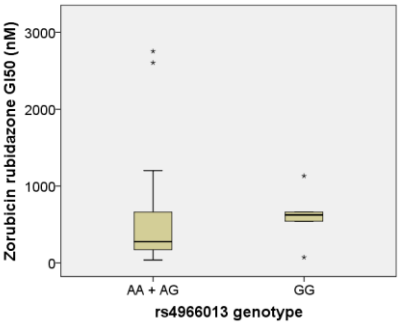

Menogaril GI50 (nM)
12000
10000
8000
6000
4000
2000
0
AA
GG
rs4966013 genotype

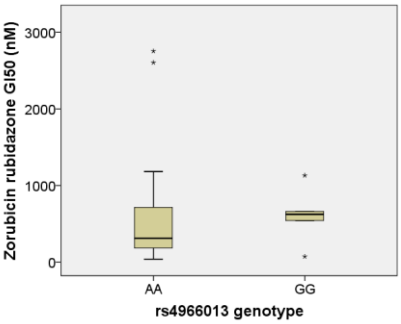

NN-Dibenzyldaunorubicin GI50 (uM)
60
50
40
30
20
10
0
AA
AG
GG
rs4966013 genotype

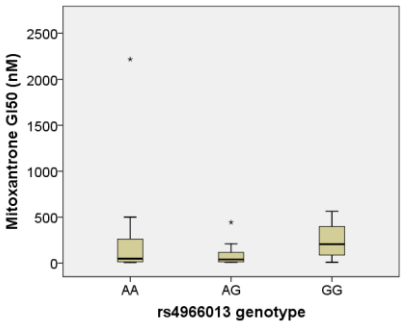

NN-Dibenzyldaunorubicin GI50 (uM)
60
50
40
30
20
10
0
AA + AG
GG
rs4966013 genotype

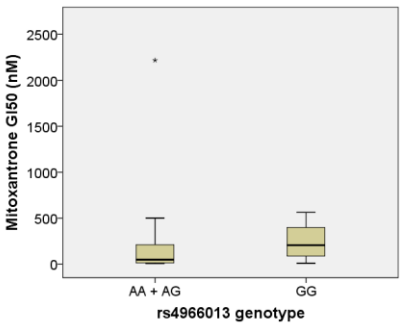

NN-Dibenzyldaunorubicin GI50 (uM)
60
50
40
30
20
10
0
AA
GG
rs4966013 genotype

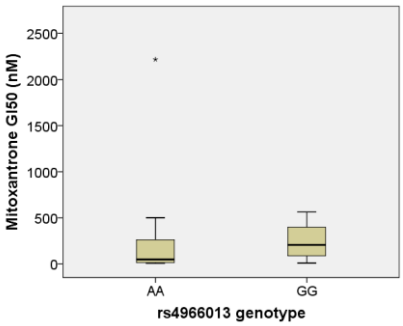

Zorubicin rubidazone GI50 (nM)
3000
2000
1000
0
AA
AG
GG
rs4966013 genotype

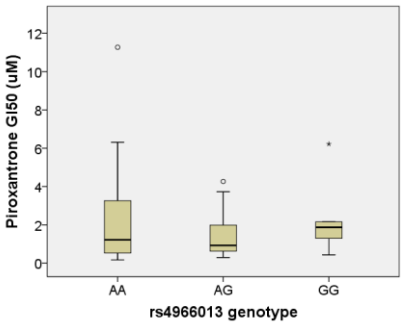

Zorubicin rubidazone GI50 (nM)
3000
2000
1000
0
AA + AG
GG
rs4966013 genotype

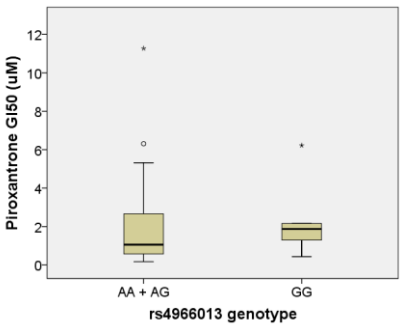

Zorubicin rubidazone GI50 (nM)
3000
2000
1000
0
AA
GG
rs4966013 genotype

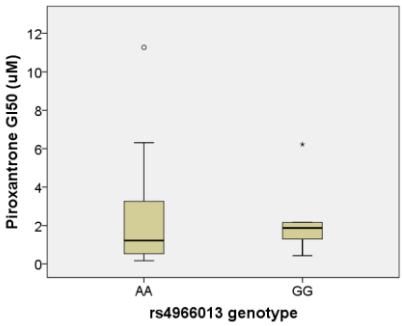

Mitoxantrone GI50 (nM)
2500
2000
1500
1000
500
0
AA
AG
GG
rs4966013 genotype

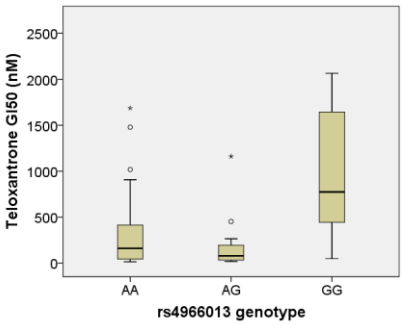

Mitoxantrone GI50 (nM)
2500
2000
1500
1000
500
0
AA + AG
GG
rs4966013 genotype

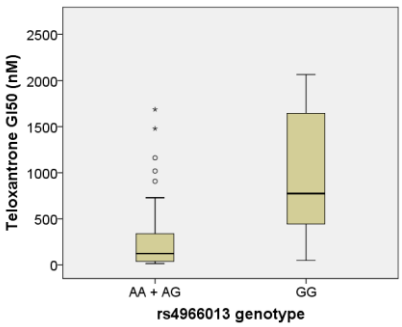

Mitoxantrone GI50 (nM)
2500
2000
1500
1000
500
0
AA
GG
rs4966013 genotype

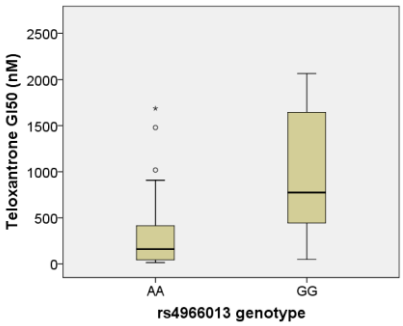

Piroxantrone GI50 (uM)
12
10
8
6
4
2
0
AA
AG
GG
rs4966013 genotype

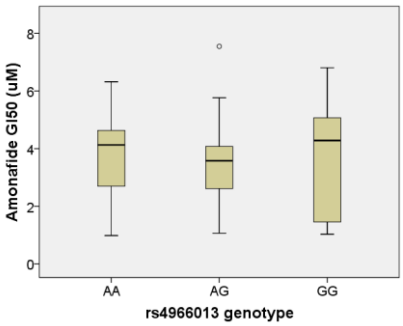

Piroxantrone GI50 (uM)
12
10
8
6
4
2
0
AA + AG
GG
rs4966013 genotype

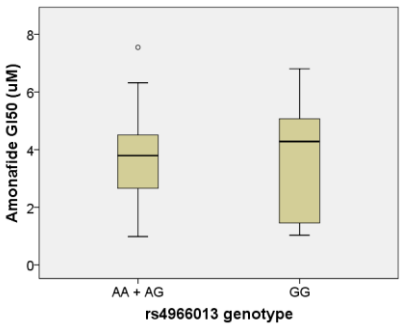

Piroxantrone GI50 (uM)
12
10
8
6
4
2
0
AA
GG
rs4966013 genotype

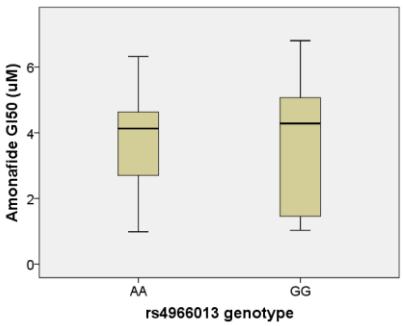

Teloxantrone GI50 (nM)
2500
2000
1500
1000
500
0
AA
AG
GG
rs4966013 genotype

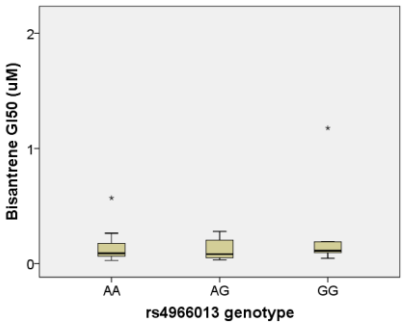

Teloxantrone GI50 (nM)
2500
2000
1500
1000
500
0
AA + AG
GG
rs4966013 genotype

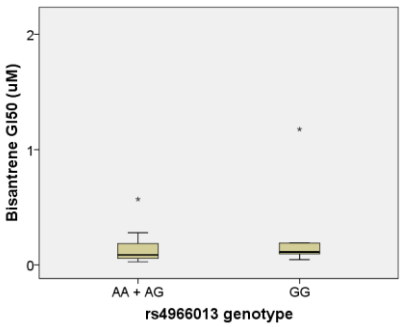

Teloxantrone GI50 (nM)
2500
2000
1500
1000
500
0
AA
GG
rs4966013 genotype

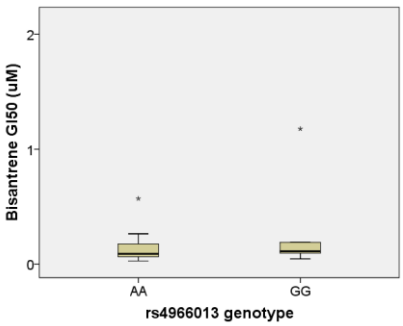

Amonafide GI50 (uM)
8
6
4
2
0
AA
AG
GG
rs4966013 genotype

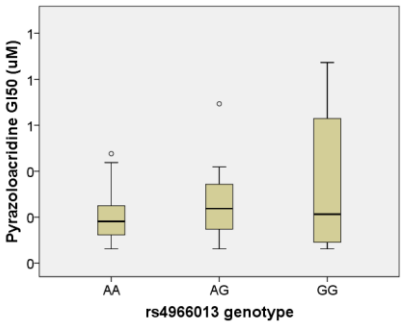

Amonafide GI50 (uM)
8
6
4
2
0
AA + AG
GG
rs4966013 genotype

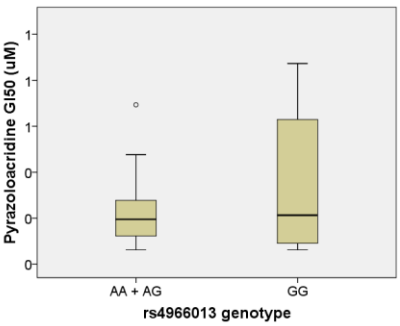

Amonafide GI50 (uM)
6
4
2
0
AA
GG
rs4966013 genotype

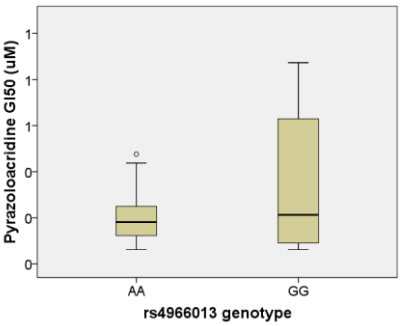

Bisantrene GI50 (uM)
2
1
0
AA
AG
GG
rs4966013 genotype

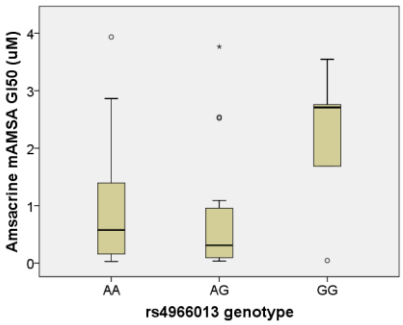

Bisantrene GI50 (uM)
2
1
0
AA + AG
GG
rs4966013 genotype

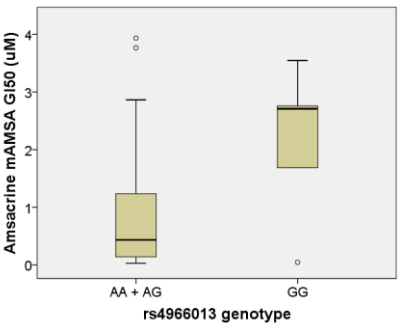

Bisantrene GI50 (uM)
2
1
0
AA
GG
rs4966013 genotype

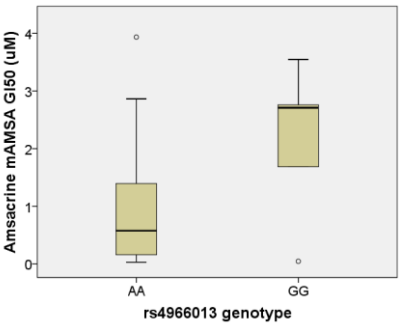

Pyrazoloacridine GI50 (uM)
AA
AG
GG
rs4966013 genotype

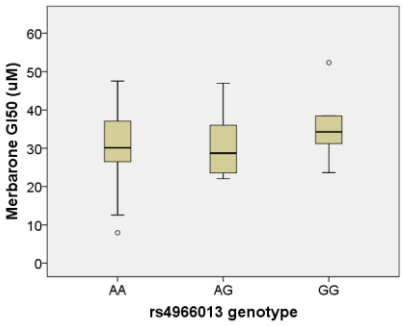

Pyrazoloacridine GI50 (uM)
AA + AG
GG
rs4966013 genotype

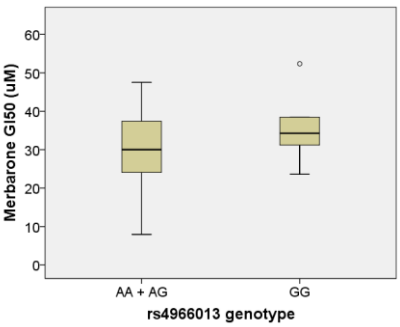

Pyrazoloacridine GI50 (uM)
AA
GG
rs4966013 genotype

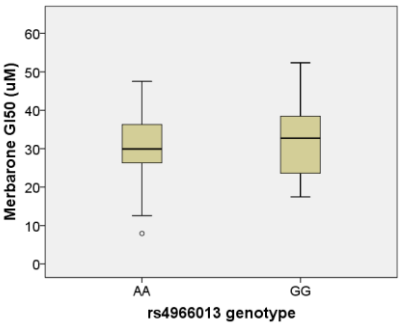

Amsacrine mAMSA GI50 (uM)
AA
AG
GG
rs4966013 genotype

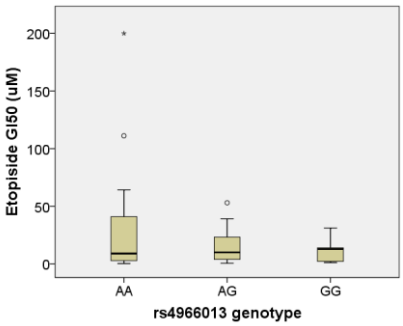

Amsacrine mAMSA GI50 (uM)
AA + AG
GG
rs4966013 genotype

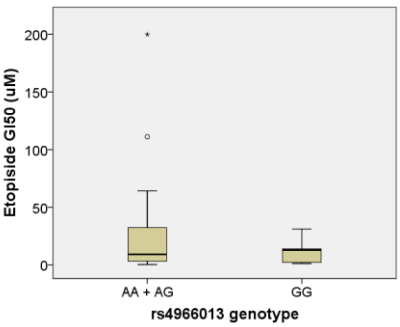

Amsacrine mAMSA GI50 (uM)
AA
GG
rs4966013 genotype

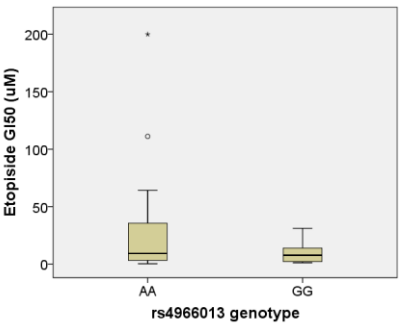

Merbarone GI50 (uM)
AA
AG
GG
rs4966013 genotype

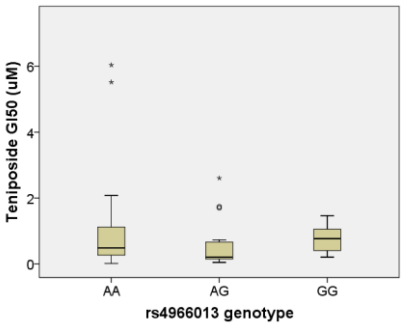

Merbarone GI50 (uM)
AA + AG
GG
rs4966013 genotype

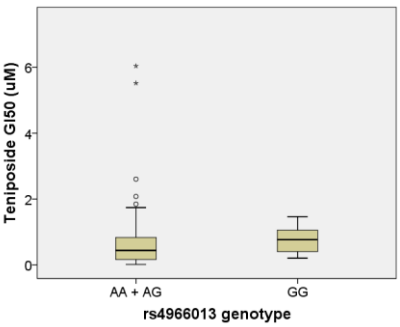

Merbarone GI50 (uM)
AA
GG
rs4966013 genotype

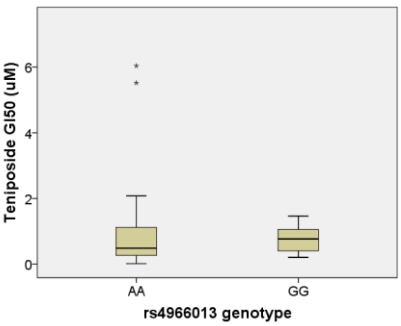

Etopiside GI50 (uM)
AA
AG
GG
rs4966013 genotype


Etopiside GI50 (uM)
AA + AG
GG
rs4966013 genotype

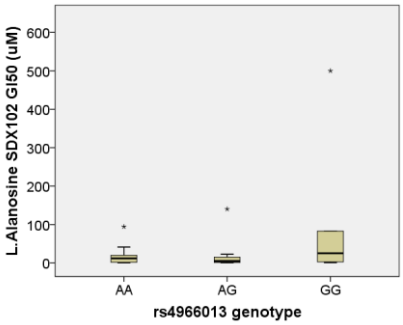

Etopiside GI50 (uM)
AA
GG
rs4966013 genotype

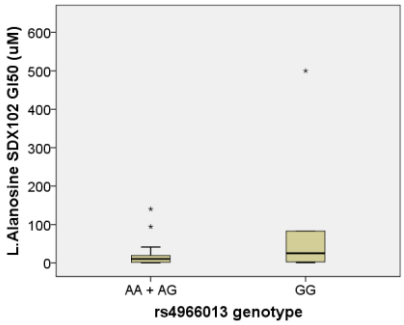

Teniposide GI50 (uM)
AA
AG
GG
rs4966013 genotype

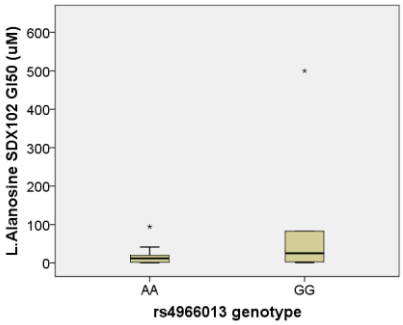

Teniposide GI50 (uM)
AA + AG
GG
rs4966013 genotype

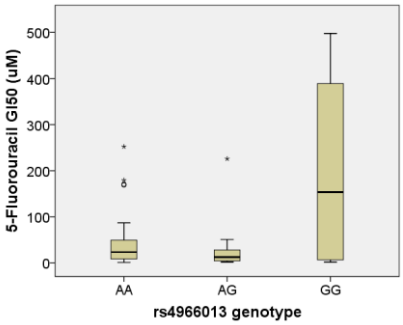

Teniposide GI50 (uM)
AA
GG
rs4966013 genotype

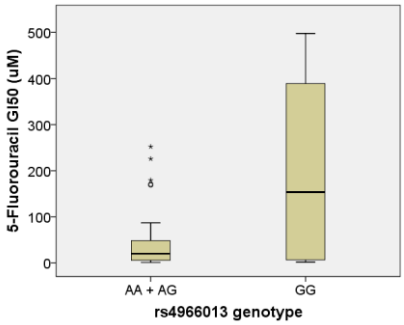
RNA/ DNA antimetabolites

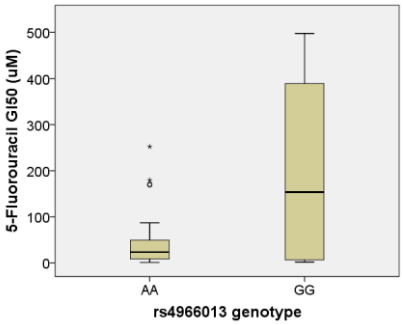


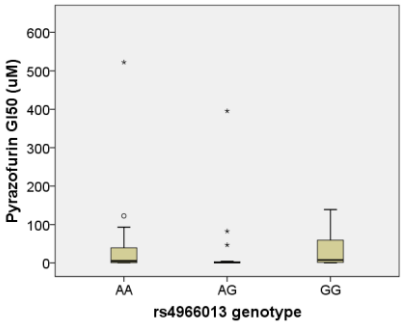


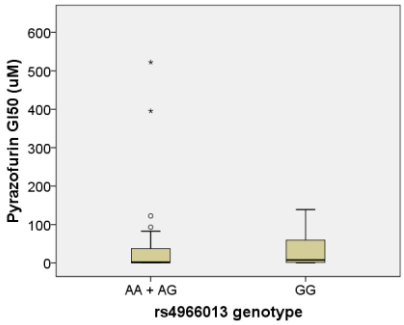


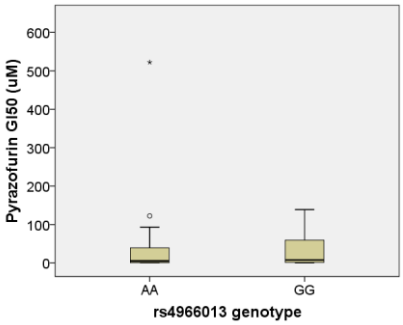


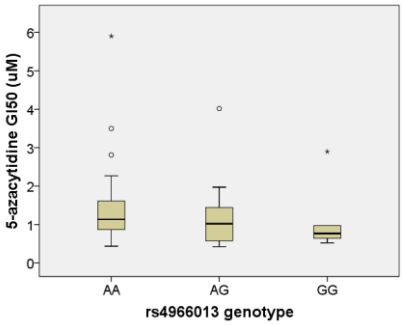


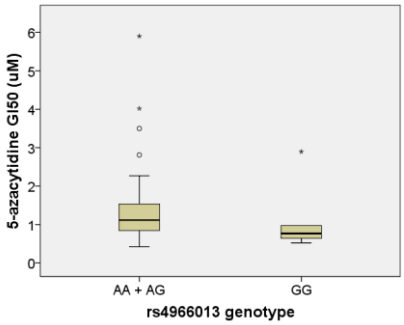


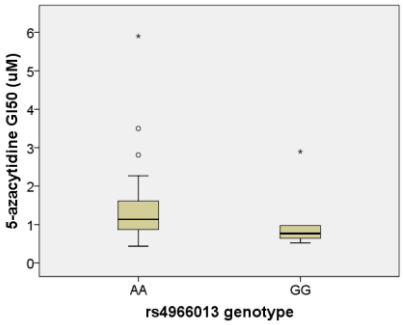


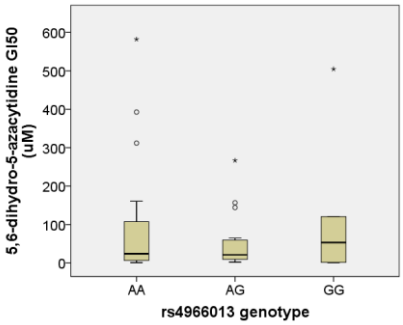


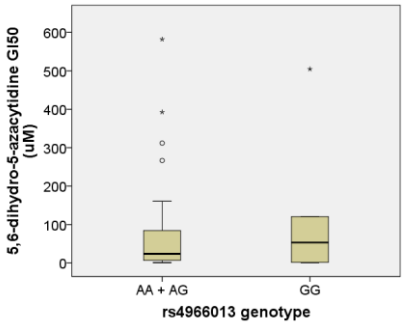


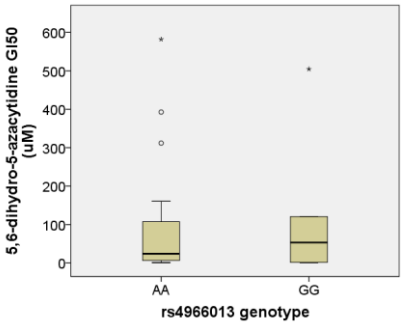


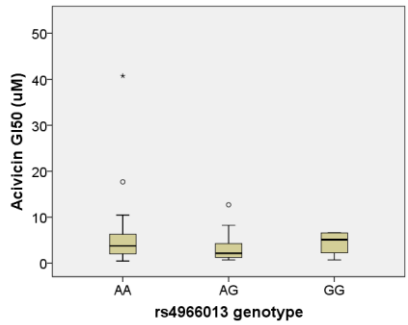


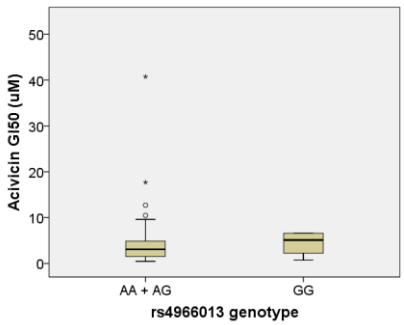


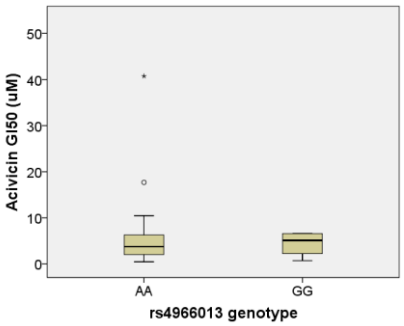


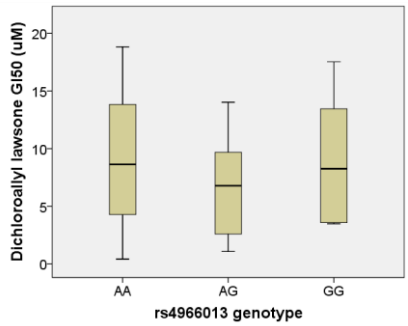


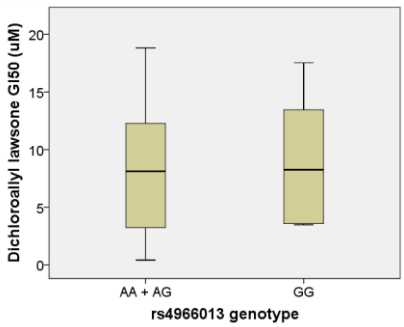


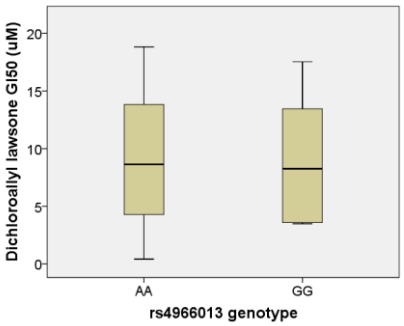

Acivicin GI50 (uM)
0
10
20
30
40
50
AA
AG
GG
rs4966013 genotype

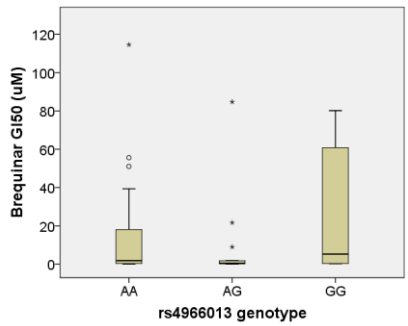

Acivicin GI50 (uM)
0
10
20
30
40
50
AA + AG
GG
rs4966013 genotype

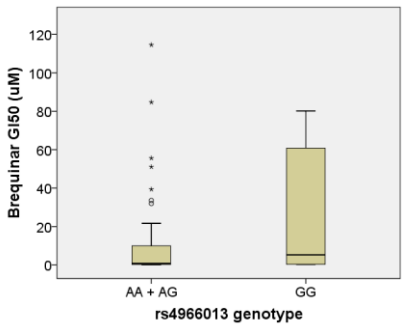

Acivicin GI50 (uM)
0
10
20
30
40
50
AA
GG
rs4966013 genotype

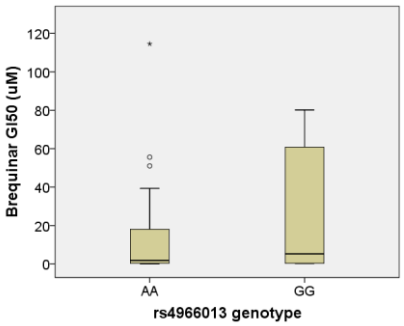

Dichloroallyl lawsone GI50 (uM)
0
5
10
15
20
AA
AG
GG
rs4966013 genotype

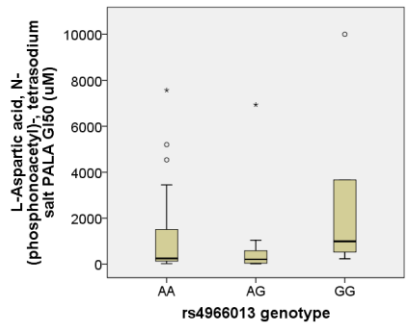

Dichloroallyl lawsone GI50 (uM)
0
5
10
15
20
AA + AG
GG
rs4966013 genotype

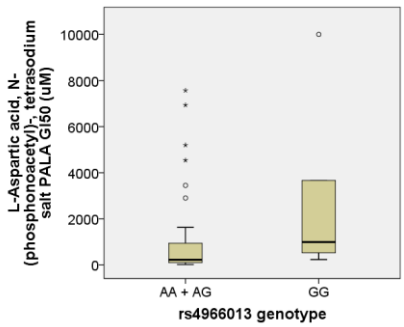

Dichloroallyl lawsone GI50 (uM)
0
5
10
15
20
AA
GG
rs4966013 genotype

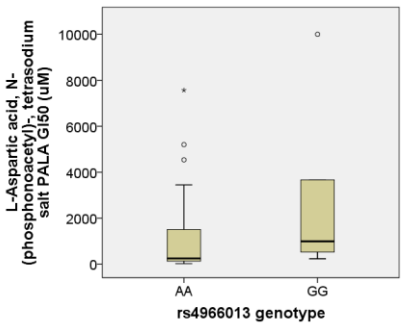

Brequinar GI50 (uM)
0
20
40
60
80
100
120
AA
AG
GG
rs4966013 genotype

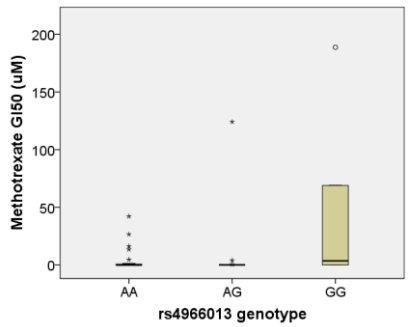

Brequinar GI50 (uM)
0
20
40
60
80
100
120
AA + AG
GG
rs4966013 genotype

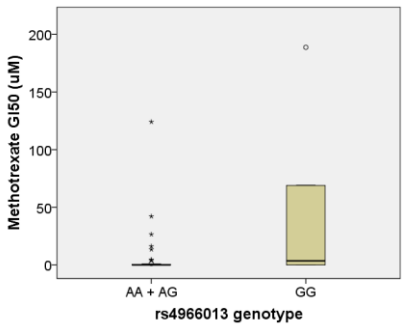

Brequinar GI50 (uM)
0
20
40
60
80
100
120
AA
GG
rs4966013 genotype

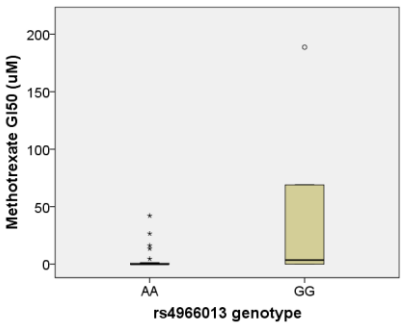

L-Aspartic acid, N-(phosphonoacetyl)-, tetrasodium salt PALA GI50 (uM)
0
2000
4000
6000
8000
10000
AA
AG
GG
rs4966013 genotype

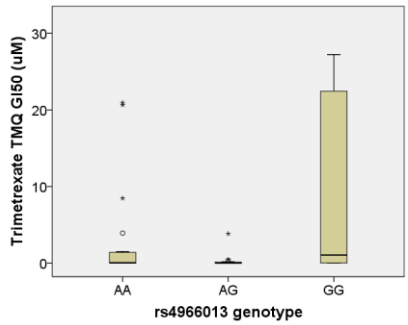

L-Aspartic acid, N-(phosphonoacetyl)-, tetrasodium salt PALA GI50 (uM)
0
2000
4000
6000
8000
10000
AA + AG
GG
rs4966013 genotype

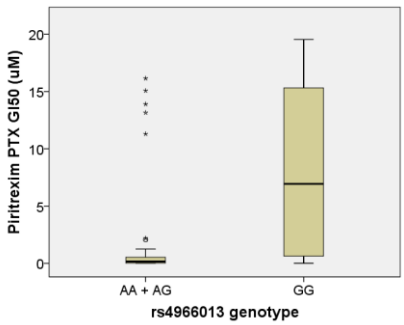

L-Aspartic acid, N-(phosphonoacetyl)-, tetrasodium salt PALA GI50 (uM)
0
2000
4000
6000
8000
10000
AA
GG
rs4966013 genotype

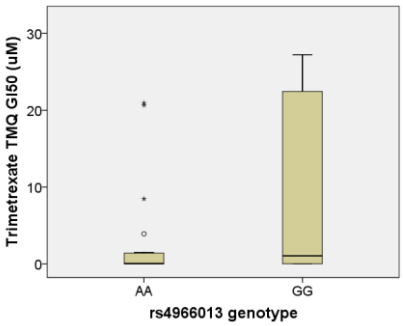

Methotrexate GI50 (uM)
0
50
100
150
200
AA
AG
GG
rs4966013 genotype

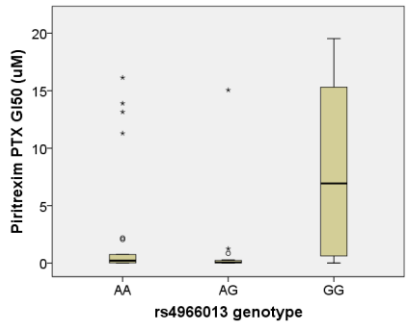

Methotrexate GI50 (uM)
0
50
100
150
200
AA + AG
GG
rs4966013 genotype

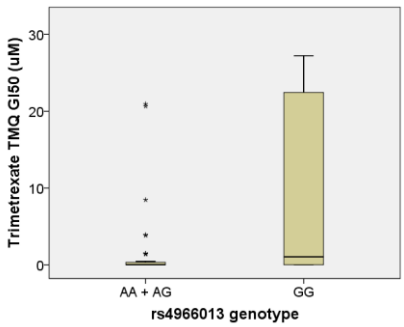

Methotrexate GI50 (uM)
0
50
100
150
200
AA
GG
rs4966013 genotype

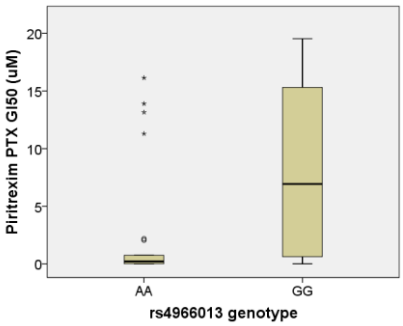

Trimetrexate TMQ GI50 (uM)
30
20
10
0
AA
AG
GG
rs4966013 genotype


Piritrexim PTX GI50 (uM)
20
15
10
5
0
AA + AG
GG
rs4966013 genotype

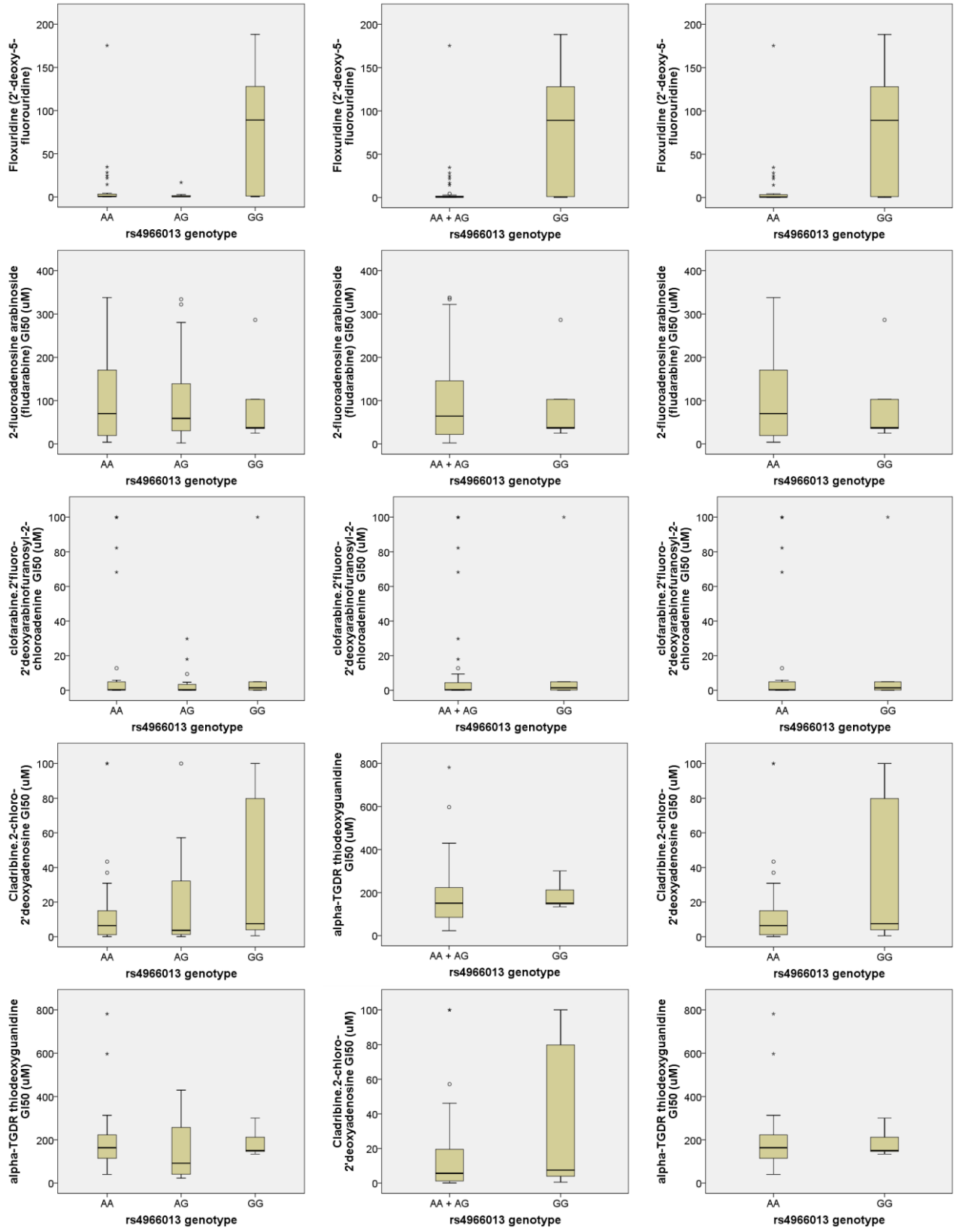

Trimetrexate TMQ GI50 (uM)
30
20
10
0
AA
GG
rs4966013 genotype

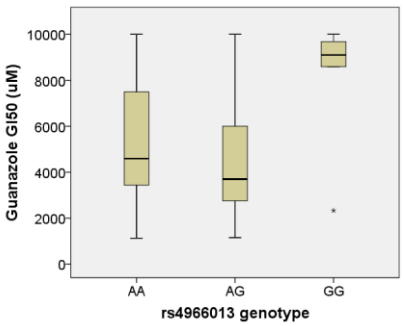

Piritrexim PTX GI50 (uM)
20
15
10
5
0
AA
AG
GG
rs4966013 genotype

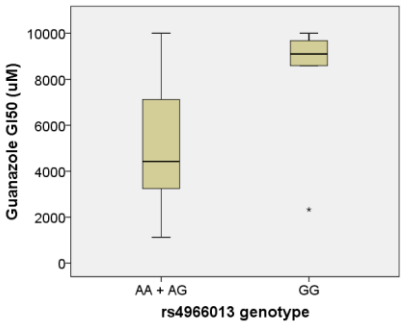

Trimetrexate TMQ GI50 (uM)
30
20
10
0
AA + AG
GG
rs4966013 genotype

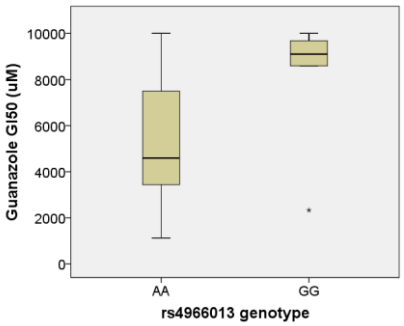

Piritrexim PTX GI50 (uM)
20
15
10
5
0
AA
GG
rs4966013 genotype

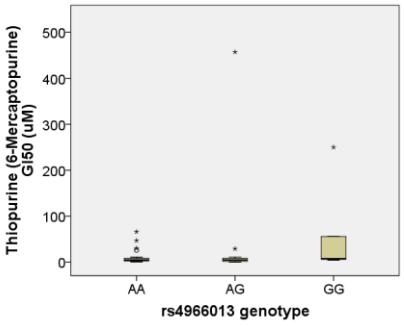
DNA antimetabolites

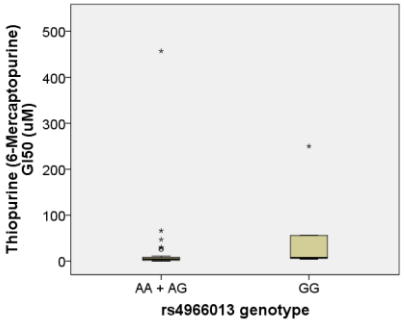


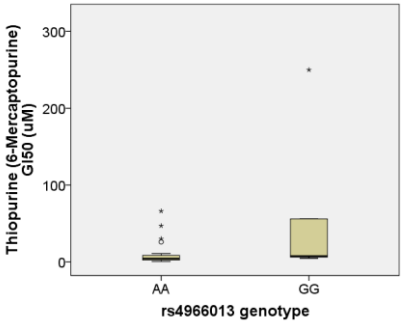

Guanazole GI50 (uM)
10000
8000
6000
4000
2000
0
AA
AG
GG
rs4966013 genotype

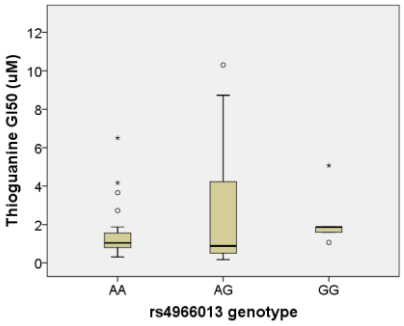

Guanazole GI50 (uM)
10000
8000
6000
4000
2000
0
AA + AG
GG
rs4966013 genotype

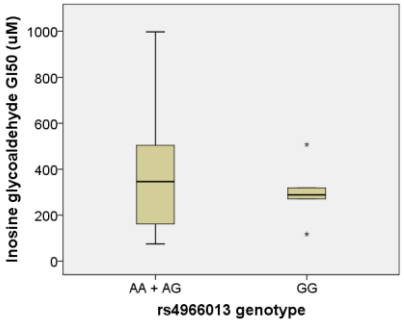

Guanazole GI50 (uM)
10000
8000
6000
4000
2000
0
AA
GG
rs4966013 genotype

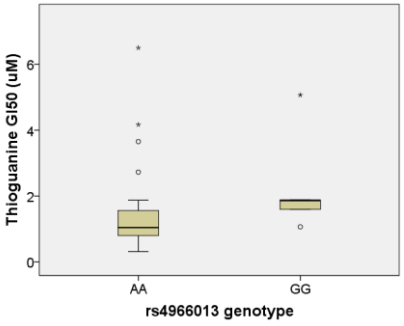

Thiopurine (6-Mercaptopurine) GI50 (uM)
500
400
300
200
100
0
AA
AG
GG
rs4966013 genotype

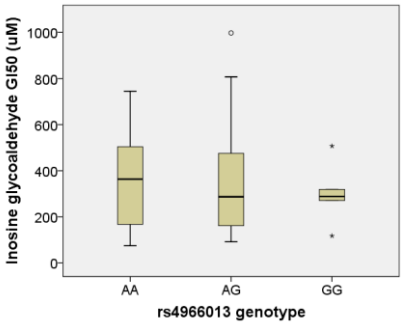

Thiopurine (6-Mercaptopurine) GI50 (uM)
500
400
300
200
100
0
AA + AG
GG
rs4966013 genotype

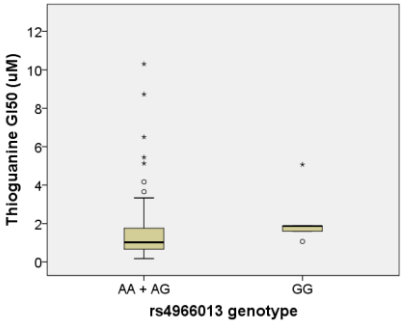

Thiopurine (6-Mercaptopurine) GI50 (uM)
300
200
100
0
AA
GG
rs4966013 genotype

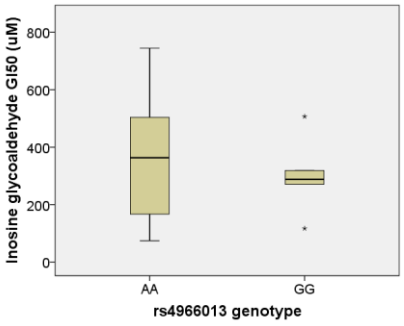

Thioguanine GI50 (uM)
12
10
8
6
4
2
0
AA
AG
GG
rs4966013 genotype

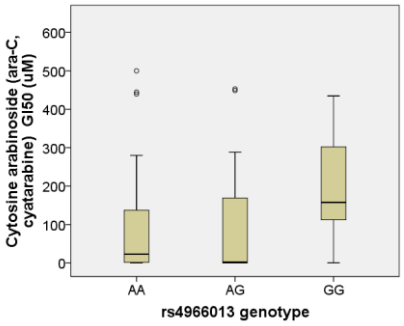

Inosine glycoaldehyde GI50 (uM)
1000
800
600
400
200
0
AA + AG
GG
rs4966013 genotype

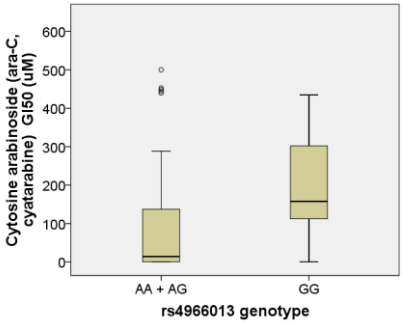

Thioguanine GI50 (uM)
6
4
2
0
AA
GG
rs4966013 genotype

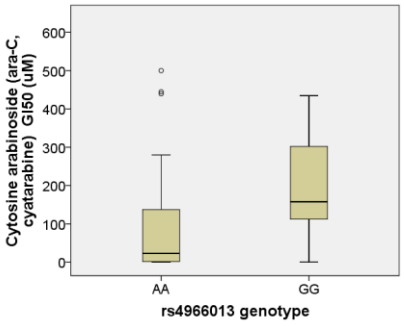

Inosine glycoaldehyde GI50 (uM)
1000
800
600
400
200
0
AA
AG
GG
rs4966013 genotype

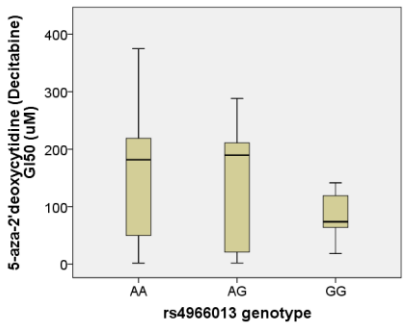

Thioguanine GI50 (uM)
12
10
8
6
4
2
0
AA + AG
GG
rs4966013 genotype

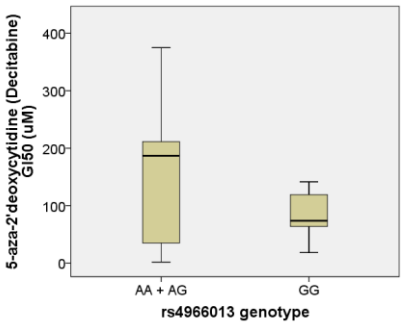

Inosine glycoaldehyde GI50 (uM)
800
600
400
200
0
AA
GG
rs4966013 genotype

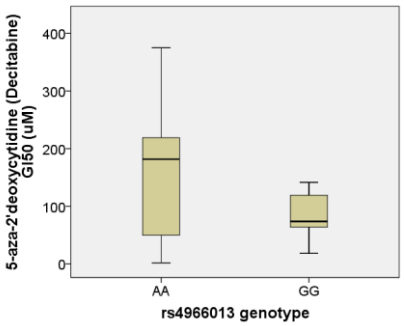

Cytosine arabinoside (ara-C, cyatarabine) GI50 (uM)
600
500
400
300
200
100
0
AA
AG
GG
rs4966013 genotype

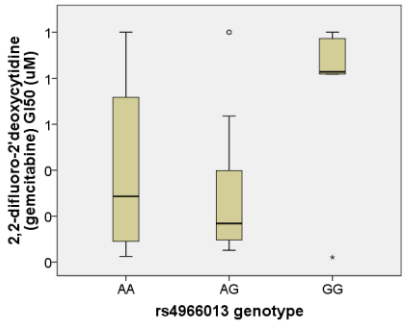

Cytosine arabinoside (ara-C, cyatarabine) GI50 (uM)
600
500
400
300
200
100
0
AA + AG
GG
rs4966013 genotype

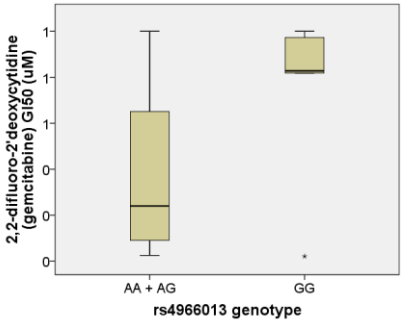

Cytosine arabinoside (ara-C, cyatarabine) GI50 (uM)
600
500
400
300
200
100
0
AA
GG
rs4966013 genotype

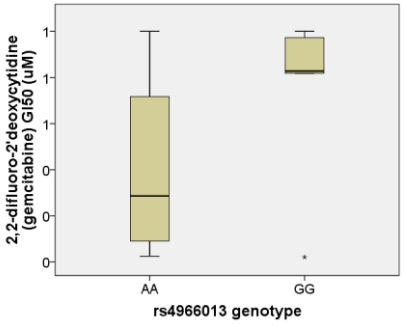

5-aza-2'deoxycytidine (Decitabine) GI50 (uM)
400
300
200
100
0
AA
AG
GG
rs4966013 genotype

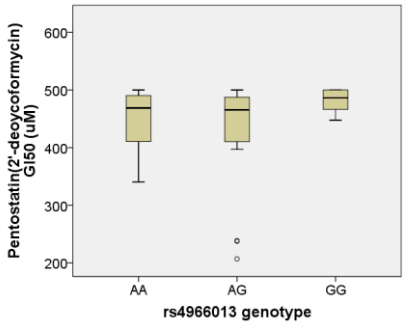

5-aza-2'deoxycytidine (Decitabine) GI50 (uM)
400
300
200
100
0
AA + AG
GG
rs4966013 genotype

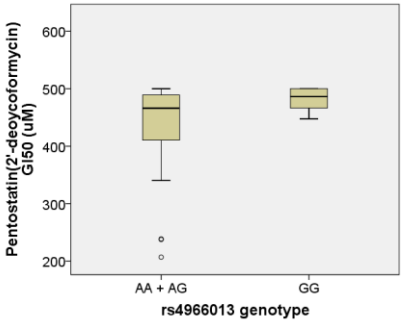

5-aza-2'deoxycytidine (Decitabine) GI50 (uM)
400
300
200
100
0
AA
GG
rs4966013 genotype

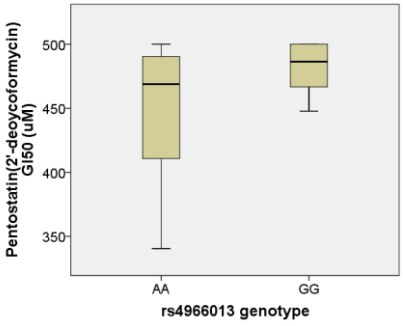

2,2-difluoro-2'deoxycytidine (gemcitabine) GI50 (uM)
1
1
1
0
0
0
AA
AG
GG
rs4966013 genotype

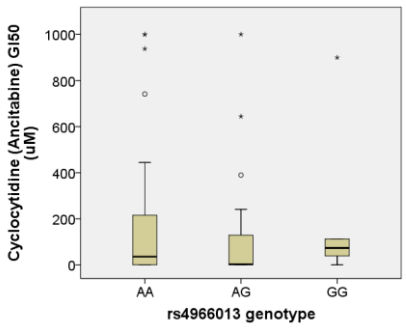

2,2-difluoro-2'deoxycytidine (gemcitabine) GI50 (uM)
1
1
1
0
0
0
AA + AG
GG
rs4966013 genotype

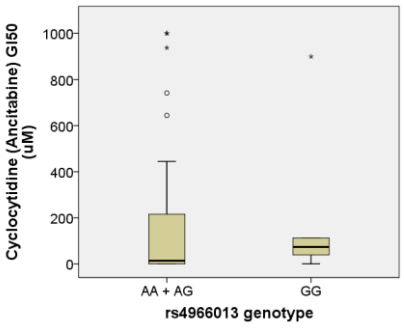

2,2-difluoro-2'deoxycytidine (gemcitabine) GI50 (uM)
1
1
1
0
0
0
AA
GG
rs4966013 genotype

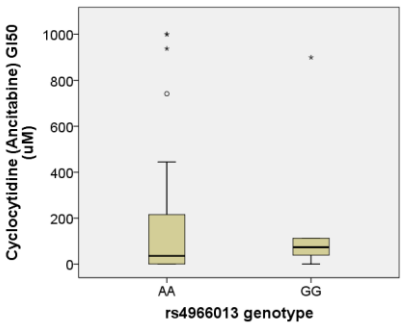

Pentostatin(2'-deoycoformycin) GI50 (uM)
600
500
400
300
200
AA
AG
GG
rs4966013 genotype

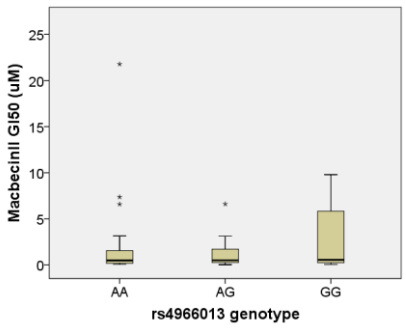

Pentostatin(2'-deoycoformycin) GI50 (uM)
600
500
400
300
200
AA + AG
GG
rs4966013 genotype

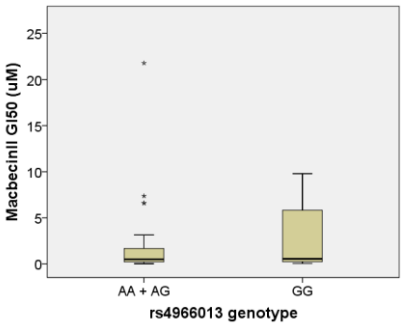

Pentostatin(2'-deoycoformycin) GI50 (uM)
500
450
400
350
AA
GG
rs4966013 genotype

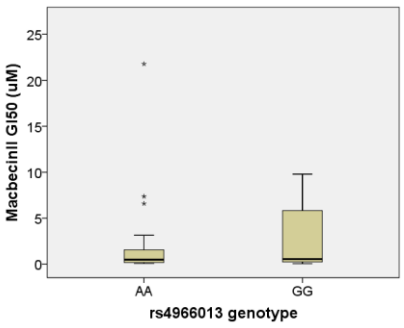

Cyclocytidine (Ancitabine) GI50 (uM)
1000
800
600
400
200
0
AA
AG
GG
rs4966013 genotype

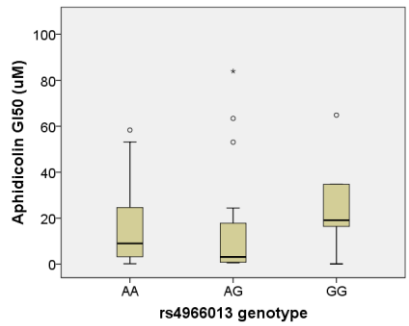

Cyclocytidine (Ancitabine) GI50 (uM)
1000
800
600
400
200
0
AA + AG
GG
rs4966013 genotype

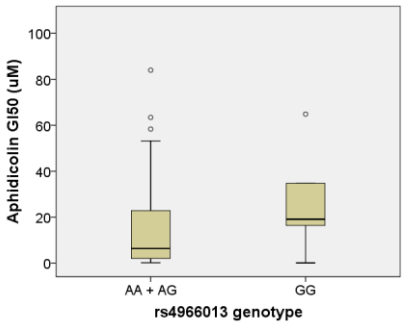

Cyclocytidine (Ancitabine) GI50 (uM)
1000
800
600
400
200
0
AA
GG
rs4966013 genotype

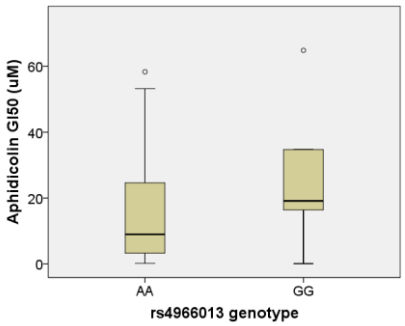

Macbecinll GI50 (uM)
25
20
15
10
5
0
AA
AG
GG
rs4966013 genotype

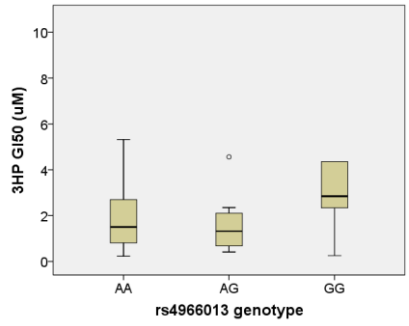

Macbecinll GI50 (uM)
25
20
15
10
5
0
AA + AG
GG
rs4966013 genotype

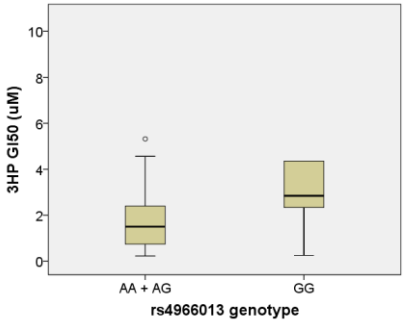

Macbecinll GI50 (uM)
25
20
15
10
5
0
AA
GG
rs4966013 genotype

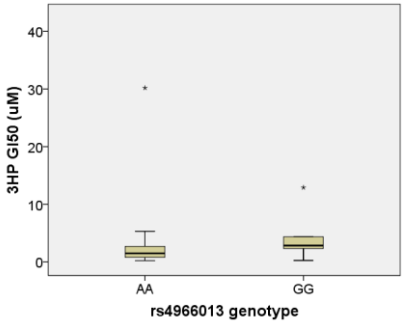

Aphidicolin GI50 (uM)
100
80
60
40
20
0
AA
AG
GG
rs4966013 genotype

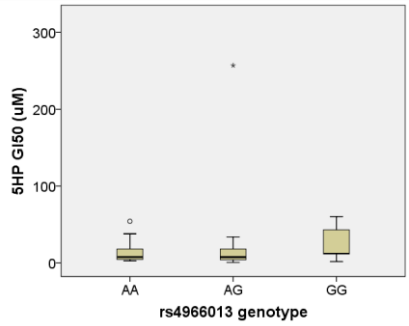

Aphidicolin GI50 (uM)
100
80
60
40
20
0
AA + AG
GG
rs4966013 genotype

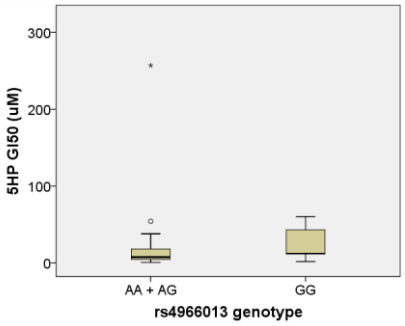

Aphidicolin GI50 (uM)
60
40
20
0
AA
GG
rs4966013 genotype

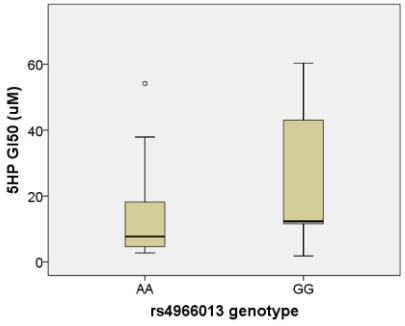

3HP GI50 (uM)
10
8
6
4
2
0
AA
AG
GG
rs4966013 genotype

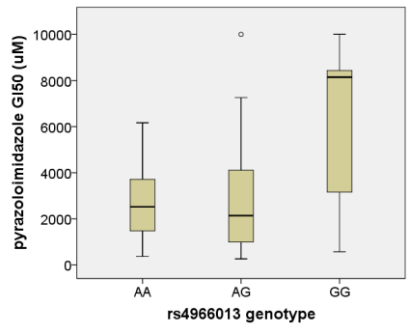

3HP GI50 (uM)
10
8
6
4
2
0
AA + AG
GG
rs4966013 genotype

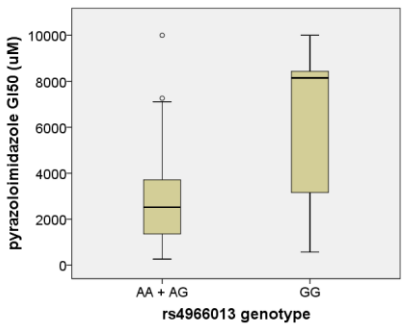

3HP GI50 (uM)
40
30
20
10
0
AA
GG
rs4966013 genotype

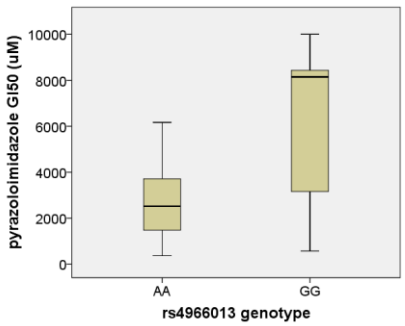

5HP GI50 (uM)
300
200
100
0
AA
AG
GG
rs4966013 genotype

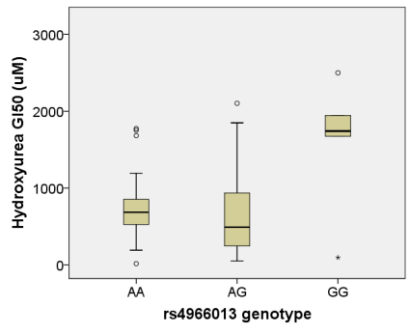

5HP GI50 (uM)
300
200
100
0
AA + AG
GG
rs4966013 genotype

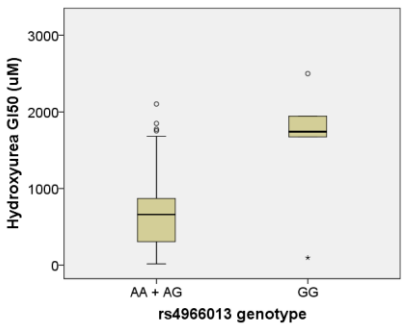

5HP GI50 (uM)
60
40
20
0
AA
GG
rs4966013 genotype

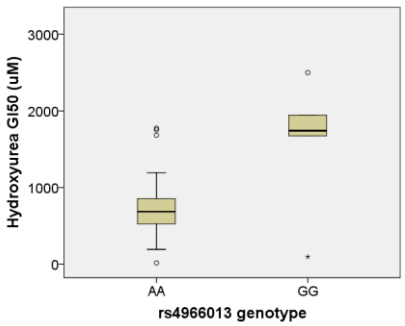

pyrazoloimidazole GI50 (uM)
10000
8000
6000
4000
2000
0
AA
AG
GG
rs4966013 genotype


pyrazoloimidazole GI50 (uM)
10000
8000
6000
4000
2000
0
AA + AG
GG
rs4966013 genotype


pyrazoloimidazole GI50 (uM)
10000
8000
6000
4000
2000
0
AA
GG
rs4966013 genotype


Hydroxyurea GI50 (uM)
3000
2000
1000
0
AA
AG
GG
rs4966013 genotype


Hydroxyurea GI50 (uM)
3000
2000
1000
0
AA + AG
GG
rs4966013 genotype


Hydroxyurea GI50 (uM)
3000
2000
1000
0
AA
GG
rs4966013 genotype

Appendix IV: Tables – drug GI_{50} by SNP genotype

Tables show associations of GI_{50} values for each chemotherapeutic agent with IGF-1R SNP rs4966013 genotype within cell lines of the NCI60 tumour panel. Comparison of GI_{50}s for different allelic populations AA vs AG vs GG using the Jonckheere Terpstra test examines the probability of an ordered association between the SNP and drug GI_{50}, assuming an additive/ non-dominant relationship between the different SNP alleles. Comparison of the significance of differences in GI_{50} between the combined AA + AG group examines the possibility of an association between SNP genotype and GI_{50} given a dominance of the A allele over the G allele. The significance of any differences in GI_{50} between allelic populations was compared using the Jonckheere Terpstra test for AA vs AG vs GG and the Mann-Whitney-U test for AA vs GG and (AA+AG) vs GG, 2 sided significances are reported. *Monte Carlo estimates of significance are reported for analyses using the Jonckheere Terpstra Test and ** Exact significances are reported for analyses using the Mann-Whitney-U Test. SNP genotyping was performed using comparative genomic hybridisation in the Bond laboratory and GI_{50} data were downloaded from the NCI60 DTP tumour screen. Associations significant at the 0.05 level are highlighted in red. The demonstration of significant associations between IGF-1R SNP, mRNA or protein expression scattered across multiple classes may reflect the level of significance chosen and the lack of use of a Bonferroni correction. However, given the clusters of associations involving the camptothecins and the nitrosorueas, it seems possible that these may represent real rather than chance effects for these two drug groups.

Alkylating agents

Drug GI_{50}	Number of Cell lines with a given genotype for SNP rs4966013				Allelic Comparison Performed		
					AA vs AG vs GG*	AA vs GG**	(AA+AG) vs GG**
	AA	AG	GG	Total	Monte Carlo Significance	Exact Significance	Exact Significance
Asaley	30	17	7	54	.560	1.000	.724
Chlorambucil	30	17	7	54	.364	.059	.067
Fluorodopan	30	16	7	53	.678	.582	.580
Ifosfamide	30	17	7	54	.371	.391	.433
Mechlorethamine (Mustine)	30	16	7	53	.976	.531	.416
Melphalan	30	16	7	53	.664	.330	.271
Uramustine (Uracil nitrogen mustard)	30	16	7	53	.327	.049	.059
AZQ	29	17	7	53	.996	.366	.248
Mitomycin C	30	17	7	54	.893	.312	.212
Actinomycin D	30	17	7	54	.371	.608	.375
Porfiromycin	30	16	7	53	.647	.582	.345
Thiotepa	30	17	7	54	.374	.084	.080
Triethylenemelamine	30	17	7	54	.612	.092	.080
Dianhydrogalacticol	29	17	7	53	.856	.387	.345
Teroxirone	30	17	7	54	.987	.719	.650
Busulfan	30	17	7	54	.670	.413	.335
Clomesone	29	17	7	53	.071	.020	.026
Cyclodisone	30	17	7	54	.273	.049	.043
Hepsulfam	29	17	7	53	.834	.366	.332
Yoshi 864	30	16	7	53	.733	.370	.319
Chlorotozocin (DCNU)	30	17	7	54	.845	.243	.095
Carmustine (BCNU)	30	17	7	54	.247	.054	.075
Lomustine (CCNU)	30	16	7	53	.871	.330	.248
PCNU	30	16	7	53	.807	.172	.067
Semustine (mCCNU)	30	16	7	53	.290	.059	.046
Dacarbazine	29	17	7	53	.781	.938	.949
Mitozolomide	30	17	7	54	.781	.199	.124
Piperazine	30	17	7	54	.731	.227	.160
Piperazinedione	29	17	7	53	.803	.206	.227
Pipobroman	30	16	7	53	.969	.293	.227
Carboplatin	30	17	7	54	.338	.059	.030
Carboxypthalatoplatinum	30	17	7	54	.882	.172	.085
Cisplatin	30	17	7	54	.399	.077	.043
Iproplatin	30	17	7	54	.950	.747	.528
Tetraplatin	30	17	7	54	.548	.249	.100

Antimitotic agents

Drug GI_{50}	Number of Cell lines with a given genotype for SNP rs4966013				Allelic Comparison Performed		
					AA vs AG vs GG*	AA vs GG**	(AA+AG) vs GG**
	AA	AG	GG	Total	Monte Carlo Significance	Exact Significance	Exact Significance
Paclitaxel (Taxol)	30	17	7	54	.762	.506	.418
Docetaxel	30	15	7	52	.590	.608	.545
Ibaxepilone (Epothilone B analogue)	29	16	7	52	.343	.206	.244
Vinblastine (NCI 60)	30	17	7	54	.549	.865	.940
Erubilin mesylate	30	17	7	54	.422	.227	.232
Colchicine derivative	30	17	7	54	.730	.865	.960
Thiocolchicine	30	17	7	54	.343	.059	.033
Maytansine	30	17	7	54	.081	.054	.035
Dolastatin10	30	16	7	53	.384	.925	.867
Dolastatin15	30	17	7	54	.766	.835	.650
Auristatin PE	30	15	7	52	.867	.435	.278
Trityl cysteine	30	16	7	53	.674	.985	.787
Monastrol	30	17	7	54	.983	.955	.940

Topoisomerase I inhibitors

Drug GI_{50}	Number of Cell lines with a given genotype for SNP rs4966013				Allelic Comparison Performed		
					AA vs AG vs GG*	AA vs GG**	(AA+AG) vs GG**
	AA	AG	GG	Total	Monte Carlo Significance	Exact Significance	Exact Significance
Camptothecin (Na salt)	30	17	7	54	.818	.059	.037
14-Chloro-20(S)-camptothecin hydrate	30	17	7	54	.938	.118	.063
MLS000766263	30	17	7	54	.330	.036	.040
Camptothecin,20-O-((4-(2-hydroxyethyl)-1-piperazino) OAC	30	17	7	54	.466	.071	.059
11-Formyl-20(RS)-camptothecin	30	17	7	54	.521	.065	.055
Camptothecin-20-O-(N,N-dimethyl)glycinate HCl	30	17	7	54	.987	.065	.046
Camptothecin glutamate HCl	30	17	7	54	.859	.084	.067
Camptothecin,n-diethyl glycinate	30	17	7	54	.758	.059	.049
Camptothecin ethylglycinate ester hydrochloride	30	17	7	54	.487	.049	.052
Topotecan	30	17	7	54	.547	.054	.046
Irinotecan	30	17	7	54	.542	.199	.212
Indotecan	30	17	7	54	.790	.435	.323
NSC 314622	30	17	7	54	.330	.662	.433
Staurosporine	30	17	7	54	.393	.213	.212
Morpholinodoxorubicin	30	17	7	54	.372	.077	.067

Topoisomerase II inhibitors

Drug GI_{50}	Number of Cell lines with a given genotype for SNP rs4966013				Allelic Comparison Performed		
					AA vs AG vs GG*	AA vs GG**	(AA+AG) vs GG**
	AA	AG	GG	Total	Monte Carlo Significance	Exact Significance	Exact Significance
Aclarubicin	29	17	7	53	.801	.433	.332
Cyanomorpholino-doxorubicin	30	17	7	54	.041	.013	.009
Daunorubicin	30	17	7	54	.877	.243	.185
Deoxydoxorubicin (Escorubicin)	30	17	7	54	.287	.556	.310
Doxorubicin	30	17	7	54	.740	.391	.203
Epirubicin	29	17	6	52	.653	.187	.059
Idarubicin	29	17	7	53	.815	.270	.217
Menogaril	30	17	7	54	.983	.259	.222
NN-Dibenzyldaunorubicin	30	17	7	54	.724	.719	.495
Zorubicin rubidazone	29	17	7	53	.564	.754	.495
Mitoxantrone	30	17	7	54	.938	.556	.448
Piroxantrone	29	17	7	53	.752	.667	.462
Teloxantrone	30	17	7	54	.803	.100	.052
Amonafide	30	17	7	54	.619	.955	.880
Bisantrene	28	16	6	50	.661	.982	.919
Pyrazoloacridine	30	17	7	54	.448	.482	.561
Amsacrine mAMSA	30	17	7	54	.987	.160	.106
Merbarone	29	17	7	53	.526	1.000	.949
Etopiside	30	17	6	53	.483	.493	.484
Teniposide	30	16	7	53	.360	.925	.634

RNA/ DNA antimetabolites

Drug GI_{50}	Number of Cell lines with a given genotype for SNP rs4966013				Allelic Comparison Performed		
	AA	AG	GG	Total	AA vs AG vs GG* Monte Carlo Significance	AA vs GG** Exact Significance	(AA+AG) vs GG** Exact Significance
L.Alanosine SDX102	29	17	7	53	.959	.480	.307
5-Fluorouracil	30	17	7	54	.764	.330	.242
Pyrazofurin	30	17	7	54	.331	.985	.632
5-azacytidine	30	16	7	53	.110	.259	.495
5,6-dihydro-5-azacytidine	29	17	7	53	.878	.938	.969
Acivicin	29	17	6	52	.439	.782	.566
Dichloroallyl lawsone	30	17	7	54	.554	.747	.448
Brequinar	28	17	7	52	.862	.406	.267
L-Aspartic acid, N-(phosphonoacetyl)-, tetrasodium salt (PALA)	30	17	7	54	.996	.213	.090
Methotrexate	30	17	7	54	.415	.059	.049
Trimetrexate TMQ	30	17	7	54	.757	.172	.071
Piritrexim PTX	29	17	7	53	.532	.049	.026

DNA antimetabolites

Drug GI_{50}	Number of Cell lines with a given genotype for SNP rs4966013				Allelic Comparison Performed		
					AA vs AG vs GG*	AA vs GG**	(AA+AG) vs GG**
	AA	AG	GG	Total	Monte Carlo Significance	Exact Significance	Exact Significance
Floxuridine (2'-deoxy-5-fluorouridine)	30	17	7	54	.725	.185	.118
Thiopurine (6-Mercaptopurine)	30	17	7	54	.832	.506	.495
Thioguanine	30	17	7	54	.842	.370	.418
2-fluoroadenosine arabinoside (Fludarabine)	30	17	6	53	.895	.852	.924
Clofarabine (2'fluoro-2'deoxyarabinofuranosyl-2-chloroadenine)	30	17	7	54	.893	.776	.762
Cladribine (2-chloro-2'deoxyadenosine)	30	17	7	54	.294	.259	.222
alpha-TGDR thiodeoxyguanidine	30	16	7	53	.442	.955	.709
Guanazole	30	16	7	53	.589	.092	.081
Cytosine arabinoside (ara-C, Cytarabine)	30	17	7	54	.803	.259	.242
5-aza-2'deoxycytidine (Decitabine)	30	16	7	53	.259	.199	.155
2,2-difluoro-2'deoxycytidine (Gemcitabine)	30	17	7	54	.530	.149	.138
Pentostatin (2'-deoycoformycin)	30	17	7	54	.507	.172	.152
Hydroxyurea	30	16	7	53	.644	.092	.063
Cyclocytidine (Ancitabine)	30	17	7	54	.711	.719	.511
pyrazoloimidazole	30	16	7	53	.473	.149	.120
3HP	29	17	7	53	.456	.221	.198
5HP	30	17	7	54	.829	.330	.286
Inosine glycoaldehyde	30	16	7	53	.562	.482	.545
MacbecinII	29	17	6	52	.676	.593	.458
Aphidicolin	29	17	7	53	.879	.345	.259

Appendix V: Tables – correlations of drug GI_{50} with IGF-1R protein and mRNA

Examination of correlations between chemotherapeutic agent GI_{50} values with IGF-1R protein and *IGF-1R* mRNA expression within cell lines of the NCI60 tumour panel. Correlation coefficients, their significance and the number of cell lines examined (n) are presented. Spearman's correlations were used, as previous examination using Kolgorov-Smirnov and Shapiro-Wilks tests revealed that many of the data sets were not normally distributed. IGF-1R protein expression and drug GI_{50} data were downloaded from the DTP NCI60 tumour screen. *IGF-1R* mRNA expression data were generated in Dr Gareth Bond's laboratory using RT-PCR and are presented as cycle thresholds at which amplification was observed, normalised to that of the housekeeping gene *GAPDH*. For IGF-1R protein and mRNA expression data, high and low values respectively corresponded to high expression; hence the largely positive correlation coefficients for protein expression with drug GI_{50} and largely negative correlation coefficients for mRNA expression. Correlations significant at the 0.05 level are highlighted in red.

Alkylating agents

Drug	Correlation of Relative IGF-1R protein expression with drug GI_{50}			Correlation of *IGF-1R* mRNA expression with drug GI_{50}		
	Spearman's correlation coefficient	Significance (2-tailed)	n	Spearman's correlation coefficient	Significance (2-tailed)	n
Asaley	.051	.709	56	.127	.353	56
Chlorambucil	.045	.741	56	-.018	.896	56
Fluorodopan	.189	.167	55	-.093	.498	55
Ifosfamide	-.160	.239	56	.047	.728	56
Mechlorethamine (Mustine)	.038	.781	55	.056	.683	55
Melphalan	.068	.623	55	-.110	.424	55
Uramustine (Uracil nitrogen mustard)	.096	.484	55	-.075	.588	55
AZQ	.146	.286	55	-.174	.205	55
Mitomycin C	-.134	.324	56	.050	.714	56
Actinomycin D	.059	.663	56	-.083	.542	56
Porfiromycin	-.213	.118	55	.127	.354	55
Thiotepa	.049	.720	56	-.100	.464	56
Triethylenemelamine	.025	.855	56	-.050	.713	56
Dianhydrogalacticol	-.024	.860	55	-.018	.898	55
Teroxirone	.128	.347	56	-.036	.790	56
Busulfan	-.030	.825	56	-.051	.710	56
Clomesone	.096	.486	55	-.133	.334	55
Cyclodisone	.130	.339	56	-.227	.093	56
Hepsulfam	.075	.588	55	-.139	.312	55
Yoshi 864	-.018	.894	55	-.052	.706	55
Chlorotozocin (DCNU)	.093	.496	56	-.152	.264	56
Carmustine (BCNU)	.276	.040	56	-.336	.011	56
Lomustine (CCNU)	.410	.002	55	-.342	.011	55
PCNU	.156	.254	55	-.300	.026	55
Semustine (mCCNU)	.306	.023	55	-.349	.009	55
Dacarbazine	.159	.245	55	-.191	.162	55
Mitozolomide	.170	.211	56	-.341	.010	56
Piperazine	.140	.302	56	-.131	.337	56
Piperazinedione	.062	.653	55	-.016	.906	55
Pipobroman	-.022	.875	55	-.035	.801	55
Carboplatin	.174	.201	56	-.148	.276	56
Carboxypthalatoplatinum	.146	.282	56	-.027	.841	56
Cisplatin	.050	.715	56	-.116	.393	56
Iproplatin	-.033	.804	58	.080	.559	56
Tertraplatin	.117	.376	59	-.039	.773	56

Antimitotic agents

Drug	Correlation of Relative IGF-1R protein expression with drug GI_{50}			Correlation of *IGF-1R* mRNA expression with drug GI_{50}		
	Spearman's correlation coefficient	Significance (2-tailed)	n	Spearman's correlation coefficient	Significance (2-tailed)	n
Paclitaxel (Taxol)	.036	.792	56	-.122	.371	56
Docetaxel	-.029	.834	54	-.001	.995	54
Ibaxepilone (Epothilone B analogue)	.193	.161	54	-.160	.247	54
Vinblastine (NCI 60)	.131	.336	56	-.134	.326	56
Erubilin mesylate	.125	.360	56	-.206	.127	56
Colchicine derivative	.095	.484	56	-.067	.625	56
Thiocolchicine	.219	.105	56	-.328	.013	56
Maytansine	.159	.241	56	-.195	.149	56
Dolastatin10	.024	.864	55	-.063	.647	55
Dolastatin15	.390	.003	56	-.332	.012	56
Auristatin PE	-.030	.830	54	-.082	.553	54
Trityl cysteine	-.048	.726	55	-.111	.418	55
Monastrol	.122	.370	56	-.125	.359	56

Topoisomerase I inhibitors

Drug	Correlation of Relative IGF-1R protein expression with drug GI_{50}			Correlation of *IGF-1R* mRNA expression with drug GI_{50}		
	Spearman's correlation coefficient	Significance (2-tailed)	n	Spearman's correlation coefficient	Significance (2-tailed)	n
Camptothecin (Na salt)	.048	.727	56	-.006	.966	56
14-Chloro-20(S)-camptothecin hydrate	.031	.822	56	-.089	.514	56
MLS000766263	.110	.420	56	-.129	.344	56
Camptothecin,20-O-((4-(2-hydroxyethyl)-1-piperazino) OAC	.166	.221	56	-.153	.260	56
11-Formyl-20(RS)-camptothecin	.137	.315	56	-.105	.440	56
Camptothecin-20-O-(N,N-dimethyl)glycinate HCl	.081	.552	56	-.102	.455	56
Camptothecin glutamate HCl	.014	.916	56	-.045	.744	56
Camptothecin,n-diethyl glycinate	.046	.736	56	-.077	.574	56
Camptothecin ethylglycinate ester hydrochloride	.010	.945	56	-.070	.608	56
Topotecan	.092	.498	56	-.065	.632	56
Irinotecan	.146	.283	56	-.178	.190	56
Indotecan	.160	.240	56	-.085	.534	56
NSC 314622	.130	.340	56	-.168	.215	56
Staurosporine	.125	.358	56	-.176	.194	56
Morpholinodoxorubicin	.060	.662	56	-.183	.178	56

Topoisomerase II inhibitors

Drug	Correlation of Relative IGF-1R protein expression with drug GI_{50}			Correlation of *IGF-1R* mRNA expression with drug GI_{50}		
	Spearman's correlation coefficient	Significance (2-tailed)	n	Spearman's correlation coefficient	Significance (2-tailed)	n
Aclarubicin	.215	.116	55	-.265	.051	55
Cyanomorpholino-doxorubicin	.178	.188	56	-.249	.064	56
Daunorubicin	.171	.208	56	-.144	.290	56
Deoxydoxorubicin (Escorubicin)	.118	.387	56	-.092	.500	56
Doxorubicin	.099	.469	56	-.052	.703	56
Epirubicin	.135	.331	54	-.141	.308	54
Idarubicin	.143	.301	54	-.038	.783	54
Menogaril	.102	.455	56	-.122	.369	56
NN-Dibenzyldaunorubicin	.201	.137	56	-.252	.061	56
Zorubicin rubidazone	.104	.449	55	-.041	.767	55
Mitoxantrone	.154	.256	56	-.218	.107	56
Piroxantrone	.041	.766	55	-.110	.424	55
Teloxantrone	.077	.573	56	-.131	.335	56
Amonafide	.092	.498	56	-.075	.582	56
Bisantrene	.041	.773	52	-.040	.780	52
Pyrazoloacridine	.230	.088	56	-.312	.019	56
Amsacrine mAMSA	.087	.523	56	-.059	.664	56
Merbarone	.177	.197	55	-.031	.824	55
Etopiside	-.176	.197	55	.067	.627	55
Teniposide	.031	.820	55	-.067	.625	55

RNA/ DNA antimetabolites

Drug	Correlation of Relative IGF-1R protein expression with drug GI_{50}			Correlation of *IGF-1R* mRNA expression with drug GI_{50}		
	Spearman's correlation coefficient	Significance (2-tailed)	n	Spearman's correlation coefficient	Significance (2-tailed)	n
L.Alanosine SDX102	-.032	.819	55	-.185	.177	55
5-Fluorouracil	.008	.956	56	.024	.861	56
Pyrazofurin	.082	.550	56	-.254	.059	56
5-azacytidine	-.040	.772	55	.168	.220	55
5,6-dihydro-5-azacytidine	.106	.443	55	-.028	.838	55
Acivicin	.026	.853	54	-.203	.141	54
Dichloroallyl lawsone	.258	.055	56	-.280	.036	56
Brequinar	.187	.175	54	-.333	.014	54
L-Aspartic acid, N-(phosphonoacetyl)-, tetrasodium salt (PALA)	.020	.882	56	-.212	.116	56
Methotrexate	.132	.333	56	-.242	.072	56
Trimetrexate TMQ	.123	.368	56	-.276	.039	56
Piritrexim PTX	.184	.180	55	-.194	.156	55

DNA antimetabolites

Drug	Correlation of Relative IGF-1R protein expression with drug GI_{50}			Correlation of *IGF-1R* mRNA expression with drug GI_{50}		
	Spearman's correlation coefficient	Significance (2-tailed)	n	Spearman's correlation coefficient	Significance (2-tailed)	n
Floxuridine (2'-deoxy-5-fluorouridine)	.013	.925	56	-.055	.686	56
Thiopurine (6-Mercaptopurine)	.169	.213	56	-.162	.233	56
Thioguanine	.126	.356	56	-.199	.142	56
2-fluoroadenosine arabinoside (fludarabine)	-.039	.779	55	.131	.342	55
clofarabine.2'fluoro-2'deoxyarabinofuranosyl-2-chloroadenine	-.106	.438	56	.121	.374	56
Cladribine (2-chloro-2'deoxyadenosine)	-.035	.799	56	.048	.725	56
alpha-TGDR thiodeoxyguanidine	.146	.289	55	-.167	.223	55
Guanazole	.066	.633	55	-.115	.404	55
Cytosine arabinoside (ara-C, Cytarabine)	.014	.921	56	-.010	.942	56
5-aza-2'deoxycytidine (Decitabine)	.013	.925	55	.004	.975	55
2,2-difluoro-2'deoxycytidine (Gemcitabine)	-.001	.994	56	.007	.959	56
Pentostatin(2'-deoycoformycin)	-.006	.968	56	.037	.789	56
Hydroxyurea	.155	.260	55	-.106	.440	55
Cyclocytidine (Ancitabine)	-.044	.747	56	.010	.939	56
pyrazoloimidazole	.054	.695	55	-.066	.633	55
3HP	.146	.289	55	-.165	.228	55
5HP	.141	.299	56	-.119	.382	56
Inosine glycoaldehyde	.251	.064	55	-.089	.518	55
MacbecinII	.113	.418	54	-.096	.491	54
Aphidicolin	.073	.597	55	-.142	.302	55